

## **ZAŁĄCZNIKI**

### **12. Kopie publikacji naukowych stanowiących podstawę rozprawy doktorskiej**

**Publikacja naukowa [A1]**

## PAPER

Cite this: *RSC Adv.*, 2016, 6, 103851

Received 15th September 2016

Accepted 12th October 2016

DOI: 10.1039/c6ra23060a

[www.rsc.org/advances](http://www.rsc.org/advances)

# Visible light photoinitiating systems based on squaraine dye: kinetic, mechanistic and laser flash photolysis studies

Janina Kabatc,<sup>\*a</sup> Katarzyna Kostrzewska,<sup>a</sup> Martyna Kozak<sup>b</sup> and Alicja Balcerak<sup>b</sup>

New two-component photoinitiator systems for radical polymerization of acrylates are presented. The systems discussed comprise a synthetic dye 1,3-bis(*p*-bromophenylamino)squaraine and borate and onium salts as coinitiator. The effect of the composition of the system on the photopolymerization kinetics was analyzed. To this end, the photophysics and photochemistry of the dye under polymerization conditions were explored by means of stationary and time-resolved spectroscopic methods. The action mechanism of the different photoinitiators systems is discussed.

## 1. Introduction

The development of new materials by means of photopolymerization requires investigations aimed at discovering more efficient photoinitiator systems.<sup>1</sup> Most traditional photoinitiating systems employ UV radiation to generate active species. Different classes of synthetic dyes play very important roles in polymer chemistry. They are very often used as photosensitizers and make the polymerization process possible in the visible light region. Therefore, the development of photoinitiators based on synthetic dyes and coinitiators has been the subject of a large amount of work.

For example, ammonium, phosphonium, sulfonium, iodonium salts, arsonium, pyridinium and organoborate salts are capable of undergoing photochemical decomposition, producing active species suitable to initiate polymerization. When these coinitiators may act as an electron acceptor, photosensitization was proposed to take place by reduction and posterior fragmentation of the cation.<sup>1–4</sup> On the other hand a coinitiator may also play a role of an electron donor, as in a case of alkyltriphenylborate salts.<sup>5</sup> The first group of coinitiators (onium salts) may act as a source of free radicals, radical cations, or Brønsted acids when exposed to light<sup>1</sup> and may be employed as efficient photoinitiators of radical, cationic, or mixed polymerization.<sup>4,6–10</sup>

Recently, the following synthetic chromophores: camphorquinone,<sup>11</sup> anthracene derivatives,<sup>12</sup> pyrene derivatives,<sup>13</sup> indanedione derivatives,<sup>14</sup> *N*-substituted quinoxalinobenzothiazine derivatives,<sup>15</sup> thiobarbituric acid derivative,<sup>16</sup> chalcone

derivatives,<sup>17</sup> acridinedione derivatives,<sup>18</sup> naphthalimide derivatives,<sup>19</sup> diketopyrrolopyrrole-thiophene or diketopyrrolopyrrole-furan derivatives,<sup>20,21</sup> violanthrone-79,<sup>22</sup> NIR sensitized polymethine dyes<sup>4</sup> and other acting as photosensitizers for onium salts were used in dye mediated photoinitiating systems.<sup>23</sup>

The squarylium dyes have been very rarely used as photosensitizers in photopolymerization process.

In 2004 Yong He and co-workers described the application of two squaraine dyes: bis(1,2,3,3-tetramethylindolenium-2-ylidene)squaraine and bis(3-methylbenzothiazol-2-ylidene)squaraine as sensitizers for three (*p*-octanoxyphenyl)phenyliodonium salts varying with a type of counterion, in radical polymerization of methyl methacrylate.<sup>24</sup>

In 2013 and 2015 Lalevée and co-workers presented the photoinitiating abilities of 2,2,3-trimethylindolenine-based squaraine dye incorporated in multicomponent systems for cationic polymerization of an epoxide or a vinyl ether as well as radical polymerization of **TMPTA**.<sup>25,26</sup> In 2016 our research group described the application of 1,3-bis(phenylamino)squaraine and conventional free radical sources, such as tetramethylammonium *n*-butyltriphenylborate, diphenyliodonium chloride and diphenyliodonium hexafluorophosphate for initiation of photopolymerization occurring *via* radical or cationic mechanism.<sup>27</sup>

From our knowledge the 1,3-bis(*p*-bromophenylamino)squaraine has not been studied in the photoinitiating systems, yet. Because, the dye under study absorbs in the region from 350 nm to 450 nm an application of the blue light sources is possible.

In the present paper, we will focus on the research carried out on the two-component photoinitiating systems for free radical polymerization of multifunctional acrylates containing three different coinitiators. We will describe two-component photoinitiating systems employing 1,3-bis(*p*-bromophenylamino)squaraine (**SQ**) as a sensitizer adequate for blue light and

<sup>a</sup>UTP, University of Science and Technology, Faculty of Chemical Technology and Engineering, Seminaryjna 3, 85-326 Bydgoszcz, Poland. E-mail: [nina@utp.edu.pl](mailto:nina@utp.edu.pl); Fax: +48 52 374 9005; Tel: +48 52 374 9112

<sup>b</sup>Student in first grade of UTP, University of Science and Technology, Faculty of Chemical Technology and Engineering, Poland

following coinitiators: tetramethylammonium *n*-butyltriphenylborate (**B2**), diphenyliodonium chloride (**I1**) and *N*-methoxy-4-phenylpyridinium tetrafluoroborate (**NO**). The photoinitiating ability of new photoinitiating systems, acting in UV-Vis light region, for initiation of free radical polymerization of di- and triacrylates was also compared with few commercially used photoinitiators.

## 2. Experimental

### 2.1. Materials

Monomers: 1,6-hexanediol diacrylate (**HDDA**), pentaerythritol triacrylate (**PETA**), 2-ethyl-2-(hydroxymethyl)-1,3-propanediol triacrylate (**TMPTA**), coinitiators (diphenyliodonium chloride (**I1**) and *N*-methoxy-4-phenylpyridinium tetrafluoroborate (**NO**)) and solvents (spectroscopic grade) were purchased from Aldrich (Poland) and used without further purification. 1,3-Bis(*p*-bromophenylamino)squaraine (**SQ**) and tetramethylammonium *n*-butyltriphenylborate (**B2**) were synthesized in our laboratory by methods described in literature.<sup>28–30</sup>

### 2.2. Spectroscopic measurements

Absorption and emission spectra were recorded at room temperature using an Agilent Technology UV-Vis Cary 60 Spectrophotometer, a Hitachi F-7000 spectrofluorimeter and UV-VIS-NIR Fluorolog 3 Spectrofluorimeter (Horiba Jobin Yvon), respectively. The spectra were recorded in following solvents: water (H<sub>2</sub>O), dimethylsulfoxide (DMSO), acetonitrile (CH<sub>3</sub>CN), *N,N*-dimethylformamide (DMF), 1-methyl-2-pyrrolidinone (MP), methanol (MeOH), ethanol (EtOH), acetone, tetrahydrofuran (THF) and diethyl ether. The final concentration of dye in solution was  $1.0 \times 10^{-5}$  M. The spectroscopic measurements were performed in mentioned above solvents containing 10% of 1-methyl-2-pyrrolidinone. For this purpose a suitable amount of the dye was dissolved in 1-methyl-2-pyrrolidinone, than 2.0 mL of the concentrated (*ca.* 1 mM) stock solution was added to a 10 mL volumetric flask containing spectroscopic grade solvents under the study.

The fluorescence lifetimes were measured using a single-photon counting system UV-VIS-NIR Fluorolog 3 Spectrofluorimeter (Horiba Jobin Yvon). The apparatus utilizes for the excitation a picosecond diode laser generating pulses of about 55 ps at 370 nm. Short laser pulses in combination with a fast microchannel plate photodetector and ultrafast electronics make a successful analysis of fluorescence decay signals with a resolution of few picoseconds possible. The dye was studied at concentration able to provide equivalent absorbance at 370 nm (0.2 in the 10 mm cell) to be obtained. The fluorescence decay was fitted to two exponentials.

The fluorescence quenching measurements were performed using a single-photon counting system UV-VIS-NIR Fluorolog 3 Spectrofluorimeter (Horiba Jobin Yvon). The apparatus uses a picosecond diode laser (370 nm) generating pulses of about 50 ps for the excitation. Short laser pulses in combination with a fast microchannel plate photodetector and ultrafast electronics make a successful analysis of fluorescence decay signals

in the range of single picoseconds possible. The dye was studied at a concentration able to provide equivalent absorbance at 370 nm (0.2 in the 10 mm cell). The rate constant for quenching of 1,3-bis(*p*-bromophenylamino)squaraine by all quenchers under studies were determined in 1-methyl-2-pyrrolidinone. The concentration of dye was  $2 \times 10^{-5}$  M and that of quenchers was in the range from  $1 \times 10^{-4}$  M to  $5.0 \times 10^{-3}$  M. The fluorescence quenching at 440 nm was measured in deaerated solution by bubbling with argon.

### 2.3. Polymerization measurements

The kinetics of polymerization of all monomers photoinitiated by: 1,3-bis(*p*-bromophenylamino)squaraine/tetramethylammonium *n*-butyltriphenylborate (**SQ/B2**), 1,3-bis(*p*-bromophenylamino)squaraine/diphenyliodonium chloride (**SQ/I1**) and 1,3-bis(*p*-bromophenylamino)squaraine/*N*-methoxy-4-phenylpyridinium tetrafluoroborate (**SQ/NO**) was measured using Differential Scanning Calorimeter TA DSC Q2000 Instrument and TA Q PCA photo unit equipped with a high-pressure mercury lamp (Photo-DSC). The heat of the photoinitiated polymerization reaction measured by means of a photo differential scanning calorimeter, is a good control of the reaction temperature. UV-visible light ( $300 \text{ nm} < \lambda < 500 \text{ nm}$ ) was applied from a high pressure mercury lamp at a constant intensity of  $30 \text{ mW cm}^{-2}$  for several min under a nitrogen flow of  $50 \text{ mL min}^{-1}$  at a prescribed temperature (isothermal mode). The weight of the samples  $30 \pm 0.1$  mg was placed into an open aluminum liquid DSC pan. The measurements were carried out under identical conditions. The sample was maintained at a prescribed temperature for 2 min before each measurement run began. Measurements were recorded at a sampling interval of 0.05 s per point. The polymerizing solution was composed of 1.8 mL of monomer, 0.2 mL of 1-methyl-2-pyrrolidinone and appropriate amount of photoinitiator. The using of 1-methyl-2-pyrrolidinone was necessary due to poor solubility of dye in the monomers studied.

The reaction heat liberated in the polymerization is directly proportional to the number of acrylates reacted in the system. By integrating the area under the exothermic peak, the conversion of the acrylate groups (*C*%) or the extent of the reaction was determined according to eqn (1):

$$C\% = \frac{\Delta H_t}{\Delta H_0} \times 100 \quad (1)$$

where  $\Delta H_t$  is the reaction heat evolved at time *t* and  $\Delta H_0$  is the theoretical heat for complete conversion. A reaction heat for an acrylate double bond polymerization of  $\Delta H_0 = 78.0 \text{ kJ mol}^{-1}$  was used. The rate of polymerization ( $R_p$ ) is directly related to the heat flow ( $dH/dt$ ) as in eqn (2):

$$R_p = \frac{dH/dt}{\Delta H_0} \quad (2)$$

### 2.4. Cyclic voltammetry measurements

The electrochemical measurements were evaluated by Cyclic Voltammetry (CV). Cyclic voltammetric measurements were

made with ER466 Integrated Potentiostat System (eDAQ, Poland) in a three-electrode configuration. The electrolyte was 0.1 M tetrabutylammonium perchlorate in dry acetonitrile. Platinum 1 mm disk electrode was applied as working electrode and platinum and Ag/AgCl were used as auxiliary and reference electrodes, respectively. All solutions were deoxygenated with N<sub>2</sub> for at least 15 min prior to measurements. The computer-controlled potentiostat was equipped with EChem Software.

### 2.5. Nanosecond laser flash photolysis

Transient absorption spectra and decay kinetics were studied out using the nanosecond laser flash photolysis method. The nanosecond laser flash photolysis experiments were performed using a LKS.60 Laser Flash Photolysis apparatus (Applied Photophysics). Laser irradiation at 355 nm from the third harmonic of the Q-switched Nd:YAG laser from a Lambda Physik/model LPY 150 operating at 65 mJ per pulse (pulse width about 4–5 ns) was used for the excitation. Transient absorbances at preselected wavelengths were monitored by a detection system consisting of a monochromator, a photomultiplier tube (Hamamatsu R955) and a pulsed xenon lamp (150 W) as a monitoring source. The signal from the photomultiplier was processed by a Helwett-Packard/Agilent an Agilent Infiniium 54810A digital storage oscilloscope and an Acorn compatible computer.

## 3. Results and discussion

The schematic structures of all compounds involved in the photoinitiating systems studied are presented in Table 1.

The synthetic dye applied in new photoinitiating systems for radical polymerization of multifunctional acrylates belongs to squaraine dyes. Generally, squaraines are a family of chromophores containing structures such as cyanine dyes, two donor groups conjugated to an electron deficient oxocyclobutenolate core, leading to highly electron delocalized structure that can be exemplified as zwitterions. Due to their planar structures and zwitterionic properties, squaraine dyes exhibit strong absorption ( $\epsilon > 10^5 \text{ dm}^3 \text{ mol}^{-1} \text{ cm}^{-1}$ ) and emission. By modifying the aromatic or heterocyclic donor moiety it is easy to modify the chromophore structure to tune the optical properties.<sup>31</sup> The dye under study possess a strong withdrawing group (–Br) in *para* position of phenyl ring.

### 3.1. Spectroscopic properties

One of the parameters that may have a significant influence on the photophysical properties of photosensitizer is a solvent medium. The solvent polarity may play a significant role in dictating spectral shifts of the absorption band of squaraine dyes.<sup>32</sup> The influence on the absorption properties of squaraine dye studied of different polarity solvents is shown in Fig. 1.

(SQ) exhibits a pronounced, well-defined absorption band with maximum from 400 nm to 415 nm. The value of molar absorption coefficient depends on the polarity of solvent and ranging from  $0.56 \times 10^4 \text{ dm}^3 \text{ mol}^{-1} \text{ cm}^{-1}$  to  $4.95 \times 10^4 \text{ dm}^3 \text{ mol}^{-1} \text{ cm}^{-1}$  from high polar to nonpolar solvents. The position

of an absorption band only slightly depends on a type of solvent. Significant variation of solvent polarity, from diethyl ether to 1-methyl-2-pyrrolidinone to water, led to negligible hypsochromic shifts (415 nm  $\rightarrow$  405 nm  $\rightarrow$  398 nm). More polar solvents lead to the blue-shift of an absorption band by 10–15 nm. Moreover, no changes in the spectral bands were observed with increasing squaraine dye concentration, thus indicating the ability of dye to remain in monomeric form even at relatively high concentrations. Similar results were observed by P. V. Kamat *et al.* for tetrahydroquinoxaline-based squaraine dyes.<sup>32</sup> Other structurally modified squaraines undergo H- and J-type aggregation upon an increase of concentration.<sup>33–35</sup>

Emission measurements revealed sharp fluorescence spectra with relatively high Stokes shifts ( $\Delta\nu_{\text{max}} \approx 5000 \text{ cm}^{-1}$ ) and fluorescence quantum yields equal  $5 \times 10^{-4}$  and  $34.5 \times 10^{-4}$  in diethyl ether and 1-methyl-2-pyrrolidinone, respectively.

As is seen, 1,3-bis(*p*-bromophenylamino)squaraine exhibit low fluorescence quantum yield and short emission lifetime about 10 ns. Fig. 2 shows the fluorescence decay observed for 1,3-bis(*p*-bromophenylamino)squaraine in 1-methyl-2-pyrrolidinone solution.

The fluorescence decay observed was fitted to two exponential curve. The dye exists in two conformers that differ in fluorescence lifetime described by the corresponding components of two exponential models, such as  $\tau_1$  and  $\tau_2$  together with the corresponding amplitudes ( $B_1$  and  $B_2$ ). This feature results from interaction of 1,3-bis(*p*-bromophenylamino)squaraine with surrounding solvent. On the basis of fitting of two exponential curve, the fluorescence lifetimes of two conformers were designated. The fluorescence lifetime of conformer appearing predominantly (over 95%) is 10.8 ns. While, the fluorescence lifetime of shorter living conformer is equal 2.7 ns.

Taking into account very small value of the fluorescence quantum yield one can conclude that there are other deactivation processes (radiative and/or nonradiative) which squaraine undergoes in its excited state. As it was mentioned in our previous paper,<sup>36</sup> the excited state of squaraine molecule may be quenched by different molecules in bimolecular reaction. The following compounds: tetramethylammonium *n*-butyltriphenylborate (**B2**), diphenyliodonium chloride (**I1**) and *N*-methoxyphenyl-4-phenylpyridinium tetrafluoroborate (**NO**) were used as a quencher. The fluorescence quenching measurements were confirmed an electron transfer between coinitiator and photosensitizer. For this purpose, the changes in fluorescence lifetime under increasing concentration of quencher (coinitiator) was studied.<sup>37,38</sup> The influence of a selected quencher on fluorescence lifetime and Stern–Volmer relationship are presented in Fig. 3, respectively.

From the comparison of the results obtained for the same chromophore and chromophore in the presence of quenchers the shortening of the average fluorescence lifetime was observed. The shortening of the fluorescence lifetime is interpreted as a result of interaction of dye with quencher molecule.

An addition of borate salt, iodonium salt and *N*-alkoxy-pyridinium salt results in a significant decrease in a lifetime of the excited singlet state of dye. Basing on this, it should be noted, that in a presence of suitable quencher the fluorescence state of

Table 1 Structures, names and abbreviations of sensitizer, electron donor, electron acceptors and monomers

<p style="text-align: center;">Sensitizer 1,3-Bis(<i>p</i>-bromophenylamino)squaraine (<b>SQ</b>)</p>		
<p style="text-align: center;">Tetramethylammonium <i>n</i>-butyltriphenylborate (<b>B2</b>)</p>	<p style="text-align: center;">Diphenyliodonium chloride (<b>I1</b>) Electron acceptor</p>	<p style="text-align: center;"><i>N</i>-Methoxy-4-phenylpyridinium tetrafluoroborate (<b>NO</b>) Electron acceptor</p>
<p style="text-align: center;">Electron donor</p> <p style="text-align: center;">2-Ethyl-2-(hydroxymethyl)-1,3-propanediol triacrylate (<b>TMPTA</b>)</p>	<p style="text-align: center;">Pentaerythritol triacrylate (<b>PETA</b>)</p>	<p style="text-align: center;">1,6-Hexanediol diacrylate (<b>HDDA</b>)</p>

1,3-bis(*p*-bromophenylamino)squaraine is quenched. The results obtained from fluorescence quenching experiments were analyzed with use the Stern–Volmer relationship eqn (3).

$$\frac{I}{I_0} = 1 + K_{SV}[Q] = 1 + k_q\tau[Q] \quad (3)$$

where:  $I_0$  and  $I$  are the fluorescence intensities of squarylium dye in absence and presence of quencher, respectively;  $K_{SV}$  is the Stern–Volmer constant, characterized the collision interaction of quencher molecules ( $Q$ ) with the excited state of fluorophore,  $k_q$  is the quenching rate constant.

From the fluorescence lifetime  $\tau$  and the slope of the linear relationship of Stern–Volmer plot (Fig. 3 right), one can calculate the  $k_q$  value.

As it was previously observed for other squaraine,<sup>36</sup> the rate of dynamic quenching of the excited singlet state depends on the type of quencher used. From the data presented in Fig. 3, it is seen the linear relationship between changes in the fluorescence lifetime and concentration of quencher. The slopes of Stern–Volmer linear relationship are as follows: 473.24, 398.33, and 328.92 for (**B2**), (**I1**) and (**NO**), respectively. From Stern–Volmer equation plot, the rate constants of fluorescence quenching reaction were obtained to be  $8.19 \times 10^{10} \text{ M}^{-1} \text{ s}^{-1}$ ,  $6.89 \times 10^{10} \text{ M}^{-1} \text{ s}^{-1}$  and  $5.69 \times 10^{10} \text{ M}^{-1} \text{ s}^{-1}$  for (**B2**), (**I1**) and (**I2**), respectively, which are nearly one order of magnitude larger than that of diffusion controlled bimolecular reaction constant ( $\sim 2 \times 10^9 \text{ M}^{-1} \text{ s}^{-1}$ ).

These results confirmed that the coinitiators under study are very effective fluorescence quenchers for excited (**SQ**) dye and the fast quenching occurs predominantly through the intramolecular ion-pair pathway.

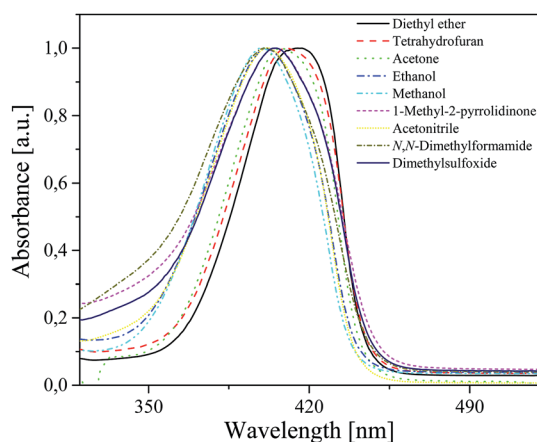


Fig. 1 The electronic absorption spectra of 1,3-bis(*p*-bromophenylamino)squaraine recorded at room temperature in solvents of different polarity.

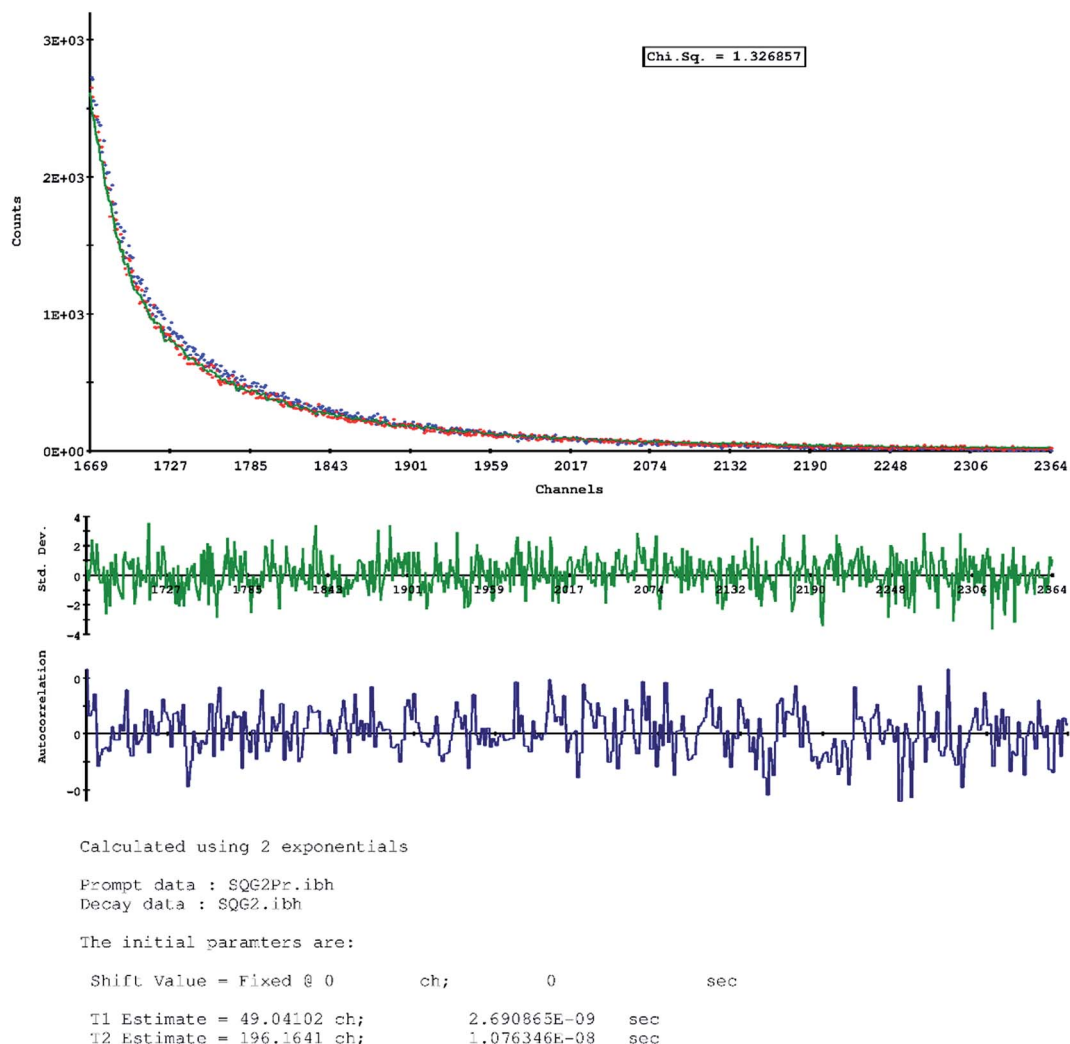


Fig. 2 The fluorescence decay recorded for 1,3-bis(*p*-bromophenylamino)squaraine in 1-methyl-2-pyrrolidinone as a solvent,  $\lambda_{\text{EX}}$  370 nm.

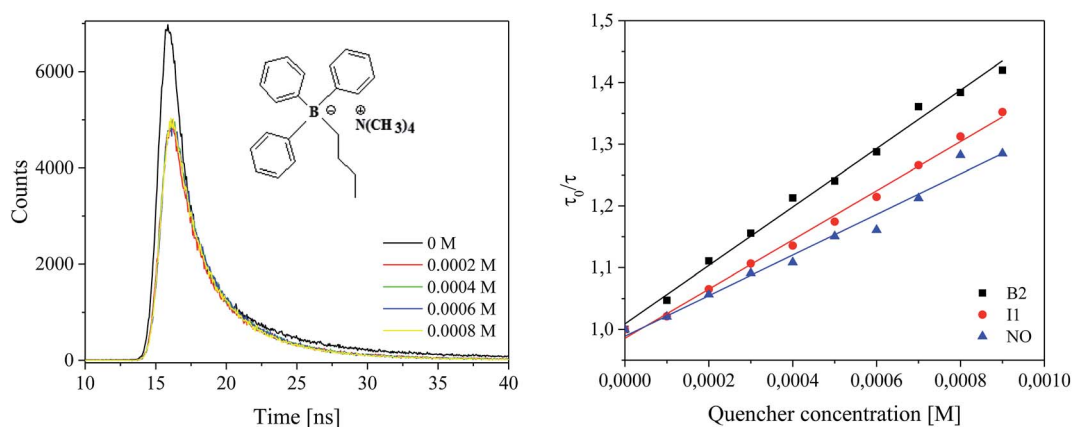


Fig. 3 Left: The effect of tetramethylammonium *n*-butyltriphenylborate (B2) on the fluorescence lifetime of 1,3-bis(*p*-bromophenylamino)squaraine in 1-methyl-2-pyrrolidinone as a solvent. Right: The Stern–Volmer plots for the quenching of fluorescence of 1,3-bis(*p*-bromophenylamino)squaraine by borate salt (B2), diphenyliodonium salt (I1) and *N*-alkoxy pyridinium salt (NO), respectively.

The influence of borate salt, iodonium salt and *N*-alkoxy pyridinium salt on the rate of fluorescence decay of dye suggests that the primary photoreaction occurs between the dye

and coinitiator in ground state. This phenomena may be a result of photoinduced electron transfer process occurred between excited dye molecule and quencher in ground state.

During photoinduced electron-transfer process squaraine may act as an electron donor or an electron acceptor depending on the electrochemical properties of both dye and quencher.

In conclusion, owing to the energy of excited (**SQ**) dye lower than that of borate and all coinitiators used, the energy transfer from excited (**SQ**) to coinitiator is impossible. Therefore, it is reasonable to consider that upon irradiation the photoinduced electron transfer reaction between excited squaraine dye and coinitiator occurs *via* intramolecular pathway, which has a large reaction rate as fluorescence quenching experiments described above.

### 3.2. Electrochemical measurements

In order to confirm, that the primary photochemical process in photoinitiating systems studied is an electron transfer, the redox properties of all components of photoinitiator were studied by cyclic voltammetry. In order to estimate thermodynamically, the activity of the squaraine dye/borate salt, squaraine dye/iodonium salt and squaraine dye/*N*-alkoxy pyridinium salt photoreaction, the values of free energy change ( $\Delta G_{el}$ ) for an electron transfer reaction were calculated according to the Rehm-Weller equation, eqn (4).<sup>39</sup>

$$\Delta G_{el} = E_{ox}(D^{+}/D) - E_{red}(A/A^{-}) - Ze^2/\epsilon a - E_{00} \quad (4)$$

in which  $E_{ox}(D^{+}/D)$  is the oxidation potential of an electron donor molecule,  $E_{red}(A/A^{-})$  is the reduction potential of electron acceptor,  $Ze^2/\epsilon a$  is the coulombic energy, normally considered negligible in high-dielectric solvents, and  $E_{00}$  is the singlet energy of the squaraine dye.

It should be noted, that in photoinitiator systems under study, the photoreducible and photooxidizable sensitization occurs. Therefore, photoexcited dye may act as an electron acceptor or an electron donor. In a case of tetramethylammonium *n*-butyltriphenylborate, the squaraine plays a role of an electron acceptor. On the other hand, squaraine dye acts as an electron donor for diphenyliodonium salt and *N*-alkoxy pyridinium salt.

For the calculation of the value of free energy change for electron transfer process the both oxidation and reduction potentials of photosensitizer must be measured. To establish the redox properties of squaraine, we used cyclic voltammetry experiment.

The electrochemical oxidation of several symmetrical squaraine dyes has been investigated earlier by Law and co-workers.<sup>40</sup> Most of squaraines exhibit two reversible oxidations, and their oxidation potentials are influenced by type of substituent.<sup>41</sup> Dye (**SQ**) exhibits only one very weak irreversible oxidation peak at 1.24 eV and reduction peak at -0.252 eV, in acetonitrile. The cyclic voltammogram of this dye is shown in Fig. 4.

The higher value of oxidation potential than that observed for other squaraine dyes<sup>32</sup> reflects a decrease in the charge-transfer character of the molecule due to the presence of zwitterionic structure of dye.

The singlet excited-state energy ( $E_{00}$ ) for 1,3-bis(*p*-bromophenylamino)squaraine was determined from the crossover

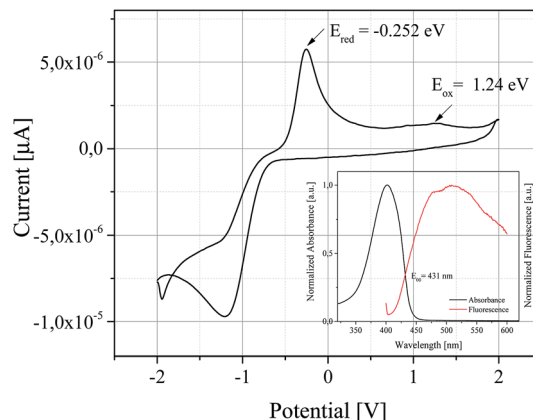


Fig. 4 Cyclic voltammograms of 1,3-bis(*p*-bromophenylamino)squaraine dyes in 0.1 M tetrabutylammonium perchlorate solution in dry acetonitrile as the supporting electrolyte. Inset: the normalized absorption and fluorescence spectra of sensitizer recorded at room temperature in acetonitrile as a solvent.

point between the normalized absorption and emission spectra and equals 2.877 eV for  $^1\text{SQ}^*$ .

Next, the values of free energy change for an electron transfer process were calculated. For this purpose the oxidation potential of 1,3-bis(*p*-bromophenylamino)squaraine ( $E_{ox} = 1.24$  eV) and reduction potentials of diphenyliodonium chloride ( $E_{red} = -0.494$  eV) and *N*-methoxyphenyl-4-phenylpyridinium tetrafluoroborate ( $E_{red} = -0.594$  eV) must be used. The thermodynamic parameters calculated ( $-110.31$  kJ mol<sup>-1</sup> and  $-100.66$  kJ mol<sup>-1</sup>) indicate that both **SQ/II** and **SQ/NO** combination systems possess high driving force,  $\Delta G_{el}$ . In the presence of tetramethylammonium *n*-butyltriphenylborate (**B2**), squaraine dye undergoes photoreduction process. In such a case the reduction potential of dye ( $E_{red} = -0.252$  eV) and the oxidation potential of coinitiator ( $E_{ox} = 1.153$  eV) were used for the calculation of  $\Delta G_{el}$  value, that is equal  $-142.06$  kJ mol<sup>-1</sup>. Negative values of  $\Delta G_{el}$  indicate, that for all photoinitiating systems under study an electron transfer reaction yielding free radicals is thermodynamically allowed.

### 3.3. Kinetics of polymerization of multifunctional acrylates

The polymerization of different monomers, such as: 1,6-hexanediol diacrylate (**HDDA**), pentaerythritol triacrylate (**PETA**), 2-ethyl-2-(hydroxymethyl)-1,3-propanediol triacrylate (**TMPTA**), with photosensitizer (squaraine dye) was performed to examine the efficiency of three different coinitiators, such as tetramethylammonium *n*-butyltriphenylborate (**B2**), diphenyliodonium chloride (**II**) and *N*-methoxy-4-phenylpyridinium tetrafluoroborate (**NO**) in radical polymerization of **HDDA**, **PETA** and **TMPTA** in the presence and absence of active species sources: coinitiators. The photopolymerizations were conducted using light wavelengths in the range from 300 nm to 500 nm and an irradiation intensity of 30 mW cm<sup>-2</sup>.

In order to evaluate the optimum conditions for the polymerization process, the effect of the concentration of photoinitiator on the rate of polymerization process was studied.

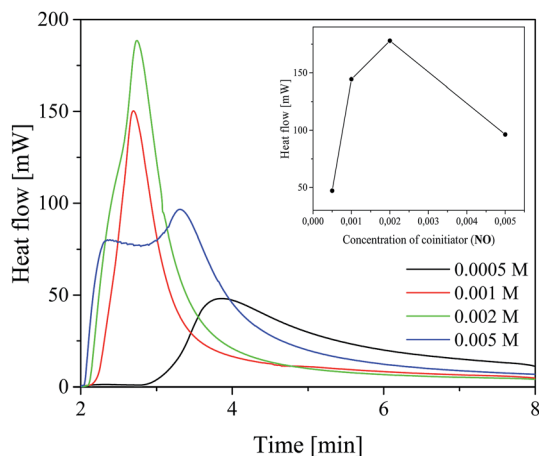


Fig. 5 Time-conversion curves recorded during the polymerization of TMPTA with 1,3-bis(*p*-bromophenylamino)squaraine at  $300 \text{ nm} < \lambda < 500 \text{ nm}$  irradiation in presence of different concentration of *N*-methoxy-*p*-phenylpyridinium tetrafluoroborate (NO) (marked in the figure). Inset: the influence of concentration of coinitiator on the kinetic of polymerization process.

To examine the effect of free radical source concentration on the initiator efficiency, polymerization with different concentration of coinitiator changing from  $5 \times 10^{-4} \text{ M}$  to  $5 \times 10^{-3} \text{ M}$  was done. Fig. 5 shows the kinetics of TMPTA polymerization with squaraine dye in presence of *N*-methoxy-4-phenylpyridinium tetrafluoroborate (NO) at four different concentrations.

The concentration of all components of photoinitiating system has a significant impact on the rate of polymerization. As the concentration of photosensitizer and coinitiator increased from  $5 \times 10^{-4} \text{ M}$  to  $5 \times 10^{-3} \text{ M}$ , the maximum polymerization rate was observed to increase from  $5 \times 10^{-4} \text{ M}$  to  $2 \times 10^{-3} \text{ M}$  in the case of *N*-methoxy-*p*-phenylpyridinium tetrafluoroborate used as coinitiator.

It is well known, that in the conventional UV/Vis photopolymerization,  $R_p$  increases when more initiator is used,

however it decreases rapidly if too much initiator is added. This effect is attributed to the “inter filter effect” and becomes more significant for photoinitiators with high molar extinction coefficient (for squaraine tested,  $\epsilon$  is about  $4 \times 10^4 \text{ dm}^3 \text{ mol}^{-1} \text{ cm}^{-1}$ ).

From the data presented in Fig. 5, it is evident that as the photoinitiator concentration is increasing, the initial rate of polymerization increases and reaches a maximum followed by a continuous mild decrease. For the tested photoinitiators under irradiation conditions the highest rate of polymerization was observed at the photoinitiator concentration of about  $2 \times 10^{-3} \text{ M}$ .

In absence of active species source (coinitiator), the photopolymerization of all monomers studied was carried out with 1,3-bis(*p*-bromophenylamino)squaraine (SQ) ( $5 \times 10^{-3} \text{ M}$ ) at irradiation ranging from 300 nm to 500 nm and no monomer conversion was observed.

Fig. 6–8 show the kinetic curves recorded during photopolymerization of radically polymerizable monomers: 1,6-hexanediol diacrylate (HDDA), pentaerythritol triacrylate (PETA) and 2-ethyl-2-(hydroxymethyl)-1,3-propanediol triacrylate (TMPTA), and, as well as the degree of double bonds conversion as a function of irradiation time.

As it is seen from the kinetic data presented above (Fig. 6–8 and Table 2) the rate of polymerization and degree of double bond conversion depend on the type of monomer and coinitiator. The best kinetic results were achieved for photoinitiator system composed of *N*-methoxy-4-phenylpyridinium tetrafluoroborate (NO) as a coinitiator. The highest efficiency for radical polymerization was observed in the case of two-functional monomer: 1,6-hexanediol diacrylate (HDDA). The radical polymerization of HDDA occurs with the degree of double bond conversion from 24% to 73% and is about two-times higher than that observed for trifunctional monomers: pentaerythritol triacrylate (PETA) and 2-ethyl-2-(hydroxymethyl)-1,3-propanediol triacrylate (TMPTA). The rates of polymerization of HDDA are higher than that achieved for triacrylates and ranging from  $0.6 \text{ mmol s}^{-1}$  to  $11.96 \text{ mmol s}^{-1}$ . The radical

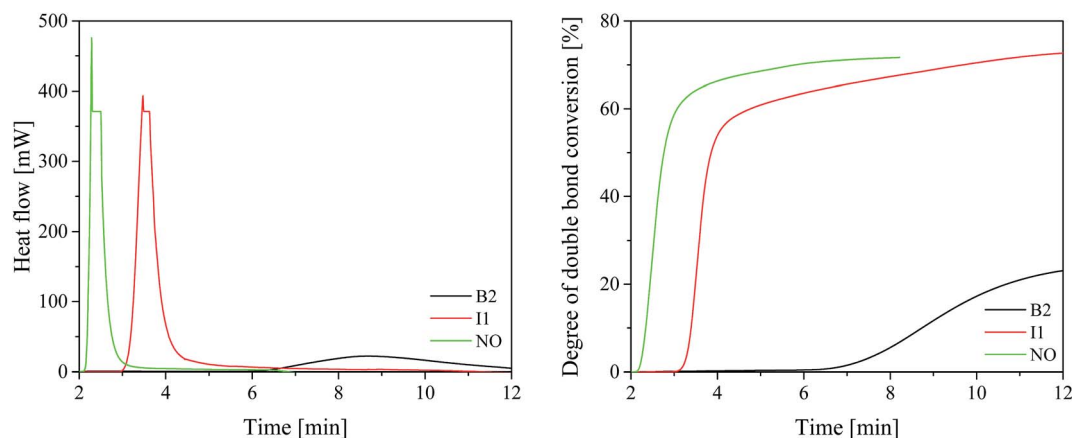


Fig. 6 The kinetic and time-conversion curves recorded during radical polymerization of HDDA initiated by 1,3-bis(*p*-bromophenylamino)squaraine in presence of different coinitiators (marked in the figure) at ambient temperature; [SQ] =  $2 \times 10^{-3} \text{ M}$ ; [coinitiator] =  $2 \times 10^{-3} \text{ M}$ . Light intensity was equal  $30 \text{ mW cm}^{-2}$ .

polymerization of triacrylates occur with the lowest rates for all coiniciators used. The efficiency of photoinitiator system composed of diphenyliodonium chloride (**I1**) to initiation of polymerization of 1,6-hexanediol diacrylate is similar to that observed when *N*-methoxy-4-phenylpyridinium tetrafluoroborate was used as coiniciator. The monomer conversion was achieved values 73.3% and 71.8% for iodonium and *N*-alkoxy-pyridinium salt, respectively.

On the other hand, the lowest efficiency of radical polymerization of all monomers studied was observed for tetramethylammonium *n*-butyltriphenylborate used as coiniciator.

The maximum conversion of **PETA** obtained during the polymerization initiated by squaraine dye in presence of (**B2**), (**I1**) and (**NO**) was found as 23.54%, 27.05% and 45.43%, respectively. The rate of polymerization is about 2 times higher for diphenyliodonium chloride in comparison with borate salt.

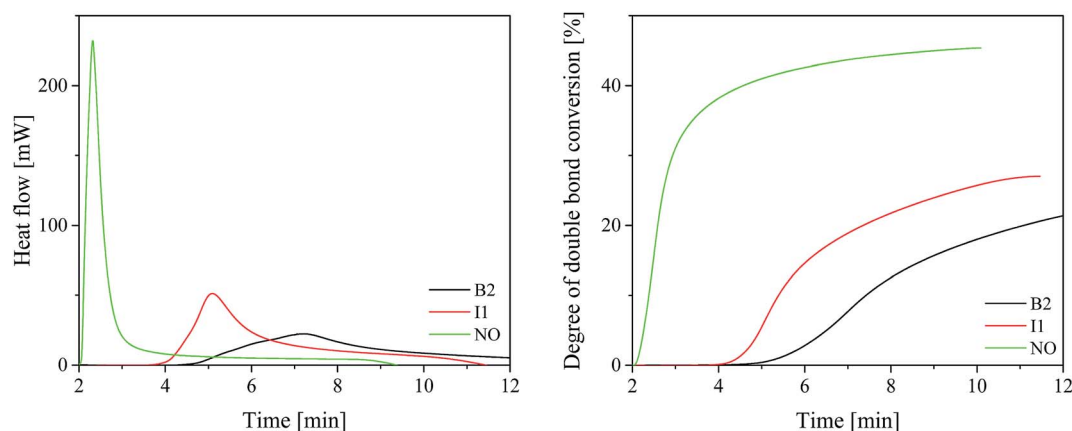


Fig. 7 The kinetic and time-conversion curves recorded during radical polymerization of **PETA** initiated by 1,3-bis(*p*-bromophenylamino) squaraine in presence of different coiniciators (marked in the figure) at ambient temperature;  $[SQ] = 2 \times 10^{-3}$  M;  $[coiniciator] = 2 \times 10^{-3}$  M. Light intensity was equal  $30 \text{ mW cm}^{-2}$ .

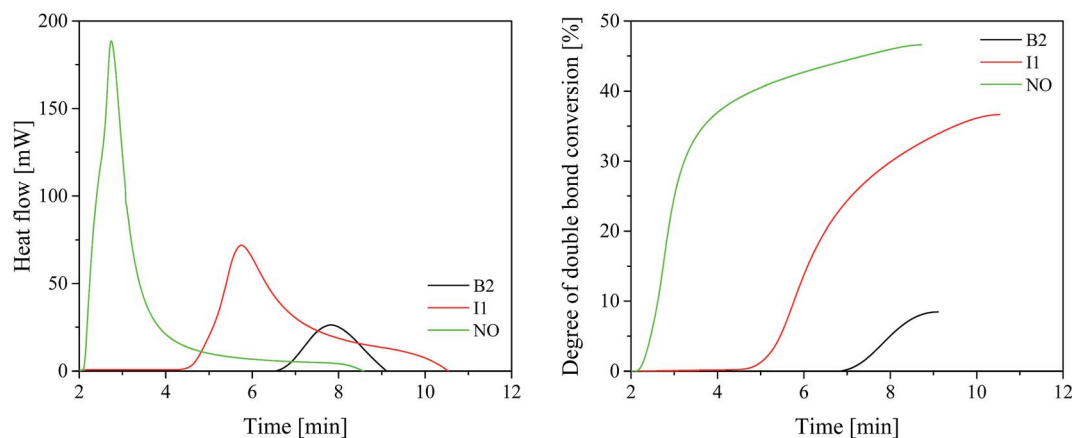


Fig. 8 The kinetic and time-conversion curves recorded during radical polymerization of **TMPTA** initiated by 1,3-bis(*p*-bromophenylamino) squaraine in presence of different coiniciators (marked in the figure) at ambient temperature;  $[SQ] = 2 \times 10^{-3}$  M;  $[coiniciator] = 2 \times 10^{-3}$  M. Light intensity was equal  $30 \text{ mW cm}^{-2}$ .

Table 2 Thermodynamic and kinetic parameters of photoinitiating systems under study

Photoinitiator	HDDA			PETA		TMPTA	
	$\Delta G_{ei}$ [kJ mol <sup>-1</sup> ]	$R_p$ [mmol s <sup>-1</sup> ]	Monomer conversion [%]	$R_p$ [mmol s <sup>-1</sup> ]	Monomer conversion [%]	$R_p$ [mmol s <sup>-1</sup> ]	Monomer conversion [%]
SQ/B2	-142.06	0.6	24.12	1.02	23.54	1.0	6.9
SQ/I1	-110.31	9.90	73.3	2.03	27.05	2.6	36.7
SQ/NO	-100.66	11.96	71.8	9.22	45.43	7.42	47.3

Similar results were obtained in the case of 2-ethyl-2-(hydroxymethyl)-1,3-propanediol triacrylate. The photo-initiating systems possessing *N*-alkoxy-pyridinium salt as an electron acceptor initiate radical polymerization about 7–9 times faster than systems composed of borate salt.

Basing on the kinetic results, the following order of coinitiators activity may be proposed: borate salt (**B2**) > iodonium salt (**I1**) > *N*-methoxy-pyridinium salt (**NO**). This trend can be explained by the difference in the decomposition rate constant and the reactivity of active species formed toward the functional group of monomer.

Therefore, *N*-methoxy-4-phenylpyridinium tetrafluoroborate is relatively more efficient radical source than others to accelerate the rate of polymerization. The higher activity of *N*-alkoxy-pyridinium salts can be explained by high efficiency of alkoxy radicals formation.<sup>42–48</sup>

The different kinetic results obtained may be also related to different properties of monomers used. It should be also noted, that the rate of radical polymerization ranges from 0.6 mmol s<sup>-1</sup> to 11.96 mmol s<sup>-1</sup> and is greater than that obtained for other squaraine dye-based photoinitiating systems composed of 1,3-bis(phenylamino)squaraine and borate salt and diphenyliodonium salts.<sup>27</sup> As it will be show below, the polymerization of radically polymerizable monomers is initiated by butyl, phenyl and methoxy radicals. The differences in photoinitiation ability observed between all coinitiators used may be related to different redox potentials of coinitiators, resulting in different values of free energy change for an electron transfer process.

In next step, for fully demonstration the interest of proposed approach, the photoinitiating ability was compared to commercially available photoinitiators. It is well known, that the photoinitiating ability is highly dependent on the nature of the light source, its intensity and wavelength, as well as on reactivity of the formulation.

For example, 1,6-hexanediol diacrylate (**HDDA**) polymerizes in presence of a initiator: bis(2,4,6-trimethylbenzoyl)phenylphosphine oxide (TMBAPO, Irgacure 819) (0.1% w/w) at light intensity 0.6 mW cm<sup>-2</sup> with total monomer conversion about 12%.<sup>49</sup> **HDDA** under 30 min of UV-irradiation initiated by triaryl sulfonium hexafluoroantimonate salt gives the monomer conversion about 50%.<sup>50</sup> In 2016 Wu and co-workers described the polymerization of 1,6-hexanediol diacrylate initiated by visible light one-component photoinitiating systems composed of 4-[(methyl)-(9-oxo-9*H*-thioxanthen-2-yl)amino]methyl phenyl acrylate. An addition of tertiary amine leads to the 60% of monomer conversion.<sup>51</sup>

The polymerization of pentaerythritoltriacrylate (**PETA**) in presence of bis(2,4,6-trimethylbenzoyl)phenylphosphine oxide as photoinitiator under irradiation of UV LED with emission maximum at 385 nm gives the total monomer conversion about 35% and 60%.<sup>52</sup>

But, the photopolymerization of an trimethylolpropane triacrylate (**TMPTA**) in presence of phosphine oxide as the photoinitiator leads to the 5% of double bond conversion under air and irradiation with Xe lamp.<sup>53</sup> Addition of 3% w/w of tris(trimethylsilyl)silane causes in an increase of conversion about 40% under the same conditions.<sup>53</sup> Monoacylphosphine oxides

such as Speedcure TPO initiates radical polymerization of **TMPTA** under irradiation with LED at 400 nm and light intensity equal 85 mW cm<sup>-2</sup>. The maximum double bond conversion was about 15%.<sup>54</sup> Arsu and co-workers<sup>55</sup> shown that the polymerization of **TMPTA** using BAPO (0.2 wt%) in the absence and presence of 2-mercaptothioxanthone (0.02 wt%), during irradiation with a medium-pressure mercury lamp with a light intensity of 20 mW cm<sup>-2</sup>, occurs with conversion about 30% and 38%, respectively.<sup>55</sup> Shi *et al.* in 2011 described a series of benzophenone-terminated hyperbranched polyester, bearing amine moieties as photoinitiator for radical polymerization of trimethylolpropane triacrylate. The maximal conversion achieved is in range from 44% to 59%.<sup>56</sup> Yang and co-workers studied the kinetics of radical polymerization using UV-lamp (200–400 nm) as a light source whit an intensity 20 mW cm<sup>-2</sup>. The dibenzoyl peroxide does not initiate polymerization of **TMPTA** under these conditions. But application of isopropyl thioxanthone or thioxanthone-based *N*-phthalimidoamino acid ammonium salt as a photoinitiator gives the final conversion about 40% and 83%, respectively.<sup>57</sup> Arsu and co-workers studied an amine linked benzophenone photoinitiator for free radical polymerization of triacrylates.<sup>58</sup> A medium pressure mercury arc lamp (220–400 nm) giving light intensity of 40 mW cm<sup>-2</sup> was used as a light source. The final conversion changes in the range from 12% to 55%.

The kinetic results shown also, that the systems under study initiate polymerization process faster than other squaraine-based photoinitiators. For example, for two-component photoinitiating systems composed of bis(1,2,3,3-tetramethylindolenium-2-ylidene)squaraine or bis(3-methylbenzothiazol-2-ylidene)squaraine, and (*p*-octanoxyphenyl)phenyliodonium salt the maximum double bond conversion of methyl methacrylate is in the range from 10% to 14% after 4 h of irradiation time.<sup>24</sup> But photopolymerization of **TMPTA** in laminate initiated by 1,3,3-trimethylindolenine-based squaraine dye and diphenyliodonium chloride (0.5%/2%, w/w) leads to the conversion of monomer about 40%.<sup>26</sup> When camphorquinone and diphenyliodonium chloride (0.5%/2%, w/w) were used to initiation of **TMPTA** polymerization under halogen lamp as a light source, final monomer conversion obtained in laminate was about 18%.<sup>55</sup> The application of 1,3-bis(phenylamino)squaraine in presence of tetramethylammonium *n*-butyl-triphenylborate for initiation of polymerization of different acrylates leads to the total monomer conversion about 10.5%, 21.6% and 27.3% for **TMPTA**, **PETA** and **HDDA**, respectively. The polymerization of triacrylates initiated by system composed of 1,3-bis(phenylamino)squaraine in presence of diphenyliodonium chloride as a coinitiator leads to about 20% of total monomer conversion using irradiation of high-pressure mercury lamp (300–500 nm) with light intensity 30 mW cm<sup>-2</sup>.<sup>27</sup>

The total conversion obtained for photoinitiating systems under study are about 73.3%, 45.43% and 47.3% for **HDDA**, **PETA** and **TMPTA**, respectively.

### 3.4. Investigation of the initiation mechanism

As it was mentioned above the three different compounds were used as coinitiators in polymerization systems under study.

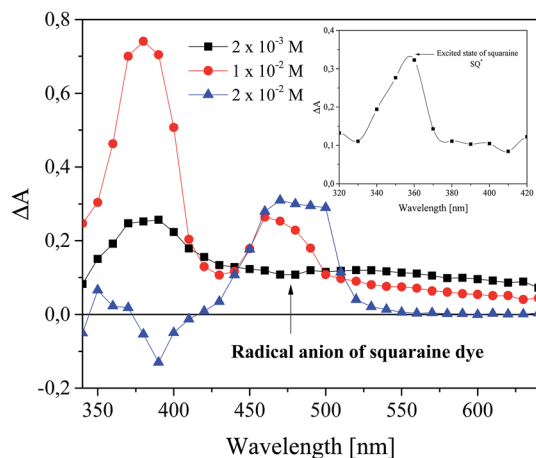


Fig. 9 Transient absorption spectra of 1,3-bis(*p*-bromophenylamino)squaraine in presence of tetramethylammonium *n*-butyltriphenylborate (B2) recorded: 2 ns (squares, circles) and 100 ns (triangles) after laser pulse. Inset: transient absorption spectra of squaraine dye recorded 100 ns after laser pulse (circles) in acetonitrile solution. Coinitiator concentration is marked in the figure.

Therefore, various species are products of primary and secondary photochemical reactions. The initiating radicals (derived from corresponding coinitiators) are different for all photoinitiating systems under study. Taking this into account, the activity of the photoinitiating systems studied depends on the reactivity and the efficiency of initiating radicals formation.

Irradiation of 1,3-bis(*p*-bromophenylamino)squaraine in acetonitrile solution, with 5 ns laser pulse results in instantaneous appearance of its excited state, which is characterized by absorption at 380 nm. The rate constant of excited state formation is equal  $2.48 \times 10^8 \text{ s}^{-1}$ . The time of decay of excited state, and the rate constant of the decay of excited state are about 2.33  $\mu\text{s}$  and  $4.29 \times 10^5 \text{ s}^{-1}$ , respectively. The lifetime of  $\text{SQ}^*$  is decreasing as concentration of borate salt increases. This means, that  $\text{SQ}^*$  is quenched by tetramethylammonium *n*-butyltriphenylborate, and a new transient with absorption at 480–500 nm is simultaneously formed. The new transient can be assigned to radical anion of squaraine dye. At the same time

the disappearance of the band corresponding to the absorption of the dye in the ground state is observed (Fig. 9).

The rate constant,  $k_q$ , for the quenching of the excited state of squaraine dye by borate salt was determined in MeCN solution. The  $k_q$  value was obtained by monitoring the excited state absorption decays of  $\text{SQ}^*$  at 380 nm for various quencher concentrations by employing the Stern–Volmer equation. The established value of this rate constant is equal  $3.31 \times 10^7 \text{ mol}^{-1} \text{ s}^{-1}$ . The time of formation of squaraine dye-based radical anion and its disappearance is equal 10 ns and 1.14  $\mu\text{s}$ , respectively.

The excited state of photosensitizer is also quenching by *N*-methoxy-*p*-phenylpyridinium tetrafluoroborate, as well as diphenyliodonium chloride. In both cases the formation of new absorption band at 480–500 nm is observed. The time of formation of new product and its disappearance is equal 20 ns and 1.47  $\mu\text{s}$ , 14 ns and about 200 ns for *N*-alkoxy-pyridinium salt and diphenyliodonium salt, respectively. New absorption band is attributed to the absorption of squaraine dye-based radical cation formation. Simultaneously the disappearance of the band at 380 nm is observed. The established value of quenching rate constant is equal  $2.31 \times 10^6 \text{ mol}^{-1} \text{ s}^{-1}$ . Fig. 10 shows the kinetic traces recorded at 480 nm for different delay times: 2 ns and 2  $\mu\text{s}$ , that present the formation and disappearance of squaraine dye radical cation.

On the basis of the above experiments, it appears that *n*-butyltriphenylborate anion is oxidized, but *N*-methoxy-*p*-phenylpyridinium cation and diphenyliodonium cation are reduced by excited state of squaraine dye. These reactions yield ground state squaraine dye, *n*-butyltriphenylboranyl radical, *N*-methoxy-*p*-phenylpyridyl radical and diphenyliodonium radical. The radicals formed undergo fast and irreversible fragmentation giving: *n*-butyl radical and triphenylboron, methoxy radical and *p*-phenylpyridinium and phenyl radical and iodobenzene.

Basing on the laser flash photolysis results and thermodynamic parameters for the electron transfer process, one can conclude, that there is the possibility of donating an electron from borate salt to squaraine dye. This process is thermodynamically allowed,  $\Delta G_{\text{el}} = -142 \text{ kJ mol}^{-1}$ . On the other hand the squaraine dye studied can also act as an electron donor for

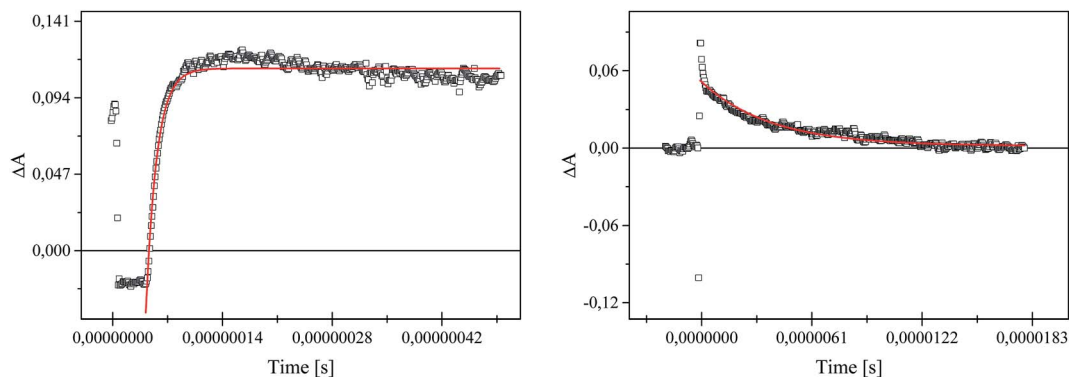


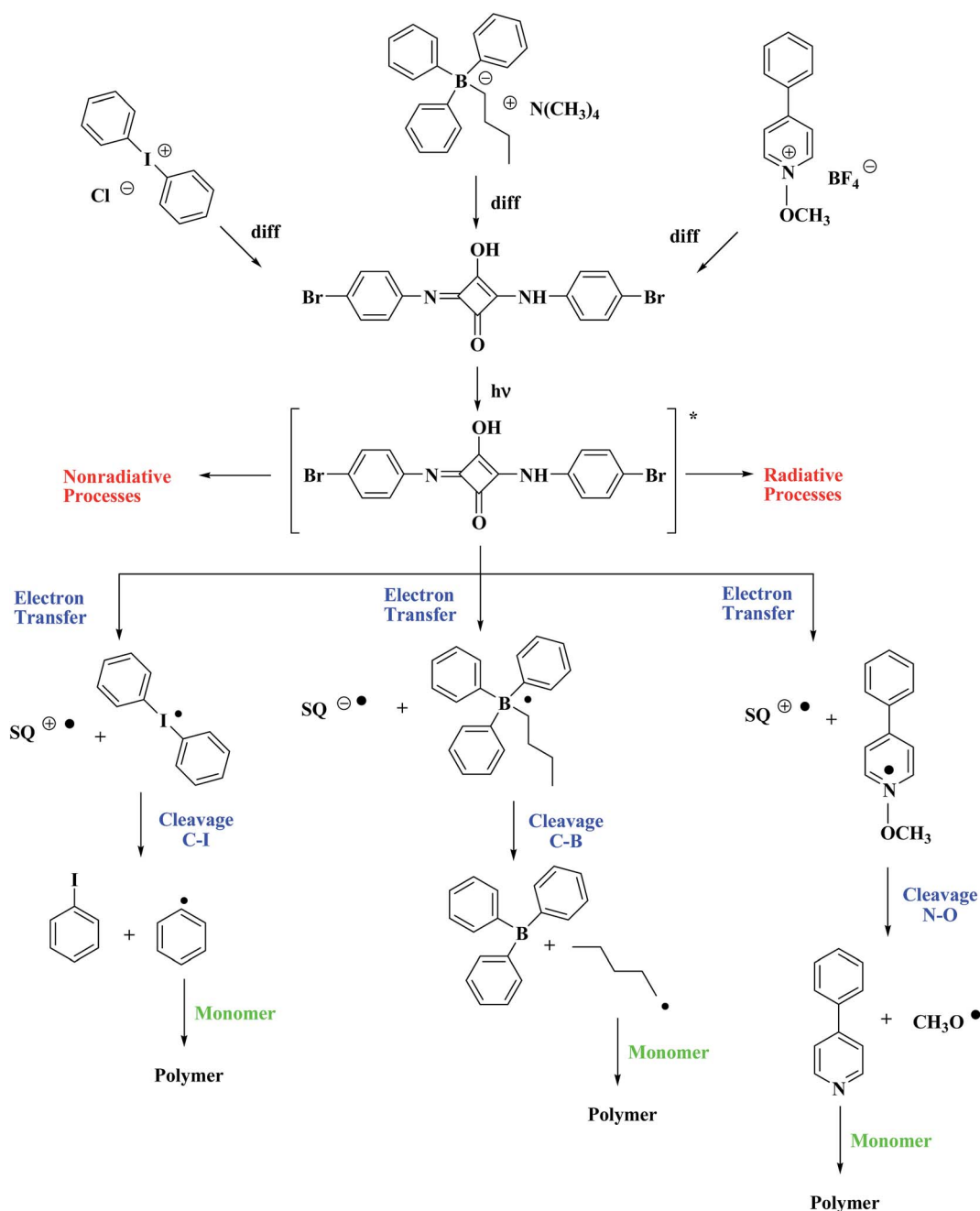
Fig. 10 The kinetic traces recorded at 480 nm for different delay times: 2 ns and 2  $\mu\text{s}$  observed after irradiation of 1,3-bis(*p*-bromophenylamino)squaraine in presence of *N*-methoxy-*p*-phenylpyridinium tetrafluoroborate. Coinitiator concentration was  $5 \times 10^{-4} \text{ M}$ .

both onium salts studied. In summary, photoinitiating systems studied may act *via* photoreducible or photooxidizable mechanism.

On the basis of the nanosecond laser flash photolysis and the thermodynamical analysis presented in this paper, the following mechanism for the primary and secondary reactions was proposed (Scheme 1) for sensitized generation of free radicals.

After irradiation of the photoinitiating system with a visible light, the excited state of squaraine ( $SQ^*$ ) is formed. The deactivation of excited state occurs by radiative and nonradiative processes. One of the nonradiative processes is an electron transfer. In presence of borate salts the squaraine dye

undergoes one-electron reduction. The dye radical anion and boranyl radical are formed. The boranyl radical undergoes carbon–boron bond cleavage, giving a butyl radical that can start the polymerization reaction. However, in the presence of diphenyliodonium salt or *N*-methoxy-*p*-phenylpyridinium salt, an electron transfer from the excited state of squaraine dye to the ground state of onium salts occurs, giving squaraine radical cation and diphenyliodonium radical or *N*-methoxy-*p*-phenylpyridinium radical. The lasts undergo fast fragmentation as a result of carbon–iodide or nitrogen–oxygen bond cleavage, forming the iodobenzene and phenyl radical or *p*-phenylpyridinium and methoxy radical.



**Scheme 1** The primary and secondary processes occurring in the photoinitiating systems under study after irradiation with visible light.

## 4. Conclusions

In this paper, the efficiency of visible light induced polymerization of multifunctional acrylates in the presence of two-component photoinitiating systems based on squaraine dye and tetramethylammonium *n*-butyltriphenylborate, diphenyliodonium chloride and *N*-methoxy-*p*-phenylpyridinium tetrafluoroborate was ascertained.

1,3-Bis(*p*-bromophenylamino)squaraine could successfully initiate photopolymerization of 1,6-hexanediol diacrylate (HDDA), trimethylolpropane triacrylate (TMPTA) and pentaerythritol triacrylate (PETA) under high-pressure mercury lamp light exposure (300 nm <  $\lambda$  < 500 nm) in the presence of *N*-methoxy-4-phenylpyridinium tetrafluoroborate, diphenyliodonium chloride and tetramethylammonium *n*-butyltriphenylborate. The best photoinitiating ability was observed for photoinitiator composed of squaraine dye as a photosensitizer and *N*-methoxy-*p*-phenylpyridinium tetrafluoroborate as a coinitiator. The rate of polymerization depends on the type of coinitiator and type of monomer. The highest values of monomer conversion were observed for diacrylate monomer polymerization. The max values reached above 73%.

Basing on the kinetic results and the laser flash photolysis experiment the mechanism of reactions occurring in new photoinitiating system composed of squaraine dye was proposed. The free radicals formation involves both, an electron transfer from borate salt to the dye and an electron transfer from dye to onium salt, as the primary photochemical reactions. Borate salt is an electron donor reducing dye, but diphenyliodonium salt and *N*-alkoxy-pyridinium salt are the electron acceptor oxidizing the excited dye. These reactions generate free radicals, which can start the polymerization chain reaction *via* photoreducible or photooxidizable series mechanism.

## Acknowledgements

This work was supported by The National Science Centre (NCN) (Cracow, Poland), Grant No. 2013/11/B/ST5/01281.

## References

- 1 M. L. Gómez, C. M. Previtali and H. A. Montejano, *Int. J. Photoenergy*, 2012, 1–9.
- 2 H. J. Timpe, K. P. Kronfeld, U. Lammel, J. P. Fouassier and D. J. Loughnot, *J. Photochem. Photobiol., A*, 1990, **52**, 111–122.
- 3 A. Kunze, U. Müller, K. Titles, J. P. Fouassier and F. Morlet-Savary, *J. Photochem. Photobiol., A*, 1997, **110**, 115–122.
- 4 T. Brömme, D. Oprych, J. Horst, P. S. Pinto and B. Strehmel, *RSC Adv.*, 2015, **5**, 69915–69924.
- 5 J. Kabatc, M. Pietrzak and J. Pączkowski, *Macromolecules*, 1998, **31**, 4651–4654.
- 6 J. P. Fouassier, D. Ruhlmann, Y. Takimoto, M. Harada and M. Kawabata, *J. Polym. Sci., Part A: Polym. Chem.*, 1993, **31**, 2245–2248.
- 7 A. Erddalane, J. P. Fouassier, F. Morlet-Savary and Y. Takimoto, *J. Polym. Sci., Part A: Polym. Chem.*, 1996, **34**, 633–642.
- 8 T. G. Yildirim, Y. Hepuzer, G. Hizal and Y. Yağci, *Polymer*, 1999, **40**, 3885–3890.
- 9 S. Dadashu-Silab, S. Doran and Y. Yağci, *Chem. Rev.*, 2016, **40**, 10212–10275.
- 10 N. Carrigan, S. Shanmugan, J. Xu and C. Boyer, *Chem. Soc. Rev.*, 2016, DOI: 10.1039/c6cs00185h.
- 11 A. Vitale, M. Sangermano, R. Bongiovanni, P. Burtscher and N. Moszner, *Materials*, 2014, **7**, 554–562.
- 12 M. A. Tehfe, J. Lalevée, F. Morlet-Savary, B. Graff, N. Blanchard and J. P. Fouassier, *ACS Macro Lett.*, 2012, **1**, 198–203.
- 13 M. A. Tehfe, F. Dumur, E. Contal, B. Graff, F. Morlet-Savary, D. Gigmes, J. P. Fouassier and J. Lalevée, *Polym. Chem.*, 2013, **4**, 1625–1634.
- 14 M. A. Tehfe, F. Dumur, B. Graff, D. Gigmes, J. P. Fouassier and J. Lalevée, *Macromolecules*, 2013, **46**, 3332–3341.
- 15 R. Podsiadły and R. Strzelczyk, *Dyes Pigm.*, 2013, **97**, 462–468.
- 16 M. A. Tehfe, F. Dumur, B. Graff, F. Morlet-Savary, D. Gigmes, J. P. Fouassier and J. Lalevée, *Polym. Chem.*, 2013, **4**, 3866–3875.
- 17 M. A. Tehfe, F. Dumur, P. Xiao, M. Delgove, B. Graff, J. P. Fouassier, D. Gigmes and J. Lalevée, *Polym. Chem.*, 2014, **5**, 382–390.
- 18 P. Xiao, F. Dumur, M. A. Tehfe, B. Graff, D. Gigmes, J. P. Fouassier and J. Lalevée, *Macromol. Chem. Phys.*, 2013, **214**, 2276–2282.
- 19 P. Xiao, F. Dumur, B. Graff, D. Gigmes, J. P. Fouassier and J. Lalevée, *Macromolecules*, 2014, **47**, 601–608.
- 20 P. Xiao, W. Hong, Y. Li, F. Dumur, B. Graff, J. P. Fouassier, D. Gigmes and J. Lalevée, *Polymer*, 2014, **55**, 746–751.
- 21 P. Xiao, W. Hong, Y. Li, F. Dumur, B. Graff, J. P. Fouassier, D. Gigmes and J. Lalevée, *Polym. Chem.*, 2014, **5**, 2293–2300.
- 22 M. A. Tehfe, D. Gigmes, F. Dumur, D. Bertin, F. Morlet-Savary, B. Graff, J. Lalevée and J. P. Fouassier, *Polym. Chem.*, 2012, **3**, 1899–1902.
- 23 M. A. Tehfe, J. Lalevée, F. Morlet-Savary, B. Graff and J. P. Fouassier, *Macromolecules*, 2011, **44**, 8374–8379.
- 24 Y. He, W. Zhou, F. Wu, M. Li and E. Wang, *J. Photochem. Photobiol., A*, 2004, **162**, 463–471.
- 25 P. Xiao, J. Zhanga, F. Dumur, M. A. Tehfe, F. Morlet-Savary, B. Graff, D. Gigmes, J. P. Fouassier and J. Lalevée, *Prog. Polym. Sci.*, 2015, **41**, 32–66.
- 26 P. Xiao, F. Dumur, T. T. Bui, F. Goubard, B. Graff, F. Morlet-Savary, J. P. Fouassier, D. Gigmes and J. Lalevée, *ACS Macro Lett.*, 2013, **2**, 736–740.
- 27 J. Kabatc, K. Kostrzewska and K. Jurek, *RSC Adv.*, 2016, **6**, 74715–74725.
- 28 R. Damincio, *J. Org. Chem.*, 1964, **29**, 1971–1976.
- 29 S.-Y. Park, K. Jun and S.-W. Oh, *Bull. Korean Chem. Soc.*, 2005, **26**, 428–432.
- 30 H. Junek, A. Hermetter, H. F. Colbrrie and H. Aigner, *Tetrahedron Lett.*, 1973, **14**, 2993–2996.
- 31 L. Hu, Z. Yan and H. Xu, *RSC Adv.*, 2013, **3**, 7667–7676.
- 32 A. Wójcik, R. Nicolaescu and P. V. Kamat, *J. Phys. Chem. A*, 2011, **114**, 2744–2750.
- 33 S. Das, T. L. Thanulingam, K. G. Thomas, P. V. Kamat and M. V. George, *J. Phys. Chem.*, 1993, **97**, 13620–13625.

- 34 S. Das, K. G. Thomas, K. J. Thomas, P. V. Kamat and M. V. George, *J. Phys. Chem.*, 1994, **98**, 9291–9296.
- 35 S. Alex, M. C. Basheer, K. T. Arun, D. Ramaiah and S. Das, *J. Phys. Chem. A*, 2007, **111**, 3226–3230.
- 36 J. Kabatc, K. Kostrzewska, K. Jurek, R. Dobosz and Ł. Orzeł, *Dyes Pigm.*, 2016, **127**, 179–186.
- 37 Y. Yağci, S. Jockusch and N. J. Turro, *Macromolecules*, 2010, **43**, 6245–6260.
- 38 S. Deniizligil, Y. Yağci and C. MacArdle, *Polymer*, 1995, **36**, 3093–3098.
- 39 D. Rehm and A. Weller, *Isr. J. Chem.*, 1970, **8**, 259.
- 40 K.-Y. Law, J. S. Facci, F. C. Balley and J. F. Yanus, *J. Imaging Sci.*, 1990, **34**, 31.
- 41 G. Sauve, P. V. Kamat, K. G. Thomas, K. J. Thomas, S. Das and M. V. George, *J. Phys. Chem.*, 1996, **100**, 2117–2124.
- 42 Y. Yağci, A. Kornowski and W. Schnabel, *J. Polym. Sci., Part A: Polym. Chem.*, 1992, **30**, 1987–1991.
- 43 P. Monecke, W. Schnabel and Y. Yağci, *Polymer*, 1997, **38**, 5389–5395.
- 44 J. Kabatc and J. Pączkowski, *Macromolecules*, 2005, **38**, 9985–9992.
- 45 J. Kabatc and J. Pączkowski, *Polymer*, 2006, **47**, 2699–2705.
- 46 J. Kabatc and J. Pączkowski, *J. Photochem. Photobiol., A*, 2006, **184**, 184–192.
- 47 E. D. Lorance, W. H. Kramer and I. R. Gould, *J. Am. Chem. Soc.*, 2004, **126**, 14071–14078.
- 48 R. Podsiadły, *J. Photochem. Photobiol., A*, 2008, **198**, 60–68.
- 49 C. Peinado, A. Alonso, E. F. Salvador, J. Baselga and F. Catalina, *Polymer*, 2002, **43**, 5355–5361.
- 50 T. H. Chiang and T.-E. Hsieh, *Int. J. Adhes. Adhes.*, 2006, **26**, 520–531.
- 51 Q. Wu, X. Wang, Y. Xiong, J. Yanga and H. Tang, *RSC Adv.*, 2016, **6**, 66098–66107.
- 52 B. Jašúrek, P. Michal, J. Vališ and O. Škola, *Photopolymerization of acrylate monomers induce by UV-LED*, RadTech, 2015.
- 53 Y. Hua and J. V. Crivello, *Macromolecules*, 2001, **34**, 2488–2494.
- 54 M. A. Tehfe, F. Louradour, J. Lalevée and J. P. Fouassier, *Appl. Sci.*, 2013, **3**, 490–514.
- 55 G. Temel, B. Enginol, M. Aydin, D. K. Balta and N. Arsu, *J. Photochem. Photobiol., A*, 2011, **219**, 26–31.
- 56 L. Hu, A. Asif, J. Xie and W. Shi, *Polym. Adv. Technol.*, 2011, **22**, 1673–1680.
- 57 W. Wu, P. Yang, L. Ma, J. Lalevée and J. Zhao, *Eur. J. Inorg. Chem.*, 2013, **2013**, 228–231.
- 58 S. Keskin, S. Jockusch, N. J. Turro and N. Arsu, *Macromolecules*, 2008, **41**, 4631–4634.

**Publikacja naukowa [A2]**

## ***N-Alkoxynium salts as coiniciators in radical polymerization sensitized with squaraine dye after irradiation with UV-visible light***

# **Sole N-alkoksonionowe jako koinicjatory w procesie polimeryzacji rodnikowej sensybilizowanej przez barwnik skwarynowy w zakresie światła UV-Vis**

DOI: 10.15199/62.2017.7.XX

Six N-alkoxyppyridinium salts were synthesized, identified and used together with 1,3-bis(4-bromophenylamino) squaraine as coiniciators in 2-component photoinitiating systems for radical polymerization of HOCH<sub>2</sub>CHEt(CH<sub>2</sub>OH)<sub>2</sub> triacrylate at 25°C and light intensity 30 mW/cm<sup>2</sup> (wave length 300–500 nm) to det. the kinetics of photopolymerization. The 2-component systems squaraine dye/N-alkoxyppyridinium salts were found very efficient for initiation of the radical polymerization.

Sole N-alkoksonionowe zastosowano jako koinicjatory w dwuskładnikowych układach inicjujących polimeryzację rodnikową triakrylanu 2-etylo-2-hydroxymetylo-1,3-propanodiolu (TMPTA). Zbadano wpływ składu układów fotoinicjujących zawierających barwnik skwarynowy na kinetykę procesu fotopolimeryzacji triakrylanu trimetylolopropanu. Opisano syntezy koinicjatorów oraz spektroskopowe

właściwości fotoinicjatorów. Stwierdzono, że dwuskładnikowe układy barwnik skwarynowy/sól N-alkoksyperydyniowa mogą być stosowane jako efektywne układy inicjujące polimeryzację rodnikową w zakresie promieniowania UV-Vis.

Proces polimeryzacji rodnikowej inicjowany promieniowaniem UV-Vis jest powszechnie stosowany do sieciowania monomerów, takich jak akrylany, metakrylany i epoksydy<sup>1)</sup>. Ze względu na wiele zalet fotopolimeryzację wykorzystuje się w różnych gałęziach przemysłu. Proces ten umożliwia m.in. utwardzanie wypełnień stomatologicznych, produkcję powłok ochronnych i dekoracyjnych, farb drukarskich oraz klejów<sup>2,3)</sup>.

Warunkiem inicjowania polimeryzacji rodnikowej jest obecność w mieszaninie polimeryzującej fotoinicjatorów stanowiących źródło rodników<sup>4)</sup>. W wyniku działania promieniowania nadfioletowego związku te ulegają fotodysocjacji tworząc cząstki reaktywne. Powszechnie wiadomo, że promieniowanie UV przy



Mgr inż. Katarzyna KOSTRZEWSKA w roku 2012 ukończyła studia na Wydziale Technologii i Inżynierii Chemicznej Uniwersytetu Technologiczno-Przyrodniczego im. Jana i Jędrzeja Śniadeckich w Bydgoszczy. Obecnie jest samodzielnym chemikiem w Zakładzie Chemii Organicznej tej uczelni. Specjalność – technologia chemiczna.

\* Autor do korespondencji:

Zakład Chemii Organicznej, Wydział Technologii i Inżynierii Chemicznej, Uniwersytet Technologiczno-Przyrodniczy im. Jana i Jędrzeja Śniadeckich, ul. Seminaryjna 3, 85-326 Bydgoszcz, tel.: (52) 374-90-64, fax: (52) 374-90-05, e-mail: katarzyna.kostrzewska@utp.edu.pl



Inż. Alicja BALCERAK jest studentką II roku studiów magisterskich na Wydziale Technologii i Inżynierii Chemicznej Uniwersytetu Technologiczno-Przyrodniczego im. Jana i Jędrzeja Śniadeckich w Bydgoszczy. W 2016 r. uzyskała stopień inżyniera na tym samym wydziale. Specjalność – analityka chemiczna i spożywcza, technologia procesów chemicznych.

większych dawkach niekorzystnie wpływa na organizm ludzki. Z tego względu tak ważne są prace nad układami inicjującymi fotopolimeryzację w zakresie światła widzialnego. Jest to możliwe dzięki zastosowaniu odpowiedniego barwnika jako sensybilizatora przesuwającego czułość układu fotoinicjującego w kierunku fal dłuższych<sup>5-7</sup>. Do grupy takich barwników należą skwaryny, które są pochodnymi 1,2-dihydroscykllobuten-3,4-dionu zwanego kwasem kwadratowym. Związki te otrzymuje się albo przez kondensację kwasu kwadratowego z bogatymi w elektrony aromatycznymi lub heterocyklicznymi zasadami metylenowymi albo etapami przez wprowadzenie do szkieletu kwasu kwadratowego związków aromatycznych lub heterocyklicznych poprzez dialkylskwarynę lub dichlorok skwaryny<sup>8</sup>.

Istnieje wiele komercyjnie dostępnych koinicjatorów inicjujących zarówno polimeryzację rodnikową, jak i kationową. Nadal jednak poszukiwane są związki pozwalające uzyskać coraz lepsze parametry procesu polimeryzacji. Do takiej grupy związków należą sole *N*-alkoksoniowe. W literaturze opisano zastosowanie tych soli w procesie polimeryzacji kationowej<sup>9, 10</sup>, a w przypadku inicjowania procesu polimeryzacji rodnikowej opisano dotychczas układy, w skład których wchodził komercyjnie dostępny tetrafluoroboran *N*-metoksy-4-fenylopirydyniowy oraz tetrafluoroboran *N,N'*-dietoksy-2,2'-bipirydylowy<sup>11-13</sup>.

## Część doświadczalna

### Materiały

Do syntezy soli *N*-alkoksoniowych (NO1–NO5) zastosowano tetrafluoroboran trimetylooksoniowy, *N*-tlenek 4-cyjanopirydyny, *N*-tlenek izochinolinoliny, *N*-tlenek chinolinoliny, *N,N'*-ditlenek 4,4'-bipirydylu i heksafluorofosforan trietylooksoniowy. Ponadto wykorzystano dichlorometan, acetonitryl, chloroform, metanol i 1-metylo-2-pirolidon jak rozpuszczalniki. Wszystkie reagenty, rozpuszczalniki, tetrafluoroboran *N*-metoksy-4-fenylopirydyny (NO) oraz triakrylan 2-etylo-2-(hydroksymetylo)-1,3-propanodiolu (TMPTA) zakupiono w firmie Aldrich (Polska).

### Syntezy

Barwnik skwarynowy 1,3-bis(4-bromofenyloamino)skwaryna (SQ) otrzymano przez kondensację kwasu kwadratowego i 4-bromoaniliny wg metody opisanej w literaturze<sup>14, 15</sup>.

**Tetrafluoroboran *N*-metoksy-4-cyjanopirydyny (NO1)** otrzymano w reakcji tetrafluoroboranu trimetylooksoniowego (1 mmol) i *N*-tlenku 4-cyjanopirydyny (1 mmol) prowadzonej w temperaturze wrzenia dichlorometanu w atmosferze gazu obojętnego przez 4 h. Związek NO1 to białe ciało stałe o temp. topnienia 101°C. Otrzymano 0,4 g NO1, co odpowiada wydajności reakcji 39,09%. <sup>1</sup>H NMR (DMSO-*d*<sub>6</sub>),  $\delta$  (ppm): 4,4898 (s, 3H, CH<sub>3</sub>); 8,8502–8,8807 (dt, 2H, Ar); 9,7766–9,8072 (dt, 2H, Ar). <sup>13</sup>C NMR (DMSO-*d*<sub>6</sub>),  $\delta$  (ppm): 70 (CH<sub>3</sub>); 115 (C); 126 (C); 130 (CH); 133 (CH); 141 (CH); 143 (CH).

**Tetrafluoroboran *N*-metoksyizochinolinoliny (NO2)** otrzymano w reakcji tetrafluoroboranu trimetylooksoniowego (7,6 mmol) i *N*-tlenku izochinolinoliny (6,9 mmol) prowadzonej w temperaturze

wrzenia dichlorometanu w atmosferze gazu obojętnego przez 4 h. Sól NO2 to białe ciało stałe o temp. topnienia 61°C. Otrzymano 1,32 g NO2. Wydajność reakcji wyniosła 77,56%. <sup>1</sup>H NMR (DMSO-*d*<sub>6</sub>),  $\delta$  (ppm): 4,5270 (s, 3H, CH<sub>3</sub>); 8,1127–8,1536 (m, 1H, Ar); 8,2771–8,3184 (m, 1H, Ar); 8,4016–8,4216 (d, *J* ≈ 8 Hz, 1H, Ar); 8,5014–8,5221 (d, *J* ≈ 8,25 Hz, 1H, Ar); 8,7100–8,7280 (d, *J* ≈ 7,2 Hz, 1H, Ar); 9,1502–9,1736 (dd, 1H, Ar); 10,4920–10,4973 (d, Hz, 1H, Ar). <sup>13</sup>C NMR (DMSO-*d*<sub>6</sub>),  $\delta$  (ppm): 70 (CH<sub>3</sub>); 128 (CH); 128 (C); 128 (CH); 131 (CH); 132 (CH); 132 (CH); 137 (C); 137 (CH); 145 (CH).

**Tetrafluoroboran *N*-metoksychinolinoliny (NO3)** otrzymano w reakcji tetrafluoroboranu trimetylooksoniowego (1 mmol) i *N*-tlenku chinolinoliny (1 mmol) prowadzonej w temperaturze wrzenia dichlorometanu w atmosferze gazu obojętnego przez 4 h. Związek NO3 to białe ciało stałe o temp. topnienia 96°C. Otrzymano 0,41 g NO3. Wydajność reakcji była równa 26,45%. <sup>1</sup>H NMR (DMSO-*d*<sub>6</sub>),  $\delta$  (ppm): 4,5568 (s, 3H, CH<sub>3</sub>); 8,1045–8,1451 (m, 1H, Ar); 8,2540–8,2906 (m, 1H, Ar); 8,3346–8,3776 (m, 1H, Ar); 8,5506–8,5837 (m, 2H, Ar); 9,3058–9,3267 (d, *J* ≈ 8,36 Hz, 1H, Ar); 9,9977–10,0163 (dd, 1H, Ar). <sup>13</sup>C NMR (DMSO-*d*<sub>6</sub>),  $\delta$  (ppm): 70 (CH<sub>3</sub>); 117 (CH); 123 (CH); 131 (CH); 131 (C); 131 (CH); 136 (C); 137 (CH); 145 (CH); 147 (CH).

**Bis(tetrafluoroboran) *N,N'*-dimetoksy-4,4'-bipirydylu (NO4)** otrzymano w reakcji tetrafluoroboranu trimetylooksoniowego (2 mmol) i *N,N'*-ditlenku 4,4'-bipirydylu (1 mmol) prowadzonej w temperaturze wrzenia acetonitrylu w atmosferze gazu obojętnego przez 4 h. Związek NO4 to białe ciało stałe o temp. topnienia 182°C. Otrzymano 0,42 g NO4. Wydajność reakcji wyniosła 43,09%. <sup>1</sup>H NMR (DMSO-*d*<sub>6</sub>),  $\delta$  (ppm): 4,5277 (s, 6H, CH<sub>3</sub>); 8,8685–8,8935 (m, 4H, Ar); 9,7782–9,8102 (m, 4H, Ar). <sup>13</sup>C NMR (DMSO-*d*<sub>6</sub>),  $\delta$  (ppm): 70 (CH<sub>3</sub>); 128 (CH); 142 (CH); 148 (C)<sup>16</sup>.

**Heksafluorofosforan *N*-etoksy-2-metylopirydyny (NO5)** otrzymano w wyniku ogrzewania heksafluorofosforanu trietylooksoniowego (1,2 mmol) z *N*-tlenkiem 2-metylopirydyny (1 mmol) w temperaturze wrzenia chloroformu w atmosferze gazu obojętnego przez 0,5 h. Sól NO5 otrzymano w postaci białego ciała stałego o temp. topnienia 70°C w ilości 1,7 g, co oznacza, że wydajność reakcji wyniosła 60,03%. <sup>1</sup>H NMR (DMSO-*d*<sub>6</sub>),  $\delta$  (ppm): 1,4235–1,4585 (t, 3H, CH<sub>3</sub>); 2,8111 (s, 3H, CH<sub>3</sub>); 4,6016–4,6541 (q, 2H, -CH<sub>2</sub>-); 8,0501–8,0893 (m, 1H, Ar); 8,1462–8,1662 (m, 1H, Ar); 8,4730–8,5150 (m, 1H, Ar); 9,3812–9,3977 (d, *J* ≈ 6,6 Hz, 1H, Ar). <sup>13</sup>C NMR (DMSO-*d*<sub>6</sub>),  $\delta$  (ppm): 13 (CH<sub>3</sub>); 17 (CH<sub>3</sub>); 79 (CH<sub>2</sub>); 127 (CH); 130 (CH); 142 (CH); 145 (CH); 154 (C)<sup>17</sup>.

Wzory barwnika SQ oraz koinicjatorów NO1–NO5 przedstawiono w tabeli 1.

## Metody badań

Widma <sup>1</sup>H i <sup>13</sup>C NMR zostały zarejestrowane za pomocą spektrometru Ascend III, Bruker (USA), pracującego przy częstotliwości 400 MHz. Stosowanym rozpuszczalnikiem był dimetylosulfotlenek (DMSO-*d*<sub>6</sub>), a wzorcem wewnętrznym tetrametylosilan.

Temperaturę topnienia oznaczono za pomocą aparatu Boeöthius PGH Rundfunk, Fernsehen Niederdorf KR, Stollberg/E.

Do pomiarów absorpcji zastosowano spektrofotometr Agilent Technology UV-Vis 60 Cary. Widma koinicjatorów zarejestrowano



Dr inż. Robert DOBOSZ w roku 2002 ukończył studia na Wydziale Technologii i Inżynierii Chemicznej Uniwersytetu Technologiczno-Przyrodniczego im. Jana i Jędrzeja Śniadeckich w Bydgoszczy. W 2007 r. uzyskał stopień doktora na tym samym wydziale. Od początku kariery zawodowej związany z UTP, gdzie obecnie jest adiunktem w Zakładzie Chemii Organicznej. Specjalność – chemia organiczna.



Dr hab. inż. Janina KABATC, prof. nadzw. UTP, w roku 1993 ukończyła studia na Wydziale Technologii i Inżynierii Chemicznej Akademii Techniczno-Rolniczej w Bydgoszczy (obecnie: Uniwersytet Technologiczno-Przyrodniczy im. Jana i Jędrzeja Śniadeckich). W 2001 r. uzyskała stopień doktora nauk chemicznych, a w 2013 r. stopień doktora habilitowanego na Uniwersytecie Mikofaję Kopernika w Toruniu. Specjalność – chemia organiczna.

Table 1. Structures, names and abbreviations of photosensitizer and coinitiators

Tabela 1. Struktury, nazwy i oznaczenia fotosensybilizatora oraz koinicjatorów

<p>1,3-Bis(4-bromofenylamino)skwaryna SQ</p>	
<p>Tetrafluoroboran <i>N</i>-metoksy-4-fenylopyridyny NO</p>	<p>Tetrafluoroboran <i>N</i>-metoksy-4-cyanopirydyny NO1</p>
<p>Tetrafluoroboran <i>N</i>-metoksyizochinoliny NO2</p>	<p>Tetrafluoroboran <i>N</i>-metoksychinoliny NO3</p>
<p>Bis(tetrafluoroboran) <i>N,N'</i>-dimetoksy-4,4'-bipirydyłu NO4</p>	<p>Heksafluorofosforan <i>N</i>-etoksy-2-metylopyridyny NO5</p>

w metanolu jako rozpuszczalniku. W celu zarejestrowania widma barwnika przygotowano roztwór Stocka. 2 mL roztworu barwnika o stężeniu  $1,2 \cdot 10^{-4}$  M w 1-metylo-2-pirolidonie przeniesiono do kolby miarowej na 10 mL i uzupełniono metanolem. Pomiary prowadzono w temperaturze pokojowej.

W celu zbadania wpływu stężenia źródła wolnych rodników (koinicjatorów) na skuteczność inicjowania dwuskładnikowych układów fotoinicjujących przeprowadzono polimeryzację TMPTA w obecności koinicjatorów o różnych stężeniach ( $5 \cdot 10^{-4}$  M,  $10^{-3}$  M,  $2 \cdot 10^{-3}$  M,  $5 \cdot 10^{-3}$  M,  $7,5 \cdot 10^{-3}$  M,  $10^{-2}$  M) i fotosensybilizatora SQ o stężeniu  $5 \cdot 10^{-3}$  M (tabela 2). Parametry kinetyczne procesu polimeryzacji TMPTA inicjowanej dwuskładnikowymi układami fotoinicjującymi: SQ/NO, SQ/NO1, SQ/NO2, SQ/NO3, SQ/NO4 oraz SQ/NO5 określono za pomocą różnicowego kalorymetru skaningowego TA DSC Q2000 Instrument, wyposażonego w przystawkę fotometryczną z wysokociśnieniową lampą rtęciową (foto-DSC). Strumień ciepła wydzielanego podczas procesu fotoinicjowanej polimeryzacji został zarejestrowany dla promieniowania UV-Vis w zakresie 300–500 nm, o mocy  $30 \text{ mW/cm}^2$ , przy przepływie azotu 50 mL/min w warunkach izotermicznych. Próbę o masie  $30 \pm 0,1$  mg umieszczano w otwartym aluminiowym tygielku. Wszystkie pomiary zostały przeprowadzone w identycznych warunkach. Przed rozpoczęciem właściwego pomiaru próbka utrzymywana była przez 2 min w zadanej temperaturze równej  $25^\circ\text{C}$ . Odczytów wyników

Table 2. Kinetic parameters of radical polymerization of TMPTA initiated with two-component photoinitiating systems under study

Tabela 2. Parametry kinetyczne polimeryzacji rodnikowej TMPTA inicjowanej przez dwuskładnikowe układy fotoinicjujące

Fotoinicjator	Stężenie fotoinicjatora mol/dm <sup>3</sup>	Strumień wydzielonego ciepła, mW	Szybkość polimeryzacji, s <sup>-1</sup>	Stopień konwersji monomeru, %
SQ/NO	$5 \cdot 10^{-4}$	168	6,64	35
	$10^{-3}$	181	7,14	46
	$2 \cdot 10^{-3}$	163	6,42	40
	$5 \cdot 10^{-3}$	136	5,37	50
	$7,5 \cdot 10^{-3}$	123	4,84	39
SQ/NO1	$10^{-2}$	123	4,84	54
	$5 \cdot 10^{-4}$	22	0,88	18
	$10^{-3}$	24	0,96	22
	$2 \cdot 10^{-3}$	34	1,36	28
	$5 \cdot 10^{-3}$	38	1,51	36
SQ/NO2	$7,5 \cdot 10^{-3}$	23	0,93	5
	$10^{-2}$	39	1,52	35
	$5 \cdot 10^{-4}$	34	1,36	24
	$10^{-3}$	170	6,70	38
	$2 \cdot 10^{-3}$	139	5,48	48
SQ/NO3	$5 \cdot 10^{-3}$	118	4,67	55
	$7,5 \cdot 10^{-3}$	111	4,39	34
	$10^{-2}$	97	3,83	51
	$5 \cdot 10^{-4}$	55	2,17	32
	$10^{-3}$	111	4,39	37
SQ/NO4	$2 \cdot 10^{-3}$	103	4,06	45
	$5 \cdot 10^{-3}$	93	3,68	45
	$7,5 \cdot 10^{-3}$	78	3,06	30
	$10^{-2}$	107	4,23	50
	$5 \cdot 10^{-4}$	59	2,31	30
SQ/NO5	$10^{-3}$	60	2,37	39
	$2 \cdot 10^{-3}$	71	2,81	37
	$5 \cdot 10^{-3}$	144	5,68	34
	$7,5 \cdot 10^{-3}$	102	4,04	47
	$10^{-2}$	365	14,40	54
SQ/NO5	$5 \cdot 10^{-4}$	19	0,75	15
	$10^{-3}$	20	0,79	17
	$2 \cdot 10^{-3}$	19	0,74	17
	$5 \cdot 10^{-3}$	22	0,88	22
	$7,5 \cdot 10^{-3}$	26	1,03	25
$10^{-2}$	28	1,09	25	

dokonywano co 0,05 s. Mieszanina polimeryzująca zawierała 1,8 mL TMPTA, 0,2 mL 1-metylo-2-pirolidonu, barwnik oraz odpowiedni koinicjator. Zastosowanie 1-metylo-2-pirolidonu było konieczne ze względu na słabą rozpuszczalność barwnika w monomerze. Dla każdego układu fotoinicjującego wykonano trzy próby, a wyniki uśredniono.

Ciepło reakcji polimeryzacji jest proporcjonalne do stopnia przereagowania wiązań podwójnych. Stopień konwersji monomeru

proporcjonalny do pola powierzchni egzotermicznego pikę wyznaczono ze wzoru (1):

$$C\% = \frac{\Delta H_t}{\Delta H_0} \cdot \frac{M_{cz}}{nm} \cdot 100 \quad (1)$$

w którym  $\Delta H_t$  oznacza całkowite ciepło wydzielone w czasie  $t$ ,  $\Delta H_0$  teoretyczne ciepło konwersji całkowitej,  $M_{cz}$  masę cząsteczkową,  $m$  masę próbki, a  $n$  odpowiada liczbie ugrupowań reaktywnych w cząsteczce monomeru<sup>18</sup>). Ciepło reakcji wiązania podwójnego akrylanów wynosiło  $\Delta H_0 = 78,0$  kJ/mol. Szybkość polimeryzacji ( $R_p$ ) bezpośrednio związaną ze strumieniem wydzielonego ciepła ( $dH/dt$ ) opisano wzorem (2)<sup>19</sup>):

$$R_p = \frac{dH/dt}{\Delta H_0} \quad (2)$$

## Wyniki badań i dyskusja

Określono kinetykę polimeryzacji rodnikowej TMPTA z zastosowaniem soli *N*-alkoksoniowych jako koinicjatorów. Związki te pełniły funkcję akceptorów elektronów pochodzących od donora, którym była 1,3-bis(4-bromofeniloamino)skwaryna. Barwnik skwarynowy w roztworze metanolu absorbował promieniowanie elektromagnetyczne w zakresie 350–450 nm. Maksimum absorpcji sensybilizatora znajdowało się przy ok. 400 nm. Dzięki temu możliwe było przesunięcie czułości badanych układów fotoinicjujących w kierunku światła widzialnego (rys. 1). Właściwości spektroskopowe barwnika SQ zostały opisane poprzednio<sup>20</sup>.

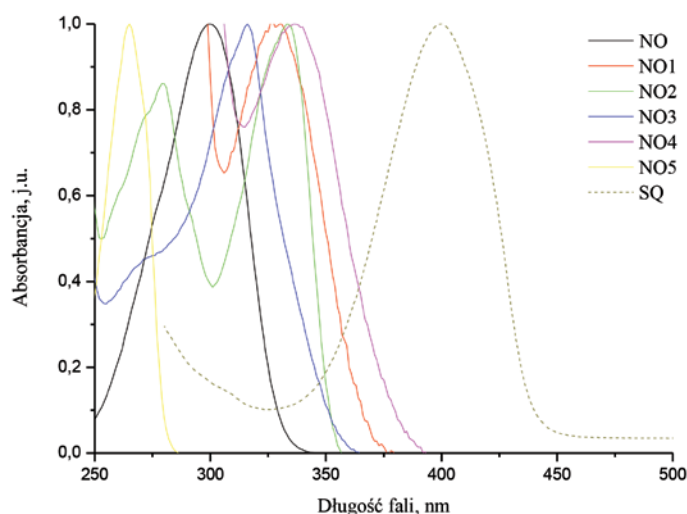


Fig. 1. The absorption spectra of coinitiators NO–NO5 and sensitizer SQ in methanol recorded at room temperature; symbols are explained in the text

Rys. 1. Widma absorpcji koinicjatorów NO–NO5 oraz sensybilizatora SQ w metanolu w temperaturze pokojowej; oznaczenia objaśniono w tekście

Wraz ze wzrostem stężenia koinicjatorów szybkość polimeryzacji rodnikowej stopniowo wzrastała do momentu osiągnięcia maksimum, po czym łagodnie zaczynała maleć. Wyjątkiem w badanej grupie układów dwuskładnikowych był układ, w którego skład wchodził koinicjator NO4.

Na rys. 2 przedstawiono zależność ilości wydzielonego ciepła oraz stopnia przereagowania wiązań podwójnych monomeru w funkcji czasu naświetlania mieszaniny polimeryzującej dla różnych stężeń koinicjatora NO4. Na podstawie danych kinetycznych stwierdzono, że szybkość polimeryzacji osiągała maksimum przy największym stężeniu koinicjatora ( $10^{-2}$  M) i była ok. 2-krotnie większa od maksymalnych szybkości polimeryzacji osiąganych w przypadku układów fotoinicjujących SQ/NO i SQ/NO2 oraz ok. czternaście razy większa od szybkości polimeryzacji inicjowanej przez układy z koinicjatorem NO1 i NO5 (tabela 2).

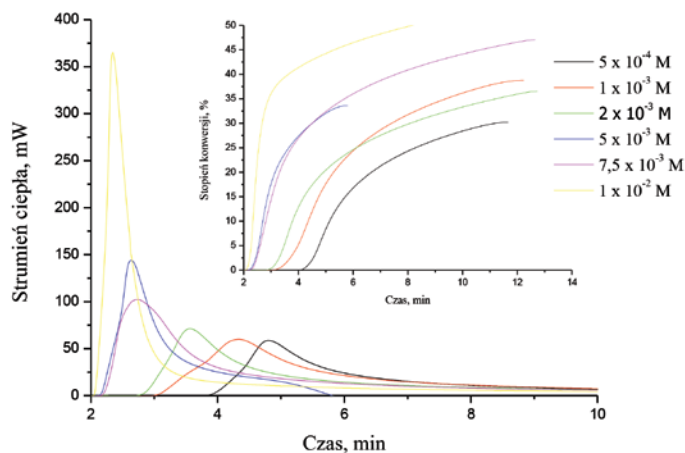


Fig. 2. The kinetic and conversion of monomer curves recorded during radical polymerization of TMPTA/MP (9:1) initiated with two-component photoinitiating system SQ/NO4; light intensity  $I_a = 30$  mW/cm<sup>2</sup>

Rys. 2. Krzywe kinetyczne oraz krzywe stopnia konwersji monomeru zarejestrowane w czasie polimeryzacji rodnikowej mieszaniny TMPTA/MP (9:1) inicjowanej przez układ dwuskładnikowy SQ/NO4; moc światła  $I_a = 30$  mW/cm<sup>2</sup>

Dla układów fotoinicjujących SQ/NO, SQ/NO2 i SQ/NO3 osiągnięto maksymalną wartość szybkości polimeryzacji przy stężeniu  $10^{-3}$  M. Dla tego samego stężenia układ SQ/NO4 inicjował polimeryzację TMPTA z szybkością 2-krotnie mniejszą. Stopnie przereagowania wiązania podwójnego monomeru dla tych czterech układów fotoinicjujących o stężeniu  $10^{-3}$  M wynosiły ok. 40%. Stężenie zastosowanego koinicjatora wpływało również na stopień konwersji wiązań podwójnych w monomerze. W warunkach doświadczalnych osiągnięto konwersję monomeru w zakresie 4,8–54,8%. Największe stopnie konwersji (przekraczające 50%) uzyskano dla fotoinicjatorów SQ/NO, SQ/NO2, SQ/NO3 i SQ/NO4 dla stężeń  $5 \cdot 10^{-3}$  M oraz  $10^{-2}$  M.

Uzyskane wysokie wartości szybkości polimeryzacji oraz stopnia konwersji TMPTA przy zastosowaniu jako koinicjatora NO4 o stężeniu  $10^{-2}$  M, związane były z jego budową (tabela 1). W tym przypadku z jednej cząsteczki koinicjatora po procesie fotoindukowanego przeniesienia elektronów można było otrzymać 2 rodniki metoksyłowe. Oznacza to, że stężenie rodników inicjujących było 2-krotnie większe niż w przypadku pozostałych koinicjatorów. Najniższą szybkość polimeryzacji oraz najmniejszą konwersję wiązań podwójnych monomeru uzyskano dla układu skomponowanego z barwnika SQ oraz koinicjatora NO5. Fakt ten można przypisać powstawaniu większego rodnika etoksyłowego, który w mniejszym stopniu inicjował proces polimeryzacji rodnikowej.

W wyniku absorpcji promieniowania elektromagnetycznego nastąpiło wzbudzenie cząsteczki barwnika, a następnie fotoindukowany był proces przeniesienia elektronu z sensybilizatora (barwnik) na koinicjator (COI). W efekcie otrzymano rodnikokation barwnika oraz rodnik koinicjatora, który ulegał dekompozycji (rozzerwanie wiązania N-O) na rodnik metoksyłowy w przypadku koinicjatorów NO–NO4 oraz rodnik etoksyłowy w przypadku soli NO5, a także na 4-fenylpirydynę z NO, 4-cyjanopirydynę z NO1, izochinolinę z NO2, chinolinę z NO3, 4,4'-bipirydydyl z NO4 oraz pirydynę z NO5. Na podstawie właściwości fotochemicznych barwników skwarynowych i soli *N*-alkoksoniowych oraz prowadzonych wcześniej badań, na rys. 3 przedstawiono mechanizm tworzenia rodników inicjujących polimeryzację<sup>11, 20–22</sup>.

## Podsumowanie i wnioski

Przeprowadzono syntezę oraz opisano właściwości fizykochemiczne soli *N*-alkoksoniowych, które wraz z opisanym wcześniej barwnikiem skwarynowym<sup>15</sup>) wchodziły w skład układów inicjujących polimeryzację rodnikową TMPTA. Dwuskładnikowe układy zawierające barwnik SQ w obecności soli *N*-alkoksoniowych, pełniących rolę

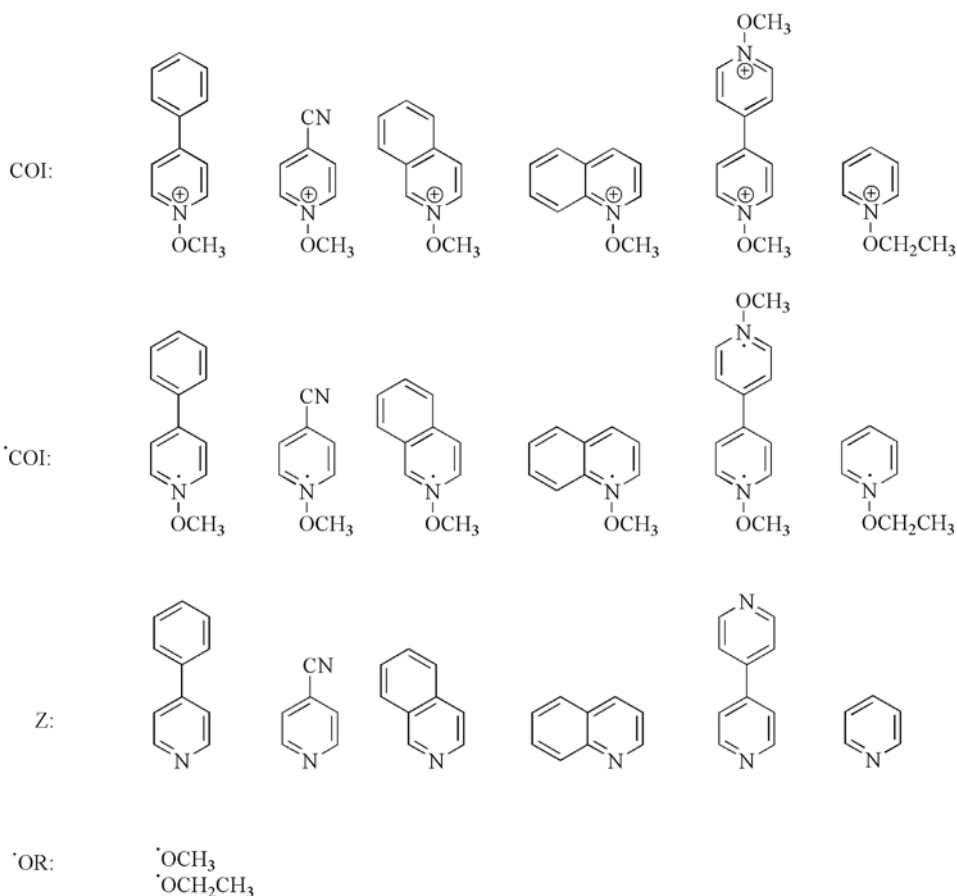
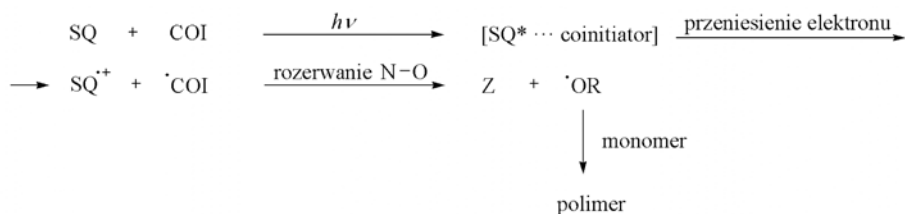


Fig. 3. Mechanizm formowania rodników inicjujących w dwuskładnikowych układach fotoinicjujących

**Rys. 3. Mechanizm powstawania rodników inicjujących w dwuskładnikowych układach fotoinicjujących**

koinicjatorów, skutecznie inicjują polimeryzację rodnikową TMPTA. Zdolność fotoinicjowania jest zróżnicowana i zależy od budowy koinicjatora, a co za tym idzie, rodnika otrzymanego w wyniku fotoindukowanego przeniesienia elektronu (rys. 3), jak również od jego stężenia (tabela 2). Największą szybkością polimeryzacji monomeru TMPTA charakteryzuje się układ fotoinicjujący SQ/NO4 o stężeniu  $10^{-2}$  M, w skład którego wchodzi pochodna bipyridylu. Fotoinicjator ten pozwala na otrzymanie znacznych szybkości polimeryzacji oraz stosunkowo wysokiej konwersji monomeru przy wysokim stężeniu koinicjatora. Zbliżone wartości stopnia konwersji monomeru i o ok. połowę mniejszą szybkość polimeryzacji osiągnięto dla układów o co najmniej 2-krotnie mniejszym stężeniu koinicjatora (SQ/NO oraz SQ/NO2). Stwierdzono, że z powodzeniem można zastąpić wcześniej

opisany układ z komercyjnie dostępnym tetrafluoroboranem *N*-metoksy-4-fenylpirydyny, nowymi fotoinicjatorami zawierającymi syntezowane sole *N*-alkoksoniowe.

Przedstawione w pracy podejście może skłaniać do syntezy nowych barwników skwarynowych, a także soli *N*-alkoksoniowych oraz do komponowania skutecznych, dwuskładnikowych układów inicjujących polimeryzację rodnikową w zakresie światła widzialnego.

Praca finansowana przez Narodowe Centrum Nauki (NCN) (Kraków, Polska), w ramach projektu badawczego 2013/11/B/ST5/01281.

Otrzymano: 22-02-2017

LITERATURA

- [1] H. Tar, D.S. Esen, M. Aydin, C. Ley, N. Arsu, X. Allonas, *Macromolecules* 2013, **46**, nr 9, 3266.
- [2] E. Andrzejewska, *Polimery* 2001, **46**, nr 2, 88.
- [3] H. Salmi, H. Tar, A. Ibrahim, C. Ley, X. Allonas *Europ. Polymer J.* 2013, **49**, 2275.
- [4] J.F. Rabek, *Współczesna wiedza o polimerach*, PWN, Warszawa 2008.
- [5] J. Kabatc, K. Jurek, *Przem. Chem.* 2013, **92**, nr 11, 1987.
- [6] J. Kabatc, J. Paczkowski, *Dyes Pigm.* 2010, **86**, 133.
- [7] J. Kabatc, *Polymer* 2010, **51**, 5028.
- [8] K. Katayama, T. Shoji, K. Naito, T. Eitoku, A. Nakayama, *J. Photochem. Photobiol. Part A: Chem.* 2010, **214**, 264.
- [9] J. Lalevée, J.P. Fouassier, *Dyes and chromophores in polymer science*, Wiley, London 2015.
- [10] Y. Yagci, T. Endo, *Adv. Polymer Sci.* 1997, **127**, 60.
- [11] J. Kabatc, K. Kostrzewska, K. Jurek, M. Kozak, A. Balcerak, Ł. Orzeł, *J. Polym. Sci., Part A: Polym. Chem.* 2017, **55**, 471.
- [12] J. Kabatc, J. Paczkowski, *J. Photochem. Photobiol., Part A: Chem.* 2006, **184**, 184.
- [13] J. Kabatc, *Mater. Chem. Phys.* 2011, **125**, 118.
- [14] S.Y. Park, K. Jun, S.W. Oh, *Bull. Korean Chem. Soc.* 2005, **26**, nr 3, 428.
- [15] J. Kabatc, K. Kostrzewska, Ł. Orzeł, *Dyes Pigm.* 2016, **130**, 226.
- [16] E.D. Lorance, W.H. Kramer, I.R. Gould, *J. Am. Chem. Soc.* 2002, **124**, nr 51, 15225.
- [17] R. Podsiadły, *J. Photochem. Photobiol., Part A: Chem.* 2008, **198**, nr 1, 60.
- [18] J. Paczkowski, *Fotochemia polimerów teoria i zastosowania*, Wydawnictwo Uniwersytetu Mikołaja Kopernika, Toruń 2003.
- [19] J. Kabatc, K. Kostrzewska, K. Jurek, *RSC Adv.* 2016, **6**, 74715.
- [20] J. Kabatc, K. Kostrzewska, M. Kozak, A. Balcerak, *RSC Adv.* 2016, **6**, 103851.
- [21] I.R. Gould, D. Shukla, D. Giesen, S. Farid, *Helvetica Chim. Acta* 2001, **84**, 2796.
- [22] D. Shukla, S.P. Adiga, W.G. Ahearn, J.P. Dinnocenzo, S. Farid, *J. Org. Chem.* 2013, **78**, 1955.

**Publikacja naukowa [A3]**

# New Squaraine-Based Two-Component Initiation Systems for UV-Blue Light Induced Radical Polymerization: Kinetic and Time-Resolved Laser Spectroscopy Studies

Janina Kabatc,<sup>1</sup> Katarzyna Kostrzewska,<sup>1</sup> Katarzyna Jurek,<sup>1</sup> Martyna Kozak,<sup>2</sup> Alicja Balcerak,<sup>2</sup> Łukasz Orzeł<sup>3</sup>

<sup>1</sup>Faculty of Chemical Technology and Engineering, UTP University of Science and Technology, Seminaryjna 3, Bydgoszcz 85-326, Poland

<sup>2</sup>Faculty of Chemical Technology and Engineering, Bachelor degree student of UTP University of Science and Technology, Seminaryjna 3, Bydgoszcz 85-326, Poland

<sup>3</sup>Faculty of Chemistry, Jagiellonian University, Ingardena 3, Cracow 30-060, Poland

Correspondence to: J. Kabatc (E-mail: nina@utp.edu.pl)

Received 14 September 2016; accepted 5 October 2016; published online 22 November 2016

DOI: 10.1002/pola.28425

**ABSTRACT:** In this article, the ability of two-component photoinitiator systems for efficient polymerization of 2-ethyl-2-(hydroxymethyl)-1,3-propanediol triacrylate was presented. The photophysics and photochemistry of squaraine dyes in the presence of an electron donor as well as an electron acceptor was investigated, and it was found that the photosensitizer in an excited state might act as an electron acceptor or an

electron donor. The excited states of squaraines may be quenched by tetramethylammonium *n*-butyltriphenylborate (**B2**), diphenyliodonium chloride (**I1**), and *N*-methoxy-4-phenylpyridinium tetrafluoroborate (**NO**). © 2016 Wiley Periodicals, Inc. *J. Polym. Sci., Part A: Polym. Chem.* **2017**, *55*, 471–484

**KEYWORDS:** dyes; initiators; kinetics; photopolymerization

**INTRODUCTION** Squaraines, which are quite often also referred to as squarylium dyes, belong to the family of polymethine dyes. Some members of this family are shown in Chart 1.

## Chart 1

Representative examples shown therein, are defined by two heteroatoms, which are connected by a polymethine chain consisting of an odd number of repeating methane units “=CH–,” which results in conjugated systems. Depending on the heteroatoms, these systems can be cationic, anionic, zwitterionic, or neutral.

As it is shown in Chart 1, the squaraines represent a real zwitterionic species. They are neutral overall, however, a neutral mesomeric structure can usually not be written with exception of special cases. One stable structure of squaraine compounds is the zwitterionic form shown, where the cyclobutene has +2 charge, and both oxygens are negatively charged. The betaine structure can be expressed either as a dipolar cyanine structure (A) or cyclobutenediylumdiolate (B). The former might be responsible that squaraines are often referred to as cyanine dyes as well as the fact that

their structure appears as if an oxocyclobutenolate core was inserted into the cyanine structure. In addition, they show some similar properties such as strong and sharp absorption in the red to NIR region. However, squaraines should be seen as a separate class because they are zwitterionic and they consist of a donor–acceptor–donor (D–A–D) structure due to the strong electron withdrawing central moiety, in contrast to cyanines. For stabilization of the D–A–D system, strong electron donating groups like heterocycles or electron rich aromatic units such as aniline derivatives are usually found in squaraine dyes.

Squaraines are interesting organic molecules due to the strong absorption in the visible region ( $\epsilon \sim 10^5 \text{ M}^{-1} \text{ cm}^{-1}$ ), intense fluorescence emission, and good photoconductivity presented in these dyes.<sup>1</sup> These features make them useful in a variety of applications in the area of imaging, nonlinear optics, photodynamic therapy, and photovoltaic cells.<sup>2</sup> Furthermore, squaraine dyes are suitable for fluorescence detection of proteins at long-wavelength excitation and labels in biological assays due their unique photochemical and photophysical properties namely light absorption in the visible red and near-infrared regions.<sup>3</sup>

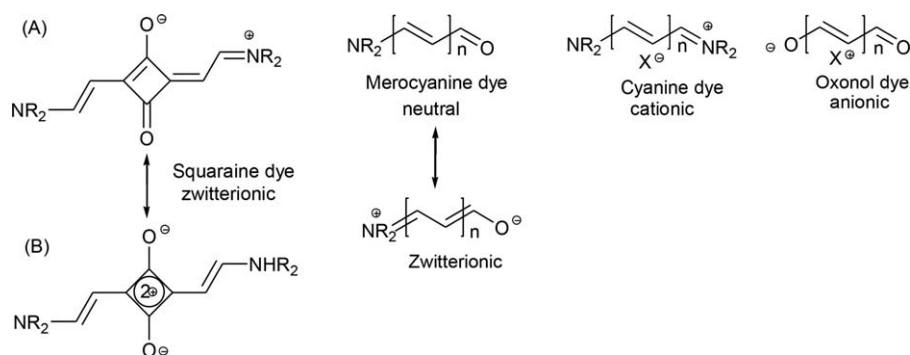


**CHART 1** The general structures of polymethine dyes.

The squaraine dyes are very rare used as photosensitizers in photopolymerization process. In 2004 Yong He and co-workers described application of two squaraine dyes: bis(1,2,3,3-tetramethylindolenium-2-ylidene) squaraine and bis(3-methylbenzothiazol-2-ylidene) squaraine as sensitizers for three (*p*-octanoxyphenyl)-phenyliodonium salts varying with a type of counterion, in radical polymerization of methyl methacrylate.<sup>4</sup> In 2013 Lavevé and coworkers presented the studies on the photoinitiating ability of 2,2,3-trimethylindolenine-based squaraine dye incorporated in multicomponent systems for cationic polymerization of an epoxide or a vinyl ether as well as radical polymerization of TMPTA.<sup>5,6</sup>

The present paper is focused on the two-component photoinitiating systems for free radical polymerization of 2-ethyl-2-(hydroxymethyl)-1,3-propanediol triacrylate (TMPTA) containing 1,3-bis(*p*-substituted phenylamino)squaraines with different substituents in *p*-position of phenyl ring and following coinitiators: tetramethylammonium *n*-butyltriphenylborate (**B2**), diphenyliodonium chloride (**I1**) and *N*-methoxy-4-phenylpyridinium tetrafluoroborate (**NO**).

## EXPERIMENTAL

### Materials

TMPTA, coinitiators (diphenyliodonium chloride (**I1**) and *N*-methoxy-4-phenylpyridinium tetrafluoroborate (**NO**)) and solvents (spectroscopic grade) were purchased from Sigma-Aldrich (Poland) and used without further purification. 1,3-Bis(*p*-substituted phenylamino)squaraines (**SQ**) and tetramethylammonium *n*-butyltriphenylborate (**B2**) were synthesized in our laboratory by methods described in literature.<sup>7–9</sup>

### Spectroscopic Measurements

Absorption and emission spectra were recorded at room temperature using an Agilent Technology UV-Vis Cary 60 Spectrophotometer, a Hitachi F-7000 spectrofluorimeter and UV-VIS-NIR Fluorolog 3 Spectrofluorimeter (Horiba Jobin Yvon), respectively. The spectra were recorded in acetonitrile (CH<sub>3</sub>CN) and 1-methyl-2-pyrrolidinone (MP). The final concentration of the dye in solution was  $1.0 \times 10^{-5}$  M.

The fluorescence lifetimes were measured using a single-photon counting system UV-VIS-NIR Fluorolog 3 Spectrofluorimeter (Horiba Jobin Yvon). The apparatus utilizes for

the excitation a picosecond diode laser generating pulses of about 55 ps at 370 nm. Short laser pulses in combination with a fast microchannel plate photodetector and ultrafast electronics make a successful analysis of fluorescence decay signals with a resolution of few picoseconds possible. The dyes were studied at concentration able to provide equivalent absorbance at 370 nm (0.2 in the 10 mm cell) to be obtained. The fluorescence decay was fitted to two exponentials.

The fluorescence quenching measurements were performed using a single-photon counting system UV-VIS-NIR Fluorolog 3 Spectrofluorimeter (Horiba Jobin Yvon). The apparatus uses a picosecond diode laser (370 nm) generating pulses of about 50 ps for the excitation. Short laser pulses in combination with a fast microchannel plate photodetector and ultrafast electronics make a successful analysis of fluorescence decay signals in the range of single picoseconds possible. The dyes were studied at a concentration able to provide equivalent absorbance at 370 nm (0.2 in the 10 mm cell). The rate constant for the quenching of 1,3-bis(*p*-substituted phenylamino)squaraines by all quenchers under studies were determined in 1-methyl-2-pyrrolidinone. The concentration of dyes were  $2 \times 10^{-5}$  M and that of the quenchers was in the range from  $1 \times 10^{-4}$  M to  $5.0 \times 10^{-3}$  M. The fluorescence quenching at 440 nm was measured in deaerated solution by bubbling with argon.

### Polymerization Measurements

The kinetics of polymerization of TMPTA photoinitiated by: 1,3-bis(*p*-substituted phenylamino)squaraine/tetramethylammonium *n*-butyltriphenylborate (**SQ/B2**), 1,3-bis(*p*-substituted phenylamino)squaraine/diphenyliodonium chloride (**SQ/I1**), and 1,3-bis(*p*-substituted phenylamino)squaraine/*N*-methoxy-4-phenylpyridinium tetrafluoroborate (**SQ/NO**) was measured using Differential Scanning Calorimeter TA DSC Q2000 Instrument and TA Q PCA photo unit equipped with a high-pressure mercury lamp (Photo-DSC). The heat of the photoinitiated polymerization reaction measured by means of a photo differential scanning calorimeter is a good control of the reaction temperature. UV-visible light (300 nm <  $\lambda$  < 500 nm) from a high pressure mercury lamp was applied at a constant intensity of 30 mW/cm<sup>2</sup> for several min under a nitrogen flow of 50 mL/min at a prescribed

temperature (isothermal mode). The weight of the samples  $30 \pm 0.1$  mg was placed into an open aluminum liquid DSC pan. The measurements were carried out under identical conditions. The sample was maintained at a prescribed temperature for 2 min before each measurement run began. Measurements were recorded at a sampling interval of 0.05 s/point. The polymerizing solution was composed of 1.8 mL of monomer, 0.2 mL of 1-methyl-2-pyrrolidinone, and appropriate amount of photoinitiator. The using of 1-methyl-2-pyrrolidinone was necessary due to the poor solubility of dye in monomer studied.

The reaction heat liberated in the polymerization is directly proportional to the number of acrylates reacted in the system. By integrating the area under the exothermic peak, the conversion of the acrylate groups ( $C\%$ ), or the extent of the reaction was determined according to eq. 1:

$$C\% = \frac{\Delta H_t}{\Delta H_0} \times 100 \quad (\text{eq. 1})$$

where  $\Delta H_t$  is the reaction heat evolved at time  $t$  and  $\Delta H_0$  is the theoretical heat for complete conversion. A reaction heat for an acrylate double bond polymerization of  $\Delta H_0 = 78.0$  kJ/mol was used. The rate of polymerization ( $R_p$ ) is directly related to the heat flow ( $dH/dt$ ) as in eq. 2:

$$R_p = \frac{dH/dt}{\Delta H_0} \quad (\text{eq. 2})$$

### Cyclic Voltammetry (CV) Measurements

The electrochemical measurements were evaluated by CV. CV measurements were made with ER466 Integrated Potentiostat System (eDAQ, Poland) in a three-electrode configuration. The electrolyte was 0.1 M tetrabutylammonium perchlorate in dry acetonitrile. Platinum 1-mm disk electrode was applied as working electrode and platinum and Ag/AgCl were used as auxiliary and reference electrodes, respectively. All solutions were deoxygenated with  $N_2$  for at least 15 min prior to measurements. The computer-controlled potentiostat was equipped with EChem Software.

### Nanosecond Laser Flash Photolysis

Transient absorption spectra and decay kinetics were recorded out using the nanosecond laser flash photolysis method. The nanosecond laser flash photolysis experiments were performed using a LKS.60 Laser Flash Photolysis apparatus (Applied Photophysics). Laser irradiation at 355 nm from the third harmonic of the Q-switched Nd:YAG laser from a Lambda Physik/model LPY 150 operating at 65 mJ/pulse (pulse width about 4-5 ns) was used for the excitation. Transient absorbance at preselected wavelengths was monitored by a detection system consisting of a monochromator, a photomultiplier tube (Hamamatsu R955) and a pulsed xenon lamp (150 W) as a monitoring source. The signal from the photomultiplier was processed by a Hewlett-Packard an Agilent Infinium 54810A digital storage oscilloscope and an Acorn compatible computer.

## RESULTS AND DISCUSSION

The structures of all compounds involved in the photoinitiating systems studied are presented in Table 1.

### Spectroscopic Properties

The most prominent feature of squaraines is their sharp and intense absorption and fluorescence in the visible blue to NIR region, very similar to cyanine dyes. This is one of the reasons why they are sometimes referred to as members of the cyanine dye family. The Stokes shift is commonly rather small, which, in addition to the narrow and intense low energy absorption, is indicative of delocalization and small reorganization energy of the excited state.

The squaraines under study absorb in the region from 350 to 450 nm, which give the possibility of application of ultraviolet-blue light sources for the irradiation of polymerizing mixture (Fig. 1).

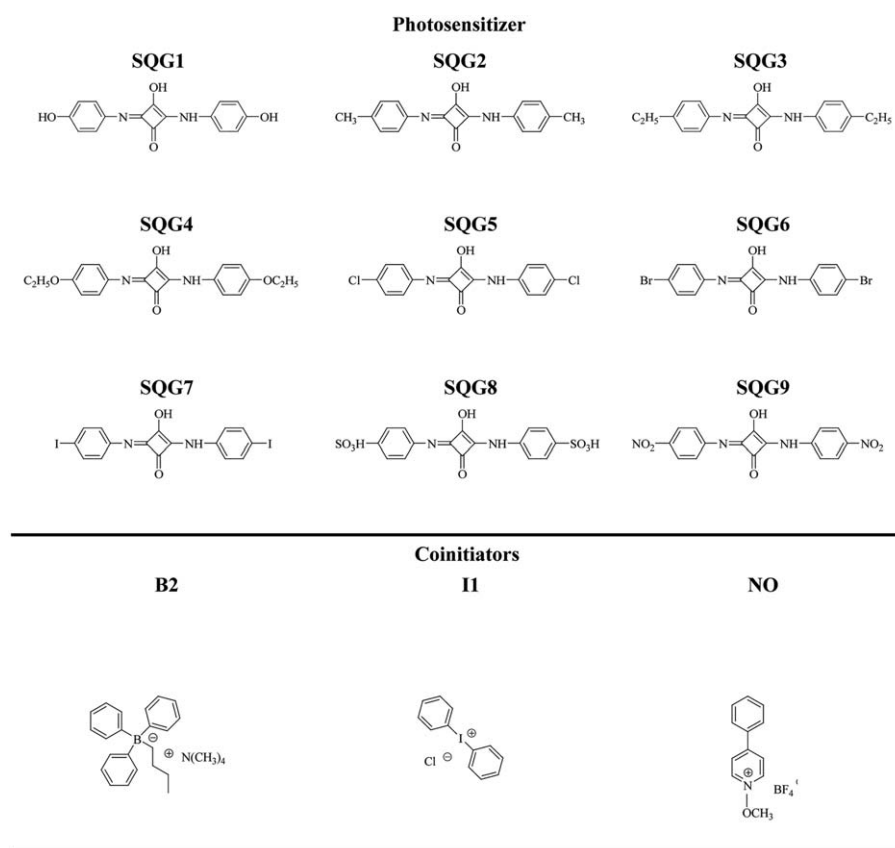
This pronounced absorption band arises from a HOMO-LUMO transition from the  $S_0$  to the  $S_1$  state of the donor-acceptor-donor structure. At higher energies, one-photon excitation into the  $S_2$  state is forbidden due to symmetry reasons and in the absorption spectra, there is a decent gap of absorption.

### The Kinetic Studies

The most common photoinitiating systems in the visible light region (400–700 nm) for radical polymerization involve a dye and an amine or organoborate salt as an electron donor.<sup>6,10–16</sup> In this case, the active radicals are formed in a bimolecular electron transfer quenching of the singlet or triplet state of the dye by the amine or borate salt. The photoinitiating systems composed of flavins, safranin, resazurin, and resorufin and amine, as well as polymethine dyes an alkyltriphenylborate salt are suitable photoinitiators of vinyl polymerization using visible irradiation.<sup>14,17–23</sup>

In this article, it was shown that the family of squaraines, in presence of borate salt and two different onium salts are efficient photoinitiators of TMPTA polymerization. The polymerization under UV-visible light irradiation (300–500 nm) in the presence of squaraine without a coinitiator was negligible. However, it proceeds efficiently in the presence of borate salt, iodonium salt, and *N*-alkoxyppyridinium salt. The comparison of photoinitiating ability of systems **SQ/B2**, **SQ/I1**, and **SQ/NO** for initiation of radical polymerization of TMPTA is presented in Figures 2–4. The kinetics of TMPTA polymerization using the high-pressure mercury lamp irradiation ( $300 \text{ nm} < \lambda < 500 \text{ nm}$ ) was followed by differential scanning calorimetry. The kinetic parameters recorded during radical polymerization are shown in Table 2.

For all initiator systems, the polymerization follows a typical radical chain mechanism with second-order termination, yielding polymers. Basing on the kinetic data presented in Figures 2–4 and Table 2, it is seen that the ability of photoinitiators under study to initiate of radical polymerization of triacrylate depends on the composition of photoinitiator. The

**TABLE 1** The Structures of Photosensitizer, Electron Donor (Borate Salt) and Electron Acceptors (Onium Salts)

chemical structure of photosensitizer and coinitiator influence on the rate of polymerization process. The rates of polymerization obtained are in the range from 0.15 to 10.87 mmol/s. The degree of double bond conversion is in the range from 7.78 to 67.60%. The lowest kinetic parameters are obtained for the photoinitiating systems composed of squaraine dye and tetramethylammonium *n*-butyltriphenylborate. The highest rate of polymerization achieved is about 2.19 mmol/s and the maximum degree of double bond conversion is equal 27.41%. Better photoinitiating efficiency shown photoinitiators in which, diphenyliodide chloride acts as coinitiator. The observed rates of polymerization and monomer conversion are about 2–4 times higher than that observed for borate salts and are in range from 0.15 to 5.97 mmol/s, and from 12.27 to 40.79%, respectively. The best kinetic results are achieved when *N*-methoxy-*p*-phenylpyridinium tetrafluoroborate is used in photoinitiator systems. The rates of polymerization are changing from 0.53 to 10.87 mmol/s. The free radical polymerization of TMPTA in this case occurs with high value of degree of double bond conversion from about 20 to 70%. It must be pointed out, that not only coinitiator type influences on the photoinitiating ability but also a type of substituent in para position of phenyl ring in squaraine dye. For all coinitiators tested the highest rates of polymerization were observed for squaraine possessing the sulphonic group. The rates of polymerization are as follows: 2.19, 5.97, and 10.87 mmol/s for borate salt,

iodonium salt and *N*-alkoxyppyridinium salt, respectively. The monomer conversions achieved are equal 27.14, 40.79, and 46.72% for (**B2**), (**I1**), and (**NO**), respectively. From the kinetic results presented above it is also seen that photoinitiating

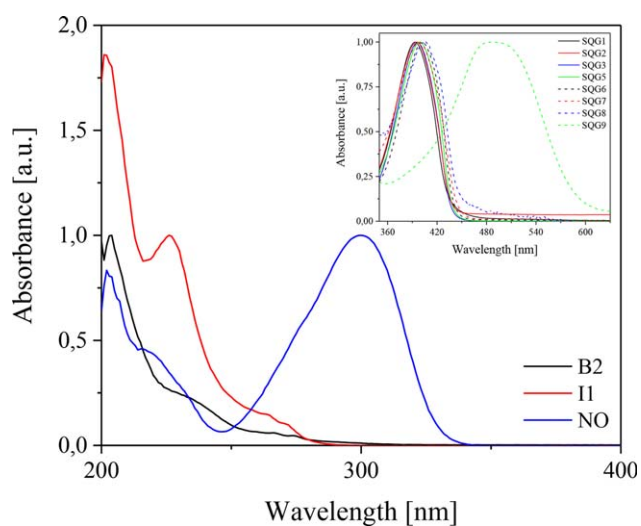


**FIGURE 1** The absorption spectra of coinitiators in 1-methyl-2-pyrrolidinone recorded at room temperature. Inset: The normalized absorption spectra of all photosensitizers in acetonitrile solution, recorded at room temperature. [Color figure can be viewed at [wileyonlinelibrary.com](http://wileyonlinelibrary.com)]

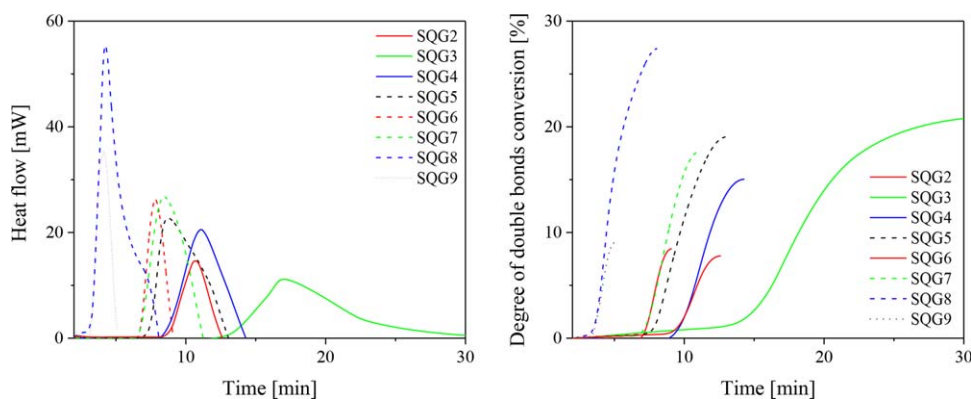


**FIGURE 2** (L): The kinetic curves recorded during the measurements of the flow of heat emitted during the photoinitiated polymerization of TMPTA/MP (9/1) mixture initiated by 1,3-bis(*p*-substituted phenylamino)squaraines in presence of tetramethylammonium *n*-butyltriphenylborate (**B2**) as a coinitiator. The dye and coinitiator concentration was  $5 \times 10^{-3}$  M.  $I_a = 30$  mW/0.196 cm<sup>2</sup>. (R) The degree of double bond conversion recorded during the polymerization process. [Color figure can be viewed at [wileyonlinelibrary.com](http://wileyonlinelibrary.com)]

systems composed of squaraine dye possessing halogen atom at para position of phenyl ring (**SQG5**, **SQG6**, and **SQG7**) initiate polymerization of TMPTA with the similar rates.

Moreover, it should be also pointed out, that for some of investigated combinations the long induction period from about 4 to 8 min was observed. The systems composed of **SQG8** or **SQG9** as sensitizers, initiate radical polymerization immediately after irradiation. In a case of photoinitiators composed of *N*-alkoxy pyridinium salt no inhibition time is observed. Basing on this one can conclude that methoxy radical faster initiate radical polymerization of TMPTA than phenyl and butyl radicals.

The spectral range (300–500 nm) used under study is rather classical for photopolymerization reaction. Therefore, the photoinitiating ability of new initiators was compared with that of commercially available photoinitiators.

For example, acylphosphine oxides are well known photoinitiators for the photopolymerization of ethylenically unsaturated

compounds, namely acrylates. Monoacylphosphine oxides such as Speedcure TPO, Speedcure TPO-L, and bisacylphosphine oxides such as Irgacure 819 (BAPO) have been commercially available for a number of years.

2,4,6-Trimethylbenzoyldiphenylphosphine oxide (TMDPO) DAROCUR TPO is a highly efficient curing agent which is used to initiate radical photopolymerization of unsaturated resins such as those based on a prepolymer, for example, acrylates in combination with mono- or multifunctional monomers as reactive thinners. In the UV-curable composition its amount is within the range between 0.3% by weight and 10% by weight, preferably between 1% by weight and 5% by weight. For example, from Arsu et al., studies, it is known, that the initiation efficiencies of photoinitiators, such as: TMDPO and bis(2,6-dimethoxybenzoyl)-2,4,4-trimethylpentylphosphine oxide (BAPO), are enhanced by addition of mercaptothioxanthone (TX-SH) to the initiator formulation. The degree of double bond conversion in TMPTA is equal 30 and 40% for initiator alone and in a presence of sensitizer,

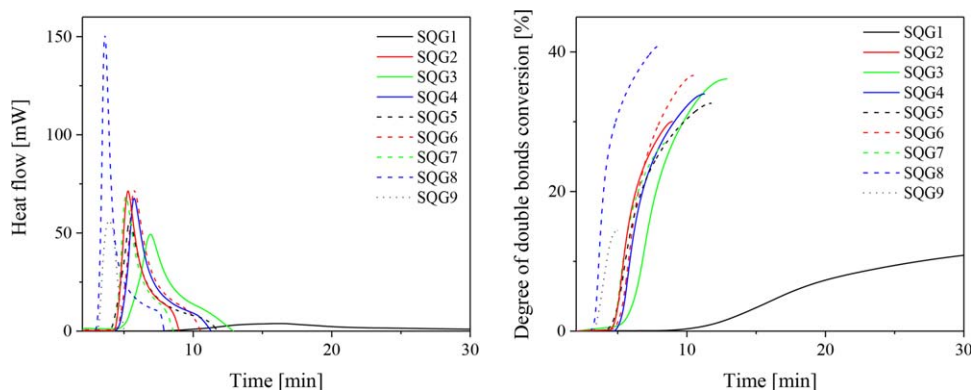


**FIGURE 3** (L): The kinetic curves recorded during the measurements of the flow of heat emitted during the photoinitiated polymerization of TMPTA/MP (9/1) mixture initiated by 1,3-bis(*p*-substituted phenylamino)squaraines in presence of diphenyliodonium chloride (**I1**) as a coinitiator. The dye and coinitiator concentration was  $5 \times 10^{-3}$  M.  $I_a = 30$  mW/0.196 cm<sup>2</sup>. (R) The degree of double bond conversion recorded during the polymerization process. [Color figure can be viewed at [wileyonlinelibrary.com](http://wileyonlinelibrary.com)]

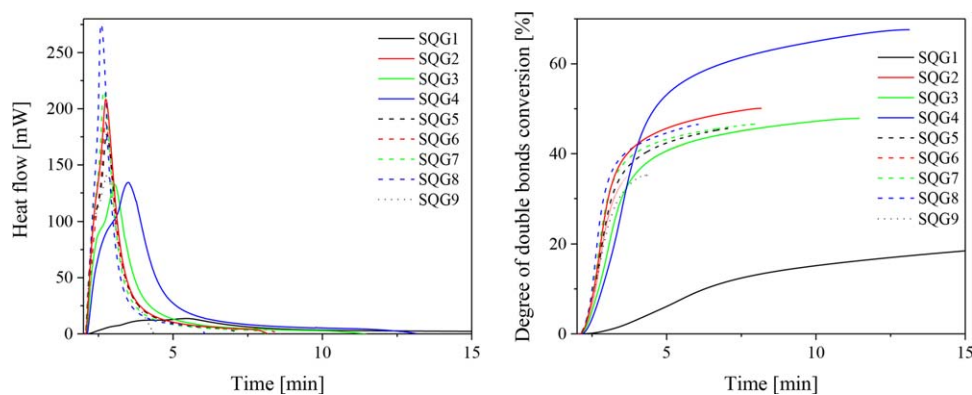


**FIGURE 4** (L): The kinetic curves recorded during the measurements of the flow of heat emitted during the photoinitiated polymerization of TMPTA/MP (9/1) mixture initiated by 1,3-bis(*p*-substituted phenylamino)squaraines in presence of *N*-methoxy-4-phenylpyridinium tetrafluoroborate (**NO**) as a coinitiator. The dye and coinitiator concentration was  $2 \times 10^{-3}$  M.  $I_a = 30$  mW/0.196 cm<sup>2</sup>. (R): The degree of double bond conversion recorded during the polymerization process. [Color figure can be viewed at [wileyonlinelibrary.com](http://wileyonlinelibrary.com)]

respectively.<sup>24</sup> Lalevée shown that the photopolymerization of trimethylolpropane triacrylate (TMPTA) in presence of BAPO in laminate and under air leads to the 5 and 60% of monomer conversion under monochromatic light of a Hg lamp (366 nm~5 mW/cm<sup>2</sup>).<sup>25</sup> The photopolymerization of an acrylate monomer (TMPTA) using a phosphine oxide as the photoinitiator in the absence or in the presence of tris(trimethylsilyl)silane (3% w/w) under 3 min of irradiation, gives the degree of monomer conversion about 10 and 45%, respectively.<sup>26</sup> The irradiation of 25 μm-thick acrylic film with xenon lamp and light intensity 110 mW/cm<sup>2</sup> under air in presence of photoinitiator BAPO/MDEA results in maximum degree of conversion about 80%.<sup>27</sup> The TMPTA polymerization under irradiation with LED at 405 nm reached of 56% of monomer conversion with the popular commercial photoinitiator BAPO.<sup>28</sup> Lai et al. in 2014 present that photopolymerization of trimethylolpropane triacrylate with photoinitiator composed of TPO (1 g) and ITX (2-isopropylthioxanthone) leads to 50% of monomer conversion.<sup>29</sup> Sehnal et al. present a range of novel phosphine oxides which show enhanced surface curing of acrylate systems

when exposed to both high pressure mercury lamps and LED's operating at 365/395 nm, without the addition of other photoinitiators.<sup>30</sup>

Acylophosphine oxides are very efficient UV-near visible light photoinitiators, but it should bear in mind, that significant disadvantage of TPO and BAPO is the strong oxygen inhibition due to the fast reaction of the phosphorous radical with oxygen.<sup>31</sup>

From the comparison presented it seen that, some of new photoinitiating systems are slightly better than those popular commercially available (TPO and BAPO), that is, are more efficient and yielded excellent final conversion of TMPTA.

#### Correlation between Kinetic Parameters and Thermodynamic Parameters

The singlet quenching rate constants were measured and they correlate well with reaction driving force as expected for an electron transfer process. Moreover, the experimental data may be fitted to a Rehm-Weller mechanism with normal parameters. This result is a further confirmation of the electron transfer occurs in the deactivation of electronically

**TABLE 2** Thermodynamic and Kinetic Parameters of Radical Polymerization of TMPTA Initiated by Systems under Study

Photoinitiator	B2		I1		NO	
	$R_p$ (mmol/s)	Monomer Conversion (%)	$R_p$ (mmol/s)	Monomer Conversion (%)	$R_p$ (mmol/s)	Monomer Conversion (%)
<b>SQG1</b>	0	0	0.15	12.27	0.53	19.96
<b>SQG2</b>	0.58	7.78	2.82	30.04	8.17	50.08
<b>SQG3</b>	0.44	20.78	1.95	36.12	5.25	47.85
<b>SQG4</b>	0.81	15.04	2.66	33.97	5.30	67.60
<b>SQG5</b>	0.90	19.07	2.20	32.64	7.05	45.69
<b>SQG6</b>	1.04	8.45	2.84	36.66	7.46	46.58
<b>SQG7</b>	1.05	17.71	2.70	27.05	8.47	46.61
<b>SQG8</b>	2.19	27.41	5.97	40.79	10.87	46.52
<b>SQG9</b>	1.38	9.07	2.21	14.42	5.60	35.19

**TABLE 3** Thermodynamic Parameters of Photoinitiating Systems under Study

Sensitizer	$E_{ox}$ (eV)	$E_{red}$ (eV)	$E_{00}$ (eV)	B2 $\Delta G_{el}$ (kJ mol <sup>-1</sup> )	I1 $\Delta G_{el}$ (kJ mol <sup>-1</sup> )	NO $\Delta G_{el}$ (kJ mol <sup>-1</sup> )
<b>SQG1</b>	0.968	-0.218	2.831	-140.90	-132.12	-122.47
<b>SQG2</b>	1.048	-0.212	2.897	-147.86	-130.78	-121.13
<b>SQG3</b>	1.102	-0.292	2.883	-138.84	-124.27	-114.62
<b>SQG4</b>	1.09	-0.258	2.696	-123.98	-107.28	-97.63
<b>SQG5</b>	0.994	-0.24	2.883	-143.86	-134.69	-125.04
<b>SQG6</b>	1.24	-0.252	2.877	-142.06	-110.31	-100.66
<b>SQG7</b>	0.89	-0.222	2.904	-147.55	-146.69	-137.04
<b>SQG8</b>	0.958	-0.236	2.932	-148.85	-142.77	-133.12
<b>SQG9</b>	1.018	-0.24	2.313	-88.83	-77.34	-67.69

excited states of squaraine dye by an electron acceptor, for example, diphenyliodonium salts. It is well known, that in squaraine-based photoinitiator systems, the initiating radicals are generated by photoinduced electron transfer. Therefore, intermolecular electron transfer between the excited dye and coinitiator must be thermodynamically allowed. Taking this into account, the values of free energy changes for electron transfer process ( $\Delta G_{el}$ ), calculated from the Rehm-Weller equation (eq. 3) must be negative.<sup>32</sup>

$$\Delta G_{el} = E_{ox}(E/E^*) - E_{red}(\text{Dye/Dye}^*) - E_{00}(\text{Dye}) - \frac{Z_1 Z_2}{\epsilon r_{12}} \quad (\text{eq. 3})$$

The value of  $\Delta G_{el}$  was calculated using the oxidation potential of tetramethylammonium *n*-butyltriphenylborate ( $E_{ox} = 1.153$  eV), the reduction potentials of diphenyliodonium chloride ( $E_{red} = -0.494$  eV) and *N*-methoxy-4-phenylpyridinium tetrafluoroborate ( $E_{red} = -0.594$  eV), the singlet excited state energy [ $E_{00}(S)$ ] of the dyes (Table 3) and the reduction and oxidation potentials of sensitizers (see data in Table 3). The Coulombic energy coefficient ( $Z_1 Z_2 / \epsilon r_{12}$ ) was omitted in these calculations because the neutral radicals of coinitiator as well as sensitizers were formed in an electron transfer process. The oxidation potential ( $E_{ox}$ ) and reduction potential ( $E_{red}$ ) of both photoredox pair components were determined using CV measurements (Table 3).

The value of energy transition between the lowest ground state and the lowest excited state ( $E_{00}$ ) was determined from the intersection of normalized absorption and fluorescence spectra of photosensitizer (Table 3). The typical result of CV measurements of squaraine dyes is presented in case of the ethyl and ethoxy-substituted dyes **SQG3** and **SQG4** in Figure 5.

As it is seen, there is one reduction process of the central squaric ring unit and two oxidation processes. For **SQG3** in acetonitrile the half-wave potential of the reduction is at a rather high potential of -1.102 eV and those of the oxidations at 0.292 and 1.134 eV. The redox properties of *p*-ethoxy substituted squaraine are similar and equal -1.09, 0.258, and 1.086 eV, respectively.

The electrochemical measurements revealed that the reduction and both oxidations are chemically irreversible.

Taking this into account, the thermodynamic parameters presented in Table 3, it is seen that all combinations of squaraine/coinitiator photoinitiating systems possess high value of driving forces for electron transfer process from -148.85 to -67.69 kJ/mol upon exposure to light. The lowest values of  $\Delta G_{el}$  were observed in the case of systems composed of tetramethylammonium *n*-butyltriphenylborate and are in range

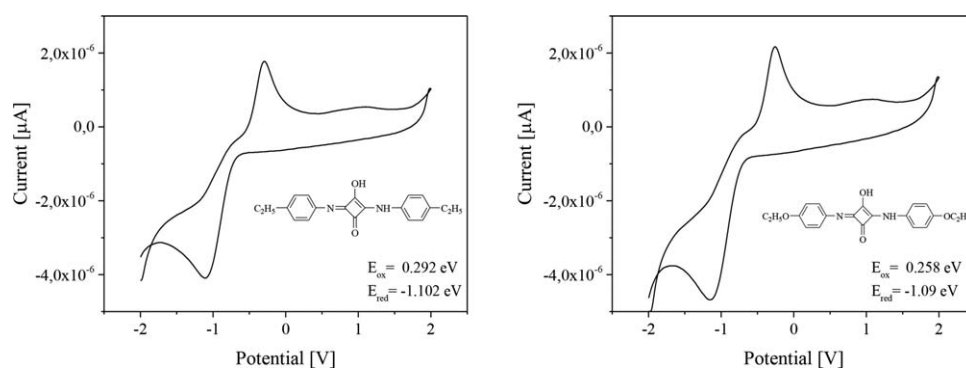


**FIGURE 5** Cyclic voltammograms of 1,3-bis(*p*-ethylphenylamino)squaraine (Left) and 1,3-bis(*p*-ethoxyphenylamino)squaraine (Right) in 0.1 M tetrabutylammonium perchlorate solution in dry acetonitrile as the supporting electrolyte.

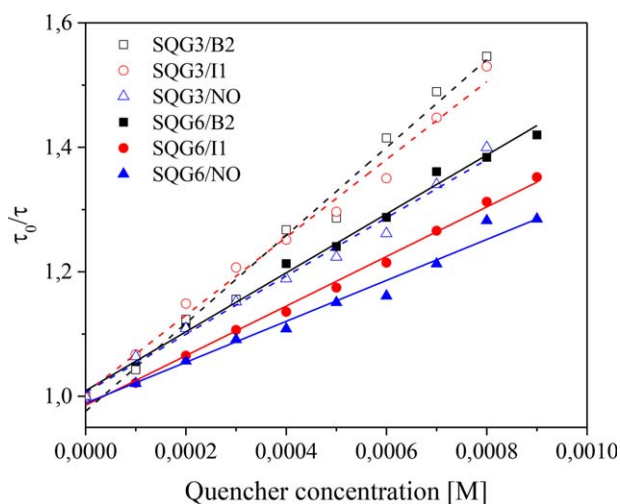


**FIGURE 6** The Stern-Volmer plots for the quenching of fluorescence of 1,3-bis(*p*-ethylphenylamino)squaraine (**SQG3**) (open points) and 1,3-bis(*p*-bromophenylamino)squaraine (**SQG6**) (solid points) by borate salt (**B2**), diphenyliodonium salt (**I1**) and *N*-alkoxy-pyridinium salt (**NO**), respectively. [Color figure can be viewed at [wileyonlinelibrary.com](http://wileyonlinelibrary.com)]

from  $-148.85$  to  $-88.83$  kJ/mol. The highest values of free energy change for electron transfer process were obtained for photoinitiating systems composed of *N*-methoxy-4-phenylpyridinium tetrafluoroborate. In this case, the  $\Delta G_{ei}$  varies from  $-137.04$  to  $-67.69$  kJ/mol.

Basing on the thermodynamic parameters one can conclude, that the best photoinitiators should be systems composed of borate salt. The kinetic results shown quite different relationship. The photoinitiating systems that possess higher values of free energy change for electron transfer initiate free radical polymerization of TMPTA with highest rates. But if we compare, the photoinitiating ability with the value of  $\Delta G_{ei}$  for only one type coinitorator, it is clear that the photoinitiators with the most negative values of free energy change of electron transfer are the best photoinitiating systems. Taking this into account it may be stated, that both the reactivity of free radicals and the rate of electron transfer process influence on the photoinitiating ability of photoinitiators studied.

#### Interactions between an Excited Singlet State of Sensitizer and Coinitiator

To understand the interactions between an excited singlet state of sensitizer and coinitorator, the fluorescence quenching experiments were performed. The quenching of the singlet excited state of squaraine dye by all coinitorators used was investigated using time-resolved fluorescence spectroscopy and nanosecond laser flash photolysis. All coinitorators used are not fluorescent compounds. 1,3-Bis(*p*-substituted phenylamino)squaraines exhibit a fluorescence emission. Figure 6 shows the Stern-Volmer plots for the quenching of fluorescence of selected squaraines (**SQG3** and **SQG6**) by **B2**, **I1**, and **NO**, respectively.

The data presented above show that tetramethylammonium *n*-butyltriphenylborate, diphenyliodonium chloride, and *N*-methoxy-4-phenylpyridinium tetrafluoroborate strongly interact with singlet fluorescent state of photosensitizer.

As it was previously observed for other squaraines,<sup>7</sup> the rate of dynamic quenching of the excited singlet state depends on the type of quencher used. From the data presented in Figure 6, it is seen the linear relationship between changes in the fluorescence lifetime and concentration of quencher. The results of Stern-Volmer relationship are summarized in Table 4.

The slopes of Stern-Volmer linear relationship are as follows: 473.24, 398.33, 328.92 for (**SQG6**) and 706.39, 625.44, and 467.61 for (**SQG3**) by (**B2**), (**I1**), and (**NO**), respectively.

Taking into account the fluorescence lifetimes for both photosensitizers:  $5.77 \times 10^{-9}$  s and  $6.24 \times 10^{-9}$  s from Stern-Volmer relationship, the rate constants of fluorescence quenching reaction were obtained to be  $8.19 \times 10^{10} \text{ M}^{-1}\text{s}^{-1}$ ,  $6.89 \times 10^{10} \text{ M}^{-1}\text{s}^{-1}$  and  $5.69 \times 10^{10} \text{ M}^{-1}\text{s}^{-1}$  for dye (**SQG6**) and  $11.32 \times 10^{10} \text{ M}^{-1}\text{s}^{-1}$ ,  $10.023 \times 10^{10} \text{ M}^{-1}\text{s}^{-1}$  and  $7.49 \times 10^{10} \text{ M}^{-1}\text{s}^{-1}$  for dye (**SQG3**) by coinitorators: (**B2**), (**I1**), and (**NO**), respectively, which are nearly one order of magnitude higher than that of diffusion controlled bimolecular reaction constant ( $\sim 2 \times 10^9 \text{ M}^{-1}\text{s}^{-1}$ ). These results confirmed that the coinitorators under study are very effective fluorescence quenchers for excited (SQ) dye and the fast quenching occurs predominantly through the intramolecular ion-pair pathway. Therefore, the quenching mechanism in squarylum dye/coinitorator system might be an electron transfer process.

From the fluorescence quenching results it is also seen, that photoinitiators possessing lower values of the fluorescence rate constants better initiate radical polymerization of triacrylate. The  $k_q\tau_0$  of dye/borate salt is much higher than that of dye/diphenyliodonium salt and dye/*N*-methoxy-pyridinium salt.

#### Mechanism of Free Radicals Formation: Nanosecond Laser Flash Photolysis

In the first step of the mechanism of generation of active species, 1,3-bis(*p*-substituted phenylamino)squaraine becomes excited by absorption of light of an appropriate wavelength. The photoexcited squaraine molecule, encounters an coinitorator

**TABLE 4** The Values of Stern-Volmer Constant ( $K_{sv}$ ) and Rate Constant of Fluorescence Quenching

Quencher	Photosensitizer			
	SQG3		SQG6	
	$K_{sv}$	$k_q \times 10^{-10} \text{ (M}^{-1}\text{s}^{-1}\text{)}$	$K_{sv}$	$k_q \times 10^{-10} \text{ (M}^{-1}\text{s}^{-1}\text{)}$
<b>B2</b>	706.39	11.32	473.24	8.19
<b>I1</b>	625.44	10.023	398.33	6.89
<b>NO</b>	467.61	7.49	328.92	5.96

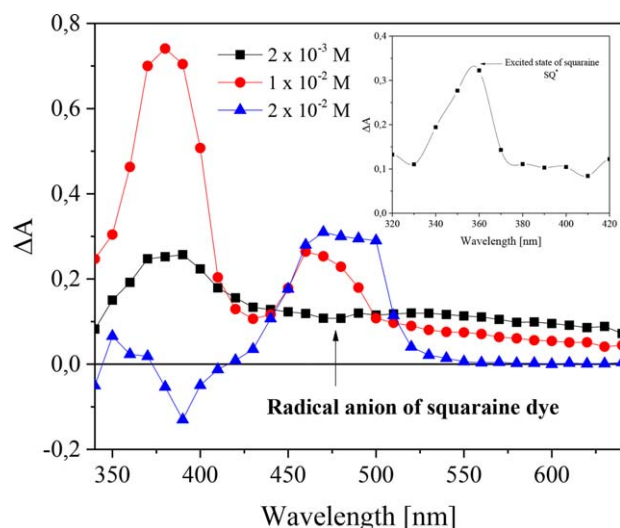


**FIGURE 7** Transient absorption spectra of 1,3-bis(*p*-bromophenylamino)squaraine in presence of tetramethylammonium *n*-butyltriphenylborate (**B2**) recorded: 2 ns (squares, circles) and 100 ns (triangles) after laser pulse. Inset: Transient absorption spectra of squaraine dye recorded 100 ns after laser pulse (circles) in acetonitrile solution. Coinitiator concentration is marked in the Figure. [Color figure can be viewed at [wileyonlinelibrary.com](http://wileyonlinelibrary.com)]

molecule, and accepts/donates an electron from/to coinitiator, forming the photosensitizer-based radical anion or radical cation, respectively.

In other words, the first step of the photoreaction occurs between squarylum dye and coinitiator. The coinitiator reacts either as an electron donor or electron acceptor with an excited state of dye.

Because the squaraines under study undergo both the photo-reduction and photooxidation, the photosensitizer may play a role of an electron acceptor as well as an electron donor. The role of photosensitizer depends on the type of coinitiator used. Therefore, two different mechanism of free radicals formation may be observed, for example, photooxidizable and photoreducible.

It should be noted, that this primary photochemical reaction occurring in photoinitiating systems under study is not only driving factors affecting the reactivity. The complex set of reactions occurring after the primary electron-transfer reaction, in which initiating radicals are formed, is likely to have a strong effect on the ability of the photoinitiating system to initiate the polymerization.

### The Photoinduced Oxidative Cleavage Squaraine/Borate Salt

Tetraorganylborate salts may be oxidized by several photoexcited oxidizing agents to release free radicals that may be used to initiate chain polymerization.<sup>33</sup> There are many examples of two-component photoinitiating systems working through electron transfer process composed of organic

borate salts. Polymethine dyes, 2,4-diiodo-6-butoxy-3-fluorone, 5,7-diiodo-3-butoxy-6-fluorone, xanthenes, fluorones, benzophenone were used as photosensitizers in such photoinitiating systems.<sup>34–39</sup> The generation of initiating radicals is a result of decomposition of unstable boranyl radical formed after electron transfer process from borate anion to an excited singlet state of photosensitizer.

The transient absorption spectra of squaraine dye in the presence of tetramethylammonium *n*-butyltriphenylborate (**B2**) in acetonitrile solution is shown in Figure 7. As it is seen, the irradiation of squaraine in acetonitrile solution, with 5 ns laser pulse results in instantaneous appearance of its excited state, which is characterized by absorption at 380 nm. The rate constant of excited state formation is equal  $2.48 \times 10^8 \text{ s}^{-1}$ . The time of decay of excited state, and the rate constant of the decay of excited state are about 2.33  $\mu\text{s}$  and  $4.29 \times 10^5 \text{ s}^{-1}$ , respectively. The lifetime of  $\text{SQ}^*$  is decreasing as concentration of borate salt increases. In other words,  $\text{SQ}^*$  is quenched by tetramethylammonium *n*-butyltriphenylborate, and a new transient with absorption at 480–500 nm is simultaneously formed. The new transient can be assigned to radical anion of squaraine dye. At the same time, the disappearance of the band corresponding to the absorption of the dye in the ground state is observed (Fig. 7).

The rate constant,  $k_q$  for the quenching of the excited state of squaraine dye by borate salt was determined in MeCN solution. The  $k_q$  value was obtained by monitoring the excited state absorption decays of  $\text{SQ}^*$  at 380 nm for various quencher concentrations by employing the Stern-Volmer equation. The established value of this rate constant is equal  $3.31 \times 10^7 \text{ mol}^{-1} \text{ s}^{-1}$ . The time of formation of squaraine dye-based radical anion and its disappearance is equal 10 ns and 1.14  $\mu\text{s}$  and its graphical presentation is shown in Figure 8.

Basing on the laser flash photolysis results and fluorescence quenching experiments the following mechanism of primary and secondary processes occurring in two-component photoinitiating system composed of squaraine dye/tetramethylammonium *n*-butyltriphenylborate is presented in Scheme 1.

### The Photoinduced Reductive Cleavage Squaraine/Iodonium Salt

Iodonium salts are among the main class of photoinitiators for cationic polymerizations.<sup>40</sup> Unfortunately, these compounds have absorption band in the UV region and are efficient photoinitiators of cationic polymerizations when irradiation is performed in UV region (230–300 nm). Many scientific papers have dealt with the mechanism of active species generation when synthetic dyes are employed as sensitizers in binary photoinitiating systems. Generally, an electron transfer and/or energy transfer from the photoexcited sensitizer to the iodonium cation were suggested as the first reaction step in the initiation mechanism.

In presence of photosensitizers, the iodonium salts act via photooxidizable mechanism in the visible light region.<sup>40–43</sup>

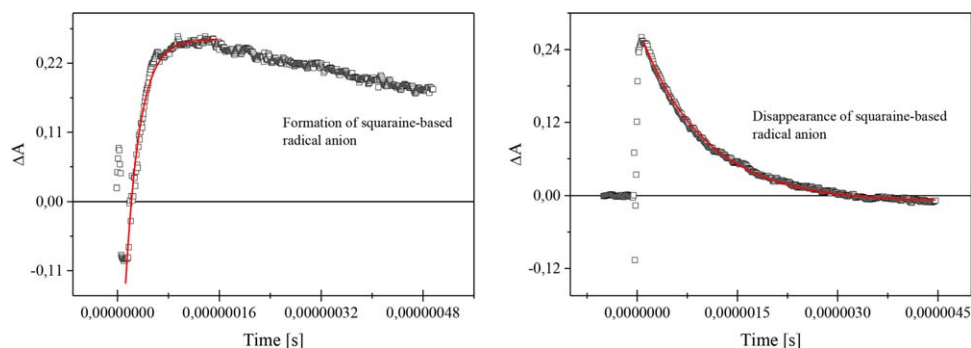
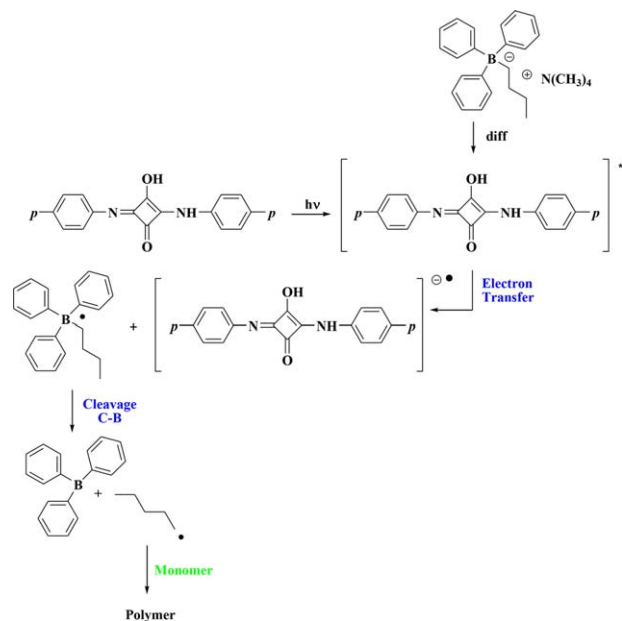


**FIGURE 8** The kinetic traces recorded at 480 nm for different delay times: 2 and 500 ns observed after irradiation of squaraine in presence of tetramethylammonium *n*-butyltriphenylborate (**B2**). Coinitiator concentration was  $1 \times 10^{-2}$  M. [Color figure can be viewed at wileyonlinelibrary.com]

In one of proposed mechanism, the iodonium salt and photosensitizer undergo bimolecular reaction via electron transfer from dye molecule, to form a dye-based radical cation and diphenyliodonium radical.<sup>44</sup> This reaction generally involves electron transfer from the photoexcited triplet state of dye to the iodonium cation, followed by rapid decomposition of iodonium radical.<sup>33</sup> The onium radical formed fragments on iodobenzene and phenyl radical. The phenyl radicals are active for initiation. The onium salts are generally used in three-component photoinitiating systems for vinyl radical polymerization.

The transient absorption spectra of squaraine in the presence of diphenyliodonium chloride is presented in Figure 9.

The lifetime of an excited state of squaraine  $SQ^*$  decreases as concentration of diphenyliodonium salt increases.



**SCHEME 1** Mechanism of primary and secondary processes occurring in two-component photoinitiating system composed of squaraine dye/tetramethylammonium *n*-butyltriphenylborate. [Color figure can be viewed at wileyonlinelibrary.com]

Therefore,  $SQ^*$  is quenched by diphenyliodonium chloride and a new transient with absorption at 510 nm is simultaneously formed. The new transient can be assigned to radical cation of squaraine dye.

The rate constant  $k_q$  for the quenching of the excited state of squaraine dye by iodonium salt was determined in MeCN solution. The  $k_q$  value was obtained by monitoring the excited state absorption decays of  $SQ^*$  at 380 nm for various quencher concentrations by employing the Stern-Volmer equation. The established value of this rate constant is equal  $3.30 \times 10^6 \text{ mol}^{-1} \text{ s}^{-1}$ . The time of formation of squaraine dye-based radical cation and its disappearance is equal 14 and 260 ns and its graphical presentation is shown in Figure 10.

Basing on the laser flash photolysis results and fluorescence quenching experiments the following mechanism of primary and secondary processes occurring in two-component photoinitiating system composed of squaraine dye/diphenyliodonium chloride presented in Scheme 2 was proposed.

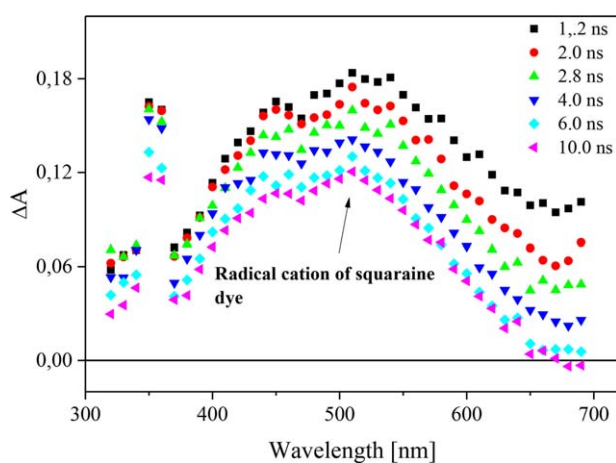


**FIGURE 9** Transient absorption spectra of 1,3-bis(*p*-bromophenylamino)squaraine in presence of diphenyliodonium chloride (**11**) recorded at different delay times after laser pulse. Coinitiator concentration was equal  $5 \times 10^{-4}$  M. [Color figure can be viewed at wileyonlinelibrary.com]

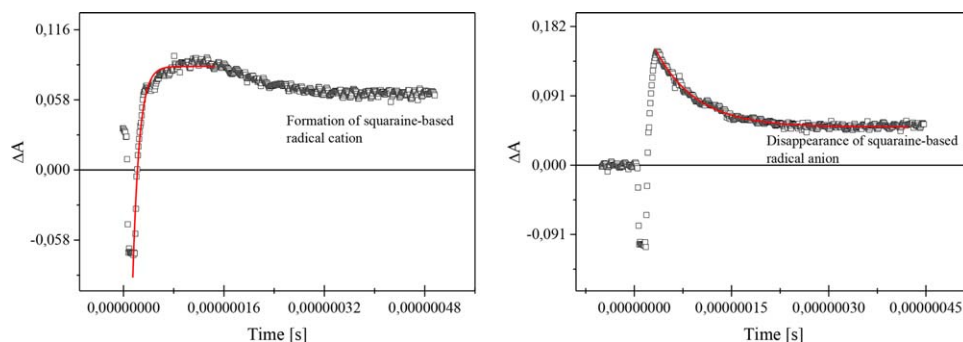
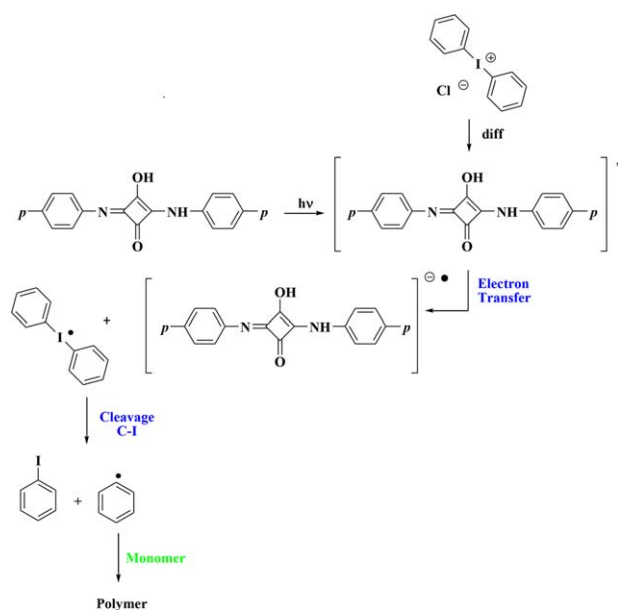


**FIGURE 10** The kinetic traces recorded at 480 nm for different delay times: 2 and 50 ns observed after irradiation of squaraine in presence of diphenyliodonium chloride (**I1**). Coinitiator concentration was  $5 \times 10^{-4}$  M. [Color figure can be viewed at wileyonlinelibrary.com]

### Dye/*N*-Alkoxyppyridinium Salts

*N*-Alkoxyppyridinium salts are very effective initiators for cationic polymerization of cyclic ethers and alkyl vinyl ethers upon irradiation at 300 nm where they are light-absorbing.<sup>45</sup> These compounds can act directly provided if they are light-absorbing. However, *N*-alkoxyppyridinium salts may act via the oxidation of photochemically or thermally generated free radicals by onium ions.<sup>46</sup> When polymerization is carried out with irradiation above 360 nm the application of suitable compound acting as a free radical source, that is, decomposing into free radicals is necessary.<sup>46</sup> Benzoin is such a compound. It decomposes spontaneously into benzoyl and hydroxybenzyl radicals after absorption of a photon. The initiation is assumed to proceed by direct action of light, that is, pyridinium radical cations are generated via homolytic scission of the N—O bond.<sup>45,46</sup>



**SCHEME 2** Mechanism of primary and secondary processes occurring in two-component photoinitiating system composed of squaraine dye/diphenyliodonium chloride. [Color figure can be viewed at wileyonlinelibrary.com]

However, the dye-sensitized fragmentation of *N*-alkoxyppyridinium salt may be used for initiation of free radical polymerization.<sup>47–49</sup> This type of photoinitiation system acts via photoinduced electron transfer process. Single electron transfer from excited dye to *N*-alkoxyppyridinium salt leads to reductive cleavage of the N—O bond to give an alkoxy radical that can initiate radical polymerization.<sup>50</sup>

The driving force for the fragmentation reaction in this case results from formation of a stable pyridine molecule.<sup>50</sup> The *N*-alkoxyppyridinium salts have been proven to be effective with a wide range of sensitizers (e.g., coumarin dyes, cyanines, oxanols, squarines, and fluoflavines) and excitation wavelengths.<sup>50–56</sup>

The transient absorption spectra of squaraine dye in the presence of *N*-methoxy-4-phenylpyridinium tetrafluoroborate is presented in Figure 11.

The excited state of photosensitizer is also quenching by *N*-methoxy-4-phenylpyridinium tetrafluoroborate. In this case

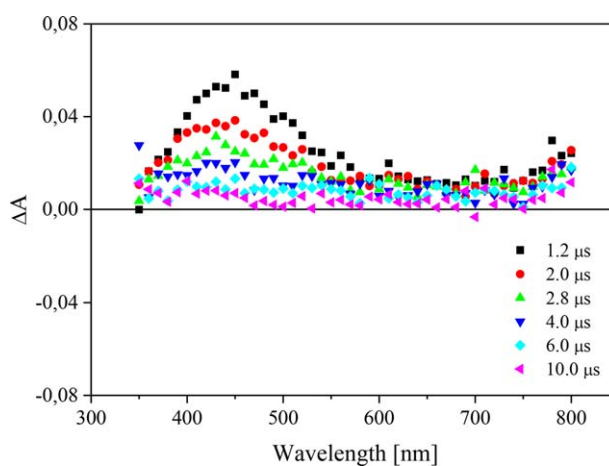


**FIGURE 11** Transient absorption spectra of 1,3-bis(*p*-bromo-phenylamino)squaraine in presence of *N*-methoxy-4-phenylpyridinium tetrafluoroborate (**NO**) recorded at different delay times after laser pulse. Coinitiator concentration was equal  $2 \times 10^{-2}$  M. [Color figure can be viewed at wileyonlinelibrary.com]

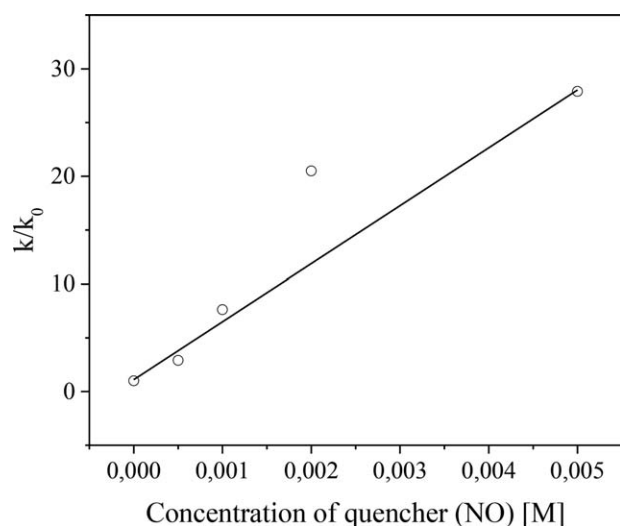


**FIGURE 12** The Stern-Volmer relationship for the quenching of an excited state of squaraine by *N*-methoxy-4-phenylpyridinium salt (**NO**) in acetonitrile solution.

the formation of new absorption band at 480–500 nm is observed. The time of formation of new product and its disappearance is equal 20 ns and 1.47  $\mu$ s, respectively. New absorption band is attributed to the absorption of squaraine dye-based radical cation formation. Simultaneously, the disappearance of the band at 380 nm is observed. The established value of quenching rate constant is equal  $2.31 \times 10^6$

$\text{mol}^{-1} \text{s}^{-1}$ . Figure 12 shows the Stern-Volmer plot for the excited state quenching by *N*-alkoxyppyridinium salt.

Similarly, as it was presented above, the mechanism of free radicals formation during irradiation of two-component photoinitiating system composed of squaraine dye/*N*-methoxyppyridinium salt shown in Scheme 3 was proposed.

In summary, the reaction of squaraine (SQ\*) with a coinitiator (electron donor or electron acceptor) competes with the deactivation reactions of the excited dye. The rate of reactions is determined by the concentration of the coinitiator and the rate constant for an electron transfer reaction. The rate of deactivation of an excited state of photosensitizer is determined by the sum of all radiative and nonradiative decay paths of squaraine dye in excited state. The next competing process is the fragmentation of the boranyl radical, diphenyliodonium radical and *N*-methoxy-4-phenylpyridyl radical, giving butyl radical, phenyl radical, and methoxy radical, and return electron transfer, which is an energy-wasting process that regenerates the starting materials.

Taking into account the kinetic results one can conclude that the reactivity order of initiating radicals, under experimental conditions, is as follows: methoxy, phenyl, and butyl.

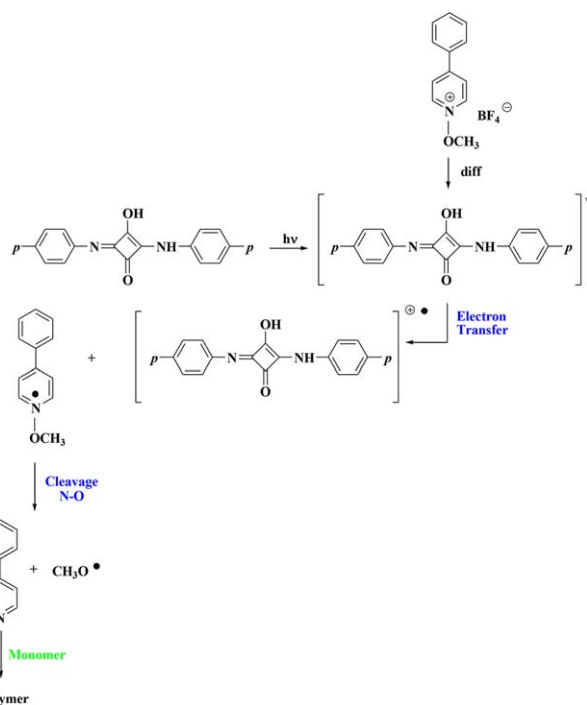
## CONCLUSIONS

In this article, the efficiency of UV-blue light induced polymerization of trifunctional acrylate in the presence of two-component photoinitiating systems based on squaraine dye and three different coinitiators (borate salt, iodonium salt, and *N*-alkoxyppyridinium salt) was ascertained.

It was found that the squaraine dye/coinitiator combination undergoes photoreaction via intermolecular electron transfer, resulting in generation of active radical species by subsequent decomposition of coinitiator-based radical. The efficiency of tetramethylammonium *n*-butyltriphenylborate (**B2**) as a coinitiator is lowest than that of diphenyliodonium chloride (**I1**) and *N*-methoxy-4-phenylpyridinium tetrafluoroborate (**NO**). The photoinitiating systems, possessing squaraine and pyridinium salt initiate free radical polymerization 3–4 times faster in comparison to system composed of borate salts.

The kinetic results obtained, shown that the systems composed of squaraine dye and diphenyliodonium salt or *N*-methoxyppyridinium salt may be considered as an attractive alternative for two-component UV-near visible light commercially available photoinitiators.

Basing on the kinetic results and the laser flash photolysis experiment, the mechanism of reactions occurring in the photoinitiating systems composed of squaraine, borate salt, iodonium salt and *N*-alkoxyppyridinium salt was proposed. After irradiation of the photoinitiator with a UV-visible light, the excited state of photosensitizer is formed. The deactivation of an excited state occurs by radiative and nonradiative processes, for example: an electron transfer process. In



**SCHEME 3** Mechanism of primary and secondary processes occurring in two-component photoinitiating system composed of squaraine dye/*N*-methoxy-4-phenylpyridinium salt. [Color figure can be viewed at [wileyonlinelibrary.com](http://wileyonlinelibrary.com)]

presence of borate salt, the squaraine undergoes one-electron reduction. The squaraine-based radical anion and boranyl radical are formed. The boranyl radical undergoes C-B bond cleavage, giving butyl radical that can start the polymerization reaction. In this system the photoreducible sensitization occurs. However, in the presence of diphenyliodonium salt or *N*-methoxy-4-phenylpyridinium salt, an electron transfer from the excited state of squaraine to the ground state of diphenyliodonium cation or *N*-methoxy-4-phenylpyridinium cation, giving squaraine-based radical cation and diphenyliodonium radical and *N*-methoxy-4-phenylpyridinium radical occurs. The latter undergo fast fragmentation forming the iodobenzene and phenyl radical as a result of C–I bond cleavage, and methoxy radical and stable 4-phenylpyridine as a result of N–O bond cleavage. In such photoinitiating systems the photooxidizable sensitization occurs. These reactions generate free radicals, which can start the polymerization chain reaction. The photoinitiating ability depends on the reactivity of free radical and increases in following order: butyl radical, phenyl radical, and methoxy radical.

#### ACKNOWLEDGMENTS

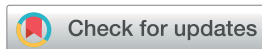
This work was supported by The National Science Centre (NCN) (Cracow, Poland), Grant No. 2013/11/B/ST5/01281.

#### REFERENCES AND NOTES

- 1 K. D. Volkova, V. B. Kovalska, A. L. Tatarets, L. D. Patsenker, D. V. Kryvorotenko, S. M. K. Yarmoluk, *Dyes Pigments* **2007**, *72*, 285–292.
- 2 J. Fabian, *Chem. Rev.* **1992**, *92*, 1197–1226.
- 3 F. Welder, B. Paul, H. Nakazumi, S. Yagi, C. L. Colyer, *J. Chromatogr. B* **2003**, *793*, 93–105.
- 4 Y. He, W. Zhou, F. Wu, M. Li, E. Wang, *J. Photochem. Photobiol. A* **2004**, *162*, 463–471.
- 5 P. Xiao, F. Dumur, T. T. Bui, F. Goubard, B. Graff, F. Morlet-Savary, J. P. Fouassier, D. Gigmes, J. Lalevée, *ACS Macro. Lett.* **2013**, *2*, 736–740.
- 6 P. Xiao, J. Zhanga, F. Dumur, M. A. Tehfe, F. Morlet-Savary, B. Graff, D. Gigmes, J. P. Fouassier, J. Lalevée, *Prog. Polym. Sci.* **2015**, *41*, 32–66.
- 7 J. Kabatc, K. Kostrzewska, K. Jurek, R. Dobosz, Ł. Orzeł, *Dyes Pigments* **2016**, *127*, 179–186.
- 8 K. Jurek, J. Kabatc, K. Kostrzewska, *Dyes Pigments* **2016**, *133*, 273–279.
- 9 R. Daminco, *J. Org. Chem.* **1964**, *29*, 1971–1976.
- 10 M. L. Gómez, C. M. Previtali, H. A. Montejano, *Int. J. Photoenergy.* **2012**, 1–9.
- 11 M.V. Encinas, E.A. Lissi, *Polymeric Materials Encyclopedia*, vol. 7; Edited by J.C. Salomone, Ed.; CRC: Boca Raton, Florida, USA, **1996**.
- 12 C. M. Previtali, S. G. Bertolotti, M. G. Neumann, I. A. Pastre, A. M. Rufs, M. V. Encinas, *Macromolecules* **1994**, *27*, 7454–7458.
- 13 M. V. Encinas, A. M. Rufs, M. G. Neumann, C. M. Previtali, *Polymer* **1996**, *37*, 1395–1398.
- 14 L. Villegas, M. V. Encinas, A. M. Rufs, C. Bueno, S. Bertolotti, C. M. Previtali, *J. Polym. Sci. Part A: Polym. Chem.* **2001**, *39*, 4074–4082.
- 15 S. Chatterjee, P. Gottschalk, P. D. Davis, G. B. Schuster, *J. Am. Chem. Soc.* **1988**, *110*, 2326.
- 16 S. Murphy, X. Yang, G. B. Schuster, *J. Org. Chem.* **1995**, *60*, 2411.
- 17 M. V. Encinas, C. M. Previtali, S. G. Bertolotti, M. Neumann, *Photochem. Photobiol. A* **1995**, *62*, 65–70.
- 18 G. Porcal, S. G. Bertolotti, C. M. Previtali, M. V. Encinas, *Phys. Chem. Chem. Phys.* **2003**, *5*, 4123–4128.
- 19 M. G. Neumann, C. C. Schmitt, C. M. Previtali, S. G. Bertolotti, *Dyes Pigments* **1996**, *32*, 93–99.
- 20 C. Bueno, M. L. Villegas, S. G. Bertolotti, C. M. Previtali, M. G. Neumann, M. V. Encinas, *Photochem. Photobiol. A* **2002**, *76*, 385–390.
- 21 J. Kabatc, J. Pączkowski, *J. Appl. Polym. Sci.* **2010**, *117*, 2669–2675.
- 22 J. Kabatc, M. Pietrzak, J. Pączkowski, *J. Chem. Soc., Perkin Trans.* **2002**, *2*, 287–295.
- 23 J. Kabatc, M. Kaczorowska, B. Jędrzejewska, J. Pączkowski, *J. Appl. Polym. Sci.* **2008**, *108*, 1636–1645.
- 24 S. Keskin, S. Jockusch, N. J. Turro, N. Arsu, *Macromolecules* **2008**, *41*, 4631–4634.
- 25 J.P. Fouassier, J. Lalevée, *Photoinitiators for Polymer Synthesis: Scope, Reactivity, and Efficiency*; Wiley-VCH: Weinheim, Germany, **W2012**, p 163.
- 26 M. A. Tehfe, F. Louradour, J. Lalevée, J. P. Fouassier, *Appl. Sci.* **2013**, *3*, 490–514.
- 27 F. Mauguière, M. Dossot, H. Obeid, D. Burget, J.P. Fouassier, A. Merlin, *Photochemistry and UV Curing: New Trends*; J.P. Fouassier, Ed.; Research Signpost: India, **2006**; p 141–152.
- 28 N. Zivic, J. Zhang, D. Bardelang, F. Dumur, P. Xiao, T. Jet, D.-L. Versace, C. Dietlin, F. Morlet-Savary, B. Graff, J. P. Fouassier, D. Gigmes, J. Lalevée, *Polym. Chem.* **2016**, *7*, 418–429.
- 29 W. Lai, X. Li, H. Liu, L. Han, Y. Zhao, X. Li, *J. Chem.* **2014**, 1–6.
- 30 P. Sehnal, K. Harper, A.T. Rose, D.G. Anderson, W.A. Green, B. Husár, M. Griesser, R. Liska, *Novel Phosphine Oxide Photoinitiators*; RadTech Conference, Rosemont, **2014**.
- 31 G. W. Sluggett, P. F. McGarry, I. V. Koptuyg, N. J. Turro, *J. Am. Chem. Soc.* **1996**, *118*, 7367.
- 32 D. Rehm, A. Weller, *Isr. J. Chem.* **1970**, *8*, 259.
- 33 A. M. Sarker, A. Y. Polykarpov, A. M. De Raaff, T. L. Marino, D. C. Neckers, *J. Polym. Sci. Part A: Polym. Chem.* **1996**, *34*, 2817–2824.
- 34 O. M. Valdes-Aguilera, C. P. Pathak, J. Shi, D. Watson, D. C. Neckers, *Macromolecules* **1992**, *25*, 541–547.
- 35 S. Hassoon, D. C. Neckers, *J. Phys. Chem.* **1995**, *99*, 9416–9424.
- 36 A. M. Sarker, A. Lungu, D. C. Neckers, *Macromolecules* **1996**, *29*, 8047–8052.
- 37 A. Y. Polykarpov, S. Hassoon, D. C. Neckers, *Macromolecules* **1996**, *29*, 8274–8276.
- 38 J. Kabatc, M. Pietrzak, J. Pączkowski, *Macromolecules* **1998**, *31*, 4651–4654.
- 39 J. Kabatc, J. Pączkowski, *J. Polym. Sci. Part A: Polym. Chem.* **2009**, *47*, 4636–4654.
- 40 M. L. Gómez, C. M. Previtali, H. A. Montejano, *Polymer* **2007**, *48*, 2355–2361.
- 41 R. Podsiadły, A. Maruszewska, R. Michalski, A. Marcinek, J. Kolińska, *Dyes Pigments* **2012**, *95*, 252–259.

- 42** J. Kolińska, R. Podsiadły, J. Sokołowska, *Coloration Technol.* **2008**, *124*, 341–347.
- 43** D. Kim, A. B. Scranton, *J. Polym. Sci. Part A: Polym. Chem.* **2004**, *42*, 5863–5871.
- 44** K. S. Padon, A. B. Scranton, *J. Polym. Sci. Part A: Polym. Chem.* **2000**, *38*, 2057–2066.
- 45** Y. Yağci, A. Kornowski, W. Schnabel, *J. Polym. Sci. Part A: Polym. Chem.* **1992**, *30*, 1987–1991.
- 46** P. Monecke, W. Schnabel, Y. Yağci, *Polymer* **1997**, *38*, 5389–5395.
- 47** J. Kabatc, J. Pączkowski, *Macromolecules* **2005**, *38*, 9985–9992.
- 48** J. Kabatc, J. Pączkowski, *Polymer* **2006**, *47*, 2699–2705.
- 49** J. Kabatc, J. Pączkowski, *J. Photochem. Photobiol. A* **2006**, *184*, 184–192.
- 50** I. R. Gould, D. Shukla, D. Giesen, S. Farid, *Helv. Chim. Acta* **2001**, *84*, 2796–2812.
- 51** E. D. Lorange, W. H. Kramer, I. R. Gould, *J. Am. Chem. Soc.* **2004**, *126*, 14071–14078.
- 52** R. Podsiadły, *J. Photochem. Photobiol. A* **2008**, *198*, 60–68.
- 53** J. Fu, L. A. Padilha, D. J. Hagan, E. W. Van Stryland, O. V. Przhonska, M. V. Bondar, Y. L. Slominsky, A. D. Kachkovski, *J. Opt. Soc. Am. B* **2007**, *24*, 67–76.
- 54** S. Dadashu-Silab, S. Doran, Y. Yağci, *Chem. Rev.* **2016**, *40*, 10212–10275.
- 55** N. Carrigan, S. Shanmugan, J. Xu, C. Boyer, *Chem. Soc. Rev.*, **2016**, *45*, 6165–6212.
- 56** Q. Wu, X. Wang, Y. Xiong, J. Yanga, H. Tang, *RSC Adv.* **2016**, *6*, 66098–66107.

**Publikacja naukowa [A4]**


 Cite this: *RSC Adv.*, 2020, 10, 24817

# Onium salts improve the kinetics of photopolymerization of acrylate activated with visible light

 Janina Kabatc,<sup>id</sup>\*<sup>a</sup> Katarzyna Iwińska,<sup>a</sup> Alicja Balcerak,<sup>a</sup> Dominika Kwiatkowska,<sup>a</sup> Agnieszka Skotnicka,<sup>a</sup> Zbigniew Czech<sup>b</sup> and Marcin Bartkowiak<sup>b</sup>

The aim was study the influence of onium salts on the kinetics of photopolymerization in the visible light region. Trimethylolpropane triacrylate TMPTA was selected as a monomer, and activated by 1,3-bis(phenylamino)squaraine (SQ) used as a photosensitizer in addition to tetramethylammonium *n*-butyltriphenylborate (B2). The iodonium salt [A–I–B]<sup>+</sup>X<sup>–</sup> functioned as a second radical initiator, bearing a different substitution pattern for the cation. The ternary system was formulated with different concentrations of both borate and diphenyliodonium salts. Differential scanning calorimetry was used to investigate the polymerization reaction over the photoactivation time carried out at 300 nm < λ < 500 nm irradiation. When the squaraine dye/borate salt was used as photoinitiator, a slow polymerization reaction was observed and a lower monomer conversion. The addition of a third component (onium salt) increased the polymerization rate and conversion. Ternary photoinitiator systems showed improvement in the polymerization rate of triacrylate leading to high conversion in a short photoactivation time. The photoinitiating ability of bi- and tri-component photoinitiators acting in the UV-Vis region for initiation polymerization of triacrylate was compared with those of some commercially used photoinitiating systems. It was also found, that, the parallel electron transfer from an excited state of the sensitizer to [A–I–B]<sup>+</sup>X<sup>–</sup>, and an electron transfer from a ground state of R(Ph)<sub>3</sub>B<sup>–</sup>N(CH<sub>3</sub>)<sub>4</sub><sup>+</sup> to an excited state of the sensitizer results in two types of initiating radical.

 Received 28th April 2020  
 Accepted 18th June 2020

DOI: 10.1039/d0ra03818k

[rsc.li/rsc-advances](http://rsc.li/rsc-advances)

## Introduction

One of the modern and rapidly developing technologies is production of various types of polymeric materials in polymerization reaction. That process may be initiated, for example photochemically or thermally. The light activated polymerization is called photopolymerization. This process is characterized by: (i) low energy consumption, (ii) the possibility of using non-solvent compositions, (iii) high efficiency, and others.<sup>1,2</sup> The photopolymerization occurs *via* radical (radical polymerization RP) or ionic mechanisms (cationic/anionic polymerization CP/AP). A photoinitiator plays a key role in radical initiated chain reaction. Because of this, many research groups still design new or improve known photoinitiators, especially those operating in the visible region of the spectrum.<sup>3–5</sup> For example, diaryliodonium salts are efficient photoinitiators for cationically initiated polymerization. The very low energy of the C–I

bond allows the decomposition of iodonium salt after irradiation with ultraviolet light.

As a result, an iodophenyl radical cation and a reactive phenyl radical are formed.<sup>6,7</sup> On the other hand, alkyltriphenylborate salts may be other example of onium salts used in activation of polymerization reaction.<sup>8</sup> The active radicals are also formed as a result of bimolecular electron transfer quenching of photoexcited sensitizer. For an activation of these photoinitiators UV light sources are very often used for paints and coatings. It is well known, that the use of UV light is not recommended in the biological field. In that case, it is possible to apply dye, that absorbs in the visible light region as sensitizer, that allow a reaction with onium salt, promoting its decomposition. Therefore, the onium salts can also act in the radical polymerization of acrylates.<sup>6,9,10</sup> Many different organic dyes have been investigated as the visible light sensitizers, for example: camphorquinone,<sup>11–13</sup> indoles,<sup>14</sup> coumarine,<sup>15</sup> ketocoumarin and derivatives,<sup>16</sup> xanthenic dyes,<sup>17,18</sup> polymethines,<sup>19</sup> hemicyanines,<sup>20</sup> squaraines,<sup>21–23</sup> pyrromethenes,<sup>24</sup> 2-amino-4,6-diphenyl-benzene-1,3-dicarbonitrile derivatives,<sup>4</sup> 2-(diethylamino)-4,6-diphenyl-benzene-1,3-dicarbonitrile derivatives,<sup>5</sup> resazurin, flavins, safranine and others.<sup>8,25–29</sup>

An electron transfer process builds the main driving source to generate initiating radicals in UV-Vis photopolymerization.<sup>19</sup>

<sup>a</sup>University of Science and Technology, Faculty of Chemical Technology and Engineering, Seminaryjna 3, 85-326 Bydgoszcz, Poland. E-mail: [nina@utp.edu.pl](mailto:nina@utp.edu.pl); Fax: +48 52 374 9005; Tel: +48 52 374 9112

<sup>b</sup>West Pomeranian University of Technology, Institute of Chemical Organic Technology, Pułaskiego 10, 70-322 Szczecin, Poland



The first excited singlet state of dye (sensitizer) transfers/accepts an electron to/from coinitiator resulting in formation of initiating radicals.

In our previous papers it was shown that, squaraine dyes act as photosensitizers for alkyltriphenylborate salts, *N*-alkoxy-pyrrolidinium salts and diphenyliodonium salts, which do not absorb light in the visible region.<sup>8,30–32</sup> It was hypothesized, that squaraine may act as photosensitizer simultaneously for two different onium salts. Such approach can improve the reactivity of photoinitiator system. The aim of this study was to evaluate an influence of onium salts on the kinetics of polymerization of triacrylate (TMPTA) during irradiation with the visible light.

Generally, the squarylium dyes have been rarely used in dyeing photoinitiating systems. There are only few papers described their photoinitiating ability of polymerization of acrylates, epoxides, vinyl ether. In such photoinitiators, various 2,3,3-trimethylindolenine-based or 2-methylbenzothiazole-based squaraine dyes were applied.<sup>33,34</sup>

It should be also noted, that trimethylindolenine-based squaraines (green/red light photosensitizers) absorb at longer wavelength than dye studied by us (blue light photosensitizer). A characteristic feature of bis-phenylamino squaraine is a presence of nitrogen atom in the conjugated double bonds system. There are not any amine and iminium terminals in chromophore structure in contrast to mentioned above photosensitizers. Therefore, in order to improve the knowledge on the ability of bis-phenylamino squaraine to initiation of radical polymerization of triacrylate was described in our article.

Moreover, bis-phenylaminosquaraine dyes have not been studied in the multicomponent photoinitiating systems, yet.

The novelty of the present work is the enhancement of the photoinitiating efficiency of blue-light sensitizer-based initiator by simple modification of chemical composition of photoinitiator. It was shown here, that an introduction of a second onium salt results in better kinetic parameters of blue-light activated polymerization of triacrylate.

In this paper, we look for some iodonium and/or alkyltriphenyl borate salts, that in a presence of suitable photosensitizer are able to initiate the radical polymerization of 2-ethyl-2-(hydroxymethyl)-1,3-propanediol triacrylate under irradiation with blue light.

## Experimental part

### Materials

Diphenyliodonium chloride (I1), diphenyliodonium hexafluorophosphate (I2), 2-ethyl-2-(hydroxymethyl)-1,3-propanediol triacrylate (TMPTA), 1-methyl-2-pyrrolidinone (MP) were supplied by Aldrich Chemical Co. (Poland) and used without further purification. 1,3-Bis(phenylamino)squaraine (SQ) and tetramethylammonium *n*-butyltriphenylborate (B2) were synthesized in our laboratory, as it was described previously.<sup>35,36</sup> Onium salts, such as: (4-methoxyphenyl)phenyliodonium *p*-toluenesulfonate (I77), (4-methoxyphenyl)-(4-nitrophenyl)iodonium *p*-toluenesulfonate (I81), (3-bromophenyl)-(4-methoxyphenyl)iodonium *p*-toluenesulfonate (I84), (4-fluorophenyl)-(4-methoxyphenyl)iodonium *p*-toluenesulfonate (I93)

were synthesized by PhD J. Ortyl from Cracow University of Technology, as described in the literature.<sup>37</sup> All substrates and solvents necessary for the preparation of coinitiators were purchased from Aldrich Chemical Co. (Poland) and used without further purification.

### The fluorescence quenching measurements

The fluorescence quenching measurements were performed using a single-photon counting system UV-VIS-NIR Fluorolog 3 Spectrofluorimeter (Horiba Jobin Yvon). The apparatus uses a picosecond diode laser (370 nm) generating pulses of about 50 ps for the excitation. Short laser pulses in combination with a fast microchannel plate photodetector and ultrafast electronics make a successful analysis of fluorescence decay signals in the range of single picoseconds possible. The dye was studied at a concentration able to provide equivalent absorbance at 370 nm (0.2 in the 10 mm cell). The rate constant for fluorescence quenching was determined in 1-methyl-2-pyrrolidinone as a solvent. The concentration of dye was  $2 \times 10^{-5}$  M and that of quenchers was in the range from  $1 \times 10^{-4}$  M to  $1 \times 10^{-3}$  M. The fluorescence quenching at 440 nm was measured in deaerated solution by bubbling with argon.

### Kinetics of polymerization by photo-differential scanning calorimetry

A regular photo-DSC setup was used to determine the photoinitiation efficiency of the UV-Vis photoinitiator systems in acrylate. For this purpose, the kinetic parameters of free radical polymerization of 2-ethyl-2-(hydroxymethyl)-1,3-propanediol triacrylate photoinitiated by bi- and tri-component photoinitiating systems composed of 1,3-bis(phenylamino)squaraine in the presence of diphenyliodonium salt or/and borate salt were determined using a Differential Scanning Calorimeter TA DSC Q2000 Instrument equipped with a high-pressure mercury lamp (Photo-DSC). The heat evolved during reaction was registered for radiation range 300–500 nm and at a constant intensity of  $30 \text{ mW cm}^{-2}$ . The measurements were performed at a sampling interval of 0.05 s per point in isothermal conditions under a nitrogen flow of  $50 \text{ mL min}^{-1}$ . Samples weighing  $30 \pm 0.1 \text{ mg}$  were placed into an open aluminum liquid DSC pan. The measurements were carried out under identical conditions. The sample was maintained at a prescribed temperature for 2 min before each measurement run began. The polymerization mixture was composed of 1.8 mL of monomer, 0.2 mL of 1-methyl-2-pyrrolidinone, the sensitizer and an appropriate coinitiator. The concentration of photoinitiators was in the range from  $1 \times 10^{-3}$  to  $3 \times 10^{-3}$  M. 1-Methyl-2-pyrrolidinone was necessary due to the poor solubility of sensitizer in monomer. The polymerizing solution without a coinitiator was used as the reference sample. The degree of conversion ( $C_{\%}$ ) is directly proportional to the number of reactive groups (double bonds) in the monomer molecule. This parameter was calculated using eqn (1):

$$C_{\%} = \frac{\Delta H_t}{\Delta H_0} \times 100 \quad (1)$$



where  $\Delta H_t$  is the reaction heat evolved at time  $t$  and  $\Delta H_0$  is the theoretical heat for the complete degree of conversion (for acrylates:  $\Delta H_0 = 78.0 \text{ kJ mol}^{-1}$ ).

The rate of polymerization ( $R_p$ ) is derived from the amount of heat released during the process, which is expressed by eqn (2):

$$R_p = \frac{dH/dt}{H_0} \quad (2)$$

where  $dH/dt$  is a heat flow in the polymerization reaction.

The overall ability to the initiation reaction was calculated using eqn (3):

$$I_p = \frac{R_{p(\max)}}{t_{\max}} \quad (3)$$

where  $I_p$  is the photoinitiation index,  $R_{p(\max)}$  is the maximum rate of polymerization, and  $t_{\max}$  is the time required for the maximum rate of heat release.

### Cyclic voltammetry measurements

The electrochemical measurements were evaluated by Cyclic Voltammetry (CV) using the ER466 Integrated Potentiostat System (eDAQ, Poland) in a three-electrode configuration. The electrolyte was 0.1 M tetrabutylammonium perchlorate in dry acetonitrile. 1 mm platinum disk electrode was used as a working electrode, platinum and Ag/AgCl were used as auxiliary and references electrodes, respectively. All solutions were

deoxygenated with  $N_2$  for at least 15 min prior to measurements. The computer-controlled potentiostat was equipped with EChem Software.

### Nanosecond laser flash photolysis experiment

Transient absorption spectra and decay kinetics were carried out using the nanosecond laser flash photolysis method. The experiments were performed using a LKS.60 Laser Flash Photolysis apparatus (Applied Photophysics). Laser irradiation at 355 nm from the third harmonic of the Q-switched Nd:YAG laser from a Lambda Physik/model LPY 150 operating at 65 mJ per pulse (pulse width about 4–5 ns) was used for the excitation. Transient absorbances at preselected wavelengths were monitored by a detection system consisting of a monochromator, a photomultiplier tube (Hamamatsu R955) and a pulsed xenon lamp (150 W) as a monitoring source. The signal from the photomultiplier was processed by a Hewlett–Packard/Agilent an Agilent Infiniium 54810A digital storage oscilloscope and an Acron compatible computer.

## Results and discussion

2-Ethyl-2-(hydroxymethyl)-1,3-propanediol triacrylate as multifunctional monomer was chosen to study the reactivity of UV-Vis photoinitiator systems. A combination of squarylium dye (1,3-bis(phenylamino)squaraine (SQ)) and a radical initiator, an

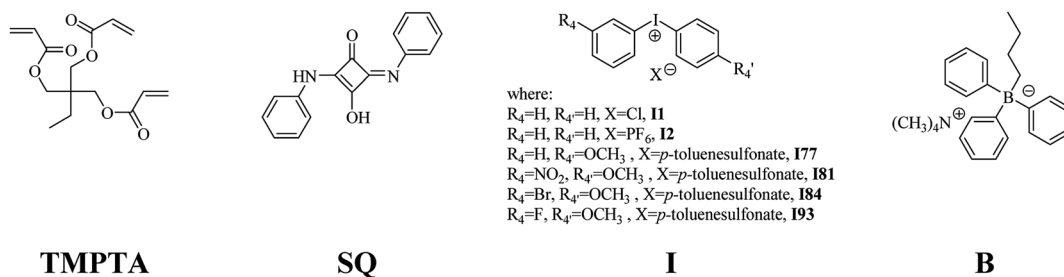
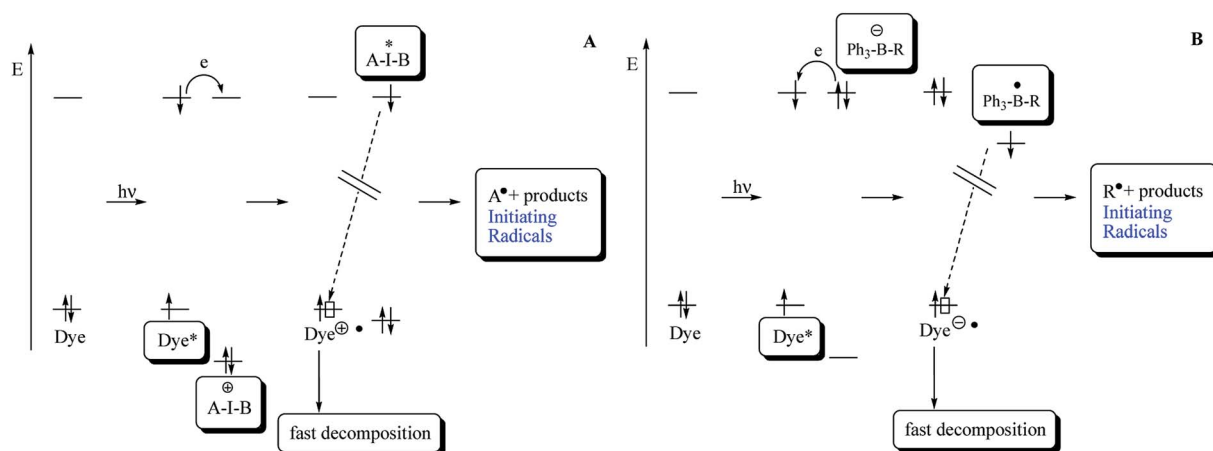


Chart 1 The composition of polymerizing mixture composed of: monomer, photosensitizer and selected coinitiator or coinitiators.



Scheme 1 Reactions occurring during UV-Vis-initiated radical polymerization based on electron transfer.



**Table 1** Thermodynamic data, the photobleaching rate constants ( $k_{bl}$ ) and fluorescence quenching rate constants ( $k_q$ ) for dye, iodonium salt and borate salt

Electron acceptor	$E_{red}$ [eV]	$\Delta G_{et}^a$ [kJ mol <sup>-1</sup> ]	$k_{bl} \times 10^4$ [s <sup>-1</sup> ]	$k_q \times 10^{-10}$ [M <sup>-1</sup> s <sup>-1</sup> ]
I1	-0.494	-126.8	5.64	6.26
I2	-1.00	-72.01	0.946	4.0
I77	-0.206	-154.6	0.7	8.12
I81	-0.554	-121.06	0.159	6.1
I84	-0.175	-157.6		
I93	-0.302	-145.4		53.1
Electron donor	$E_{ox}$ [eV]	$\Delta G_{et}^a$ [kJ mol <sup>-1</sup> ]	$k_{bl} \times 10^4$ [s <sup>-1</sup> ]	$k_q \times 10^{-10}$ [M <sup>-1</sup> s <sup>-1</sup> ]
B2	1.153	-159.9	1.3	2.69

<sup>a</sup> Calculated using the singlet state energy  $0 \rightarrow 0$  for SQ  $E_{00} = 2.938$  eV.

onium salt (iodonium or/and borate), was selected as photo-initiator system (see Chart 1).

Following bi- and tri-component photoinitiators: SQ/I, SQ/B2 and SQ/I/B2 were studied.

The sensitizer absorbs light from 320 nm to 450 nm with the maximum at 400 nm in 1-methyl-2-pyrrolidinone used as a solvent.<sup>30</sup> All cointiators studied absorb below 300 nm. In this case, only squaraine dye is excited by light source used, because an almost satisfied overlap exists between absorption of sensitizer and emission of the high-pressure mercury lamp (Omnicure 2000) used in photo-DSC studies.

Scheme 1 describes the necessary pathways to generate initiating radicals in the redox system comprising the dye (sensitizer) as an electron donating moiety and the iodonium salt with the general cation structure  $[A-I-B]^+$  as electron

acceptor, functioning as radical initiator. On the other hand, the pathways to generate initiating radicals in redox system comprising squaraine dye as electron acceptor and an alkyl-triphenylborate salt as electron donating moiety as radical initiator is different.

Excitation of dye results in formation of first excited singlet state Dye\*. Electrochemical data allow a rough estimate of the HOMO and LUMO energies of Dye and iodonium and borate salts, respectively. Electron transfer from Dye\* to  $[A-I-B]^+$  results in reduction of the iodonium salt and yields the iodyl radical  $[A-I-B]^{\cdot}$ . The short-living intermediate cleavages with a high efficiency and yields initiating aryl radicals A'. In the case of alkyltriphenylborate salt, an electron transfer from  $[Ph_3-B-R]^-$  to Dye\* results in reduction of dye, and yields the boranyl radical  $[Ph_3-B-R]^{\cdot}$ . The short-living intermediate cleavages with a high efficiency and yields initiating alkyl radicals R'. The fast decomposition of  $[A-I-B]^{\cdot}$ ,  $[Ph_3-B-R]^{\cdot}$ , Dye<sup>•+</sup> and Dye<sup>•-</sup> results in decrease of the efficiency of back electron transfer.

It was found, that the irradiation of a photosensitizer alone with visible light does not induce polymerization reaction.

The main factor that controls the rate constant of electron transfer is the exothermicity of the reaction. This value may be estimated using the oxidation potential of an electron donor and the reduction potential of an electron acceptor. The possibility of electron-transfer from donor to acceptor molecules was determined on the basis of electrochemical properties of all components of photoinitiating systems. For this purpose, the redox potentials were measured using cyclic voltammetry. The values of free energy change  $\Delta G_{el}$  for electron transfer were calculated according to Rehm-Weller equation.<sup>30,38</sup> In this study, diphenyliodonium salts were used as the electron acceptors and squaraine dye as electron donor, but borate salt as electron donor with sensitizer acting as electron acceptor.

These iodonium salts with various substituents in 4- or 4'-positions possess reduction potentials ( $E_{red}$ ) in the range from -1.00 eV to -0.175 eV,<sup>20</sup> while squaraine dye (SQ) exhibits an oxidation potential ( $E_{ox}$ ) of 1.13 eV and reduction potential of -0.128 eV. The oxidation potential of borate salt is 1.153 eV. SQ possesses an excitation energy ( $E_{00}$ ) of 2.938 eV derived from the

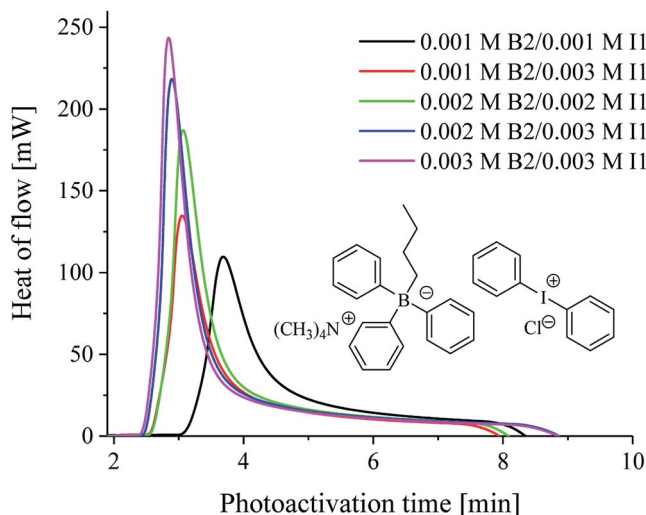


**Fig. 1** The kinetic curves recorded during radical polymerization of TMPTA initiated by 1,3-bis(phenylamino)squaraine in a presence of two cointiators marked in the figure. The concentration of sensitizer was  $1 \times 10^{-3}$  M, the concentration of borate and iodonium salts is marked in the figure. The irradiation range was from 300 nm to 500 nm with intensity  $30 \text{ mW cm}^{-2}$ .



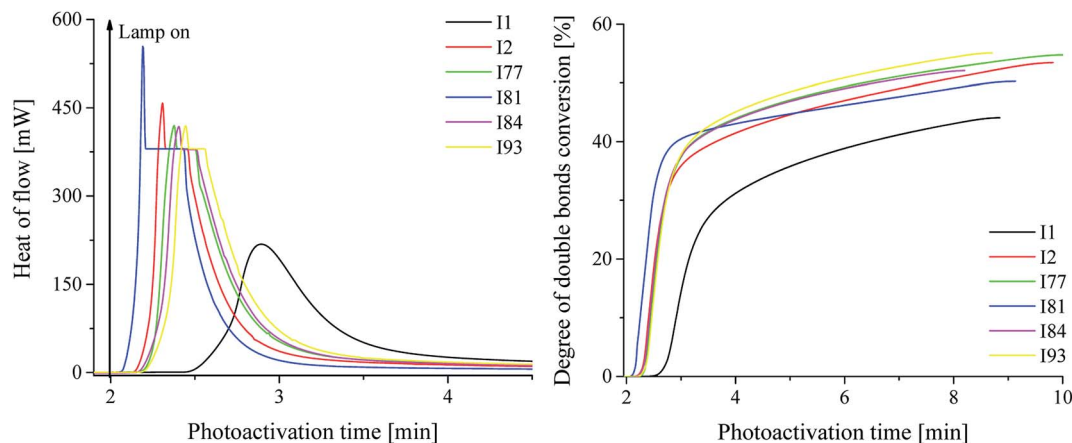


Fig. 2 L: the kinetic curves recorded during radical polymerization of TMPTA initiated by 1,3-bis(phenylamino)squaraine in a presence of two coinitiators marked in the figure. P: degree of double bonds conversion versus irradiation time. The concentration of sensitizer was  $1 \times 10^{-3}$  M, and concentration of borate and idonium salts was  $2 \times 10^{-3}$  M and  $3 \times 10^{-3}$  M, respectively. The irradiation range was from 300 nm to 500 nm with intensity  $30 \text{ mW cm}^{-2}$ .

absorption and fluorescence spectrum. These electrochemical data ( $E_{\text{ox}}$ ,  $E_{\text{red}}$ ,  $E_{00}$ ) allow calculating the free enthalpy of electron transfer  $\Delta G_{\text{el}}$ , eqn (4), resulting in the range form  $-159.9 \text{ kJ mol}^{-1}$  to  $-72 \text{ kJ mol}^{-1}$ . The negative values of  $\Delta G_{\text{el}}$  demonstrated that as a result of an electron transfer reaction between photosensitizer and coinitiators for all initiating systems under study, the radicals initiating polymerization process are formed.

The thermodynamic data presented in Table 1 confirmed, that these reactions are possible from thermodynamic point of view, that should lead to similar reactivity (expect to salt I2) between excited dye and  $[\text{A-I-B}]$  and  $\text{Dye}^*$  and  $[\text{Ph}_3\text{-B-R}]^-$ .

$$\Delta G_{\text{el}} = E_{\text{ox}} - E_{\text{red}} - E_{00} \quad (4)$$

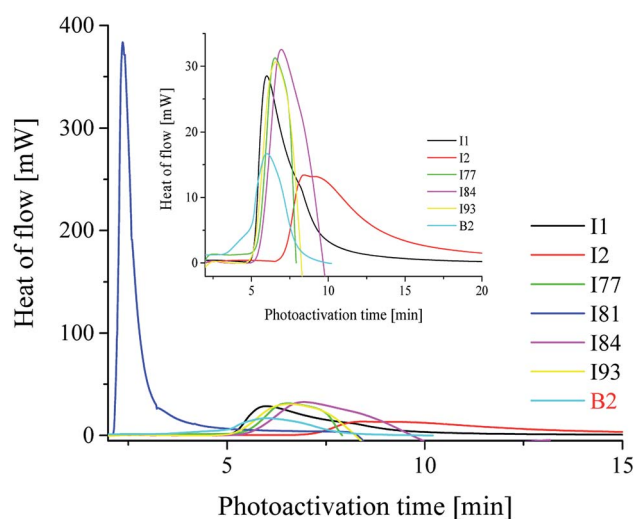


Fig. 3 The kinetic curves recorded during radical polymerization of TMPTA initiated by 1,3-bis(phenylamino)squaraine in a presence of coinitiator marked in the figure. The concentration of sensitizer and coinitiator was  $5 \times 10^{-3}$  M. The irradiation range was from 300 nm to 500 nm with intensity  $30 \text{ mW cm}^{-2}$ .

However, the kinetic results obtained (Fig. 1–3 and Table 2) show that the thermodynamic data do not fit with this hypothesis.

The representative polymerization curves and conversions of monomer during polymerization at different times of irradiation are shown in Fig. 1–3.

In Fig. 1, the typical kinetic curves of a photoinitiated polymerization, show the heat flow as a function of the photoactivation time, as well as the influence of borate salt and diphenyliodonium salt on the polymerization rate for the tertiary systems.

The influence of different initiator systems on the kinetics of photopolymerization is presented in Fig. 2, as well as the degree of monomer conversion as a function of the photoactivation time, using a ternary initiator systems.

For the comparison the photoinitiating ability of bi-component photoinitiators on the kinetic of polymerization of TMPTA is shown in Fig. 3.

The kinetic parameters of polymerization observed for different compositions of photoinitiators are shown in Table 2.

The maximum of polymerization heat roughly describes the reactivity of a photopolymer system<sup>19,39</sup> because the system crosslinks during exposure. It is a characteristic point where auto-acceleration and verification are equivalent. Thus, diffusion processes control the reactivity and reaction rate constants change with conversion. Furthermore, termination kinetics often changes from bimolecular termination to termination by initiator radicals at higher conversion degrees.<sup>19,39</sup> Nevertheless, choosing of maximum heat flow forms a reasonable compromise to describe the reactivity, because this quantity relates somehow to the initiation efficiency. In other words, the initiator efficiency is defined as the ability of the investigated photoinitiators to initiate free radical polymerization and is expressed as its rate ( $R_p$ ) (see the data in Table 2).



Table 2 The kinetic results of radical polymerization of TMPTA initiated by bi- and tri-component photoinitiators<sup>a</sup>

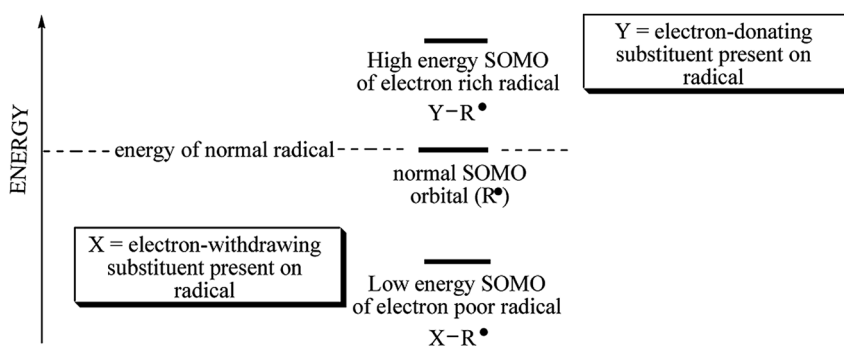
Coinitiator	$Q_{\max}$ [mW]	$t_{\max}$ [min]	$R_p \times 10^3$ [s <sup>-1</sup> ]	$I_p \times 10^3$	$R_p/R_{p(B2)}$	$C_p$ [%]
I1	28.5	6.01	1.12	3.11	2.12	16.9
I2	13.4	8.46	0.53	1.10	1	6
I77	31.3	6.55	1.23	3.41	2.33	
I81	383.7	2.36	15.15	126	28.57	48
I84	32.6	6.97	1.28	3.54	2.42	
I93	30.7	6.6	1.21	3.35	2.28	
<b>B2</b>	<b>16.7</b>	<b>6.01</b>	<b>0.66</b>	<b>1.83</b>	<b>1</b>	<b>10.5</b>
I1/B2	218.44	2.9	8.62	68.7	13.09	44.1
I2/B2	457.9	2.3	18.07	148	27.44	54
I77/B2	419.86	2.37	16.57	138	25.16	54.7
I81/B2	554.09	2.19	21.87	166	33.20	50.3
I84/B2	417.93	2.4	16.50	135	25.04	52
I93/B2	419.12	2.44	16.54	113	25.11	55.1

<sup>a</sup>  $t_{\max}$  is the time needed for reach of the maximum value of heat flow.

Barner-Kowollik *et al.* determined the initiation efficiency of a photoinitiator *via* a trifold combination of pulsed laser polymerization and subsequent ionization mass spectrometry and femtosecond transient absorption spectroscopy (PLP-ESIMS).<sup>30,40</sup> This method is suitable only for initiators forming identical radical fragments originating from disparate source molecules. The photoinitiators studied dissociate into different radicals (*e.g.* phenyl, *p*-methoxyphenyl, *p*-nitrophenyl, *p*-bromophenyl, *p*-fluorophenyl and *n*-butyl). The quantitative initiation evaluation of different fragments originating from disparate sources molecules requires additional information regarding the radicals' reactivity towards vinyl bonds and/or stability of initiating radicals or other factors.<sup>30</sup> It is well known, that the stability of radicals decreases from primary alkyl radical (*n*-butyl) to phenyl radicals. Radicals possess single occupied molecular orbital which is quite higher in energy. Any factors, that decrease energy of SOMO result in increase of radical stability and decrease its reactivity. Type of substituent attached may influence on the stability of radical formed. An electron-donating and an electron-withdrawing properties depend on the energy of SOMO (see Scheme 2).

As it was mentioned above, several different *p*-substituted phenyl radicals are formed as a result of carbon–iodide bond cleavage in diphenyliodol radical. The substitution in *para*

position of phenyl ring may stabilize a radical formed. Generally, the increased substitution improves the stability of radical formed, and less energy is required for its formation. When both electron-donating and electron-withdrawing groups are present in the same molecule, with a suitable separation between them, an additional captodative stabilization of radical occurs.<sup>41</sup> The methoxy-, nitro-, bromo- and fluoro-substituted diphenyliodonium salts were chosen for the study. Substituent effects on radical stabilization energy (RSE) values can be interpreted as a combination of three different molecular orbital interactions: (a) resonance stabilization through interaction of the radical center with *p*-systems; (b) stabilization through hyperconjugation of the radical center with adjacent C–H bonds; and (c) stabilization through interaction of the radical center with high lying orbitals describing lone pair electrons.<sup>42</sup> The RSE value for sigma radical derived from *n*-butyltriphenylboranyl radical is about 12.2 kJ mol<sup>-1</sup>.<sup>42</sup> The substituent effect on RSE values may be observed for the *p*-substituted diphenyliodonium salts under study. The substituent attached at the *para* position of phenyl ring may stabilize a radical. The methoxy group with unshared electron pairs stabilizes the radical by means of three electron bonding. Basing on Coote *et al.*,<sup>42</sup> the radical stabilization energies theoretically calculated at G3(MP2)-RAD level, for phenyl, *p*-



Scheme 2 Illustrative diagram of energy of radicals.



methoxyphenyl and *p*-nitrophenyl are  $-37 \text{ kJ mol}^{-1}$ ,  $-41.6 \text{ kJ mol}^{-1}$  and  $-40.4 \text{ kJ mol}^{-1}$ , respectively. Taking this into account, more stable *p*-nitro, *p*-bromo and *p*-fluorophenyl radicals are formed in the case of iodonium salt, than *n*-butyl radical.

Basing on the Scheme 2 and literature focused on the estimation of radical stabilization energies (RSEs) one can conclude, that coinitiator-based radical possessing of electron-withdrawing substituent in *para* position of phenyl ring decomposes faster than diphenyliodonium with electron-donating group.<sup>41</sup> This fact may be a reason of an excellent photoinitiating ability of (4-methoxyphenyl)-(4-nitrophenyl) iodonium *p*-toluenesulfonate (I81).

From the data presented in Table 2 and Fig. 3, it is seen that most of the iodonium salts (I1, I2, I77, I84, I93) exhibit no large differences regarding the reactivity in triacrylate (TMPTA). On the other hand, the effect of diphenyliodonium salt as second coinitiator dramatically reduced the photoactivation time required to reach a higher rate of polymerization and conversion of monomer when compared with the system without iodonium salt. It should be mentioned, that the concentration of coinitiator in bimolecular systems was higher than in three-component ones and equal  $5 \times 10^{-3} \text{ M}$ . It was found, that when only  $5 \times 10^{-3} \text{ M}$  of iodonium salt or borate salt was used, the maximum rate of polymerization ( $R_{p(\text{max})} (\text{s}^{-1})$ ) values equal  $15 \times 10^{-3} \text{ s}^{-1}$  was observed for diphenyliodonium salt (I81) possessing nitro ( $\text{NO}_2$ ) and methoxy ( $\text{CH}_3\text{O}$ ) groups at *para* position in both phenyl rings. Similar results were observed for 2-(*p*-*N,N*-dimethylaminostyryl)benzoxazole used as a photosensitizer and described in earlier paper.<sup>20</sup> Other bi-component photoinitiators initiate radical polymerization of triacrylate with very low and comparable rates, e.g. about  $1.2 \times 10^{-3} \text{ M}$ . The worst photoinitiating ability possesses photoinitiator composed of squaraine dye and tetramethylammonium *n*-butyl-triphenylborate salt (SQ/B2). However, for the ternary photoinitiator systems, the  $R_{p(\text{max})}$  was about 20–30-times higher than for SQ/B2 system. When bis(*p*-substituted)diphenyliodonium salt was used as a coinitiator, the  $R_{p(\text{max})}$  values were: 0.009, 0.018, 0.017, 0.022, 0.016 and 0.017 for  $3 \times 10^{-3} \text{ M}$  iodonium salt. When equimolar concentration of borate salt and iodonium salt, e.g.  $2 \times 10^{-3} \text{ M}$  was used, a slight inhibitory was observed and the  $R_{p(\text{max})}$  decreased about 20% (see Fig. 1).

The ternary photoinitiator system, formed by squarylium dye, borate salt and diphenyliodonium salt, showed an expressively higher  $R_{p(\text{max})}$  on the photoactivated polymerization. As presented in Table 1, the  $R_{p(\text{max})}$  for SQ/B2/I systems reached from  $8.62 \times 10^{-3} \text{ s}^{-1}$  to  $21.87 \times 10^{-3} \text{ s}^{-1}$ , while the binary system SQ/B2, at the same reaction conditions reached  $0.66 \times 10^{-3} \text{ s}^{-1}$ . After 60 s of photoactivation using ternary system, the monomer conversion was about 40% (except for salt I1), the total degree of double bonds conversion reached about 55% and for the binary system the total monomer conversion was achieved about 17, 6, and 48% for salts I1, I2 and I81, respectively after 4–5 min of irradiation. For the binary systems composed of sensitizer and borate salt the total degree of double bonds conversion was reached 10.5% after 8 min of photoactivation. It should be noted,

that in binary systems the concentration of coinitiators was 2–2.5-times higher than in ternary photoinitiators.

The values of photoinitiation index ( $I_p$ ) expressed as a quotient of maximum rate of polymerization and time required to reach the maximum rate of heat release, obtained from the exothermal curve,<sup>31</sup> show that all of the compounds used as coinitiators in the polymerization, possess different effectiveness to the generation of active centers. The photoinitiation index is ranging from 0.001 to 0.17 (see data in Table 2). The highest values were achieved for bi-component photoinitiator: SQ/I81 of about 0.126, and tri-component: I2/B2 and I81/B2 of about 0.148 and 0.166, respectively.

The spectral range (300–500 nm) used under study is classical for photopolymerization. Therefore, the photoinitiating ability of new initiators was compared with that of commercially available initiators. It should be also mentioned, that the ability to initiation of polymerization of triacrylate by tertiary systems is better than that observed for commercially available initiators. For the comparison, camphorquinone (CQ) as a popular sensitizer was used in presence of following coinitiators: ethyl *p*-(*N,N*-dimethylamino)benzoate (EDMAB), diphenyliodonium chloride (I1), *N*-methyl-diethanolamine (MDEA), and *N*-phenylglycine. The kinetic curves are shown in Fig. 4.

The rates of polymerization initiated by commercial photoinitiators under experimental conditions are in the range from  $0.0017 \text{ s}^{-1}$  to  $0.018 \text{ s}^{-1}$ . The best photoinitiating ability shows initiator composed of camphorquinone and *N*-methyl-diethanolamine (MDEA), that is similar to photoinitiating efficiency of system: squaraine dye/*p*-substituted diphenyliodonium salt (I81). The initiation efficiency of camphorquinone and diphenyliodide (I1) is comparable with that observed for bimolecular systems: squaraine dye and diphenyliodonium salts

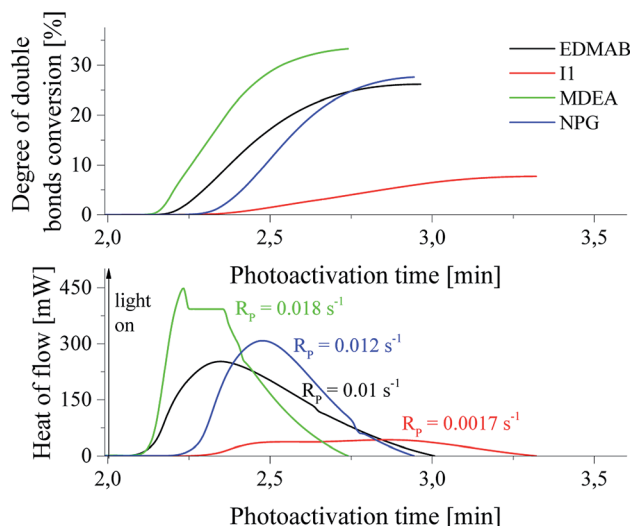
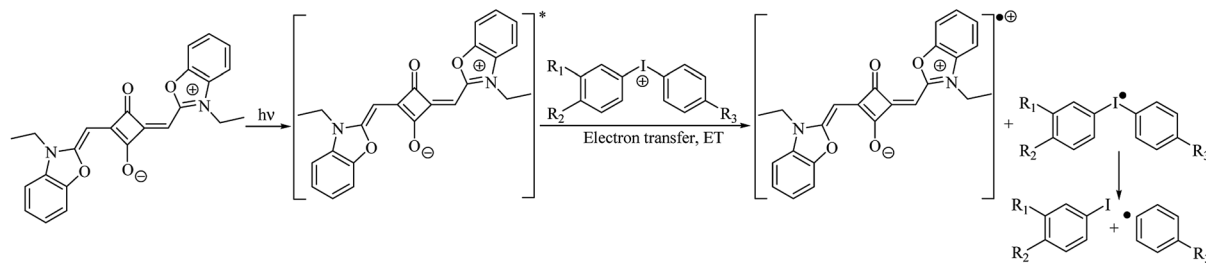


Fig. 4 The photoinitiating ability of commercially available photoinitiators: CQ/ethyl *p*-(*N,N*-dimethylamino)benzoate (EDMAB), CQ/diphenyliodonium chloride (I1), CQ/*N*-methyl-diethanolamine (MDEA), CQ/*N*-phenylglycine (NPG) for initiation of polymerization of TMPTA under irradiation with light 300 nm–500 nm,  $I_a = 30 \text{ mW cm}^{-2}$ . The photoinitiator concentration was  $5 \times 10^{-3} \text{ M}$ .





Scheme 3 Mechanism of free radicals formation in bimolecular photoinitiating system.

possessing: hydrogen, bromine, fluorine atoms in *para* position of phenyl ring. Ternary initiators are similarly effective in initiating of TMPTA polymerization as the most effective commercially available system: CQ/MDEA. The rate of polymerization observed in a case of initiator: squaraine/(4-methoxyphenyl)-(4-nitrophenyl)iodonium *p*-toluenesulfonate (I81) is about 20% higher than that observed for the best commercial initiator studied. It should be also noted, that the degree of TMPTA conversion achieved for commercial photoinitiators is relatively low and reaches values ranging from 12.4 to 33.5%. Polymerization initiated by the best photoinitiators under study leads to higher values of double bond conversion in TMPTA and ranging from 44% to 55%.

It should be also noted, that for all tested bimolecular photoinitiators a long inhibition time was observed. An introduction of iodonium salt to bimolecular system SQ/B2 distinctly decreases the inhibition time and leads immediately to a start of the photopolymerization process. It was found, that the maximum rates of polymerization were observed below 60 s of irradiation, in the most cases after 10 or 20 seconds.

The diphenyliodonium salt concentration has little effect on  $R_{p(\max)}$ , indicating that even at low concentrations, this salt participate efficiently in the monomer polymerization. The beneficial role of the diphenyliodonium salt in photoinitiated free radical polymerization has been well recognized. Iodonium salts are very effective in reacting with an excited Dye\*, accepting an electron and generating free radicals, that can start the polymerization, as viewed in Scheme 3.<sup>32</sup>

Additionally formed, phenyl radicals are highly reactive toward vinyl bonds and demonstrated high addition rate constants to double bonds of acrylate monomers in free radical polymerization, thus resulting in the shortened induction period (Fig. 2). On the other hand, the free volume effect also could contribute to the high polymerization efficiency. Namely, the polymerization rate is faster than the volume shrinkage, leading to an increase in free-volume formation.<sup>43,44</sup> This phenomenon increases the mobility of the residual double bond and resulting in an increase in the final conversion.

The values of  $R_p/R_{p(B2)}$  given in Table 2 represent the ratio between the rate observed for given photoinitiating system and that with the lowest polymerization rate, *e.g.* SQ/borate salt (B2). As it is seen, the following order in terms of the efficiency of polymerization is observed:

$$B2 \approx I2 < I1 < I77 \approx I84 \approx I93 < I1/B2 < I2/B2 \approx I77/B2 \approx I84/B2 \approx I93/B2 < I81 < I81/B2.$$

It was also found, that photoinitiators used were bleaching during radical polymerization process. This suggests that the photoinduced decomposition of sensitizer and photoinitiators is caused by photoinduced intermolecular electron transfer.<sup>30,45</sup> The changes of absorption spectra of squaraine dye in a presence of selected cointiators are shown in Fig. 5.

The photobleaching ratio may be calculated using eqn (5):

$$w\% = \frac{\Delta A}{A_0} = \frac{(A_0 - A_t)}{A_0} \quad (5)$$

where:  $A_0$  is an absorbance at the maximal absorption wavelength before light irradiation, and  $A_t$  represents the absorption at 402 nm after ( $t$ ) of visible light irradiation.

Fig. 6 shows a decrease of absorbance of photosensitizer in presence of selected cointiators during irradiation with visible light.

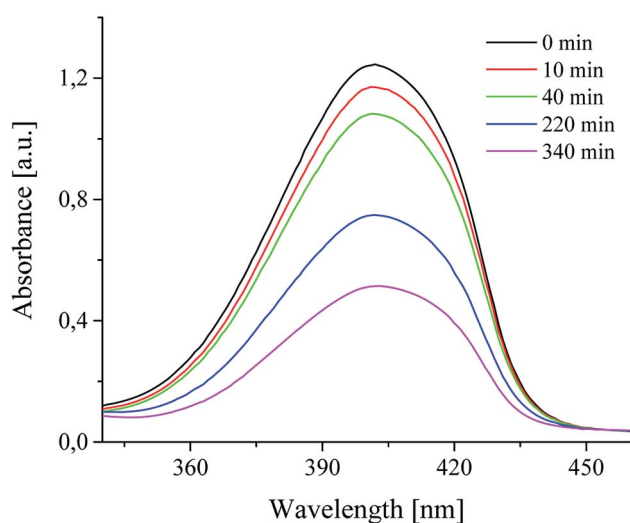


Fig. 5 The changes of absorption spectra of squaraine dye in 1-methyl-2-pyrrolidinone as a solvent, in presence of diphenyliodonium hexafluorophosphate (I2) observed during irradiation ( $300 \text{ nm} < \lambda < 500 \text{ nm}$ ) in selected periods of time. The light intensity was  $30 \text{ mW cm}^{-2}$ .



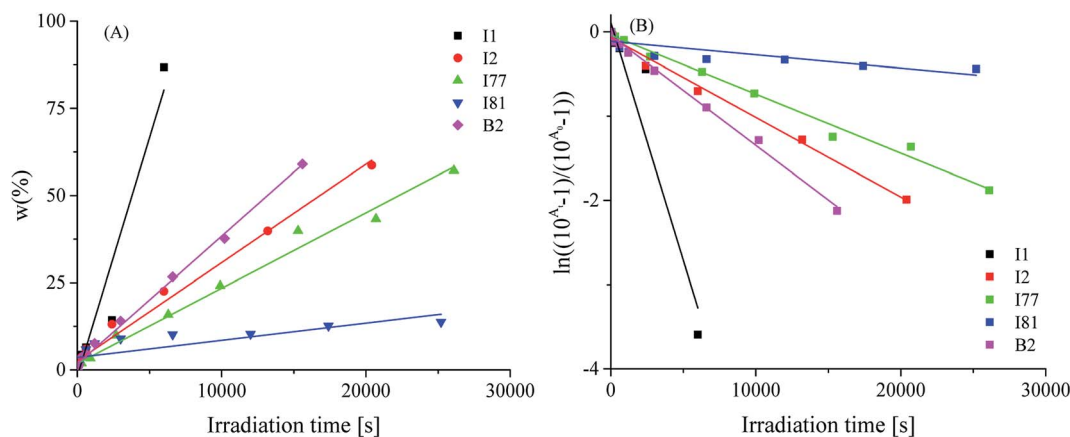


Fig. 6 The changes of photobleaching ratios at 402 nm under various visible light irradiation time.

The photobleaching process may also be presented as a relationship expressed by eqn (6).

$$\ln\left(\frac{10^A - 1}{10^{A_0} - 1}\right) = -k_{bl}\Delta t \quad (6)$$

where  $A_0$  and  $A$  are the absorbances of sensitizer at 402 nm at time 0 and  $t$ , respectively. The term  $k_{bl}$  describes the photobleaching rate constant.

For almost all cointiators, the linear relationship between the changes of absorbance and irradiation time is observed, except to cointiator I81 for which the relationship is exponential. The linear fitting coefficients are in the range from 0.985 to 0.996. The values of  $R^2$  for linear fitting for cointiator I81 is about 0.66. Better result is achieved for exponential fitting. The fitting coefficient equals 0.95. Basing on the eqn (6) the photobleaching rate constants were calculated and summarized in Table 1. They are ranging from  $1.59 \times 10^{-5} \text{ s}^{-1}$  to  $5.64 \times 10^{-4} \text{ s}^{-1}$ . Based on the kinetics of photobleaching, it is seen that the squaraine dye faster photobleaching in presence of diphenyliodonium chloride and tetramethylammonium *n*-butyltriphenylborate. Therefore, this may be a reason of very low ability to initiation of radical polymerization by systems composed of I1 and B2 salts. Taking this into account, one can conclude, that the phenyl and butyl radicals faster react in other way, than the addition to monomer molecule. In that case the photobleaching is faster than photoinitiation. In other words, the photobleaching process competes with the initiation of polymerization. It was found earlier,<sup>30</sup> that in presence of cointiator I81, the sensitizer studied undergoes photobleaching very slow, and the relationship between the decrease of absorbance and irradiation time is not linear. The system composed of this cointiator is the best bimolecular initiator for radical polymerization of TMPTA.

In the next step, an effect of concentration of cointiator on the quenching of the excited singlet state of sensitizer was studied. The fluorescence quenching experiment was carried out to determine the interactions between photoexcited sensitizer and cointiators. Tetramethylammonium *n*-butyltriphenylborate and diphenyliodonium *p*-toluenesulphonates

were used are not fluorescent compounds. For this purpose, both spectroscopic methods were used: time-resolved fluorescence spectroscopy and nanosecond laser flash photolysis. The results obtained as the Stern-Volmer plots are presented in Fig. 7.

Basing on the Stern-Volmer equation,<sup>30</sup> the fluorescence quenching rate constants  $k_q$  were calculated and summarized in Table 1. The kinetics of quenching changes from  $2.69 \times 10^{10} \text{ M}^{-1} \text{ s}^{-1}$  to  $53.1 \times 10^{10} \text{ M}^{-1} \text{ s}^{-1}$  and is nearly one order of magnitude higher than that of the diffusion controlled bimolecular reaction constant (about  $2 \times 10^9 \text{ M}^{-1} \text{ s}^{-1}$ ). It was found here, that the fluorescence quenching rate constants depend on a type of cointiator. These results confirmed that cointiators studied are effective fluorescence quenchers for photoexcited sensitizer, due to strong interactions with photosensitizer in excited singlet state. Therefore, it might be conclude, that the quenching occurs predominantly through the intramolecular ion-pair pathway, *e.g.* electron transfer process. The highest

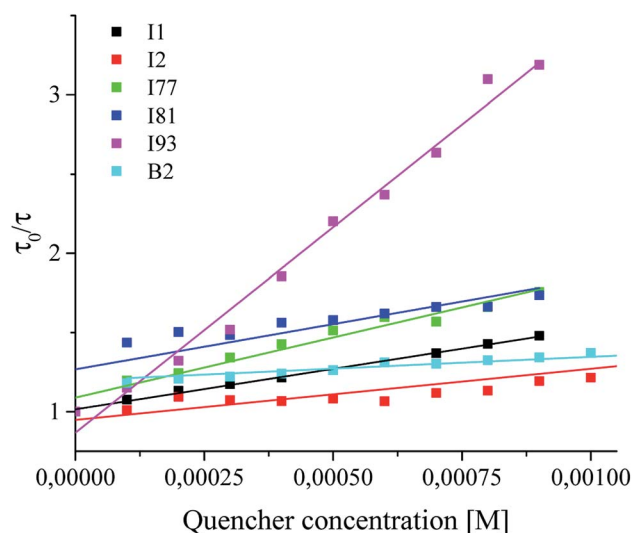
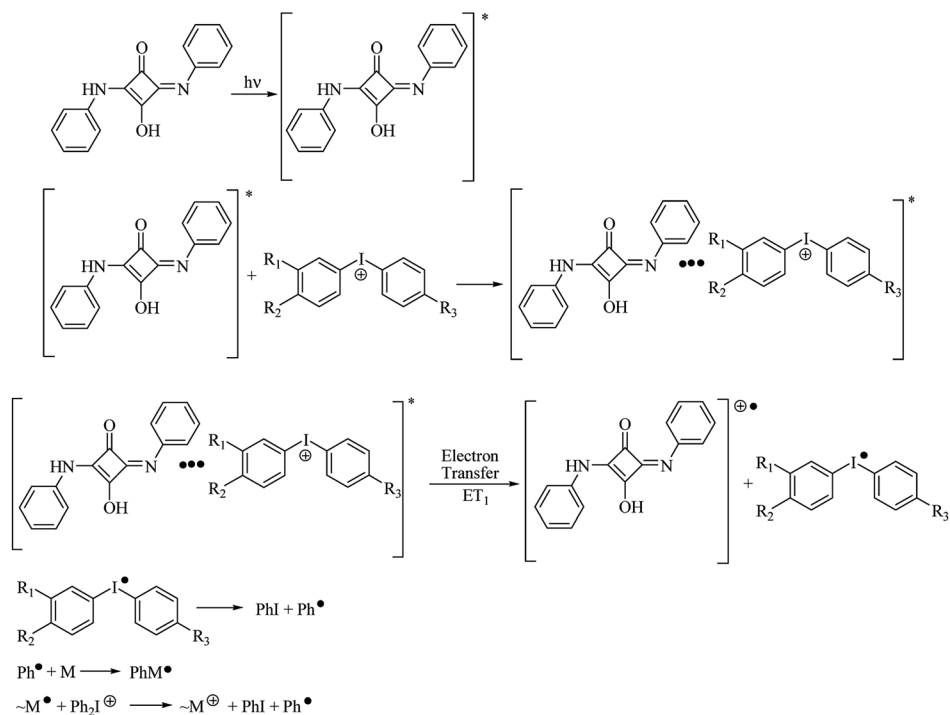


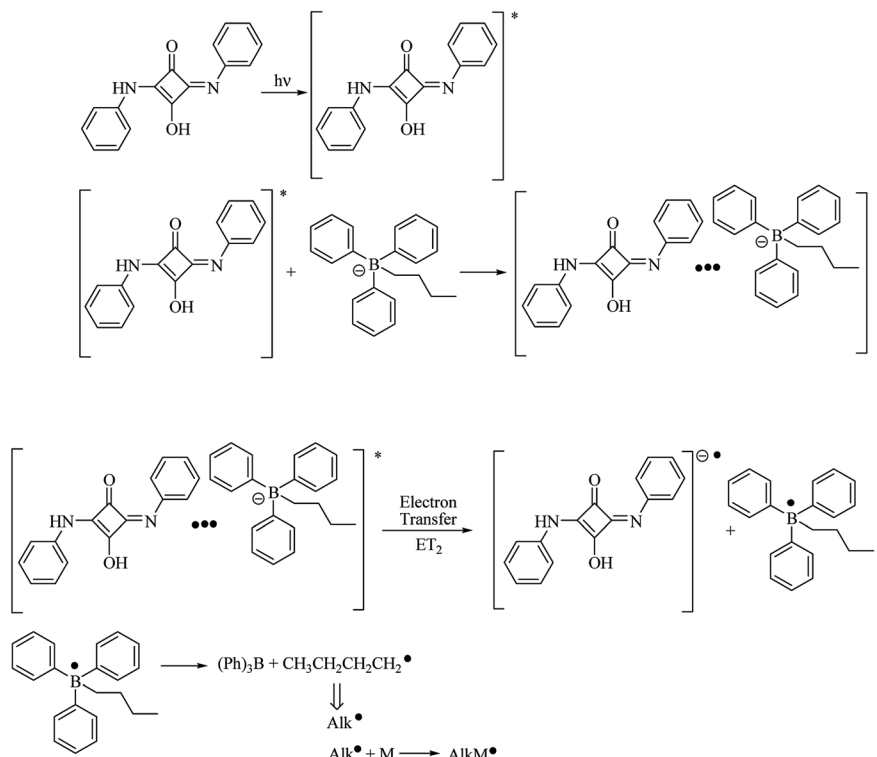
Fig. 7 An effect of type and concentration of quencher on the fluorescence of photosensitizer.



## Path 1



## Path 2



Scheme 4 Mechanism of initiating radicals formation in bi- and tri-component photoinitiating systems.

values of  $k_q$  is observed for coinitiator I93, but the lowest for borate salt B2. There is not any correlation between the rate of polymerization and the rate of fluorescence quenching. It can be seen that in the case of coinitiators (I2 and B2), which cause

very fast photobleaching of sensitizer, the lowest values of the fluorescence quenching rate constants and at the same time the lowest rates of initiation of free radical polymerization of TMPTA are also observed.



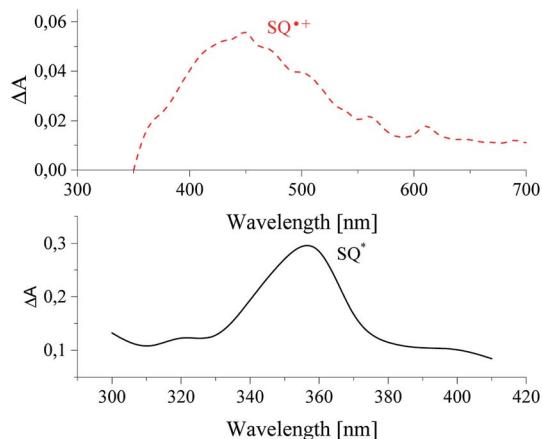


Fig. 8 Transient absorption spectra recorded for sensitizer alone (down) and in presence of diphenyliodonium hexafluorophosphate (up) in acetonitrile solution.

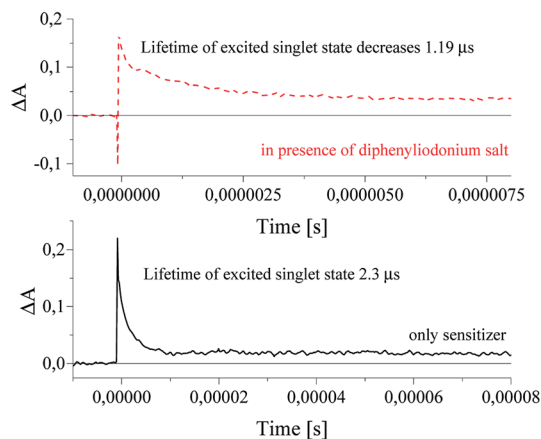


Fig. 9 The kinetic curves recorded 1  $\mu$ s after laser pulse at 380 nm. The concentration of diphenyliodonium salt was  $2 \times 10^{-3}$  M.

The mechanism of free radicals formation in a ternary photoinitiator system is more complicated, than that for bimolecular ones. Therefore, for the explanation of a role of both onium salts as cointiators, when squarylium dye is used as a photosensitizer, the nanosecond laser flash photolysis experiments were done. From our previous studies it is known, that the electron-transfer photosensitization involves the absorption of light by squarylium dye and formation of photoexcited sensitizer ( $SQ^*$ ). In presence of cointiator, the excited complex is formed, and two parallel redox processes occur. They are reduction of iodonium salt and/or oxidation of borate salt, *via* electron transfer. Next, diphenyliodonyl radical and alkyltriphenyl boranyl radicals decompose rapidly into iodobenzene and phenyl radical, and/or triphenylborate and alkyl radical, making the reaction irreversible. The phenyl and alkyl reactive species are effective in initiating of the polymerization reaction. Radicals generated in the polymerization propagation are effective in cleaving both C-I (path 1) and C-B (path 2) bonds, as

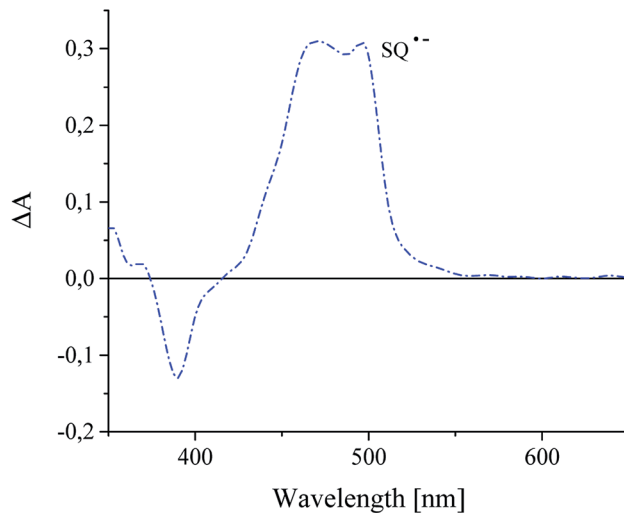


Fig. 10 Transient absorption spectra of recorded for squaraine dye in presence of tetramethylammonium *n*-butyltriphenylborate recorded 100 ns after laser pulse in acetonitrile as a solvent.

viewed in Scheme 4, releasing another phenyl radical and/or alkyl radical and allowing the polymerization reaction occur.<sup>6,8</sup>

It is seen, that the cointiator plays a role of an electron donor or an electron acceptor. The electrochemical properties of sensitizer influence on its behavior insight photoexcited complex.

This hypothesis is supported by a nanosecond laser flash photolysis experiment.

It was found, that sensitizer in deaerated solution in acetonitrile undergoes excitation with 355 nm laser pulse. One transient absorption band about 360 nm is observed in nanoseconds time scale, as a result of excited state of squaraine formation (see Fig. 8).

An addition of diphenyliodonium salt results in disappearance of the excited state absorption band, and new absorption band with maximum at 460 nm is formed. That is assigned to the product of oxidation of sensitizer (radical cation of squaraine) (see Fig. 8 upper curve).

The curves in Fig. 9 shown the disappearance of the excited singlet state of sensitizer alone (lower curve) and in a presence of diphenyliodonium salt (upper curve). It was found, that an addition of diphenyliodonium salt results in a decrease of lifetime of excited state of photosensitizer by about 1  $\mu$ s, and increases the rate constant of decay of sensitizer from  $4.29 \times 10^5 \text{ s}^{-1}$  to  $8.37 \times 10^5 \text{ s}^{-1}$ .<sup>30</sup> The lifetime was changed with an increasing concentration of cointiator. Basing on Stern-Volmer relationship, the rate constant of quenching of excited state of sensitizer was calculated. The values  $k_q$  depend on the chemical structure of diphenyliodonium salt and are equal  $0.16 \times 10^6 \text{ M}^{-1} \text{ s}^{-1}$  and  $2.41 \times 10^6 \text{ M}^{-1} \text{ s}^{-1}$  for salts I1 and I81, respectively.<sup>30</sup>

In presence of an alkyltriphenylborate salt, photoexcited squaraine undergoes immediate disappearance, that was observed at 360 nm wavelength. The time of decay of excited sensitizer is about 2.33  $\mu$ s, but the rate constant of the decay is



equal  $3.31 \times 10^7 \text{ s}^{-1}$ . A new absorption band at 480–500 nm assigned to the radical anion of sensitizer was appear (Fig. 10).

It was found, that the times of formation and disappearance of product of oxidization and reduction of squaraine dyes are different.<sup>8</sup> Their values for dye-based radical cation are 14 ns and 260 ns, but for dye-based radical anion are 10 ns and 1.14  $\mu\text{s}$ , respectively.<sup>32</sup>

On the basis of nanosecond laser flash photolysis results, it was found that *n*-butyltriphenylborate anion is oxidized, but diphenyliodonium cation is reduced by photoexcited sensitizer. The initiating radicals are formed in the secondary reactions. These results are in good accordance with thermodynamic parameters calculated for both electron transfer processes and given in Table 1.

## Conclusions

UV-Vis irradiation from the range 300 nm to 500 nm initiates radical photopolymerization of multifunctional acrylic monomer comprising a squaraine dye and iodonium salts with distinct substitution pattern or/and alkyltriphenylborate salt. One of reasons of addition of onium salt to a bimolecular photoinitiator is the significant increase the polymerization rate which is very important in systems that need a fast cure. The negative values of free energy change for the electron transfer process suggest that in such photoinitiating systems the intermolecular electron transfer occurs. The free radicals are formed as a results of electron transfer processes between sensitizer and both coinitiators. In first, an electron transfer from photoexcited sensitizer to diphenyliodonium salt (ET<sub>1</sub>), and second an electron transfer from borate salt to sensitizer in excited state (ET<sub>2</sub>) occur. Both processes take place simultaneously but with different rates. The rate of electron transfer ET<sub>1</sub> depends on the an electron acceptor structure and changes from  $0.16 \times 10^6 \text{ M}^{-1} \text{ s}^{-1}$  and  $2.41 \times 10^6 \text{ M}^{-1} \text{ s}^{-1}$ . The photoinitiating systems composed of sensitizer and an electron donor and an electron acceptor are more efficient initiators for triacrylate polymerization under visible light than the selected commercially available photoinitiators acting at the same conditions.

From our results, the studied systems: squaraine dye/borate salt/iodonium salt should be considered as remarkable photoinitiators, which is valuable for practical and industrial applications. The kinetic results also shown, that the systems composed of squaraine/diphenyliodonium salt/alkyltriphenylborate salt may be considered as an attractive alternative for UV-near visible light commercially available photoinitiators. New dye mediated photoinitiators are important for new and advanced applications, especially in the field of visible light curing.

## Conflicts of interest

There are no conflicts to declare.

## References

- 1 F. Dumur, D. Gigmès, J. P. Fouassier and J. Lalevée, *Acc. Chem. Res.*, 2016, **49**, 1980–1989.
- 2 J. Ortyl, M. Topa, I. Kamińska-Borek and R. Popielarz, *Eur. Polym. J.*, 2019, **116**, 45–55.
- 3 S. Dadashi-Silab, S. Doran and Y. Yagci, *Chem. Rev.*, 2016, **116**, 10212–10275.
- 4 E. Hola, M. Pilch, M. Galek and J. Ortyl, *Polym. Chem.*, 2020, **11**, 480–495.
- 5 E. Hola, J. Ortyl, M. Jankowska, M. Pilch, M. Galek, F. Morlet-Savary, B. Graff, C. Dietlin and J. Lalevée, *Polym. Chem.*, 2020, **11**, 922–935.
- 6 F. A. Ogliairi, C. Ely, C. L. Petzhold, F. F. Demarco and E. Piva, *J. Dent.*, 2007, **35**, 583–587.
- 7 J. V. Crivello and J. H. W. Lam, *Macromolecules*, 1977, **10**, 1307–1315.
- 8 J. Kabatc, K. Kostrzewska, K. Jurek, M. Kozak, A. Balcerak and Ł. Orzeł, *J. Polym. Sci., Part A: Polym. Chem.*, 2017, **55**, 471–484.
- 9 Y. Lin and J. W. Stransbury, *Polymer*, 2003, **44**, 4781–4789.
- 10 H. J. Timpe, S. Ulrich, C. Decker and J. P. Fouassier, *Macromolecules*, 1993, **26**, 4560–4566.
- 11 J. Kirschner, J. Paillard, M. Bouzrati-Zeerelli, J. M. Becht, J. E. Klee, S. Chelli, S. Lakhdar and J. Lalevée, *Molecules*, 2019, **24**, 2913.
- 12 P. Xiao, F. Dumur, B. Graff, J. Zhang, F. Morlet-Savary, D. Gigmès, J. P. Fouassier and J. Lalevée, *J. Polym. Sci., Part A: Polym. Chem.*, 2015, **53**, 567–575.
- 13 M. Bouzrati-Zerelli, M. Maier, C. Dietlin, F. Morlet-Savary, J. P. Fouassier, J. E. Klee and J. Lalevée, *Dent. Mater.*, 2016, **32**, 1226–1234.
- 14 D. Wang, P. Garra, J. P. Fouassier, B. Graff, Y. Yagci and J. Lalevée, *Polym. Chem.*, 2019, **10**, 4991–5000.
- 15 M. Abdallah, A. Hijazi, B. Graff, J. P. Fouassier, G. Rodghiero, A. Gualandii, F. Dumur, P. G. Cozzi and J. Lalevée, *Polym. Chem.*, 2019, **10**, 872–884.
- 16 H. Salmi, H. Tar, A. Ibrahim, C. Ley and X. Allonas, *Eur. Polym. J.*, 2013, **49**, 2275–2279.
- 17 H. Tar, D. S. Esen, M. Aydin, Ch. Ley, N. Arsu and X. Allonas, *Macromolecules*, 2013, **46**, 3266–3272.
- 18 J. Qiu and J. Wei, *J. Polym. Res.*, 2014, **21**, 1–7.
- 19 T. Brömme, D. Oprych, J. Horst, P. S. Pinto and B. Strehmel, *RSC Adv.*, 2015, **5**, 69915–69924.
- 20 A. Balcerak and J. Kabatc, *RSC Adv.*, 2019, **9**, 28490–28499.
- 21 K. Kawamura, J. Schmitt, M. Barnet, H. Salmi, Ch. Ley and X. Allonas, *Chem.-Eur. J.*, 2013, **19**, 12853–12858.
- 22 Y. He, W. Zhou, F. Wu, M. Li and E. Wang, *J. Photochem. Photobiol., A*, 2004, **162**, 463–471.
- 23 H. Yong, W. Zhou, G. Liu, L. M. Zhen and E. Wang, *J. Photopolym. Sci. Technol.*, 2000, **13**, 253–254.
- 24 O. I. Tarzi, X. Allonas, C. Ley and J. P. Fouassier, *J. Polym. Sci., Part A: Polym. Chem.*, 2010, **48**, 2594–2603.
- 25 E. Andrzejewska, *Polym. Int.*, 2017, **66**, 366–381.
- 26 M. Sangermano, N. Razza and J. V. Crivello, *Macromol. Mater. Eng.*, 2014, **299**, 775–793.



## Paper

- 27 P. Xiao, F. Dumur, J. Zhang, M. Bouzrati-Zerelli, B. Graff, D. Gigmes, J. P. Fouassier and J. Lalevée, *J. Polym. Sci., Part A: Polym. Chem.*, 2015, **53**, 1806–1815.
- 28 J. V. Crivello and U. Bulut, *J. Polym. Sci., Part A: Polym. Chem.*, 2005, **43**, 5217–5231.
- 29 F. Morlet-Savary, J. E. Klee, F. Pfefferkorn, J. P. Fouassier and J. Lalevée, *Macromol. Chem. Phys.*, 2015, **216**, 2161–2170.
- 30 K. Kostrzewska, J. Ortyl, R. Dobosz and J. Kabatc, *Polym. Chem.*, 2017, **8**, 3464–3474.
- 31 J. Kabatc, *J. Polym. Sci., Part A: Polym. Chem.*, 2017, **55**, 1575–1589.
- 32 J. Kabatc, K. Kostrzewska, M. Kozak and A. Balcerak, *RSC Adv.*, 2016, **6**, 103851–103863.
- 33 P. Xiao, J. Zhanga, F. Dumur, M. A. Tehfe, F. Morlet-Savary, B. Graff, D. Gigmes, J. P. Fouassier and J. Lalevée, *Prog. Polym. Sci.*, 2015, **41**, 32–66.
- 34 P. Xiao, F. Dumur, T. T. Bui, F. Goubard, B. Graff, F. Morlet-Savary, J. P. Fouassier, D. Gigmes and J. Lalevée, *ACS Macro Lett.*, 2013, **2**, 736–740.
- 35 S.-Y. Park, K. Jun and S.-W. Oh, *Bull. Korean Chem. Soc.*, 2005, **26**, 428–432.
- 36 R. J. Damico, *Org. Chem.*, 1964, **29**, 1971.
- 37 J. Kabatc, J. Ortyl and K. Kostrzewska, *RSC Adv.*, 2017, **7**, 41619–41629.
- 38 D. Rehm and A. Weller, *Isr. J. Chem.*, 1970, **8**, 259–271.
- 39 M. D. Goodner and C. N. Bowman, *Macromolecules*, 1999, **32**, 6552–6559.
- 40 E. Frick, H. A. Ernst, D. Voll, T. J. A. Wolf, A.-N. Unterreiner and C. Barner-Kowollik, *Polym. Chem.*, 2014, **5**, 5053–5068.
- 41 F. G. Bordwell and T.-Y. Lynch, *J. Am. Chem. Soc.*, 1989, **111**, 7558–7562.
- 42 M. L. Coote, C. Y. Lin and H. Zipse, The stability of carbon-centered radicals, in *Carbon-Centered Free Radicals and Radical Cations: Structure, Reactivity, and Dynamics*, ed. M. D. E. Forbes, John Wiley & Sons, Inc., Publication, 2010, pp. 83–104.
- 43 F. Sun, N. Zhang, J. Nie and H. Du, *J. Mater. Chem.*, 2011, **21**, 17290–17296.
- 44 B. R. Nayak and L. J. Mathias, *J. Polym. Sci., Part A: Polym. Chem.*, 2005, **43**, 5661–5670.
- 45 J. Kabatc, K. Kostrzewska and K. Jurek, *RSC Adv.*, 2016, **6**, 74715–74725.



**Publikacja naukowa [A5]**

PAPER



Cite this: *Polym. Chem.*, 2020, **11**, 5500

# Highly efficient UV-Vis light activated three-component photoinitiators composed of tris(trimethylsilyl)silane for polymerization of acrylates†

Alicja Balcerak, Dominika Kwiatkowska, Katarzyna Iwińska and Janina Kabatc \*

The goal of this paper concerns the evaluation of the efficiency of novel three-component systems for initiating the photopolymerization process of 2-ethyl-2-(hydroxymethyl)-1,3-propanediol triacrylate (TMPTA). Combinations of 1,3-bis(phenylamino)squaraine (SQG1) with different types of co-initiators are proposed as effective UV-Vis light photoinitiators. The co-initiators used in the experiments, such as silane (TTMSS), borate salt (B2), carbazole (NVC) and a set of iodonium salts (I1, I2, I77, I81), are active radical sources for initiation of the polymerization of TMPTA. The effect of the composition of the system on the photopolymerization kinetics was analyzed. The optimal photoinitiator concentration that gives high monomer conversions and high values of the rate of polymerization is indicated and presented in this article.

Received 26th May 2020,  
Accepted 22nd July 2020

DOI: 10.1039/d0py00763c

rsc.li/polymers

## 1. Introduction

In recent years, interest in light induced polymerization processes has rapidly increased. Photopolymerization reactions are relevant for green chemistry because of their many advantages, for example they are highly efficient, energy-saving, economic, solvent-free and environmentally friendly.<sup>1–3</sup> This advanced technique has resulted in enormous progress in the development of novel adhesives, photocurable coatings, varnishes, printing inks, 3D printing, various composites, dental filling materials and many others.<sup>4–8</sup>

In general, the photopolymerization process requires the presence of an appropriate photoinitiator (PI). This compound undergoes a photochemical reaction after absorption of light and forms reactive species (radicals or cations) that initiate the chain reaction and transform the monomer into a polymer.<sup>9,10</sup> These photochemical reactions include  $\alpha$ -cleavage of bonds and atom abstraction, known as Norrish type I and type II reactions, respectively.<sup>11</sup> An effective photoinitiator should decompose after irradiation with the light source used and efficiently react with the monomer. Moreover, high initiation performance, high reactivity of the radical towards the monomer, good stability and non-toxicity are required.<sup>12,13</sup>

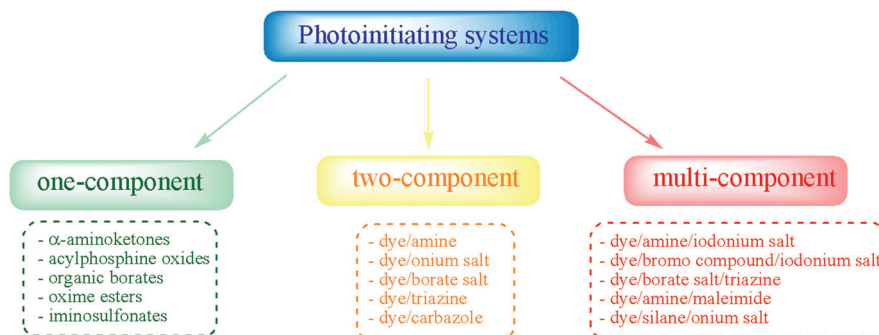
The design and development of new, high speed photoinitiating systems (PISs) is extremely important for producing novel polymer materials exhibiting many functional properties and applicable in different areas of science, technology, engineering, medicine, *etc.*<sup>14</sup> Many photoinitiators (PIs), used both in free radical polymerization (FRP) and cationic polymerization (CP), have been widely described in recent years. However, novel effective photoinitiating systems operating in the visible region of the spectrum, as well as panchromatic photoinitiators, have invariably attracted interest from many researchers.<sup>15</sup> The use of UV radiation as a light source may be problematic, due to high heat build-up, harmfulness for human health and limited curing of thick samples.<sup>16</sup>

Generally, a typical photoinitiating system contains the monomer or oligomer, the photoinitiator (sensitizer + co-initiator) and appropriate additives, which impart the required properties.<sup>17</sup> A general classification of photoinitiating systems depending on the number of components and examples of designed PISs are shown in Scheme 1.<sup>18–20</sup>

In one-component systems, the initiation of radical polymerization occurs only in the presence of an active molecule as sensitizer (*e.g.* dye). In this case, the radicals are produced through homolytic bond cleavage.<sup>20,21</sup> Introduction of more compounds (co-initiators) to the system results in an improvement in the performance of these photoinitiators. The most popular PISs contain two or three components. The formation of active species in dual systems involves energy/electron transfer, electron/proton transfer or direct hydrogen atom transfer. However, the efficiency of the initiation step may be

UTP University of Science and Technology, Faculty of Chemical Technology and Engineering, Seminaryjna 3, 85-326 Bydgoszcz, Poland. E-mail: nina@utp.edu.pl

† Electronic supplementary information (ESI) available. See DOI: 10.1039/d0py00763c



Scheme 1 Types of photoinitiating systems.

affected by various kinetic limitations, *e.g.* inactive dye-based radicals are able to terminate this step in growing polymer chains.<sup>22–24</sup> These systems may be improved by the addition of a second co-initiator. Multi-component PISs contain a light absorber and donors and acceptors of electrons or protons. The mechanism of generation of active species is more complex and includes several chemical reactions. An appropriate combination of components provides high polymerization efficiency and the ability to work under well-defined conditions.<sup>25,26</sup>

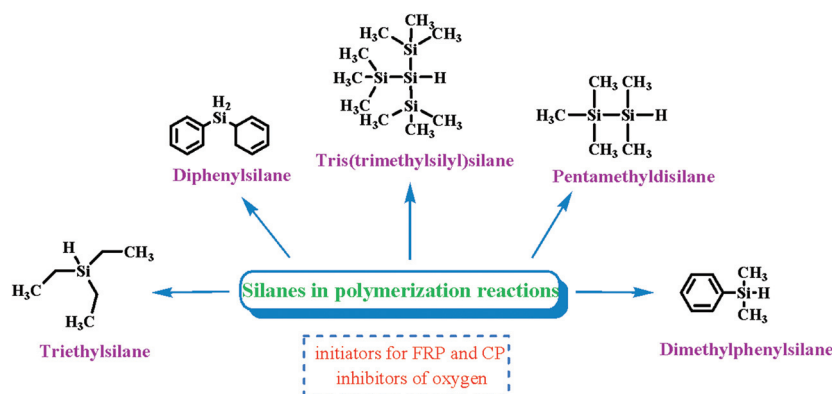
Different types of radicals are used as initiating agents for crosslinking reactions. Silanes were recently proposed as very efficient co-initiators for photoinitiated radical polymerization.<sup>27</sup> Various silane derivatives used in photoinitiating systems have been described in the literature. Some examples of these compounds are presented in Scheme 2.<sup>28,29</sup>

Systems comprising a PI combined with silane derivatives show high reactivity. The active species are mainly generated from (i) bond cleavage between silicon and other atoms or (ii) Si–H bond abstraction. Importantly, silanes have potential for reduction of oxygen inhibition.<sup>30,31</sup> The silyl radicals act as “peroxide scavengers”. As a result, the concentration of reactive species increases, which is shown in Scheme 3.<sup>32</sup> The formation of radicals occurs in several reactions. The photosensitizer (PS) absorbs light and then reacts with silane ( $R_3SiH$ ), generating the active form ( $R_3Si^\cdot$ ). The silyl radicals ( $R_3Si^\cdot$ ) and

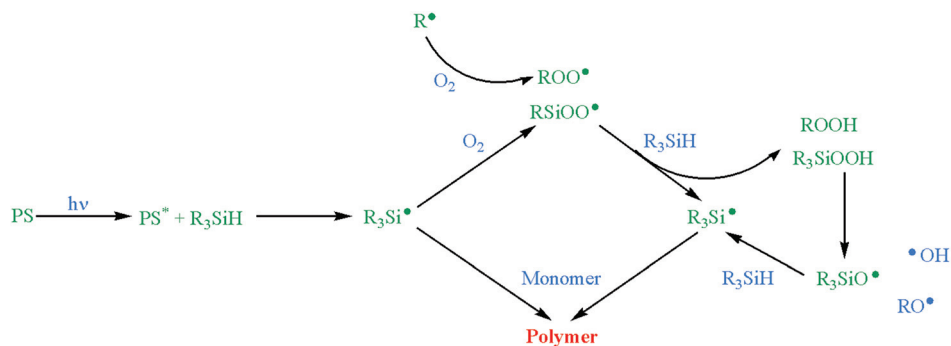
$R^\cdot$  radicals arising from interactions between the PS and the other co-initiators bind to oxygen molecules ( $O_2$ ). The inhibition of oxygen and scavenging of the peroxy radicals increase the total amount of  $R_3Si^\cdot$  radicals that react with the monomer and lead to polymer formation.<sup>27,33,34</sup>

A large series of silanes were studied as co-initiators for radical polymerization initiated by systems containing isopropylthioxanthone as a photosensitizer, as described by J. Lalevée *et al.*<sup>28</sup> One of the silanes was tris(trimethylsilyl)silane, also studied by us. This compound exhibits weak oxygen inhibition and is very efficient when combined with isopropylthioxanthone (ITX) for photopolymerization of Ebecryl 605 and 1,6-hexanediol diacrylate, under both laminated and aerated conditions. In this system, the silyl radical formation results from the interaction between the triplet state of thioxanthone derivative and silane. The rate constant and quantum yield characterizing the formation and reactivity of silyl radicals formed from tris(trimethylsilyl)silane are  $4.1 \times 10^7 \text{ M}^{-1} \text{ s}^{-1}$  and 0.7, respectively. It was found that silanes are very effective for visible light induced polymerization under aerated conditions.<sup>28</sup>

Recently, novel PISs based on silane derivatives were described in 2020 by Wang and coworkers. These systems are an alternative to the popular, previously proposed photoinitiators based on silanes, because of the lack of aromatic amines and peroxides showing toxic effects. This group of researchers



Scheme 2 Examples of silanes used as co-initiators in photoinitiating systems.



**Scheme 3** The mechanism of radical formation in a silyl-based photoinitiating system in the presence of oxygen molecules.

proposed highly effective systems containing camphorquinone or 2-isopropylthioxanthone as sensitizers combined with various silane/iodonium salt as co-initiators. It was proved that these versatile three-component systems are appropriate for radical and cationic polymerizations of acrylates and epoxides initiated by redox reactions, light or temperature. A significant advantage of the new PISs is their storage stability in different photo or thermal curing resins. Importantly, no viscosity changes of the prepared composites occurred. The concentration of sensitizer with respect to the silane/iodonium salt co-initiators and various types of additives, *e.g.* stabilizers, played a key role in the gelation times. The newly developed strategy based on dual curing different mixtures of monomers is associated with the possibility of creating composite materials with good mechanical and thermal properties.<sup>35</sup>

An important group of compounds that initiate polymerization are polymeric photoinitiators.<sup>36,37</sup> These macromolecules are well-defined polymers containing side or chain chromophores showing sensitivity towards light. The presence of polymeric chains improves compatibility and reduces the migration of additives in the created materials. Moreover, these photoinitiators can be used as pre-polymers for preparation of various block copolymers or complex polymeric systems.<sup>38,39</sup> For example, in 2020, Yang *et al.* reported highly efficient macrophotoinitiators for radical polymerization of acrylates upon LED exposure at 405 nm. A series of novel multifunctional PIs were synthesized by the reaction of naphthalimides and siloxanes containing a silicon hydride unit. These photoinitiators generate two types of radicals: silyl and carbon. The increased concentration of active species results in a more efficient initiation step. Significantly, the silyl radicals are also reactive towards O<sub>2</sub> molecules, which eliminates the oxygen inhibition phenomenon in photopolymerization. A high monomer conversion of about 80% was observed. The proposed photoinitiators show reduced toxicity and stability towards migration from cured materials, thus they can be used in medicine and food industry.<sup>40</sup>

The present paper is focused on three-component photoinitiating systems for free radical polymerization of TMPTA. We describe new systems which are a combination of 1,3-bis(phenylamino)squaraine as a sensitizer with tris(trimethylsilyl)

silane and a second co-initiator corresponding to a borate salt, carbazole or iodonium salt. The innovation of our study is the application of a squaraine dye as a photosensitizer for silane compound. To the best of our knowledge, the ability of PISs composed of squaraine and tris(trimethylsilyl)silane to initiate free radical polymerization has not been described before. It was also shown that enhancement of the photoinitiating efficiency of the blue-light sensitizer-based initiator may be achieved by simple modification of the chemical composition of photoinitiator. The introduction of a second onium salt results in better kinetic parameters for the blue-light activated polymerization of triacrylate. The efficiency of the photoinitiating systems has been evaluated by determining the kinetic parameters of polymerization, *i.e.* monomer conversion ( $C_{\%}$ ) and rate of polymerization ( $R_p$ ). The proposed new photoinitiators can be used as ingredients for photocuring compositions, which are essential for production of adhesives, inks, coatings, 3D printing, *etc.*

## 2. Experimental

### 2.1. Materials

2-Ethyl-2-(hydroxymethyl)-1,3-propanediol triacrylate (TMPTA), 1-methyl-2-pyrrolidinone (MP), and the commercially available co-initiators tris(trimethylsilyl)silane (TTMSS), *N*-vinylcarbazole (NVC), diphenyliodonium chloride (I1) and diphenyliodonium hexafluorophosphate (I2) were purchased from Sigma-Aldrich (Poland) and used without further purification. The other co-initiators,<sup>41</sup> tetramethylammonium *n*-butyltriphenylborate (B2), (4-methoxyphenyl)-phenyliodonium *p*-toluenesulfonate (I77), and (4-methoxyphenyl)-(4-nitrophenyl)iodonium *p*-toluenesulfonate (I81), as well as the photosensitizer 1,3-bis(phenylamino)squaraine (SQG1)<sup>42</sup> were synthesized according to the methods described in other articles.

### 2.2. Polymerization experiments

The photopolymerization experiments were carried out by the use of a DSC Q 2000 differential scanning calorimeter (TA Instruments) and a TA Q PCA photo unit equipped with a high

pressure mercury lamp (Photo-DSC). The measurements were performed under isothermal conditions at 25 °C under a nitrogen flow of 50 mL min<sup>-1</sup>. Radiation in the UV-Vis range (300–500 nm) at a constant intensity equal to 30 mW cm<sup>-2</sup> was applied as a light source.

The polymerization solutions were composed of the sensitizer, an appropriate co-initiator, the solvent and the monomer. The reference sample did not contain an initiator. Measurements were also carried out on a reference sample without a photosensitizer (ESI, Fig. S4†). 1-Methyl-2-pyrrolidinone was used for the preparation of the tested samples and the reference, because of poor solubility of SQG1 dye in TMPTA. In general, the samples for the polymerization studies were prepared as follows: an appropriate amount of photoinitiator (dye: 1 × 10<sup>-3</sup> M; co-initiators: 1 × 10<sup>-3</sup> M, 2 × 10<sup>-3</sup> M, 3 × 10<sup>-3</sup> M or 5 × 10<sup>-3</sup> M) was dissolved in 0.2 mL of 1-methyl-2-pyrrolidinone, and then 1.8 mL of 2-ethyl-2-(hydroxymethyl)-1,3-propanediol triacrylate was added to the solution and mixed. A sample weight (tested samples and reference) of 30 ± 0.1 mg was placed into an open aluminum liquid DSC pan and then maintained at the prescribed temperature (25 °C) for 2 min before each measurement run began. The obtained data were recorded at sampling intervals of 0.05 s per point.

The degree of monomer conversion ( $C_{\%}$ ) was calculated based on the amount of heat released during the polymerization reaction. The liberated heat amount is directly proportional to the number of reactive moieties in the monomer molecule (acrylate groups). The conversion percentages were obtained by integrating the area under the exothermic peak using eqn (1):

$$C_{\%} = \frac{\Delta H_t}{\Delta H_0^{\text{theor}}} \times 100 \quad (1)$$

where  $\Delta H_t$  is the heat evolved at time  $t$  during the polymerization reaction, and  $\Delta H_0^{\text{theor}}$  is the theoretical heat corresponding to complete conversion of the reactive group. For calculation of the  $C_{\%}$  parameter, the value of theoretical enthalpy for an acrylate double bond polymerization of  $\Delta H_0^{\text{theor}} = 78.0$  kJ mol<sup>-1</sup> was used.<sup>43</sup>

The rate of polymerization ( $R_p$ ) is directly related to the heat flow liberated in the reaction and is expressed by eqn (2):

$$R_p = \frac{dC}{dt} = \frac{dH/dt}{\Delta H_0^{\text{theor}}} \quad (2)$$

where  $dH/dt$  is the heat flow evolved during the polymerization reaction.

The overall initiation efficiency was calculated as the photo-initiation index  $I_p$ , which may be defined according to eqn (3):

$$I_p = \frac{R_p^{\text{max}}}{t^{\text{max}}} \quad (3)$$

where  $t^{\text{max}}$  is the time required to reach the maximum rate of heat ( $H^{\text{max}}$ ) release obtained from the exothermic kinetic curve.

The kinetic parameters listed above were calculated for each of the investigated systems. Based on the obtained data, the optimal conditions for the polymerization process, under which the photoinitiator works the most effectively, were proposed.

## 3. Results and discussion

### 3.1. Characterization of initiators

The structures of the sensitizer, monomer and co-initiators involved in the polymerization experiments are presented in Chart 1.

The role of the sensitizer in the investigated PISs was played by 1,3-bis(phenylamino)squaraine (SQG1), which belongs to the group of squaraines. Because of their specific features, such as sharp and strong absorption and emission in the visible (Vis) light region, high molar extinction coefficients, high fluorescence quantum yields, pH stability and photostability, squaraines are widely used as photosensitizers in various fields.<sup>44–46</sup>

The SQG1 dye was synthesized by a condensation reaction of 1,2-dihydroxycyclobuten-3,4-dione (squaric acid) with two molar equivalents of aniline in a mixture of 1-butanol and toluene, as depicted in Scheme 4.

The dye possesses a single, sharp absorption band in the UV-Vis region with a maximum located at 393 nm in 1-methyl-2-pyrrolidinone (MP). The emission band is broad and the fluorescence maximum is at 495 nm (value for the dye dissolved in MP).<sup>47</sup> More information about the spectroscopic properties and application of SQG1 squaraine in photoinitiating systems can be found in our previous papers.<sup>9,42,47,48</sup>

Tris(trimethylsilyl)silane (TTMSS) combined with a second co-initiator was selected as the initiating radical generator in the photoinitiating systems under study. The role of the second co-initiator was played by compounds belonging to different groups, such as borate salts (B2), carbazoles (NVC) and iodonium salts (I1–I81). We examined the ability of a typical pair of co-initiators, silane/iodonium salt,<sup>19</sup> and compared with other systems comprising silane/electron donor (TTMSS/B2), and silane/radical activator (TTMSS/NVC).

One of the important preconditions of polymerization processes is the selection of an appropriate light source. The spectroscopic properties of the investigated compounds were studied at room temperature in 1-methyl-2-pyrrolidinone (MP) and ethyl acetate as solvents. The spectroscopic data are presented in Table 1 and in the ESI (Fig. S1 and S2†).

All investigated compounds absorb in the range from about 250 nm to 350 nm. The maximum absorption is between 252 nm and 270 nm. The longest wavelengths of absorption were observed for tris(trimethylsilyl)silane and *N*-vinylcarbazole. The position of the absorption band and the molar extinction coefficient are affected by the type of solvent and the chemical structure of initiator. The lowest value of molar extinction coefficient was measured for tris(trimethylsilyl)silane in ethyl acetate solvent.

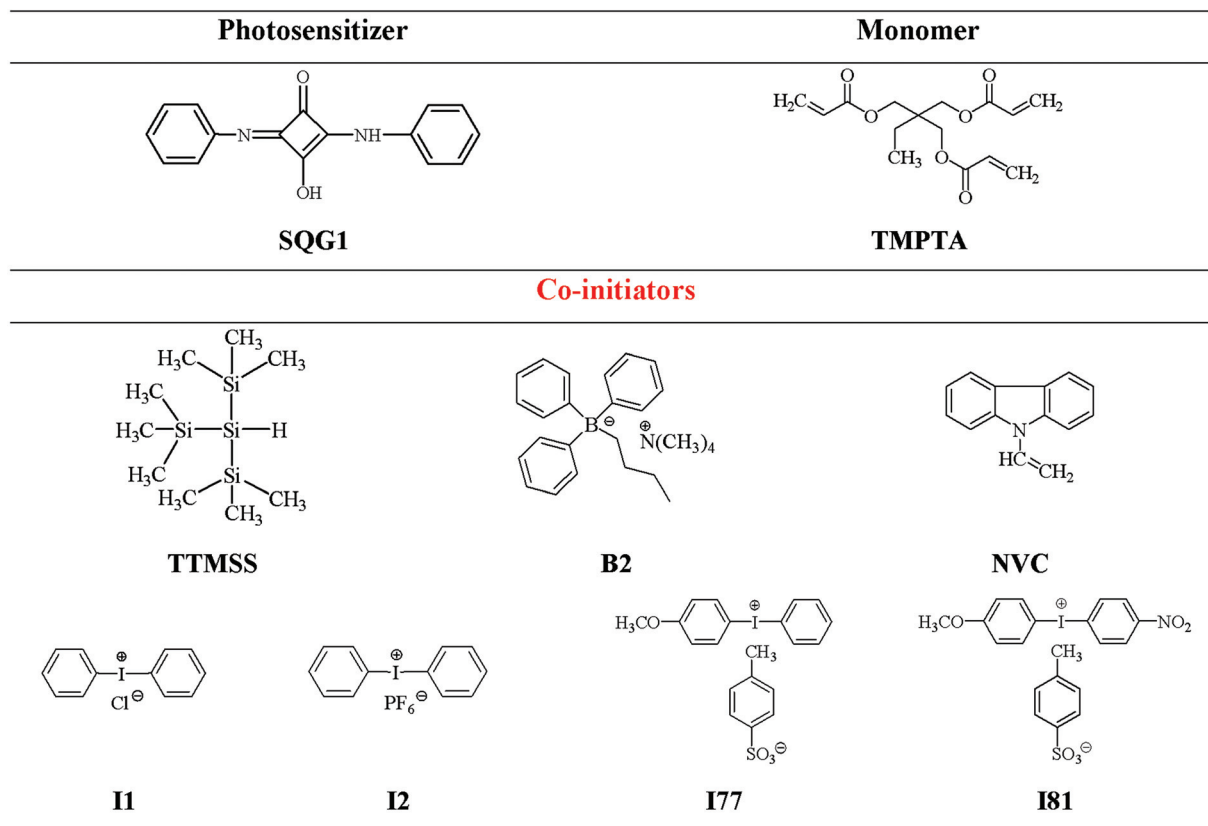
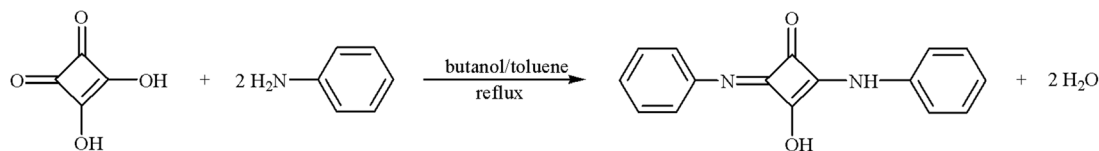


**Chart 1** Chemical structures and abbreviations of the components of the photoinitiating systems studied.



**Scheme 4** Method of synthesis of SQG1 dye.

**Table 1** The spectroscopic data of the investigated compounds

Initiator	1-Methyl-2-pyrrolidone		Ethyl acetate	
	$\lambda_{\max}$ ab (nm)	$\epsilon_{\max}$ ( $M^{-1} \text{ cm}^{-1}$ )	$\lambda_{\max}$ ab (nm)	$\epsilon_{\max}$ ( $M^{-1} \text{ cm}^{-1}$ )
Tris(trimethylsilyl)silane			275	107
<i>N</i> -Vinylcarbazole	294	6833		
	340	4196		
Diphenyliodonium chloride			252	1747
Diphenyliodonium hexafluorophosphate	260	3687	253	3557
(4-Methoxyphenyl)-phenyliodonium <i>p</i> -toluenesulfonate	263	12 147	252	11 385
(4-Methoxyphenyl)-(4-nitrophenyl)iodonium <i>p</i> -toluenesulfonate	272	2164	269	5089
Tetramethylammonium <i>n</i> -butyltriphenylborate			252	6768

It is required that the source of emitted radiation includes the absorption range of the photosensitizer. As mentioned above, the sensitizer has a main absorption band with a maximum located at about 400 nm. Thus, the light emitted from the high pressure mercury lamp (300 nm <  $\lambda$  < 500 nm)

overlaps with the absorption region of the squaraine dye. The emission spectrum of the OmniCure S2000 lamp is provided in the ESI (Fig. S3†). The high pressure mercury lamp used as a light source emits light from 300 nm to 600 nm. The highest power of the lamp above 110 mW  $\text{cm}^{-1}$  was measured for

three wavelengths: 365 nm, 410 nm and 440 nm. Most of the co-initiators studied strongly absorb light below 300 nm. Based on this, it is seen that all co-initiators used could not decompose in order to form reactive species for free radical polymerization of TMPTA.

Other factors that affect the kinetic parameters of photopolymerization are the redox properties of the components of photoinitiator systems. They may be established based on the Rehm–Weller equation by estimating the value of the free energy change for an electron transfer process.

The oxidation potential of tris(trimethylsilyl)silane is lower than 1.7 V.<sup>28</sup> The  $E_{\text{ox}}$  measured by cyclic voltammetry is 0.436 V. Using a reduction potential of  $-0.128$  V and a singlet state energy of 2.938 eV for 1,3-bis(phenylamino)squaraine, an exothermic electron transfer reaction ( $-2.374$  eV) can be expected based on the classical Rehm–Weller equation (eqn (4))

$$\Delta G_{\text{et}} = E_{\text{ox}} - E_{\text{red}} - E_{00} + C \quad (4)$$

where  $\Delta G_{\text{et}}$ ,  $E_{\text{ox}}$ ,  $E_{\text{red}}$ ,  $E_{00}$  and  $C$  are the free energy change for the electron transfer reaction, the oxidation potential of donor, the reduction potential of acceptor, the singlet state energy, and the coulombic term for the formed initial ion pair, respectively. This result supports the fact that the  $^1\text{SQG1}/\text{tris}(\text{trimethylsilyl})\text{silane}$  reaction probably corresponds to an electron/proton transfer sequence and not to a pure hydrogen transfer process,<sup>28</sup> unlike the system containing isopropylthioxanthone and tris(trimethylsilyl)silane in which a pure hydrogen transfer occurs.<sup>28</sup> The free energy change for the electron transfer from tetramethylammonium *n*-butyltriphenylborate ( $E_{\text{ox}} = 1.153$  V) is  $-1.65$  eV, but for the iodonium salts I1, I2, I77 and I81 possessing the reduction potentials

$-0.494$  V,  $-1.0$  V,  $-0.206$  V and  $-0.554$  V, respectively, the values of  $\Delta G_{\text{et}}$  are in the range from  $-1.60$  eV to  $-0.747$  eV. Selected cyclic voltammograms are provided in the ESI (Fig. S5–S9†).

### 3.2. Kinetic studies of the photopolymerization process and the role of each component in the photoinitiating systems

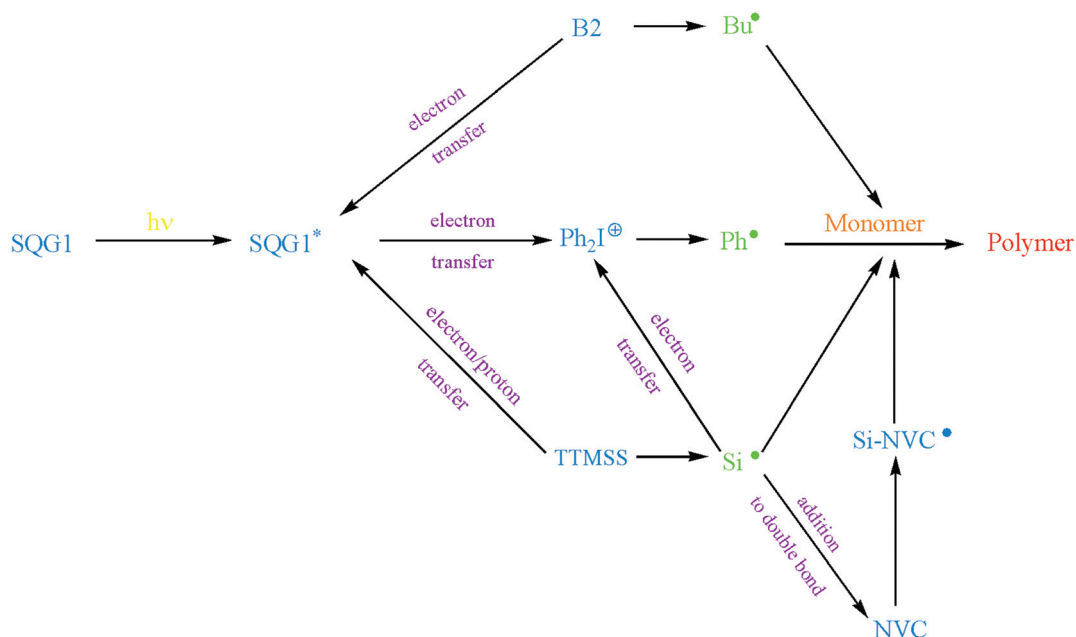
The influence of several combinations of squaraine dye with different co-initiators on the polymerization of triacrylate was evaluated using the differential scanning calorimetry technique.

The performances in initiating the radical polymerization of TMPTA by three-component photoinitiating systems containing the SQG1 sensitizer and various radical sources, namely TTMSS combined with a second co-initiator (B2, NVC, I1, I2, I77 or I81), were tested and compared with the two-component systems SQG1/B2 and SQG1/TTMSS. The experiments were carried out for various concentrations of pairs of co-initiators.

The photoinitiating systems studied comprised 1,3-bis(phenylamino)squaraine, tris(trimethylsilyl)silane (TTMSS) as a co-initiator and various types of additives, such as diphenyliodonium salt, borate salt or *N*-vinylcarbazole.

The role of each studied component in the investigated photoinitiating systems is presented in Scheme 5.

As can be seen in Scheme 5, the presence of each component involved in the photoinitiating system is crucial for the formation of radicals that can initiate the polymerization reaction. The dye molecule 1,3-bis(phenylamino)squaraine (SQG1) plays the role of sensitizer in the investigated PISs. The sensitizer absorbs light, which leads to formation of an excited state of the sensitizer molecule (SQG1\*). The first step of the photo-



**Scheme 5** The presentation of the role of all components of photoinitiating systems.

reaction occurs between the dye and the co-initiator. The squaraine dye may undergo both photoreduction and photo-oxidation reactions in the PIS. Depending on the type of co-initiator, the photosensitizer may act as an electron donor/acceptor or proton acceptor.

In the presence of the borate salt (B2), the deactivation of the excited state of sensitizer occurs *via* electron transfer from co-initiator to the sensitizer. The boranyl radical undergoes carbon–boron bond cleavage, giving a butyl radical that can start the polymerization reaction.

In the PIS comprising squaraine dye and iodonium salt, the electron transfer process occurs from the excited state of sensitizer to the ground state of onium salt. In this case, the squaraine radical cation and the diphenyliodonium radical are formed. In the next step, the diphenyliodonium radical undergoes fragmentation *via* carbon–iodine bond cleavage which forms the active species (phenyl radicals).

In the photoinitiating system based on *N*-vinylcarbazole, the active species are formed because of interactions between NVC and other radicals present in the PIS (*e.g.* silyl radicals). The addition of silyl radicals to the double bond of the carbazole molecule gives Si-NVC radicals, initiating polymerization.

In the photoinitiating system containing TTMSS, the initiating radicals are formed *via* proton/electron transfer from the co-initiator to the sensitizer. The combination of tris(trimethylsilyl)silane with the second co-initiator increases the concentration of initiating radicals. This is due to the reaction between silyl radicals and the iodonium salt which generates highly reactive phenyl radicals. Therefore, three-component

photoinitiating systems are more effective than their two-component analogues.

Generally, the excited photosensitizer undergoes proton/electron transfer from tris(trimethylsilyl)silane. The active silyl radicals are formed as a result of this process. On the other hand, in the presence of diphenyliodonium salt, the excited photosensitizer acts as an electron donor and undergoes an oxidation process. Taking this into account, the photosensitizer may be oxidized or reduced depending on the type of additive.

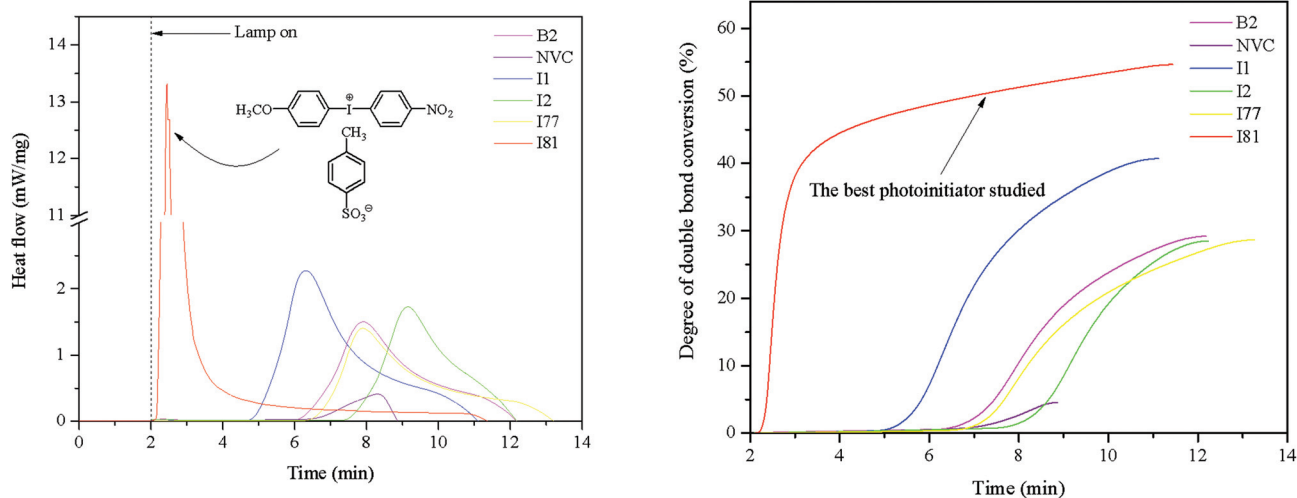
The data for the most effective photoinitiating systems used in the radical polymerization of the triacrylate monomer are presented in Table 2.

Fig. 1 illustrates the effect of different pairs of co-initiators on the kinetics of photopolymerization process. Depending on the type of photoinitiating system used, various values of the rate of polymerization ( $R_p$ ), as well as the degree of double bond conversion ( $C\%$ ), for the acrylate monomer were observed.

From the kinetics curves depicted in Fig. 1, it can be concluded that the efficiency of the formation of initiating radicals is related to the type of second co-initiator used in the polymerization mixture. The obtained results clearly indicate that among the tested three-component systems, the highest performance photoinitiator is the combination of 1,3-bis(phenylamino)squaraine (SQG1) with tris(trimethylsilyl)silane (TTMSS) and (4-methoxyphenyl)-(4-nitrophenyl)iodonium *p*-toluenesulfonate (I81). The amount of heat released during the polymerization reaction reached *ca.* 14 mW mg<sup>-1</sup>. This value is about 10 times higher compared to other systems. It

**Table 2** Kinetic parameters of the radical polymerization of TMPTA initiated by three-component photoinitiating systems based on squaraine dye and various types of radical sources (concentration of SQG1 was  $1 \times 10^{-3}$  M)

Radical source	Parameter					
	Co-initiator concentration (M)	Max. heat flow (mW mg <sup>-1</sup> )	$t^{\max}$ (min)	$R_p^{\max}$ ( $10^{-3}$ s <sup>-1</sup> )	$C\%$ (%)	$I_p$ ( $10^{-6}$ s <sup>-2</sup> )
TTMSS/B2	$1 \times 10^{-3}/2 \times 10^{-3}$	1.17	8.43	1.48	18.32	2.93
	$2 \times 10^{-3}/3 \times 10^{-3}$	1.38	6.90	1.75	26.51	4.23
	$2 \times 10^{-3}/5 \times 10^{-3}$	1.50	5.91	1.90	29.20	5.36
	$5 \times 10^{-3}/2 \times 10^{-3}$	1.24	7.42	1.57	20.14	3.53
TTMSS/NVC	$1 \times 10^{-3}/2 \times 10^{-3}$	0.97	6.80	1.22	12.05	2.99
	$2 \times 10^{-3}/3 \times 10^{-3}$	0.66	6.57	0.83	9.38	2.11
	$2 \times 10^{-3}/5 \times 10^{-3}$	0.41	6.31	0.52	4.54	1.37
	$5 \times 10^{-3}/2 \times 10^{-3}$	0.98	5.97	1.24	15.68	3.46
TTMSS/I1	$1 \times 10^{-3}/2 \times 10^{-3}$	2.09	4.54	2.64	34.27	9.69
	$2 \times 10^{-3}/3 \times 10^{-3}$	2.36	4.00	3.00	35.50	12.50
	$2 \times 10^{-3}/5 \times 10^{-3}$	2.27	4.30	2.88	40.70	11.16
	$5 \times 10^{-3}/2 \times 10^{-3}$	2.13	4.97	2.70	36.33	9.05
TTMSS/I2	$1 \times 10^{-3}/2 \times 10^{-3}$	1.27	8.85	1.60	17.44	3.01
	$2 \times 10^{-3}/3 \times 10^{-3}$	1.39	8.74	1.77	19.95	3.38
	$2 \times 10^{-3}/5 \times 10^{-3}$	1.73	7.15	2.19	28.49	5.10
	$5 \times 10^{-3}/2 \times 10^{-3}$	1.21	9.79	1.54	17.81	2.62
TTMSS/I77	$1 \times 10^{-3}/2 \times 10^{-3}$	1.38	8.11	1.75	21.94	3.60
	$2 \times 10^{-3}/3 \times 10^{-3}$	1.51	7.29	1.92	26.70	4.39
	$2 \times 10^{-3}/5 \times 10^{-3}$	1.41	5.90	1.78	28.66	5.03
	$5 \times 10^{-3}/2 \times 10^{-3}$	1.55	7.50	1.96	24.28	4.36
TTMSS/I81	$1 \times 10^{-3}/2 \times 10^{-3}$	9.31	0.83	11.79	56.18	236.75
	$2 \times 10^{-3}/3 \times 10^{-3}$	12.73	0.57	16.12	57.88	471.35
	$2 \times 10^{-3}/5 \times 10^{-3}$	13.32	0.44	16.87	54.67	639.02
	$5 \times 10^{-3}/2 \times 10^{-3}$	11.90	0.65	15.06	58.81	386.15



**Fig. 1** The kinetic profiles recorded during radical polymerization of a mixture of TMPTA/MP (9 : 1) initiated by three-component photoinitiating systems composed of [SQG1] =  $1 \times 10^{-3}$  M, [TTMSS] =  $2 \times 10^{-3}$  M and [second co-initiator] =  $5 \times 10^{-3}$  M. The second co-initiators used in the experiments are marked on the figure.

should be noted that irradiation of the polymerization mixture TMPTA/MP/SQG1/TTMSS/I81 caused an immediate exothermic effect and the time for the crosslinking reaction of triacrylate was about 25 s. In the other cases, an initiation time for photopolymerization equal to 3–5 min was observed. The degree of double bond conversion of TMPTA for PISs containing TTMSS and I81 as co-initiators exceeded 54%. This may be related to the higher efficiency of radical formation and/or radical reactivity. The final conversion for the other systems varies in the range from 5% for *N*-vinylcarbazole to 41% for the SQG1/TTMSS/I1 photoinitiator.

As can be seen in Table 2, the highest effectiveness for the initiation of polymerization was obtained for the combination of squaraine dye with silane and one of the iodonium salts. In this case, the kinetic parameters of the polymerization process may be associated with the structure of used co-initiator. The monomer conversions observed for almost all photoinitiators are in the range from 30% to 60% and the rates of polymerization achieved values of about  $2 \times 10^{-3} \text{ s}^{-1}$ . The exception is the photoinitiating system composed of 1,3-bis(phenylamino) squaraine (SQG1), tris(trimethylsilyl)silane (TTMSS) and (4-methoxyphenyl)-(4-nitrophenyl)iodonium *p*-toluenesulfonate (I81). This system exhibited the highest  $C_0$  and  $R_p$  parameters, which is attributed to the presence of a strongly electron-withdrawing substituent ( $-\text{NO}_2$ ) attached to the phenyl ring in the *para* position in the co-initiator structure.

As mentioned above, four different diphenyliodonium salts were chosen for the studies. First, we had to study the effect of the anion structure on the photoinitiating efficiency of diphenyliodonium salts with the same chemical structure of the cation. Better initiating efficiency was observed for the diphenyliodonium cation paired with the chloride anion (I1) than the same cation with hexafluorophosphate as counter-ion (I2). This may be a result of the higher quantum yield for free radical formation for co-initiator I1.

In the case of diphenyliodonium salts, which play the role of electron acceptor, and squaraine, various initiating radicals are formed: phenyl from salts I1, I2 and I77 and *p*-nitrophenyl from salt I81. The substitution in the *para* position of the phenyl ring stabilizes the radical formed, and less energy is required for its formation. The presence of both electron-donating (methoxy) and electron-withdrawing substituents in one molecule with an appropriate separation between them results in additional stabilization of the free radical formed. The radical stabilization energy depends on three different molecular orbital interactions: resonance stabilization through interaction of the radical center with *p*-systems, stabilization through hyperconjugation of the radical center with adjacent C–H bonds and stabilization through interaction of the radical center with high lying orbitals containing lone pair electrons. The substituent effect on the radical stabilization energy is observed for the *p*-substituted diphenyliodonium co-initiators. The radical stabilization energies theoretically calculated for phenyl and *p*-nitrophenyl radicals are  $-37 \text{ kJ mol}^{-1}$  and  $-40.4 \text{ kJ mol}^{-1}$ , respectively. The *p*-nitrophenyl radical is more stable, which is reflected in its excellent photoinitiating efficiency.

The efficiency of the photoinitiated polymerization reaction in the presence of a co-initiator belonging to the group of borate salts (B2) is similar to that of the photoinitiating systems containing diphenyliodonium hexafluorophosphate (I2). The maximum rates of polymerization were about  $1.5\text{--}2.2 \times 10^{-3} \text{ s}^{-1}$  and the monomer conversion achieved values from 18% to 30%.

On the other hand, the lowest ability to initiate the radical polymerization of TMPTA of all photoinitiators studied was observed for *N*-vinylcarbazole as co-initiator. The values of the degree of double bond conversion were in the range from 4.54% to 15.68%. The polymerization rate ( $R_p$ ) achieved values of *ca.*  $1 \times 10^{-3} \text{ s}^{-1}$ . This poor efficiency is probably due to the

lower reactivity of carbazole radicals toward the double bond of triacrylate.

Generally, the maximum rate of polymerization of TMPTA ranged from  $0.52 \times 10^{-3} \text{ s}^{-1}$  for the SQG1/TTMSS/NVC system to  $16.87 \times 10^{-3} \text{ s}^{-1}$  for SQG1/TTMSS/I81, and the monomer conversion varied from 4.54% to 58.81%, respectively for these photoinitiators. As mentioned above, the shortest times for polymerization were observed for systems with the I81 co-initiator. The maximum rate of heat release during the exothermic reaction occurred at about 30 s for the best photoinitiator studied and 4.00 min to 9.79 min for the other systems. The values of the photoinitiation index ( $I_p$ ) show that systems comprising B2, I2 or I77 as co-initiators exhibit similar effectiveness for the generation of active species. This parameter was about  $4 \times 10^{-6} \text{ s}^{-2}$ . For the most effective photoinitiating system, SQG1/TTMSS/I81, the initial polymerization rate is about 50–170 times higher than that estimated for the other systems.

Taking into account the kinetic results for the polymerization process of TMPTA, the following order of co-initiator activity in three-component photoinitiating systems comprising TTMSS may be proposed: I81 > I1 > I77 > I2 > B2 > NVC. This sequence may be explained by a difference in the rate of formation of active species as a result of decomposition of the intermediate product formed in a primary photochemical reaction and/or the reactivity of the radicals toward the functional groups of the monomer. Moreover, the higher activity of iodonium salts is also a result of their high quantum efficiency for generating radicals.<sup>9,49</sup>

In order to examine the effect of radical source concentration (co-initiator) on the efficiency of the photoinitiator, polymerization was carried out using various concentrations of the second co-initiator from  $1 \times 10^{-3} \text{ M}$  to  $5 \times 10^{-3} \text{ M}$ . The influence of the second co-initiator concentration on the kinetic parameters of TMPTA polymerization (heat flow, rate,

photoinitiation index) and monomer conversion is shown in Fig. 2.

Generally, it can be concluded that the concentration of co-initiator has a significant impact on the rate of polymerization of triacrylate. As seen in Fig. 2, increasing the value of this parameter results in higher amounts of heat being released and shortening of the initiation time. Moreover, the conversion of monomer increases from 45% to 58%. Importantly, the increase in  $C_{\%}$  value is observed up to a certain point, above which the higher concentration of co-initiator used does not influence the monomer conversion.

For all tested photoinitiating systems, a pronounced relation between second co-initiator concentration and rate of polymerization was observed. Taking into account the kinetic results, it is seen that the rate of polymerization as well as the photoinitiation index increases as the concentration of the second co-initiator changes from  $1 \times 10^{-3} \text{ M}$  to  $5 \times 10^{-3} \text{ M}$ . The kinetic curves for both parameters increase proportionally to the concentration. However, from  $3 \times 10^{-3} \text{ M}$  to  $5 \times 10^{-3} \text{ M}$ , the increases in  $R_p$  and  $I_p$  are not so sharp and the curves flatten.

As is well known, in conventional photopolymerization reactions, the rate of polymerization increases when more co-initiator is added to the mixture. However, too high a concentration of photoinitiator may induce “the inner filter effect”. Thus, the selection of appropriate proportions of components for photoinitiating systems is really important. By estimation of the optimal conditions for the polymerization process, the most effective photoinitiator was proposed. The highest performance system is a combination of  $2 \times 10^{-3} \text{ M}$  tris(trimethylsilyl)silane (TTMSS) and  $5 \times 10^{-3} \text{ M}$  second co-initiator.

In order to confirm the crucial influence of the third component (second co-initiator) on the improvement of the kinetic parameters of acrylate polymerization, experiments using two-component photoinitiating systems were carried out.

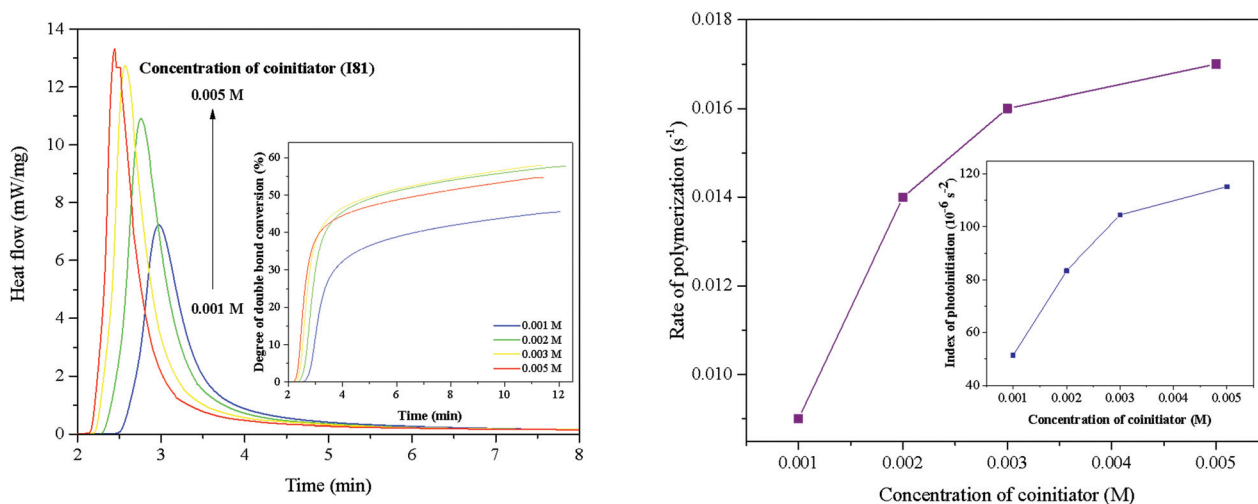
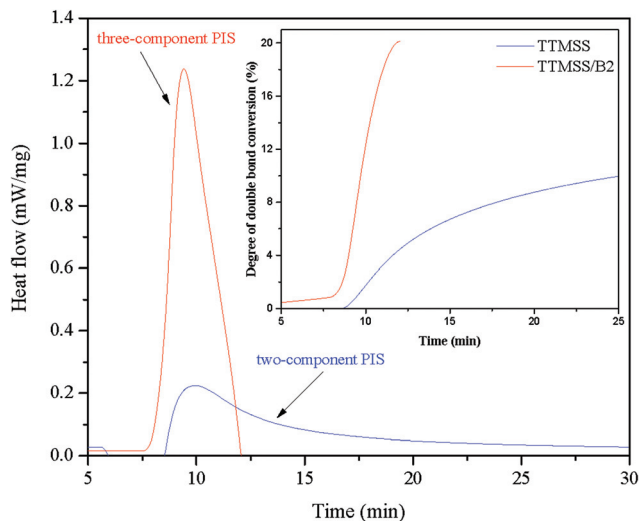


Fig. 2 The effect of concentration of the second co-initiator on the kinetics of the polymerization of TMPTA in the presence of (4-methoxyphenyl)-(4-nitrophenyl)iodonium *p*-toluenesulfonate (I81). The concentrations of the other components of the PIS: [SQG1] =  $1 \times 10^{-3} \text{ M}$ ; [TTMSS] =  $2 \times 10^{-3} \text{ M}$ . The concentration of I81 is marked on the figure.



**Fig. 3** The kinetic curves recorded during radical polymerization of TMPTA initiated by two- and three-component photoinitiating systems containing SQG1 dye as sensitizer and appropriate co-initiators. The concentrations of the components of the PISs: [SQG1]/[TTMSS] =  $5 \times 10^{-3}$  M/ $5 \times 10^{-3}$  M, [SQG1]/[TTMSS]/[B2] =  $1 \times 10^{-3}$  M/ $5 \times 10^{-3}$  M/ $1 \times 10^{-3}$  M.

Based on the kinetic data presented in Fig. 3 and Tables 2 and 3, it is seen that the ability of the photoinitiators studied to initiate the polymerization process of triacrylate depends on the number of components, *i.e.* the composition of the photoinitiator. The polymerization process of TMPTA in the presence of a three-component photoinitiating system is more effective than that when two-component photoinitiators are used.

The fundamental differences between the photoinitiators studied are noticeable in Fig. 3. Three-component PISs provide higher monomer conversions. Moreover, the overall time for polymerization of the monomer is shorter, which is important for rapid curing of polymer coatings.

The rate of polymerization and monomer conversion depend on the concentration of the used photoinitiator. The efficiency of SQG1/B2 systems increases proportionally to the increased concentration of radical source. However, the degree of double bond monomer conversion is relatively low. It

should be noted that the introduction of a third component to the PIS results in better kinetic parameters for polymerization of the triacrylate monomer initiated under UV-Vis light.

Based on the kinetic results, one can conclude that in two-component photoinitiating systems composed of squaraine dye and tris(trimethylsilyl)silane, the active radicals (silyl radicals) for the polymerization process are formed as a result of a primary photochemical reaction between an excited singlet state of photosensitizer and the co-initiator. Addition of a second co-initiator to the photoinitiator system results in other types of primary photochemical process that lead to the generation of other types of initiating radicals. For three-component photoinitiators, both primary photochemical processes and subsequent secondary processes lead to an increase in the number of radicals initiating polymerization and consequently to better kinetic parameters for the process.

### 3.3. Comparison of the photoinitiator systems presented with other systems

The photoinitiating efficiency of the co-initiators studied was compared with that of systems composed of 1,3-bis(*p*-substituted phenylamino)squaraines as photosensitizers and *n*-butyl-triphenylborate salt (B2), diphenyliodonium chloride (I1) and *N*-methoxy-4-phenylpyridinium tetrafluoroborate (NO) as co-initiators. These photoinitiating systems for the radical polymerization of TMPTA were studied and described in a previous paper.<sup>50</sup> The degree of double bond conversion was in the range from 7.78% to 67.60%. Similar to the photoinitiators described here, the lowest kinetic parameters were obtained for systems composed of 1,3-bis(*p*-substituted phenylamino)squaraines and borate salt B2 ( $C_{\%}$ : 7.78%–27.41%). Diphenyliodonium chloride (I1) was better co-initiator for *p*-substituted squaraines. The monomer conversions were about 2–4 times higher than those observed for the borate salt (B2) and achieved values from 12.27% to 40.79%. The best kinetic results were obtained for systems composed of the *N*-alkoxy-pyridinium salt (conversion of monomer: 20%–70%). Based on this, one can conclude that the photoinitiating efficiency depends on the sensitizer structure as well as the co-initiator. The photosensitizer possessing a sulphonyl group in the *para* position of the phenyl ring is the best component for a photoinitiator system. The photoinitiating ability of systems

**Table 3** Comparison of the kinetic parameters of the radical polymerization of TMPTA initiated by two- and three-component photoinitiating systems

Photoinitiator <sup>a</sup>	Parameter					
	Co-initiator concentration (M)	Max. heat flow (mW mg <sup>-1</sup> )	$t^{\max}$ (min)	$R_p^{\max}$ (10 <sup>-3</sup> s <sup>-1</sup> )	$C_{\%}$ (%)	$I_p$ (10 <sup>-6</sup> s <sup>-2</sup> )
SQG1/B2	$2 \times 10^{-3}$	0.14	8.62	0.18	5.97	0.35
	$5 \times 10^{-3}$	0.52	6.64	0.66	9.98	1.66
SQG1/TTMSS	$2 \times 10^{-3}$	0.48	7.44	0.61	3.26	1.37
	$5 \times 10^{-3}$	0.22	10.01	0.28	11.67	0.47
SQG1/TTMSS/B2	$5 \times 10^{-3}/1 \times 10^{-3}$	1.24	9.42	1.57	20.14	2.78

<sup>a</sup> Concentration of SQG1 for the two-component PISs was the same as that of the appropriate co-initiator. Concentration of SQG1 was  $1 \times 10^{-3}$  M for the three-component photoinitiating system.

composed of other squaraine dyes is similar to that observed for the two-component photoinitiators described here. The efficiency of the two-component system exhibiting the highest degree of monomer double bond conversion<sup>50</sup> is comparable with that of the three-component system SQG1/TTMSS/I81.

Next, the photoinitiating ability of the best photoinitiator system studied was compared with systems containing the commercially available sensitizer thioxanthone with different co-initiators: diphenyliodonium chloride (I1), methyl-ethanoldiamine (MEDA), mercaptobenzoxazole (MO), *N*-phenylglycine (NPG) and ethyl 4-*N,N*-dimethyl-aminobenzoate (EDMAB). The concentration of commercial sensitizer and co-initiator was  $5 \times 10^{-3}$  M and was higher than that for the best photoinitiator proposed by us (Fig. 4).

As seen, all photoinitiating systems are very efficient for free radical polymerization of triacrylate (TMPTA) under irradiation with UV-Vis light. However, the degree of double bond conversion achieved higher values in the case of the three-component photoinitiator composed of 1,3-bis(phenyl-amino)squaraine, tris(trimethylsilyl)silane and (4-methoxyphenyl)-(4-nitrophenyl)iodonium *p*-toluenesulphonate. The highest values of  $C_{\%}$  reached for commercially available sensitizers are about 7% and 25%.

We proposed new three-component photoinitiating systems composed of tris(trimethylsilyl)silane (TTMSS) for polymerization of 2-ethyl-2-(hydroxymethyl)-1,3-propanediol triacrylate (TMPTA). These systems are different from those described in the literature due to the presence of a new sensitizer, which belongs to the group of squaraines. In comparison with typical PISs containing TTMSS and commercially available sensitizers, our photoinitiators lead to higher monomer conversions. The polymerization process of TMPTA using the presented three-

component photoinitiating systems is more effective than that using two-component photoinitiating systems. In 2011, Lalev e and coworkers<sup>18</sup> proposed Type II PI/organosilane systems using a thioxanthone derivative (isopropylthioxanthone – ITX) and camphorquinone (CQ). In these cases, the degree of monomer conversion ( $C_{\%}$ ) achieved values of 20% and 40%–60% for ITX and CQ, respectively. For the investigated three-component PISs based on SQG1 dye we obtained  $C_{\%}$  values from 30% to *ca.* 60% for systems containing silane and iodonium salt as the second co-initiator. The high values of the kinetic parameters of the polymerization of TMPTA may be related to increased concentration of initiating radicals due to the interactions between both the sensitizer and the co-initiator and the co-initiator (TTMSS) and the second co-initiator (*e.g.* iodonium salt).<sup>18</sup>

## 4. Conclusions

In this paper, the efficiency of the photoinitiated polymerization of the acrylate monomer (TMPTA) in the presence of two- and three-component systems based on squaraine dye and various types of co-initiators was ascertained. For systems containing three components (sensitizer and two co-initiators), rates of polymerization of about  $2 \times 10^{-3} \text{ s}^{-1}$  (*ca.*  $17 \times 10^{-3} \text{ s}^{-1}$  for the highest performance system SQG1/TTMSS/I81) and monomer conversions in the range from 10% to 60% were obtained.

The systems composed of  $1 \times 10^{-3}$  M SQG1,  $2 \times 10^{-3}$  M TTMSS and  $5 \times 10^{-3}$  M second co-initiator show the most effective photoinitiation of the polymerization reaction.

On the basis of the obtained results, one may conclude that three-component photoinitiating systems comprising tris(trimethylsilyl)silane are more effective than their two-component analogues. The introduction of a second co-initiator to the photoinitiating system results in improvement of the kinetic parameters of the radical polymerization of acrylates.

The proposed new systems acting in the UV-Vis light region may be used as effective photoinitiators in photopolymerization reactions for the production of novel polymer materials. Moreover, these PISs show an important advantage, namely the ability to prevent oxygen inhibition, which is one of the problems encountered during curing of polymerization mixtures.

## Conflicts of interest

There are no conflicts to declare.

## Acknowledgements

This work was supported by the National Science Centre – NCN (Cracow, Poland), Grant No. 2013/11/B/ST5/01281.

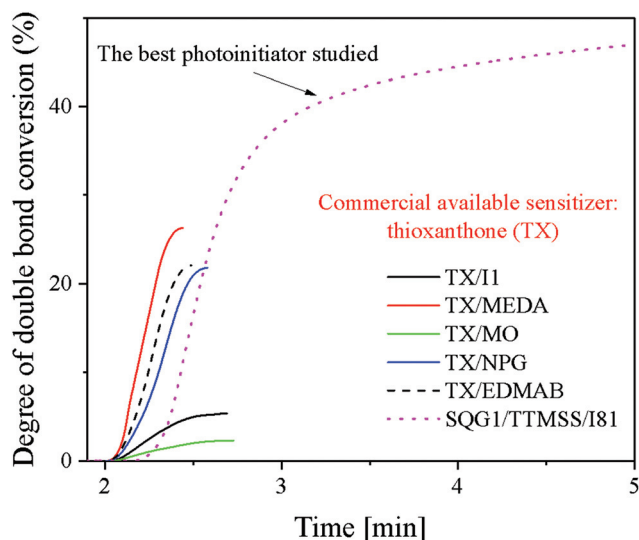


Fig. 4 The kinetic curves recorded during radical polymerization of TMPTA initiated by two-component photoinitiating systems composed of the commercially available photosensitizer thioxanthone (TX) and various co-initiators, and by the best three-component photoinitiator studied.

## References

- 1 W. Liao, C. Xu, X. Wu, Q. Liao, Y. Xiong, Z. Li and H. Tang, *Dyes Pigm.*, 2020, **178**, 108350.
- 2 R. Cui, K. Wang, G. Ma, B. Qian, J. Yang, Q. Yu and J. Nie, *J. Appl. Polym. Sci.*, 2011, **120**, 2754–2759.
- 3 C. Dietlin, S. Schweizer, P. Xiao, J. Zhang, F. Morlet-Savary, B. Graff, J. P. Fouassier and J. Lalevée, *Polym. Chem.*, 2015, **6**, 3895–3912.
- 4 K. Podemska, R. Podsiadły, A. M. Szymczak and J. Sokołowska, *Dyes Pigm.*, 2012, **94**, 113–119.
- 5 S. You, P. Wang, J. Schimelman, H. H. Hwang and S. Chen, *Addit. Manuf.*, 2019, **30**, 100834.
- 6 J. Kirschner, J. Paillard, B. Graff, J. M. Becht, J. E. Klee and J. Lalevée, *Macromol. Chem. Phys.*, 2020, **221**, 1900495.
- 7 K. B. Riad, A. A. Arnold, J. P. Claverie, S. V. Hoa and P. M. Wood-Adams, *ACS Appl. Nano Mater.*, 2020, **3**, 2875–2880.
- 8 A. Bagheri and J. Jin, *ACS Appl. Polym. Mater.*, 2019, **1**, 593–611.
- 9 J. Kabatc, *J. Polym. Sci., Part A: Polym. Chem.*, 2017, **55**, 1575–1589.
- 10 S. Erdur, G. Yilmaz, D. G. Colak, I. Cianga and Y. Yagci, *Macromolecules*, 2014, **47**, 7296–7302.
- 11 M. Szycher, *Szycher's handbook of polyurethanes*, CRC Press, USA, 2nd edn, 2012.
- 12 D. C. R. S. De Oliveira, M. G. Rocha, A. Gatti, A. B. Correr, J. Ferracane and M. A. C. Sinhoret, *J. Dent.*, 2015, **43**, 1565–1572.
- 13 A. Eibel, D. E. Fast and G. Gescheidt, *Polym. Chem.*, 2018, **9**, 5107–5115.
- 14 B. Fang, M. Jin, X. Wu, Y. Zhang and D. Wang, *Dyes Pigm.*, 2016, **126**, 54–61.
- 15 J. Zhang, N. Zivic, F. Dumur, C. Guo, Y. Li, P. Xiao, B. Graff, D. Gimes, J. P. Fouassier and J. Lalevée, *Mater. Today Commun.*, 2015, **4**, 101–108.
- 16 A. Nejadbrahim, M. Ebrahimi, X. Allonas, C. Croutxé-Bargghorn, C. Ley and B. Métral, *RSC Adv.*, 2019, **9**, 39709–39720.
- 17 C. Ley, C. Carré, A. Ibrahim and X. Allonas, Application of high performance photoinitiating systems for holographic grating recording, in *Holographic materials and optical systems*, InTech, 2017, ch. 17.
- 18 J. Lalevée, M. A. Tehfe, F. Morlet-Savary, B. Graff, X. Allonas and J. P. Fouassier, *Prog. Org. Coat.*, 2011, **70**, 83–90.
- 19 J. Lalevée and J. P. Fouassier, *Dyes and chromophores in polymer science*, Wiley, 2015.
- 20 J. P. Fouassier, F. Morlet-Savary, J. Lalevée, X. Allonas and C. Ley, *Materials*, 2010, **3**, 5130–5142.
- 21 J. Kabatc and K. Jurek, *Polymer*, 2012, **53**, 1973–1980.
- 22 X. Ma, D. Cao, H. Fu, J. You, R. Gu, B. Fan and J. Nie, *Prog. Org. Coat.*, 2019, **135**, 517–524.
- 23 J. Kabatc, *Polymer*, 2010, **51**, 5028–5036.
- 24 P. Xiao, J. Zhang, F. Dumur, M. A. Tehfe, F. Morlet-Savary, B. Graff, D. Gimes, J. P. Fouassier and J. Lalevée, *Prog. Polym. Sci.*, 2015, **41**, 32–66.
- 25 X. Peng, D. Zhu and P. Xiao, *Eur. Polym. J.*, 2020, **127**, 109569.
- 26 J. P. Fouassier and J. Lalevée, *RSC Adv.*, 2012, **2**, 2621–2629.
- 27 J. P. Fouassier and J. Lalevée, *Photoinitiators for polymer synthesis: Scope, reactivity and efficiency*, Wiley, 2012.
- 28 J. Lalevée, A. Dirani, M. El-Roz, X. Allonas and J. P. Fouassier, *Macromolecules*, 2008, **41**, 2003–2010.
- 29 Y. Chen, Q. Jia, Y. Ding, S. Sato, L. Xu, C. Zang, X. Shen and T. Kakuchi, *Macromolecules*, 2019, **52**, 844–856.
- 30 J. Lalevée, M. El-Roz, X. Allonas and J. P. Fouassier, *Prog. Org. Coat.*, 2009, **65**, 457–461.
- 31 J. Steindl, T. Koch, N. Moszner and C. Gorsche, *Macromolecules*, 2017, **50**, 7448–7457.
- 32 J. Lalevée, M. A. Tehfe, F. Morlet-Savary, B. Graff, X. Allonas and J. P. Fouassier, *Prog. Org. Coat.*, 2011, **70**, 23–31.
- 33 L. Song, Q. Ye, X. Ge, A. Misra and P. Spencer, *Dent. Mater.*, 2016, **32**, 102–113.
- 34 M. A. Tehfe, M. El-Roz, J. Lalevée, F. Morlet-Savary, B. Graff and J. P. Fouassier, *Eur. Polym. J.*, 2012, **48**, 956–962.
- 35 D. Wang, P. Garra, J. P. Fouassier and J. Lalevée, *Polym. Chem.*, 2020, **11**, 857–866.
- 36 J. Tan, B. Wu, J. Yang, Y. Zhu and Z. Zeng, *Polymer*, 2010, **51**, 3394–3401.
- 37 Z. Uyar, M. Durgun, M. S. Yavuz, M. B. Abaci, U. Arslan and M. Degirmenci, *Polymer*, 2017, **123**, 153–168.
- 38 Z. Uyar, F. Turgut, U. Arslan, M. Durgun and M. Degirmenci, *Eur. Polym. J.*, 2019, **119**, 102–113.
- 39 T. Corrales, F. Catalina, C. Peinado and N. S. Allen, *J. Photochem. Photobiol., A*, 2003, **159**, 103–114.
- 40 J. Yang, C. Xu, W. Liao, Y. Xiong, X. Wang and H. Tang, *Prog. Org. Coat.*, 2020, **138**, 105410.
- 41 J. Kabatc, J. Ortyl and K. Kostrzewska, *RSC Adv.*, 2017, **7**, 41619.
- 42 K. Jurek, J. Kabatc and K. Kostrzewska, *Dyes Pigm.*, 2016, **133**, 273–279.
- 43 J. Brandrup and E. H. Immergut, *Polymer Handbook*, John Wiley & Sons, Inc., New York, Chichester, Brisbane, Toronto, Singapore, 3rd edn, 1989.
- 44 A. Balcerak, K. Iwińska and J. Kabatc, *Dyes Pigm.*, 2019, **170**, 107596.
- 45 S. Khopkar and G. Shankarling, *Dyes Pigm.*, 2019, **170**, 107645.
- 46 G. Alberto, N. Barbero, C. Divieto, E. Rebba, M. P. Sassi, G. Viscardi and G. Martra, *Colloids Surf., A*, 2019, **568**, 123–130.
- 47 J. Kabatc, K. Kostrzewska and Ł. Orzeł, *Dyes Pigm.*, 2016, **130**, 226–232.
- 48 J. Kabatc, K. Kostrzewska and K. Jurek, *RSC Adv.*, 2016, **6**, 74715–74725.
- 49 J. Kabatc, K. Kostrzewska, M. Kozak and A. Balcerak, *RSC Adv.*, 2016, **6**, 103851–103863.
- 50 J. Kabatc, K. Kostrzewska, K. Jurek, M. Kozak and A. Balcerak, *J. Polym. Sci., Part A: Polym. Chem.*, 2017, **55**, 471–484.

## Supporting Information

### **Highly efficient UV-Vis light activated three-component photoinitiators comprising of *tris(trimethylsilyl)silane* for polymerization of acrylates**

Alicja Balcerak, Dominika Kwiatkowska, Katarzyna Iwińska and Janina Kabatc\*

*UTP University of Science and Technology, Faculty of Chemical Technology and Engineering,  
Seminaryjna 3, 85-326 Bydgoszcz, Poland*

\* Corresponding author.

*E-mail address: nina@utp.edu.pl (J. Kabatc)*

## 1. Spectroscopic properties of co-initiators used in photopolymerization experiments.

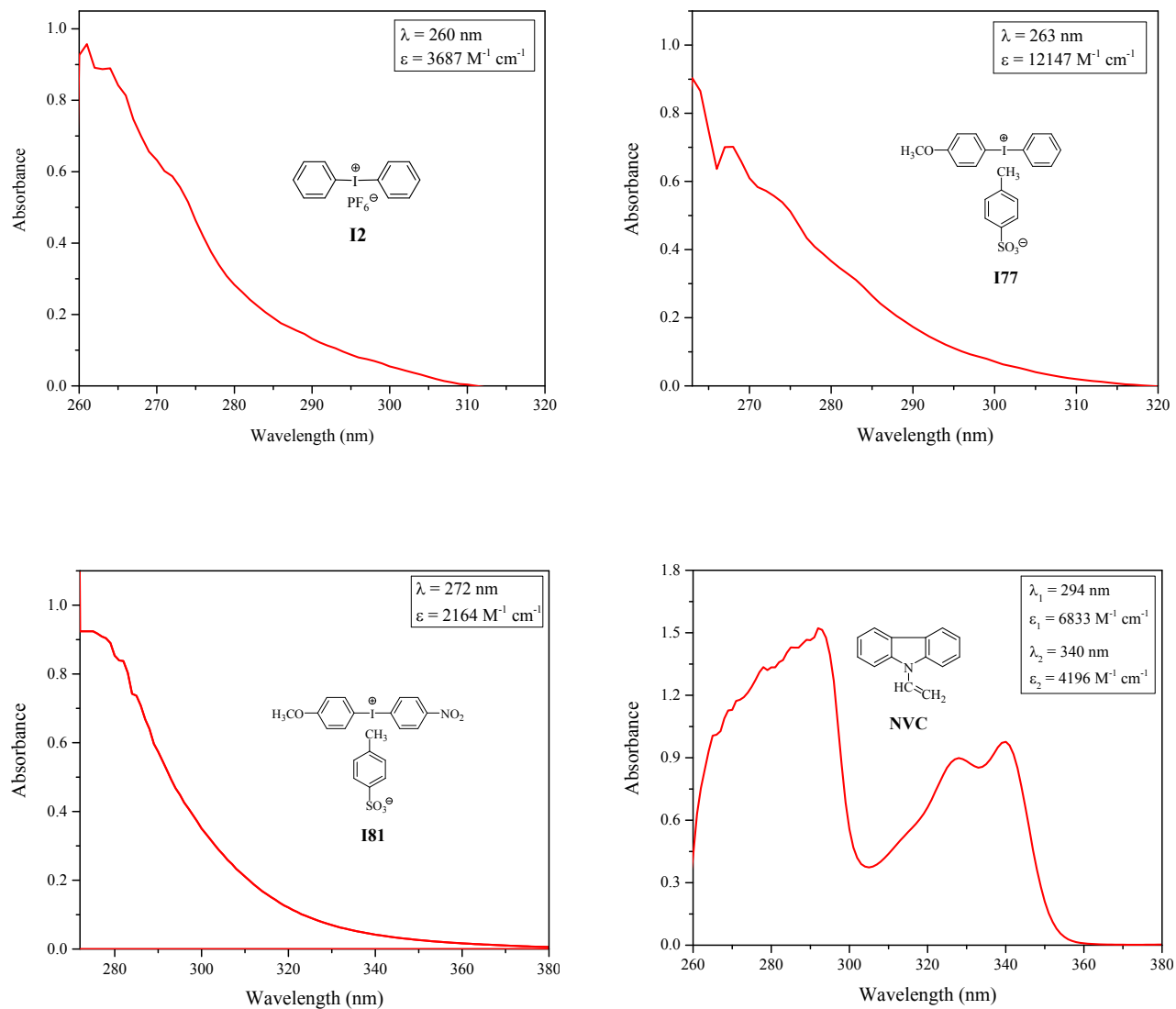


**Fig. S1** The normalized absorption spectra of initiators: I2, I77, I81 and NVC in 1-methyl-2-pyrrolidinone (MP), recorded at room temperature.

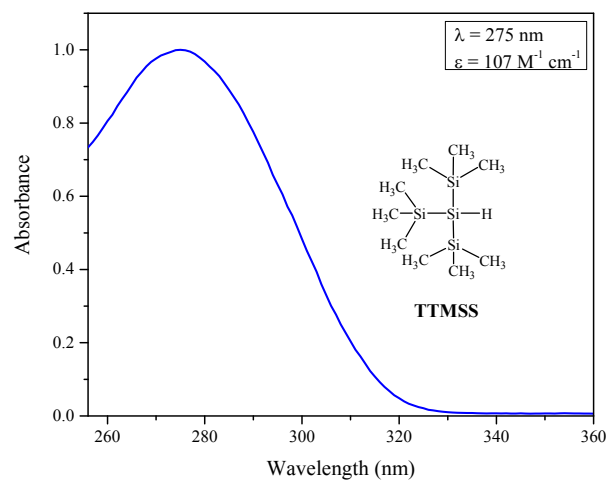
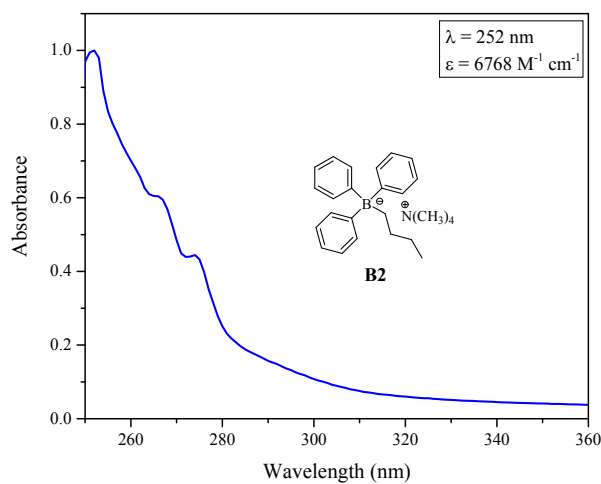
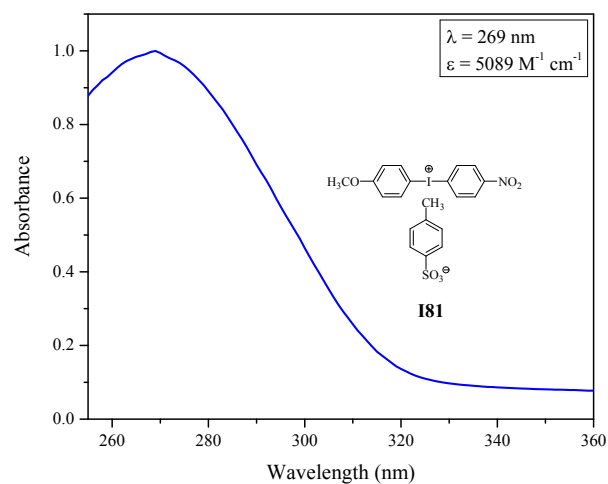
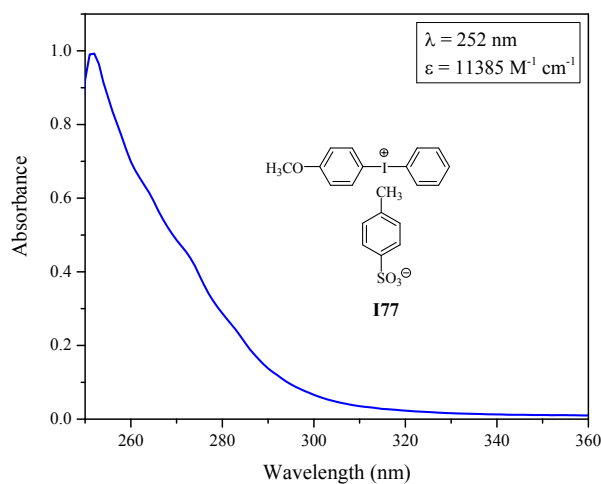
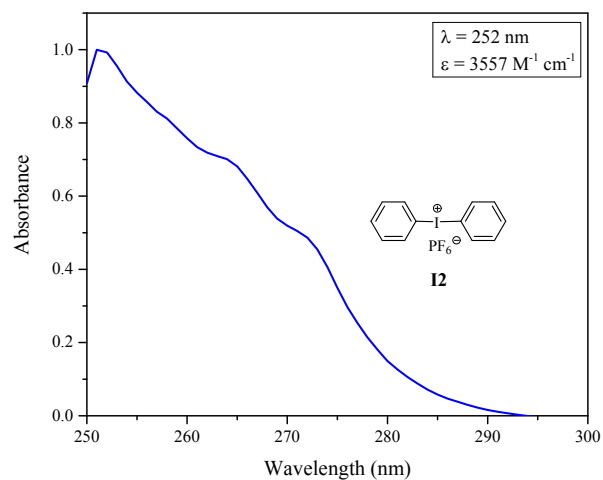
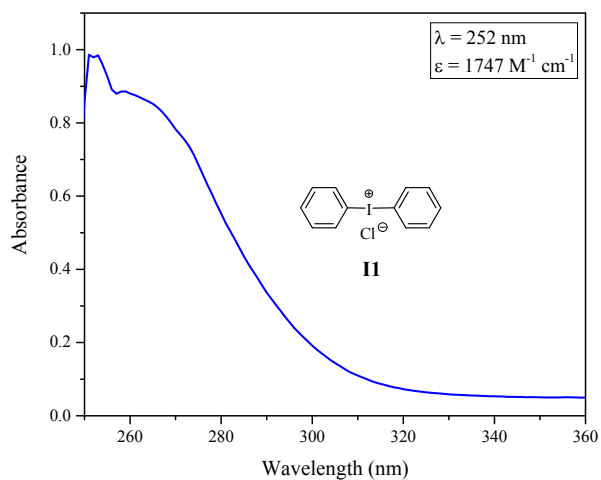


**Fig. S2** Normalized absorption spectra of initiators: I1, I2, I77, I81, B2 and TTMSS in ethyl acetate (AcOEt) recorded at room temperature.

## 2. Emission spectrum of high-pressure mercury lamp (OmniCure S2000)

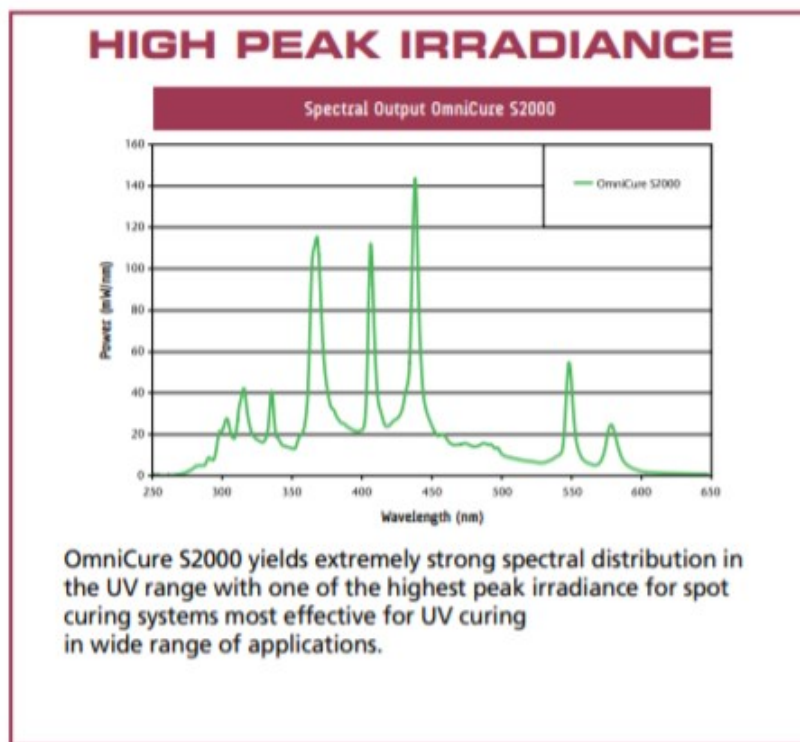


**Fig. S3** Emission spectrum of the lamp OmniCure S2000.

## 3. Kinetic effect registered depending of type of reference sample.

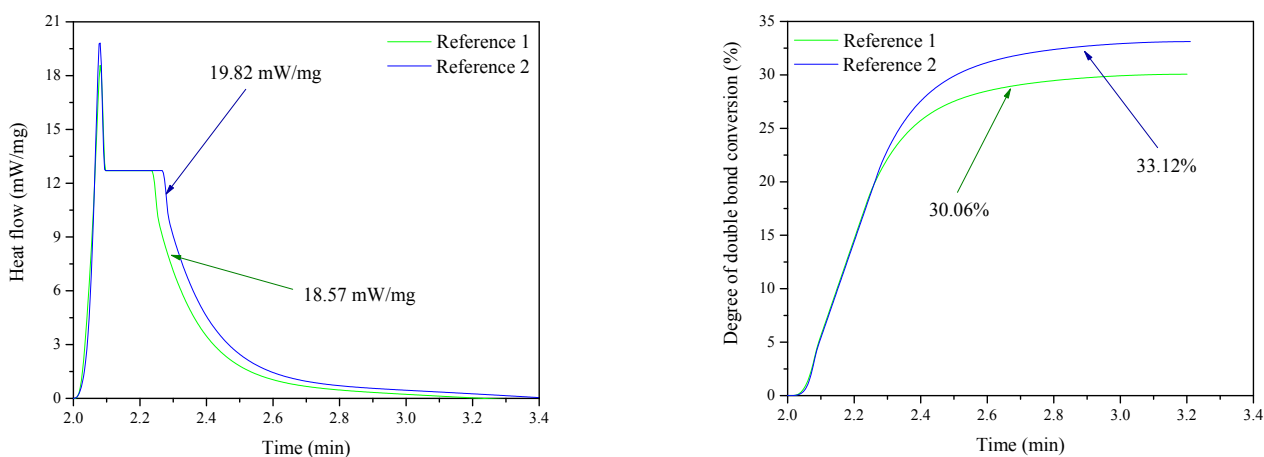


**Fig. S4** The kinetic curves registered during radical polymerization of TMPTA initiated by three-component photoinitiating systems containing SQG1 dye as sensitizer, I81 and TTMSS as co-initiators. The concentration of components of PISs was  $2 \times 10^{-3}$  M. The heat effects were recorded in the presence of different polymerization mixture: Reference 1 - SQG1/MP/TMPTA; Reference 2 – MP/TMPTA.

**4. Cyclic voltammetry curves showing oxidation and reduction processes of selected components of photoinitiating systems in acetonitrile.**

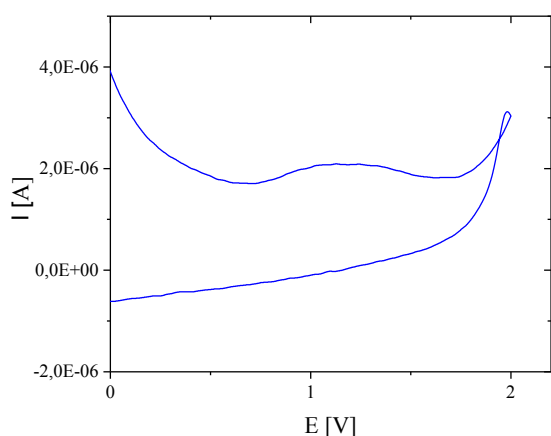


**Figure S5** Cyclic voltammogram curves of the 1,3-bis(phenylamino)squaraine oxidation in acetonitrile.

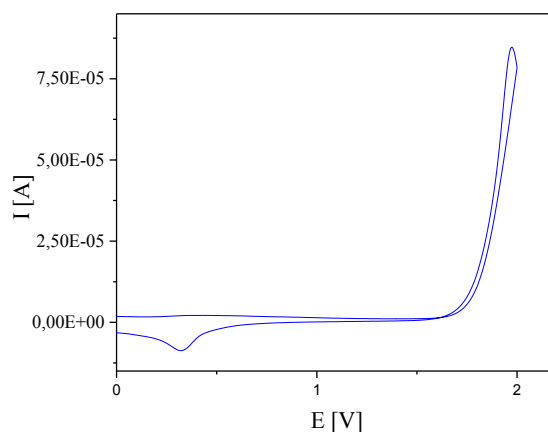


**Figure S6** Cyclic voltammogram curves of the tris(trimethylsilyl)silane oxidation in acetonitrile.

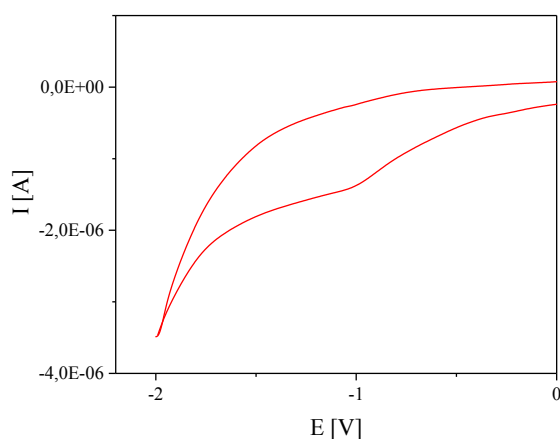


**Figure S7** Cyclic voltammogram curves of the diphenyliodonium hexafluorophosphate reduction in acetonitrile.

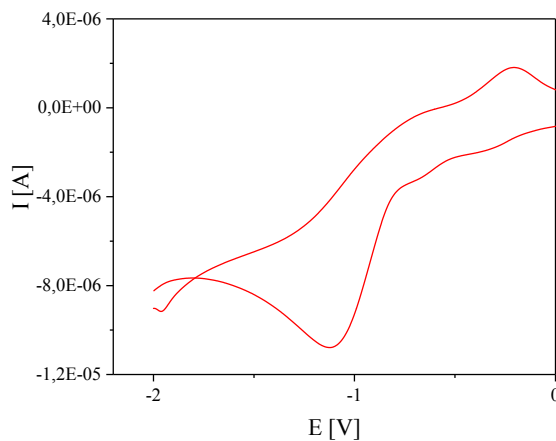


**Figure S8** Cyclic voltammogram curves of the (4-methoxyphenyl)-phenyliodonium *p*-toluenesulfonate reduction in acetonitrile.

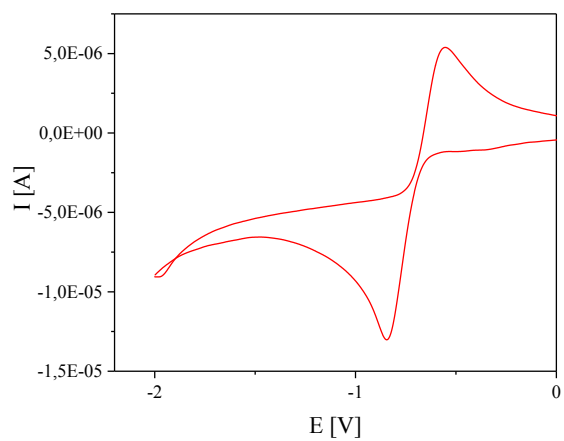


**Figure S9** Cyclic voltammogram curves of the (4-methoxyphenyl)-(4-nitrophenyl)iodonium *p*-toluenesulfonate reduction in acetonitrile

**Publikacja naukowa [A6]**

## Article

# High-Performance UV-Vis Light Induces Radical Photopolymerization Using Novel 2-Aminobenzothiazole-Based Photosensitizers

Alicja Balcerak <sup>1,\*</sup>, Janina Kabatc <sup>1</sup>, Zbigniew Czech <sup>2,\*</sup>, Małgorzata Nowak <sup>2</sup> and Karolina Mozelewska <sup>2</sup>

<sup>1</sup> Department of Organic Chemistry, Faculty of Chemical Technology and Engineering, Bydgoszcz University of Science and Technology, Seminaryjna 3, 85-326 Bydgoszcz, Poland; nina@pbs.edu.pl

<sup>2</sup> International Laboratory of Adhesives and Self-Adhesive Materials, Department of Chemical Organic Technology and Polymeric Materials, Faculty of Chemical Technology and Engineering, West Pomeranian University of Technology in Szczecin, Pułaskiego 10, 70-322 Szczecin, Poland; nowak.malgorzata@zut.edu.pl (M.N.); karolina\_mozelewska@zut.edu.pl (K.M.)

\* Correspondence: alicja.balcerak@pbs.edu.pl (A.B.); psa\_czech@wp.pl (Z.C.)

**Abstract:** The popularity of using the photopolymerization reactions in various areas of science and technique is constantly gaining importance. Light-induced photopolymerization is the basic process for the production of various polymeric materials. The key role in the polymerization reaction is the photoinitiator. The huge demand for radical and cationic initiators results from the dynamic development of the medical sector, and the optoelectronic, paints, coatings, varnishes and adhesives industries. For this reason, we dealt with the subject of designing new, highly-efficient radical photoinitiators. This paper describes novel photoinitiating systems operating in UV-Vis light for radical polymerization of acrylates. The proposed photoinitiators are composed of squaraine (SQ) as a light absorber and various diphenyliodonium (Iod) salts as co-initiators. The kinetic parameters of radical polymerization of trimethylolpropane triacrylate (TMPTA), such as the degree of double bonds conversion ( $C\%$ ), the rate of photopolymerization ( $R_p$ ), as well as the photoinitiation index ( $I_p$ ) were calculated. It was found that 2-aminobenzothiazole derivatives in the presence of iodonium salts effectively initiated the polymerization of TMPTA. The rates of polymerization were at about  $2 \times 10^{-2} \text{ s}^{-1}$  and the degree of conversion of acrylate groups from 10% to 36% were observed. The values of the photoinitiating indexes for the most optimal initiator concentration, i.e.,  $5 \times 10^{-3} \text{ M}$  were in the range from  $1 \times 10^{-3} \text{ s}^{-2}$  even to above  $9 \times 10^{-3} \text{ s}^{-2}$ . The photoinitiating efficiency of new radical initiators depends on the concentration and chemical structure of used photoinitiator. The role of squaraine-based photoinitiating systems as effective dyeing photoinitiators for radical polymerization is highlighted in this article.

**Keywords:** UV-Vis light photoinitiators; 2-aminobenzothiazole derivatives; squaraine dyes; iodonium salts; radical polymerization



**Citation:** Balcerak, A.; Kabatc, J.; Czech, Z.; Nowak, M.; Mozelewska, K. High-Performance UV-Vis Light Induces Radical Photopolymerization Using Novel 2-Aminobenzothiazole-Based Photosensitizers. *Materials* **2021**, *14*, 7814. <https://doi.org/10.3390/ma14247814>

Academic Editor: Gerard Lligadas

Received: 19 November 2021

Accepted: 13 December 2021

Published: 17 December 2021

**Publisher's Note:** MDPI stays neutral with regard to jurisdictional claims in published maps and institutional affiliations.



**Copyright:** © 2021 by the authors. Licensee MDPI, Basel, Switzerland. This article is an open access article distributed under the terms and conditions of the Creative Commons Attribution (CC BY) license (<https://creativecommons.org/licenses/by/4.0/>).

## 1. Introduction

Currently, a large number of polymer materials is produced by photopolymerization [1]. Generally, photochemically induced polymerization is defined as a process in which reactive species (radicals or ions) formed from light-activated molecules, called photoinitiators (PI), initiate a series of chemical reactions and as a result transform liquid monomers into cross-linked polymer structures.

The photopolymerization is considered as one of the most widespread, modern and rapidly developing technologies used in the chemical industry [2–4]. Photoinitiated polymerization reactions show a huge potential in the simple and fast synthesis of polymeric materials with specified features. In comparison with the conventional curing techniques, the interest towards photochemically initiated polymerization is constantly gaining importance [5]. The increasing popularity of photopolymerization is related to numerous unique

advantages, such as low economic costs [6,7], high efficiency [8,9], the possibility of spatial and temporal control over the process [10,11] and a fast-curing rate [12]. These techniques are referred to as eco-friendly because of the possibility of using solvent-free polymerizable compositions with zero or a very low index of volatile organic compounds (VOCs), which are one of the major sources of environmental pollution. Moreover, there is the possibility of the easy recycling of waste generated during the production of process [13,14].

Due to many advantages, the light-activated polymerization has a wide range of applications. This process is used in many areas of science and technology, such as: medicine, paint and varnish industry, printing, production of adhesives, nanotechnology, electronic sector and many others [15,16]. Some examples of applications of photopolymerization in different areas are presented in Figure 1.



Figure 1. Areas of applications of photopolymerization processes.

One of the main uses of the photopolymerization process in medicine is the production of dental fillings. Novel, durable and aesthetic light-cured dental composites displaced the traditional amalgams and became the basic materials used to fill cavities in teeth. However, the requirements for new composites are still enormous and pose huge challenges for designing dental fillings [17,18]. The light-cured dental fillings should show high durability, attrition strength, as well as chemical and physical resistance factors, such as: salivary enzymes, acids and bacterial metabolism products and others. Moreover, it is extremely important that these types of materials exhibit high biocompatibility in relation to oral tissues, good dimensional stability during crosslinking and resistance for yellowing [19].

The subject of design and the development of new hydrogels is also more and more popular. These elastic and highly hydrated biomaterials possess great and unique properties, which enables them usage in regenerative medicine [20]. Especially important features of hydrogels are: biocompatibility, biodegradability, extreme water-binding capacity and the ability to adjust the physicochemical properties. Hydrogels exhibit an excellent ability to heal wounds, which was confirmed by a large group of scientists [21–23].

The photopolymerization is a key process in the production of various types of polymer coatings. Innovative varnishes with excellent antibacterial and antimicrobial properties for dentistry [24,25], novel paints for the degradation of organic pollutants in water [26], biocompatible film-forming polymer adhesives activated by natural sunlight [27], and

programmable shape-shifting 3D structures [28] are just a few examples of new inventions that represent an important step towards the progress of new technologies.

Notably, in recent years, a dynamic progress of 3D printing technique was observed, which offers many benefits compared to traditional manufacturing processes of novel polymer materials [29,30]. First of all, the use of 3D printing techniques enables us to accelerate the time of introducing novel products to the worldwide market. Moreover, this technology eliminates the need of expensive apparatus and thus significantly decreases the production costs. The additional benefits include: accuracy, speed and flexibility towards manufacturing a wide range of materials. What is important is that 3D printing guarantees less waste production than traditional methods [31,32]. An interesting work about the application of these technique was presented in 2021 by Bai and co-workers [33]. A group of scientists described 3D concrete printing (3DCP), which is a new and promising construction technology. The researcher group introduced the possibility of using underutilized solids and waste solid aggregates for the production of concrete. Three-dimensional printing has become extremely important also during the current COVID-19 pandemic, what is confirmed by numerous publications on this topic [34–37]. The use of this technology has proved invaluable in eliminating the shortage of basic personal protective supplies and healthcare equipment for medical personnel. The 3D printing technique is used to produce medical face shields, respirators, biodegradable mask filters and 3D bioprinted tissue models for coronavirus research. The dynamics of the research in the field of 3D printing has become a very important aspect in the fight against the pandemic.

Numerous examples of the use of photopolymerization processes in various areas of science and technology show how important these topics are and prove the high potential of this technology in the production of various polymer materials. Hence, searching for new photoinitiating systems (PISs) and designing new photocurable compositions is a key aspect for progress in the development of novel techniques such as photopolymerization.

Typical photocurable composition is comprised of monomer or mixtures of monomers and oligomers, photoinitiator and other ingredients: solvents, fillers, substances improving the stability of formulations and others [38,39]. Nowadays, a wide variety of monomers is commercially available. The most commonly used compounds are acrylates and methacrylates, epoxides, esters, urethanes, etc. A large number of photoinitiators for radical as well as ionic polymerization have been already described in the literature. However, a large number of scientific works is directed towards searching for new, high-performance photoinitiating systems. Next generation photoinitiators exhibit high activity even under low intensities of light. Moreover, an increasing number of novel compounds work not only in the range of ultraviolet (UV), but also in visible light (Vis) [40–42].

The wide group of photoinitiators are systems based on dyes acting as light absorbers. The introduction of dye molecules into the photoinitiating system enables a shift in the band of absorption towards longer wavelengths and, significantly, expands the area of application of the photoinitiator. The dye molecule acts as a sensitizer for other compounds, such as co-initiators, which work as electron donors or electron acceptors. In this type of system, the main process leading to the generation of initiating radicals is an electron transfer process (ET) [3].

The example of highly efficient initiators dedicated to radical polymerization are the two-component PISs containing of sensitizer molecule and co-initiator. In such bimolecular systems, the role of light absorbers can be played by various types of organic dyes, which was presented in Figure 2 [43].



**Figure 2.** Examples of dyes used as photosensitizers in dyeing photoinitiating systems [43].

The application of many of these compounds as photosensitizers in dye-based photoinitiating systems was described in the literature. However, the information about photosensitizers in the form of squaraines (SQs) are limited. The first paper mentioning the use of squaraine dyes as photosensitizers for radical polymerization was reported in 2004 by Wang and co-workers [44]. In 2021, Giacometto and co-workers [45] presented an overview paper regarding recent advances on squaraine-based photoinitiators. It turns out that squaraines are a promising group of useful dyes for various innovative applications because of their unique features, such as the easiness of the methods of synthesis, the low costs of manufacturing and good photochemical stability [45,46]. For these reasons, the design of novel squaraine acid derivatives seems to be really important.

The 2-aminobenzothiazole derivatives are an interesting group of compounds showing a wide range of applications due to their specific properties. For example, in 2016 Joseph and Boomadevi Janaki [47] described new copper complexes of Schiff base ligands of 2-aminobenzothiazole derivatives. These compounds were synthesized by the condensation of Knoevenagel of acetoacetanilide and 2-aminobenzothiazole. The copper complexes are characterized by a wide range of absorption, from 200 nm to ca. 800 nm. Moreover, all synthesized compounds show high antioxidant activity, antibacterial and antifungal properties. For this reason, it is possible to use of these copper complexes based on 2-aminobenzothiazole to decrease ROS levels or reduce oxidative stress in Alzheimer's patients [47].

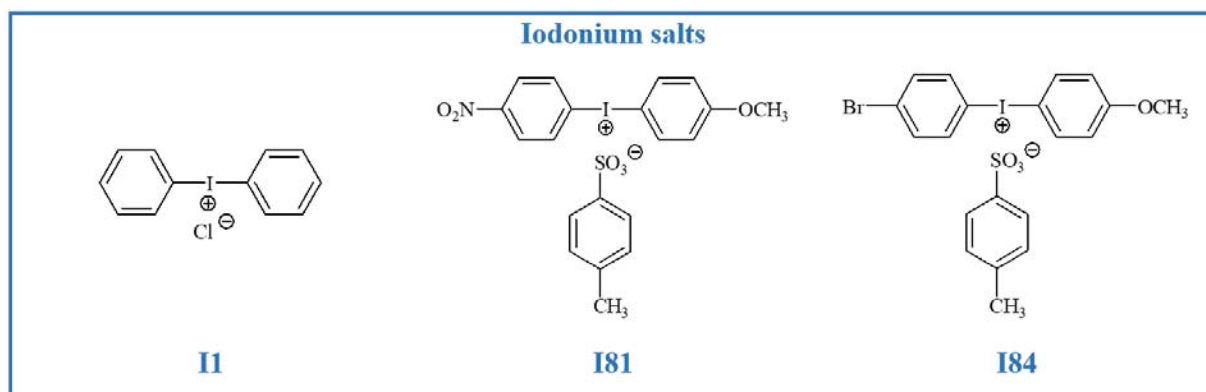
In this paper, we focused on determining the efficiency of novel two-component systems based on newly synthesized 2-aminobenzothiazole derivatives for the photoinitiation of radical polymerization of acrylate monomer. We decided to use these dyes as UV-Vis light absorbers and combined them with various iodonium salts to obtain a high performance photoinitiators. The similar compounds were used as sensitizers for radical polymerization of 1,6-hexanediacylate (HDDA) and gave promising results of kinetics of photopolymerization reaction, which was described by Zhao and co-workers in 2020 [48]. Novel *S*-benzoheterocycle thiobenzoates photoinitiators showed an excellent photoinitiating ability and cured polymeric films possessed comparable or better mechanical properties in comparison with commercially available photoinitiators, such as benzophenone (BP) and irgacure 184 [48]. Due to the high-performance of photoinitiating systems composed

of dye as sensitizer and co-initiator in the form of iodonium salt, what was proposed by Zhang and co-workers in 2019 [49] we examined the kinetics of the radical polymerization of trimethylolpropane triacrylate (TMPTA) using novel photoinitiators based on 2-aminobenzothiazole derivatives and various diphenyliodonium salts.

## 2. Materials and Methods

### 2.1. Materials

All reagents used for the synthesis of 2-aminobenzothiazole derivatives, such as: 3,4-dihydroxy-3-cyclobutene-1,2-dione (squaric acid), 2-aminobenzothiazole, 2-amino-6-bromobenzothiazole, 2-amino-6-methylbenzothiazole, 1-butanol and toluene were purchased from Aldrich Chemical Co. (Milwaukee, WI, USA) and used without further purification. The spectroscopic grade solvents *N,N*-dimethylformamide (DMF), and 1-methyl-2-pyrrolidinone (MP) were supplied by Alfa Aesar (Heysham, Lancashire, UK) and Aldrich Chemical Co. (Milwaukee, WI, USA). Diphenyliodonium chloride (I1) was purchased from Acros Organics (Carlsbad, CA, USA) and other iodonium salts, such as: (4-methoxyphenyl)-(4-nitrophenyl) iodonium *p*-toluenesulfonate (I81) and (3-bromophenyl)-(4-methoxyphenyl)iodonium *p*-toluenesulfonate (I84) were synthesized by scientists from Cracow University of Technology, as described in the literature [50]. The chemical structures of iodonium salts I1, I81 and I84 used as co-initiators in photopolymerization experiments are shown in Scheme 1. Trimethylolpropane triacrylate (TMPTA, from Sigma Aldrich, Burlington, MA, USA) was applied as a model acrylate monomer for the composition polymerized by a radical mechanism.



**Scheme 1.** The chemical structures of co-initiators.

### 2.2. General Procedure for the Synthesis of 2-Aminobenzothiazole Derivatives

The series of novel 2-aminobenzothiazoles, which played a role of photosensitizers in two-component photoinitiating systems, i.e.: 1,3-bis(benzothiazoleamino)squaraine (SQM1), 1,3-bis(6-bromobenzothiazoleamino)squaraine (SQM2) and 1,3-bis(6-methylbenzothiazoleamino)squaraine (SQM3), was synthesized in one-step reaction. The condensation reaction of 1 eqv. of squaric acid with 2 eqv. of 6-substituted 2-aminobenzothiazoles leads to squaraine dye formation, as presented in Scheme 2.

The squaraines SQM1-SQM3 were synthesized, as follows: 1,2-dihydroxycyclobuten-3,4-dione (2.5 mmol) was heated under reflux in a mixture of 1-butanol (40 mL) and toluene (20 mL). The water was distilled off azeotropically using a Dean-Stark trap. After 1 h of heating, an appropriate 6-substituted 2-aminobenzothiazole derivative (5 mmol) was added and the reaction mixture refluxed for additional 4 h. After that, the reaction mixture was cooled and the solvent removed under vacuum. The solid was dried at room temperature [46]. The 2-aminobenzothiazole derivatives were used as photosensitizers in photopolymerization experiments. The chemical structures of these compounds are depicted in Scheme 3. The  $^1\text{H}$  and  $^{13}\text{C}$  NMR spectra of SQM1-SQM3 compounds are available in Supplementary Materials (Figures S1–S6).



emission intensities for the dye and reference,  $n_{\text{dye}}$  and  $n_{\text{ref}}$  are the refractive indexes of the solvents used for the dye and reference, respectively.

The steady-state photolysis experiments were carried out to investigate the interactions between photosensitizer and co-initiator. The changes of the absorption of the photosensitizer and photosensitizer in the presence of an appropriate co-initiator in *N,N*-dimethylformamide (DMF) as a solvent after irradiation with an argon-ion laser at an intensity of  $50 \text{ mW} \times \text{cm}^{-2}$  were registered. The absorption measurements after 0 s, 10 s, 30 s, 60 s, 10 min, 20 min, 30 min and 60 min of irradiation were registered using an UV-Vis Cary 60 spectrophotometer (Agilent Technology). The concentration of co-initiator was  $1 \times 10^{-3} \text{ M}$ .

#### 2.4. Photopolymerization Experiments

The general procedure for photopolymerization experiments included several fundamental steps:

- The synthesis and spectral characterization of novel photosensitizers;
- The preparation of polymerizable compositions containing an appropriate concentration of photoinitiator;
- The selection of curing conditions of the polymerizing mixture, i.e.,: light source, intensity and range of light radiation and flow of inert gas (nitrogen).

The basic steps for the photopolymerization experiments are shown in Figure 3. The preparation of the appropriate polymerizable composition required the synthesis of new photosensitizers. These compounds were prepared according to the general procedure described in Section 2.2. In the next step, the squaraine dyes were combined with different co-initiators. These combinations were two-component photoinitiating systems for radical polymerization of trimethylolpropane triacrylate (TMPTA). The polymerization mixture was composed of 1.8 mL of monomer (TMPTA), 0.2 mL of solvent (MP), appropriate photosensitizer (SQM1/SQM2/SQM3) and co-initiator (I1/I81/I84). The use of 1-methyl-2-pyrrolidinone (MP) was necessary due to poor solubility of dye in monomer. The experiments were carried out for various concentration of photoinitiators:  $5 \times 10^{-4} \text{ M}$ ,  $1 \times 10^{-3} \text{ M}$ ,  $2 \times 10^{-3} \text{ M}$  and  $5 \times 10^{-3} \text{ M}$ . The monomer composition without a co-initiator was used as a reference sample.

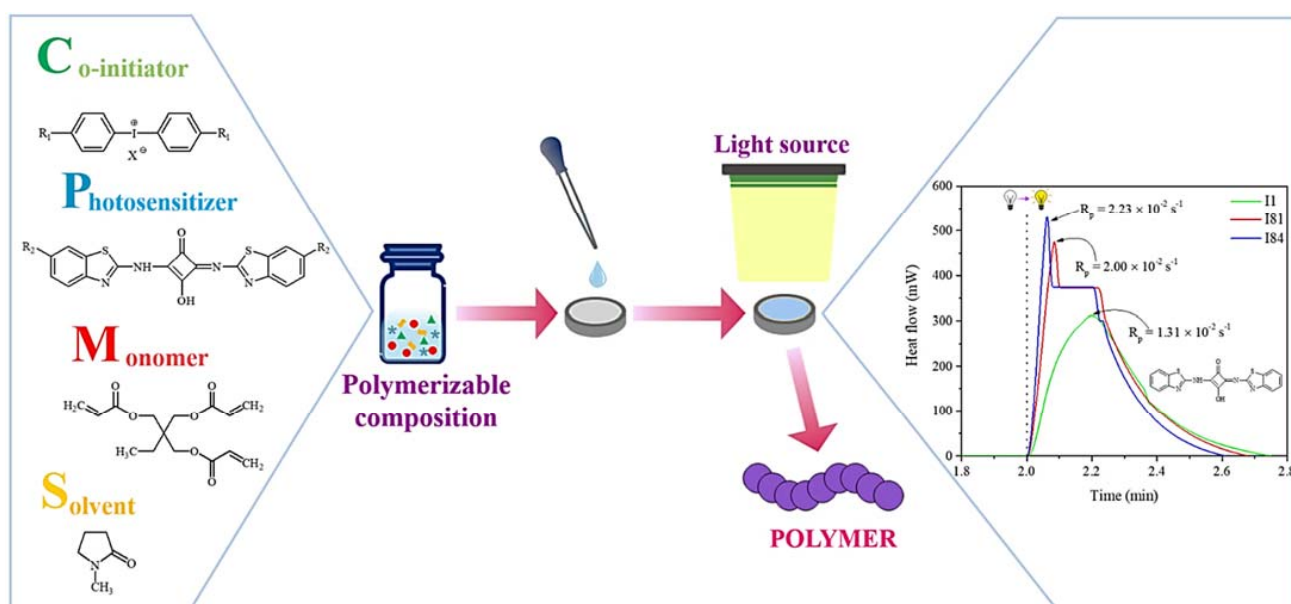


**Figure 3.** Schematic steps representation of photopolymerization experiments.

In order to determine the photoinitiation efficiency of the proposed systems, a regular photo-DSC setup was used. The photopolymerization experiments were carried out

using differential scanning calorimeter—DSC Q2000 (TA Instruments, New Castle, DE, USA) connected with TA Q PCA photo unit equipped with a high-pressure mercury lamp—OmniCure S2000 (Excelitas Technologies, Waltham, MA, USA). The radiation in the UV-Vis range (300–500 nm) at constant light intensity equal to  $30 \text{ mW} \times \text{cm}^{-2}$  was used as a light source. All measurements were performed under isothermal conditions at  $25 \text{ }^\circ\text{C}$  and nitrogen flow of  $50 \text{ mL} \times \text{min}^{-1}$ . The tested and reference samples weighing  $30 \pm 0.1 \text{ mg}$  were placed into an open aluminum DSC pan and then maintained at the prescribed temperature, i.e.,  $25 \text{ }^\circ\text{C}$  for 2 min before each measurement run began. The heat evolved during the exothermal reaction and was registered at sampling intervals of 0.05 s per point.

On the basis of the obtained data, the kinetic parameters of photopolymerization process, such as: the degree of monomer conversion ( $C\%$ ), the rate of polymerization ( $R_p$ ) and photoinitiation index ( $I_p$ ) were calculated. The value of  $C\%$  parameter is directly proportional to the number of reactive moieties in the monomer molecule, which corresponds to the acrylate groups. The conversion percentages were determined on the basis of the integrated area under exothermic peak using Equation (2):

$$C\% = \frac{\Delta H_t}{\Delta H_0} \times 100 \quad (2)$$

where  $\Delta H_t$  is the heat evolved at time  $t$  during reaction,  $\Delta H_0$  is the theoretical enthalpy for the complete degree of monomer conversion (for acrylates:  $\Delta H_0 = 78.0 \text{ kJ} \times \text{mol}^{-1}$  [52]).

The rate of polymerization ( $R_p$ ) corresponds to the amount of heat released during the chain reaction. This parameter was estimated using Equation (3):

$$R_p = \frac{dH/dt}{\Delta H_0} \quad (3)$$

where  $dH/dt$  denotes how the heat flow evolved during the polymerization reaction.

Taking into account the maximum rate of polymerization ( $R_{p(\text{max})}$ ) and the time required for the maximum rate of heat released in the polymerization reaction ( $t_{\text{max}}$ ), the overall ability to the initiation of polymerization reaction ( $I_p$ ) may be calculated on the basis of the formula presented below (Equation (4)):

$$I_p = \frac{R_{p(\text{max})}}{t_{\text{max}}} \quad (4)$$

The kinetic parameters of polymerization process expressed by Equations (2)–(4) were used as a determinants for the evaluation of the photoinitiation efficiency of new squaraine-based photoinitiators. On the basis of these parameters, the most effective photoinitiating systems for radical polymerization of acrylate monomers has been detailed in this article.

### 3. Results and Discussion

#### 3.1. Characteristics of Photoinitiators

As mentioned above, in this article we proposed new bimolecular photoinitiators composed of squaraine dye as a photosensitizer and iodonium salt in the role of a co-initiator. The chemical structure of synthesized photosensitizers was confirmed by the NMR technique. The  $^1\text{H}$  and  $^{13}\text{C}$  NMR spectra clearly confirmed the chemical structure of dyes (SQM1–SQM3). The structure analysis of squaraines is presented below. The  $^1\text{H}$  and  $^{13}\text{C}$  NMR spectra of all synthesized compounds are available in the ESI file. The structure characteristics data of 2-aminobenzothiazole derivatives are as follows:

- 1,3-Bis(benzothiazoleamino)squaraine (SQM1)

$^1\text{H}$  NMR (DMSO- $d_6$ ),  $\delta$  (ppm): 8.49 (s, 1H, -OH); 7.98–7.96 (d, 2H, Ar,  $J = 8 \text{ Hz}$ ); 7.78–7.72 (m, 2H, Ar); 7.48–7.40 (m, 3H, Ar); 7.34–7.30 (m, 2H, Ar).

$^{13}\text{C}$  NMR (DMSO- $d_6$ ),  $\delta$  (ppm): 187.2; 171.8; 168.1; 162.8; 146.9; 130.6; 127.4; 126.8; 124.5; 123.0; 122.8; 122.3; 118.9; 116.7; 60.8; 19.1; 18.6; 14.3.

The SQM1 dye was obtained as orange solid, yield: 49.54%, mp. 190–227 °C.

- 1,3-Bis(6-bromobenzothiazoleamino)squaraine (SQM2)

$^1\text{H}$  NMR (DMSO- $d_6$ ),  $\delta$  (ppm): 8.21 (s, 1H, Ar); 8.20 (s, 2H, -NH, -OH); 8.04 (s, 1H, Ar); 7.95–7.94 (d, 1H, Ar,  $J = 4$  Hz); 7.57–7.54 (dd, 1H, Ar,  $J = 12$  Hz); 7.41–7.38 (dd, 1H, Ar,  $J = 12$  Hz); 7.29–7.27 (d, 1H, Ar,  $J = 8$  Hz).

$^{13}\text{C}$  NMR (DMSO- $d_6$ ),  $\delta$  (ppm): 187.1; 172.0; 168.0; 162.7; 150.1; 148.1; 133.8; 132.4; 130.0; 129.1; 125.1; 124.1; 121.2; 119.0; 115.8; 113.2.

The SQM2 dye was obtained as orange solid, yield: 80.39%, mp. 206–230 °C.

- 1,3-Bis(6-methylbenzothiazoleamino)squaraine (SQM3)

$^1\text{H}$  NMR (DMSO- $d_6$ ),  $\delta$  (ppm): 8.26 (s, 2H, -NH, -OH); 7.79 (s, 1H, Ar); 7.65–7.62 (dd, 1H, Ar,  $J = 12$ ); 7.61–7.60 (s, 1H, Ar); 7.37–7.35 (d, 1H, Ar,  $J = 8$  Hz); 7.33–7.29 (m, 1H, Ar); 7.19–7.16 (dd, 1H, Ar,  $J = 12$ ); 2.45 (s, 3H, -CH<sub>3</sub>); 2.39 (s, 3H, -CH<sub>3</sub>).

$^{13}\text{C}$  NMR (DMSO- $d_6$ ),  $\delta$  (ppm): 187.5; 172.6; 167.3; 161.9; 146.1; 145.3; 133.8; 131.8; 131.0; 128.9; 128.4; 127.6; 122.5; 122.0; 118.6; 116.6; 70.8; 21.4; 21.2; 18.7; 14.0.

The SQM3 dye was obtained as orange solid, yield: 80.42%, mp. 128–153 °C.

One of the most important preconditions of photopolymerization experiments is the selection of a proper light source. For this reason, the spectroscopic properties of photoinitiators were studied.

From the data presented in Figure 4a and summarized in Table 1, it can be concluded that all 2-aminobenzothiazole derivatives absorb in narrow range of spectrum. The absorption bands are intensive and range from 300 nm to ca. 460 nm. The maximum absorption ( $\lambda_{\text{ab(max)}}$ ) of all squaraines is about 345 nm. Moreover, the molar extinction coefficients for SQs achieve high values and are in the order of  $2 \times 10^4 \text{ dm}^3 \times \text{mol}^{-1} \times \text{cm}^{-1}$  for SQM1 and about  $1 \times 10^3 \text{ dm}^3 \times \text{mol}^{-1} \times \text{cm}^{-1}$  for other. The spectral data of investigated dyes are summarized in Table 1. The 1-methyl-2-pyrrolidinone was used as solvent in spectroscopic studies.

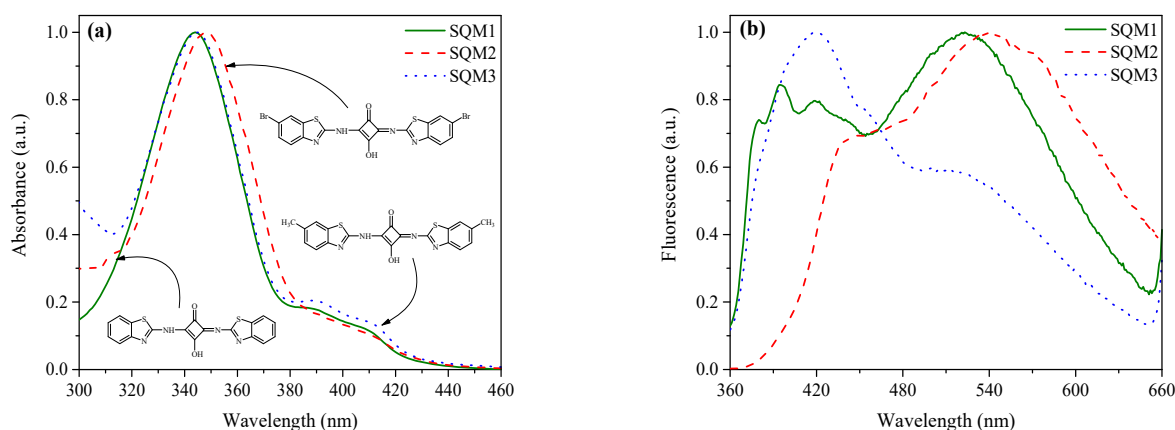


**Figure 4.** Normalized absorption (a) and fluorescence (b) spectra of squaraines SQM1-SQM3 in 1-methyl-2-pyrrolidinone (MP) recorded at room temperature.

**Table 1.** The spectroscopic properties of investigated photosensitizers.

Compound	$\lambda_{\text{ab(max)}}$ (nm)	$\epsilon(\text{max})$ ( $\text{dm}^3 \times \text{mol}^{-1} \times \text{cm}^{-1}$ )	$\lambda_{\text{fl(max)}}$ (nm)	$\Delta\nu_{\text{St}}$ ( $\text{cm}^{-1}$ )	$\Phi_{\text{fl}}$ ( $10^{-2}$ )
SQM1	344	24,500	523	9949	1.64
SQM2	348	9700	538	10,148	1.17
SQM3	345	8300	418	5062	1.40

As shown in Figure 4b, the fluorescence bands are broad and ranging from 360 nm to 660 nm. The position of the fluorescence bands depends both on the structure of the

dye, as well as, the type of solvent used. In comparison to the absorption maxima, the values of  $\lambda_{fl(max)}$  for SQM1-SQM3 compounds are different. Interestingly, the squaraine dyes have two characteristic fluorescence maxima. It may be explained by the presence of three emission bands, i.e., free dye, dye-solvent complex and twisted excited state resulting from C-N bond rotation [53]. The main maximum of fluorescence is 523 nm for SQM1, 538 nm for SQM2 and 418 nm for SQM3, respectively.

The Stokes shifts ( $\Delta\nu_{St}$ ) reached high values, from  $5 \times 10^3 \text{ cm}^{-1}$  to  $10 \times 10^3 \text{ cm}^{-1}$ . The fluorescence quantum yields ( $\Phi_{fl}$ ) are similar for all studied dyes. As is clearly seen, the proposed squaraines show excellent spectroscopic properties for their application as photosensitizers in photoinitiating systems.

On the other hand, the iodonium salts: I1, I81 and I84 absorb light below 300 nm [3]. Due to the absorption range of these compounds in the ultraviolet, usually the iodonium salts need to be combined with other molecules, which absorb light in the visible range of spectrum. Therefore, the introduction of squaraine dye into photoinitiating system is necessary, because it shifts the sensitivity of the photoinitiator towards longer wavelengths. The light source emitted from the high-pressure mercury lamp (OmniCure S2000) cover the range from 300 nm to 600 nm and in this case overlaps with the absorption region of squaraine dye. To summarize, the combination of squaraine dye with iodonium salt is a promising system, which can be used for initiation of the radical polymerization of acrylates.

The steady state photolysis experiments showed that the exposure of the dye solution to laser radiation results in a gradual bleaching of photosensitizer. It can be observed by the difference in light absorption. The longer exposure time of the sample causes the lower absorption intensity. For example, the changes in the intensity of absorption bands both of SQM1 dye solution, as well as the combination of squaraine dye SQM1 with iodonium salt, are presented in Figure 5.

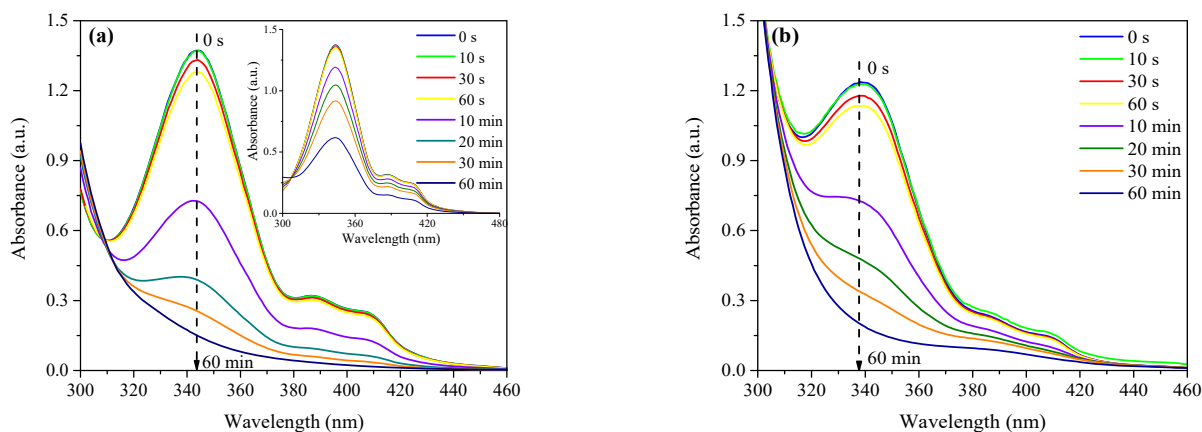


**Figure 5.** The steady state photolysis of (a) SQM1/I1 and (b) SQM1/I84 in *N,N*-dimethylformamide (DMF) upon the argon ion laser exposure ( $I_0 = 50 \text{ mW} \times \text{cm}^{-2}$ ). The concentration of iodonium salt was  $1 \times 10^{-3} \text{ M}$ . Inset: The photobleaching of squaraine dye (SQM1) as a result of laser irradiation.

As is clearly seen, the irradiation of squaraine dye solution results in a decrease in the intensity of absorption from about 1.5 to ca. 0.5 after 0 s and 60 min of irradiation, respectively. On the other hand, the presence of iodonium salt, I1, I81 and I84 leads to fast decrease of absorption intensity (even only 1 min of irradiation). The fastest photobleaching of squaraines was observed in the presence of (4-methoxyphenyl)-(4-nitrophenyl) iodonium *p*-toluenesulfonate (I81). The absorbance quenching processes are similar to that, when squaraine dye is combined with diphenyliodonium chloride (I1) or (3-bromophenyl)-(4-methoxyphenyl)iodonium *p*-toluenesulfonate (I84).

Therefore, the fastest interaction of SQ/Iod pair after light action is observed for the combination of squaraine dye with I81 salt. In other cases, the interaction dye-iodonium

salt is similar. These differences may be observed in the photoinitiation efficiencies of novel radical photoinitiators.

### 3.2. Kinetic Studies of Photopolymerization Process

The influence of combinations of different photosensitizers in the form of squaraine dye with various diphenyliodonium salts on the kinetics parameters of the radical polymerization of trimethylolpropane triacrylate (TMPTA) was estimated. The photopolymerization experiments were conducted for different pairs of photosensitizer/co-initiator. The squaraine dyes, such as: 1,3-bis(benzothiazoleamino)squaraine (SQM1), 1,3-bis(6-bromobenzothiazoleamino)squaraine (SQM2) and 1,3-bis(6-methylbenzothiazoleamino)squaraine (SQM3) were used as UV-Vis light absorbers. Three diphenyliodonium salts: diphenyliodonium chloride (I1), (4-methoxyphenyl)-(4-nitrophenyl) iodonium *p*-toluenesulfonate (I81) and (3-bromophenyl)-(4-methoxyphenyl)iodonium *p*-toluenesulfonate (I84) played the role of co-initiators. The photopolymerization experiments were carried out for different initiator concentrations.

In order to find the most optimal concentration of the photoinitiator in polymerizable mixture, that gives the highest kinetic parameters of radical polymerization of TMPTA, the kinetic studies for systems containing of  $5 \times 10^{-4}$  M,  $1 \times 10^{-3}$  M,  $2 \times 10^{-3}$  M and  $5 \times 10^{-3}$  M of SQ/Iod pair were carried out. The influence of initiator concentration on the rate of polymerization reaction of acrylate monomer was illustrated in Figure 6. The experiments were performed for all combinations of squaraine dye and diphenyliodonium salt. For example, the kinetic results of polymerization reaction for different concentration of SQM3/Iod pairs were presented in Table 2.

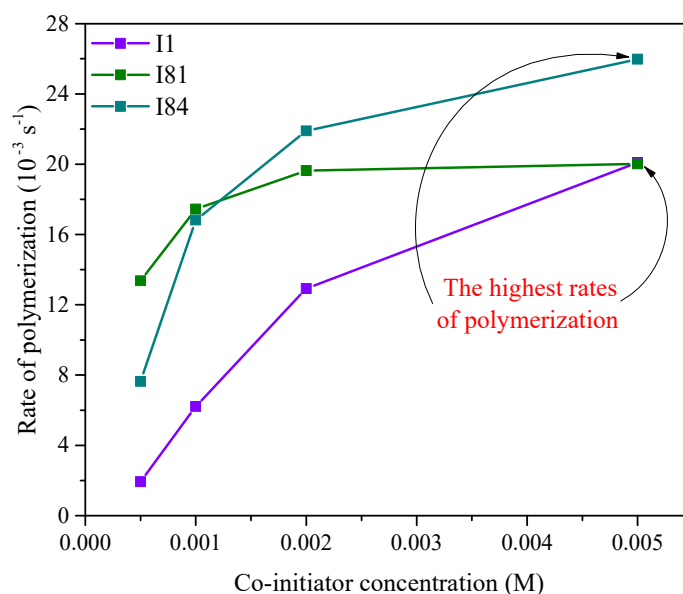


**Figure 6.** The effect of concentration of photoinitiator on the rate of the radical polymerization of TMPTA. The concentration of 1,3-bis(6-methylbenzothiazoleamino)squaraine (SQM3) was the same as for appropriate co-initiators and was marked on the figure.

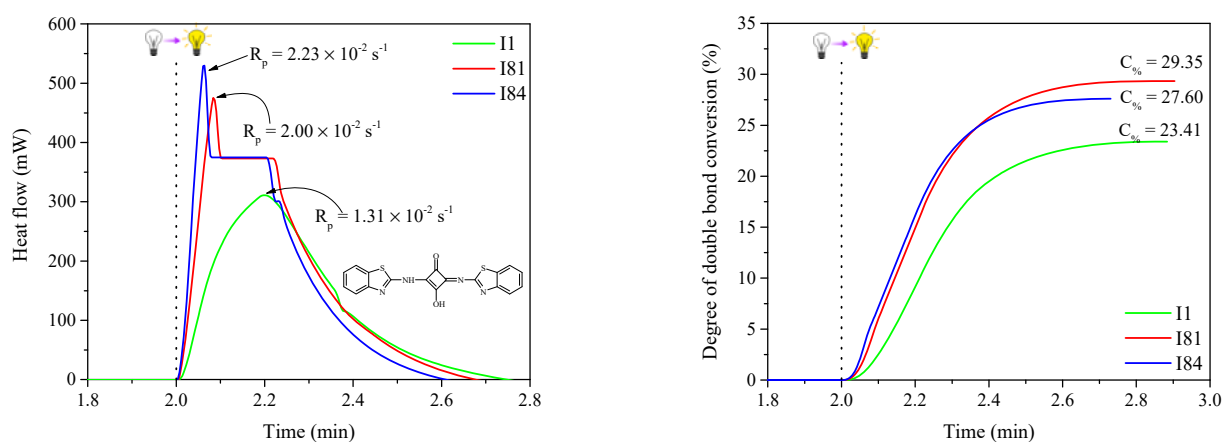
As shown in Figure 6, the concentration both of the sensitizer and the co-initiator, had an important impact on the kinetics of radical polymerization of triacrylate (TMPTA). The rate of polymerization increases as the initiator concentration in the polymerization mixture changed from  $5 \times 10^{-4}$  M to  $5 \times 10^{-3}$  M. The rate-initiator concentration curves for SQM3/I1 and SQM3/I84 are similar. The highest  $R_p$  values were observed for the highest concentration of photoinitiator, i.e.,  $5 \times 10^{-3}$  M. It should be noted that concentrations of initiators of  $2 \times 10^{-3}$  M and  $5 \times 10^{-3}$  M give similar and the highest rates of polymerization, at about  $20 \times 10^{-3} \text{ s}^{-1}$ .

**Table 2.** The influence of photoinitiator concentration for kinetic parameters of radical polymerization of TMPTA initiated by squaraine dye (SQM3) with the combination of different iodonium salts: I1, I81 and I84.

Photoinitiator	Photoinitiator Concentration (M)							
	$5 \times 10^{-4}$		$1 \times 10^{-3}$		$2 \times 10^{-3}$		$5 \times 10^{-3}$	
	$R_p$ ( $\times 10^{-3} \text{ s}^{-1}$ )	$C\%$ (%)	$R_p$ ( $\times 10^{-3} \text{ s}^{-1}$ )	$C\%$ (%)	$R_p$ ( $\times 10^{-3} \text{ s}^{-1}$ )	$C\%$ (%)	$R_p$ ( $\times 10^{-3} \text{ s}^{-1}$ )	$C\%$ (%)
SQM3/I1	1.93	12.25	6.21	26.43	12.92	29.56	20.10	34.27
SQM3/I81	9.94	25.16	20.02	34.70	21.77	35.68	23.37	35.71
SQM3/I84	7.64	24.63	16.82	30.00	21.90	30.56	25.98	33.45

On the basis of the data summarized in Table 2, it can be concluded, that the highest final monomer conversions are observed for the photoinitiating systems comprised of  $5 \times 10^{-3}$  M of photoinitiator. The values of degree of double bond monomer conversion ranging from about 10% for SQM3/I1 photoinitiating system (concentration of initiator:  $5 \times 10^{-4}$  M) to above 35% for SQM3/I81 combination (concentration of initiator:  $5 \times 10^{-3}$  M). Similar results were obtained for combinations of SQM1 and SQM2 dyes with mentioned iodonium salts. It needs to be highlighted, that using of initiator concentration of  $2 \times 10^{-3}$  M or  $5 \times 10^{-3}$  M are the best options due to the highest kinetic parameters of radical polymerization of TMPTA.

In order to explain the influence of the type of co-initiator on the kinetics of the photopolymerization process, the efficiency of photoinitiating systems consisting of 1,3-bis(benzothiazoleamino)squaraine (SQM1) and various types of diphenyliodonium salts (I1, I81 was I84) was compared, what is shown in Figure 7.

**Figure 7.** The kinetic curves registered during radical polymerization of TMPTA initiated by two-component photoinitiating systems composed of 1,3-bis(benzothiazoleamino)squaraine (SQM1) in the presence of various co-initiators marked on the figure. The concentration of photoinitiator was  $5 \times 10^{-3}$  M. The light intensity was  $30 \text{ mW} \times \text{cm}^{-2}$ .

From the kinetics data presented in Figure 7 and summarized in Table 3, it can be concluded that the structure of the co-initiator has a significant effect the kinetics of the polymerization reaction. The highest rates of polymerization and final monomer conversion were obtained from pairs composed of squaraine dye and (3-bromophenyl)-(4-methoxyphenyl)iodonium *p*-toluenesulfonate (I84). The exothermal effect for these photoinitiating systems was the highest and ranged from 300 mW to above 600 mW. The rates of polymerization achieved values about  $2.20 \times 10^{-2} \text{ s}^{-1}$  to  $2.60 \times 10^{-2} \text{ s}^{-1}$  and the final conversion ranged from 28% to 34%.

The photoinitiation reaction of radical polymerization of acrylate monomer (TMPTA) is very fast. It should be noted that the light action of the tested sample causes an immediate reaction with the release of a large amount of heat. The photocuring of polymerizable mixture takes only few seconds. As was shown in Table 3, The maximum of released

heat during exothermal reaction was in the range from 12 s to even ca. 3 s for the most effective photoinitiator.

**Table 3.** The kinetics parameters of radical polymerization of TMPTA initiated by bimolecular photoinitiators composed of 2-aminobenzothiazole derivative (SQM1/SQM2/SQM3) and various radical sources (I1/I81/I84). The concentration of photoinitiator was  $5 \times 10^{-3}$  M.

Photoinitiator	Co-Initiator	$Q_{(max)}$ (mW)	$t_{(max)}$ (s)	$R_p$ ( $\times 10^{-2} \text{ s}^{-1}$ )	$I_p$ ( $\times 10^{-3} \text{ s}^{-2}$ )	$C\%$ (%)
SQM1	I1	311	12.03	1.31	1.09	23.41
	I81	475	5.03	2.00	3.98	29.35
	I84	529	3.83	2.23	5.82	27.60
SQM2	I1	465	6.23	1.96	3.15	25.70
	I81	547	4.03	2.31	5.73	28.18
	I84	612	2.83	2.58	9.12	29.68
SQM3	I1	476	8.23	2.01	2.44	34.27
	I81	554	4.23	2.34	5.53	35.71
	I84	616	3.23	2.60	8.05	33.45

In this paper, we studied also the influence of sensitizer structure on the polymerization process, what was presented in Figure 8.

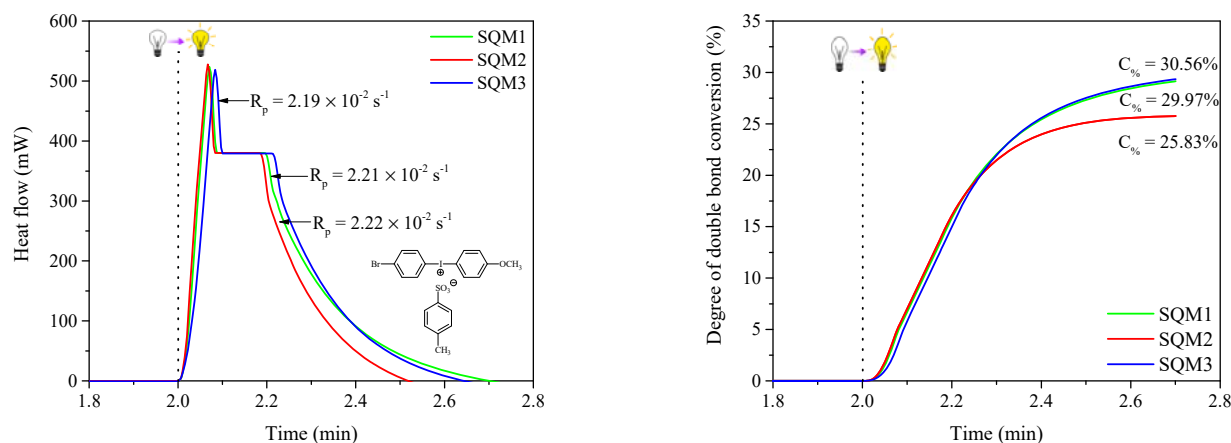


**Figure 8.** The kinetic curves registered during radical polymerization of TMPTA initiated by various two-component photoinitiating systems composed of various SQ dye and (3-bromophenyl)-(4-methoxyphenyl)iodonium *p*-toluenesulfonate (I84). The concentration of photoinitiator was  $2 \times 10^{-3}$  M. The light intensity was  $30 \text{ mW} \times \text{cm}^{-2}$ .

Apart from the initiator concentration and the structure of the co-initiator, the type of photosensitizer used in photopolymerization experiments also has a significant impact. The highest values of the kinetic parameters of reaction were obtained for photoinitiating system comprised of 1,3-bis(6-methylbenzothiazoleamino)squaraine (SQM3). Similar results were obtained for photoinitiators and consisted of SQM1 and SQM2 dyes. The final monomer conversion for photoinitiating systems containing SQM3 squaraine oscillated at about 35%. On the other hand, the combination of SQM1 or SQM2 squaraine dyes with all iodonium salts gives the degree of double-bond conversion in the range from 20% to 30%. It should be also noted that the highest values of photoinitiation indexes were obtained for bimolecular photoinitiators composed of squaraine dye and (3-bromophenyl)-(4-methoxyphenyl)iodonium *p*-toluenesulfonate (I84). In this case, this parameter is about  $10 \times 10^{-3} \text{ s}^{-2}$ .

On the basis of obtained kinetic results, one can conclude, that proposed bimolecular photoinitiators are very efficient and high-speed photoinitiating systems, which initiate the radical polymerization of acrylates with promising final monomer conversions. The

further modification of system compositions may improve the kinetic parameters of radical polymerization of acrylate monomers. In the next papers, we focused on the combination of these 2-aminobenzothiazole derivatives with other co-initiator to improve the photoinitiating ability of these systems.

#### 4. Conclusions

The proposed two-component photoinitiating systems consisting of newly synthesized 2-aminobenzothiazole derivatives and different diphenyliodonium salts may be used as ultraviolet-visible light active photoinitiators for the radical polymerization of trimethylolpropane triacrylate (TMPTA). The photoinitiation efficiency of novel photoinitiators depends on the sensitizer and co-initiator structures and their concentration in polymerizable composition. The highest values of kinetics parameters of radical polymerization of TMPTA were obtained for combination of squaraine derivatives (SQM1-SQM3) with (3-bromophenyl)-(4-methoxyphenyl)iodonium *p*-toluenesulfonate (I84). The rates of polymerization oscillates at about  $2 \times 10^{-2} \text{ s}^{-1}$  and the total monomer conversion ranged from 20% to above 35%. The proposed photoinitiating systems may be used as effective high-speed initiators for radical polymerization of acrylate monomers under sensitive light conditions.

**Supplementary Materials:** The following are available online at <https://www.mdpi.com/article/10.3390/ma14247814/s1>, Figure S1: <sup>1</sup>H NMR spectrum of SQM1 registered in DMSO-d<sub>6</sub>, Figure S2: <sup>13</sup>C NMR spectrum of SQM1 registered in DMSO-d<sub>6</sub>, Figure S3: <sup>1</sup>H NMR spectrum of SQM2 registered in DMSO-d<sub>6</sub>, Figure S4: <sup>13</sup>C NMR spectrum of SQM2 registered in DMSO-d<sub>6</sub>, Figure S5: <sup>1</sup>H NMR spectrum of SQM3 registered in DMSO-d<sub>6</sub>, Figure S6: <sup>13</sup>C NMR spectrum of SQM3 registered in DMSO-d<sub>6</sub>.

**Author Contributions:** Conceptualization, A.B. and J.K.; methodology, J.K.; validation, A.B. and J.K.; formal analysis, A.B., J.K., Z.C., M.N. and K.M.; investigation, A.B., J.K. and Z.C.; writing—original draft preparation, A.B.; writing—review and editing, J.K. and Z.C.; visualization, A.B., M.N. and K.M. All authors have read and agreed to the published version of the manuscript.

**Funding:** The APC was funded by Grant of Rector of the West Pomeranian University of Technology in Szczecin for PhD students of the Doctoral School, grant number: ZUT/65/2021.

**Institutional Review Board Statement:** Not applicable.

**Informed Consent Statement:** Not applicable.

**Data Availability Statement:** Not applicable.

**Conflicts of Interest:** The authors declare no conflict of interest.

#### References

1. Gallastegui, A.; Spesia, M.B.; dell'Erba, I.E.; Chesta, C.A.; Previtali, C.M.; Palacios, R.E.; Gómez, M.L. Controlled release of antibiotics from photopolymerized hydrogels: Kinetics and microbiological studies. *Mater. Sci. Eng. C* **2019**, *102*, 896–905. [[CrossRef](#)] [[PubMed](#)]
2. Hola, E.; Topa, M.; Chachaj-Brekiesz, A.; Plich, M.; Fiedor, P.; Galek, M.; Ortyl, J. New, highly versatile bimolecular photoinitiating systems for free-radical, cationic and thiol-ene photopolymerization process under low light intensity UV and visible LEDs for 3D printing application. *RSC Adv.* **2020**, *10*, 7509. [[CrossRef](#)]
3. Kabatc, J.; Iwińska, K.; Balcerak, A.; Kwiatkowska, D.; Skotnicka, A.; Czech, Z.; Bartkowiak, M. Onium salts improve the kinetics of photopolymerization of acrylate activated with visible light. *RSC Adv.* **2020**, *10*, 24817. [[CrossRef](#)]
4. Brighenti, R.; Cosma, M.P. Mechanical behavior of photopolymerized materials. *J. Mech. Phys. Solids* **2021**, *153*, 104456. [[CrossRef](#)]
5. Scanone, A.C.; Casado, U.; Schroeder, W.F.; Hoppe, C.E. Visible-light photopolymerization of epoxy-terminated poly (dimethylsiloxane) blends: Influence of the cycloaliphatic monomer content on the curing behavior and network properties. *Eur. Polym. J.* **2020**, *134*, 109841. [[CrossRef](#)]
6. Rahal, M.; Graff, B.; Toufaily, J.; Hamieh, T.; Dumur, F.; Lalevée, J. Design of keto-coumarin based photoinitiator for free radical photopolymerization: Towards 3D printing and photocomposites applications. *Eur. Polym. J.* **2021**, *154*, 110559. [[CrossRef](#)]
7. Balcerak, A.; Kabatc, J. The photooxidative sensitization of *bis*(*p*-substituted diphenyl)iodonium salts in the radical polymerization of acrylates. *RSC. Adv.* **2019**, *9*, 28490–28499. [[CrossRef](#)]

8. Li, J.; Li, S.; Li, Y.; Li, R.; Nie, J.; Zhu, X. In situ monitoring of photopolymerization by photoinitiator with luminescence characteristics. *J. Photochem. Photobiol. A* **2020**, *389*, 112225. [[CrossRef](#)]
9. Yuan, Y.; Li, C.; Zhang, R.; Liu, R.; Liu, J. Low volume shrinkage photopolymerization system using hydrogen-bond-based monomers. *Prog. Org. Coat.* **2019**, *137*, 105308. [[CrossRef](#)]
10. Gallastegui, A.; Zambroni, M.E.; Chesta, C.A.; Palacios, R.E.; Gómez, M.L. New bifunctional cross-linkers/co-initiators for vinyl photopolymerization: Silsesquioxanes-B2 vitamin as eco-friendly hybrid photoinitiator systems. *Polymer* **2021**, *221*, 123605. [[CrossRef](#)]
11. Liu, S.; Zhang, Y.; Sun, K.; Graff, B.; Xiao, P.; Dumur, F.; Lalevée, J. Design of photoinitiating systems based on the chalcone-anthracene scaffold for LED cationic photopolymerization and application in 3D printing. *Eur. Polym. J.* **2021**, *147*, 110300. [[CrossRef](#)]
12. Ibanez, C.; Lecamp, L.; Boust, F.; Lebaudy, P.; Burel, F. Elaboration of epoxy/silica composites by cationic photopolymerization: Kinetic study, optical and mechanical characterization. *J. Photochem. Photobiol. A* **2020**, *402*, 112798. [[CrossRef](#)]
13. Sun, G.; Wu, X.; Liu, R. A comprehensive investigation of acrylates photopolymerization shrinkage stress from micro and macro perspectives by real time MIR-photo-rheology. *Prog. Org. Coat.* **2021**, *155*, 106229. [[CrossRef](#)]
14. Dietlin, C.; Schweizer, S.; Xiao, P.; Zhang, J.; Morlet-Savary, F.; Graff, B.; Fouassier, J.-P.; Lalevée, J. Photopolymerization upon LEDs: New photoinitiating systems and strategies. *Polym. Chem.* **2015**, *6*, 3895–3912. [[CrossRef](#)]
15. Li, J.; Peng, Y.; Peña, J.; Xing, J. An initiating system with high efficiency for PEGDA photopolymerization at 532 nm. *J. Photochem. Photobiol. A* **2021**, *411*, 113216. [[CrossRef](#)]
16. Li, J.; Nie, J.; Zhu, X. Hydrogen bond complex used as visible light photoinitiating system for free radical photopolymerization: Photobleaching, water solubility. *Prog. Org. Coat.* **2021**, *151*, 106099. [[CrossRef](#)]
17. Fugolin, A.P.; Lewis, S.; Logan, M.G.; Ferracane, J.L.; Pfeifer, C.S. Methacrylamide-methacrylate hybrid monomers for dental applications. *Dent. Mater.* **2021**, *36*, 1028–1037. [[CrossRef](#)]
18. Nys, S.D.; Duca, R.C.; Vervliet, P.; Covaci, A.; Boonen, I.; Elskens, M.; Vanoirbeek, J.; Godderis, L.; Merbeek, B.V.; Landuyt, K.L.V. Bisphenol A as degradation product of monomers used in resin-based dental materials. *Dent. Mater.* **2021**, *37*, 1020–1029. [[CrossRef](#)]
19. De Oliveira, D.C.R.S.; Rocha, M.G.; Correa, I.C.; Correr, A.B.; Ferracane, J.L.; Sinhoreti, M.A.C. The effect of combining photoinitiator systems on the color and curing profile of resin-based composites. *Dent. Mater.* **2016**, *32*, 1209–1217. [[CrossRef](#)] [[PubMed](#)]
20. Catoira, M.C.; Fusaro, L.; Francesco, D.D.; Ramella, M.; Boccafosci, F. Overview of natural hydrogels for regenerative medicine applications. *J. Mater. Sci. Mater. Med.* **2019**, *30*, 115. [[CrossRef](#)]
21. Wei, W.; Zhang, Q.; Zhou, W.; Liu, Z.; Wang, Y.; Alakpa, E.V.; Ouyang, H.; Liu, H. Immunomodulatory, application of engineered hydrogels in regenerative medicine. *Appl. Mater. Today* **2019**, *14*, 126–136. [[CrossRef](#)]
22. Monteiro, N.; Thrivikraman, G.; Athirasala, A.; Tahayeri, A.; França, C.M.; Ferracane, J.L.; Bertassoni, L.E. Photopolymerization of cell-laden gelatin methacryloyl hydrogels using a dental curing light for regenerative dentistry. *Dent. Mater.* **2018**, *34*, 389–399. [[CrossRef](#)] [[PubMed](#)]
23. Chandika, P.; Kim, M.S.; Khan, F.; Kim, Y.M.; Heo, S.Y.; Oh, G.W.; Kim, N.G.; Jung, W.K. Wound healing properties of triple cross-linked poly (vinyl alcohol)/methacrylate kappa-carrageenan/chitoooligosaccharide hydrogel. *Carbohydr. Polym.* **2021**, *269*, 118272. [[CrossRef](#)]
24. Barma, M.D.; Muthupandiyam, I.; Samuel, S.R.; Amaechi, B.T. Inhibition of *Streptococcus mutans*, antioxidant property and cytotoxicity of novel nano-zinc oxide varnish. *Arch. Oral Biol.* **2021**, *126*, 105132. [[CrossRef](#)]
25. Landzberg, G.; Hussein, H.; Kischen, A. A novel self-mineralizing antibacterial tissue repair varnish to condition root-end dentin in endodontic microsurgery. *J. Endod.* **2021**, *47*, 939–946. [[CrossRef](#)]
26. Islam, M.T.; Dominguez, A.; Turley, R.S.; Kim, H.; Sultana, K.A.; Shuvo, M.A.I.; Alvarado-Tenorio, B.; Montes, M.O.; Lin, Y.; Gardea-Torresdey, J.; et al. Development of photocatalytic paint based on TiO<sub>2</sub> and photopolymer resin for the degradation of organic pollutants in water. *Sci. Total Environ.* **2020**, *704*, 135406. [[CrossRef](#)] [[PubMed](#)]
27. Tan, N.C.S.; Djordjevic, I.; Malley, J.A.; Kwang, A.L.Q.; Ikhwan, S.; Šolić, I.; Singh, J.; Wicaksono, G.; Lim, S.; Steele, T.W.J. Sunlight activated film forming adhesive polymers. *Mater. Sci. Eng. C* **2021**, *127*, 112240. [[CrossRef](#)]
28. Wang, J.; Dai, N.; Jiang, C.; Mu, X.; Zhang, B.; Ge, Q.; Wang, D. Programmable shape-shifting 3D structures via frontal photopolymerization. *Mater. Des.* **2021**, *198*, 109381. [[CrossRef](#)]
29. Quan, H.; Zhang, T.; Xu, H.; Luo, S.; Nie, J.; Zhu, X. Photo-curing 3D printing technique and its challenges. *Bioact. Mater.* **2020**, *5*, 110–115. [[CrossRef](#)]
30. Li, N.; Qiao, D.; Zhao, S.; Lin, Q.; Zhang, B.; Xie, F. 3D printing to innovative biopolymer materials for demanding applications: A review. *Mater. Today Chem.* **2021**, *20*, 100459. [[CrossRef](#)]
31. Lambert, A.; Valiulis, S.; Cheng, Q. Advances in optical sensing and bioanalysis enabled by 3D printing. *ACS Sens.* **2018**, *3*, 2475–2491. [[CrossRef](#)]
32. Palaganas, N.B.; Mangadlao, J.D.; de Leon, A.C.; Palaganas, J.O.; Pangilinan, K.D.; Lee, Y.J.; Advincula, R.C. 3D printing of photocurable cellulose nanocrystal composite for fabrication of complex architectures via stereolithography. *ACS Appl. Mater. Interfaces* **2017**, *9*, 34314–34324. [[CrossRef](#)] [[PubMed](#)]

33. Bai, G.; Wang, L.; Ma, G.; Sanjayan, J.; Bai, M. 3D printing eco-friendly concrete containing under-utilised and waste solids as aggregates. *Cem. Concr. Compos.* **2021**, *120*, 104037. [[CrossRef](#)]
34. Vakharia, V.N.; Khan, S.; Marathe, K.; Giannis, T.; Webber, L.; Choi, D. Printing in a pandemic: 3D printing solutions for healthcare during COVID-19. A protocol for a PRISMA systematic review. *Ann. 3D Print. Med.* **2021**, *2*, 100015. [[CrossRef](#)]
35. Ahmed, A.; Azam, A.; Bhutta, M.M.A.; Khan, F.A.; Aslam, R.; Tahir, Z. Discovering the technology evolution pathways for 3D printing (3DP) using bibliometric investigation and emerging applications of 3DP during COVID-19. *Clean. Environ. Syst.* **2021**, *3*, 100042. [[CrossRef](#)]
36. Oladapo, B.I.; Ismail, S.O.; Afolalu, T.D.; Olawade, D.B.; Zahedi, M. Review on 3D printing: Fight against COVID-19. *Mater. Chem. Phys.* **2021**, *258*, 123943. [[CrossRef](#)] [[PubMed](#)]
37. Nazir, A.; Azhar, A.; Nazir, U.; Liu, Y.F.; Qureshi, W.S.; Chen, J.E.; Alanazi, E. The rise of 3D printing entangled with smart computer aided design during COVID-19 era. *J. Manuf. Syst.* **2021**, *60*, 774–786. [[CrossRef](#)] [[PubMed](#)]
38. Zenasni, M.; Quintero-Jaime, A.; Salinas-Torres, D.; Benyoucef, A.; Morallón, E. Electrochemical synthesis of composite materials based on titanium carbide and titanium dioxide with poly((N-phenyl-o-phenylenediamine for selective detection of uric acid. *J. Electroanal. Chem.* **2021**, *895*, 115481. [[CrossRef](#)]
39. Khudyakov, I.V. Fast photopolymerization of acrylate coatings: Achievements and problems. *Prog. Org. Coat.* **2018**, *121*, 151–159. [[CrossRef](#)]
40. Jiao, Z.; Wang, C.; Yang, Q.; Wang, X. Preparation and characterization of UV-curable urethane acrylate oligomers modified with cycloaliphatic epoxide resin. *J. Coat. Technol. Res.* **2018**, *15*, 251–258. [[CrossRef](#)]
41. Dumur, F. Recent advances on visible light photoinitiators of polymerization based on Indane-1,3-dione and related derivatives. *Eur. Polym. J.* **2021**, *143*, 110178. [[CrossRef](#)]
42. Abdallah, M.; Magaldi, D.; Hijazi, A.; Graff, B.; Dumur, F.; Fouasier, J.-P.; Bui, T.T.; Goubard, F.; Lalevé, J. Development of new high-performance visible light photoinitiators based on carbazole scaffold and their applications in 3D printing and photocomposite synthesis. *J. Polym. Sci. Part A Polym. Chem.* **2019**, *57*, 2081–2092. [[CrossRef](#)]
43. Kabatc, J.; Kostrzewska, K.; Kozak, M.; Balcerak, A. Visible light photoinitiating systems based on squaraine dye: Kinetic, mechanistic and laser flash photolysis studies. *RSC Adv.* **2016**, *6*, 103851–103863. [[CrossRef](#)]
44. He, Y.; Zhou, W.; Wu, F.; Li, M.; Wang, E. Photoreaction and photopolymerization studies on squaraine dyes/iodonium salts combination. *J. Photochem. Photobiol. A Chem.* **2004**, *162*, 463–471. [[CrossRef](#)]
45. Giacoletto, N.; Ibrahim-Ouali, M.; Dumur, F. Recent advances on squaraine-based photoinitiators of polymerization. *Eur. Polym. J.* **2021**, *150*, 110427. [[CrossRef](#)]
46. Balcerak, A.; Iwińska, K.; Kabatc, J. Novel 1,3-bis(p-substituted phenylamino)squaraine dyes. The synthesis and spectroscopic studies. *Dye. Pigm.* **2019**, *170*, 107596. [[CrossRef](#)]
47. Joseph, J.; Janaki, G.B. Copper complexes bearing 2-aminobenzothiazole derivatives as potential antioxidant: Synthesis, characterization. *J. Photochem. Photobiol. B Biol.* **2016**, *162*, 86–92. [[CrossRef](#)]
48. Zhao, Z.; Wang, C.; Liu, F.; Zhang, B. Synthesis and application of new S-benzoheterocycle thiobenzoates photoinitiators. *Res. Chem. Intermed.* **2020**, *46*, 3717–3726. [[CrossRef](#)]
49. Zhang, J.; Lalevé, J.; Morlet-Savary, F.; Graff, B.; Xiao, P. Photopolymerization under various monochromatic UV/visible LEDs and IR lamp: Diamino-anthraquinone derivatives as versatile multicolor photoinitiators. *Eur. Polym. J.* **2019**, *112*, 591–600. [[CrossRef](#)]
50. Kabatc, J.; Ortyl, J.; Kostrzewska, K. New kinetic and mechanistic aspects of photosensitization of iodonium salts in photopolymerization of acrylates. *RSC Adv.* **2017**, *7*, 41619–41629. [[CrossRef](#)]
51. Olmsted, J. Calorimetric determinations of absolute fluorescence quantum yields. *J. Phys. Chem.* **1979**, *83*, 2581–2584. [[CrossRef](#)]
52. Balcerak, A.; Kwiatkowska, D.; Iwińska, K.; Kabatc, J. Highly efficient UV-Vis light activated three-component photoinitiators composed of tris(trimethylsilyl)silane for polymerization of acrylates. *Polym. Chem.* **2020**, *11*, 5500–5511. [[CrossRef](#)]
53. Kabatc, J.; Kostrzewska, K.; Orzeł, Ł. Factors that influence the spectroscopic properties of 1,3-bis-p-substituted-(phenylamino)squaraines. *Dye. Pigm.* **2016**, *130*, 226–232. [[CrossRef](#)]

**Publikacja naukowa [A7]**

PAPER



Cite this: *Polym. Chem.*, 2022, **13**, 220

# Novel photoinitiators based on difluoroborate complexes of squaraine dyes for radical polymerization of acrylates upon visible light†

Alicja Balcerak,  Dominika Kwiatkowska  and Janina Kabatc \*

The present article describes the efficiency of novel two-component photoinitiators based on a typical squaraine dye and its difluoroborate analogues for the radical polymerization of acrylate monomers. The role of photosensitizers in photoinitiating systems was played by squaraine derivatives, such as 2,4-bis(3,5-dimethylpyrrol-2-yl)squaraine (PSQ1) and 2,4-bis(4-ethyl-3,5-dimethylpyrrol-2-yl)squaraine (PSQ2) and difluoroborate complexes of these compounds, such as BPSQ1 and BPSQ2, named BODIPY dyes. These dyes absorb radiation in visible region of the spectrum, from 400 nm to 600 nm and show high molar absorption coefficients of about  $10^5 \text{ dm}^3 \text{ mol}^{-1} \text{ cm}^{-1}$ . Therefore, they may be used as sensitizers, e.g. in photopolymerization experiments. The synthesized dyes were combined with various co-initiators and used as visible-light photoinitiators for the radical polymerization of 2-ethyl-2-(hydroxymethyl)-1,3-propanediol triacrylate (TMPTA). The proposed systems show different photoinitiation abilities, which are related to the structure of both sensitizer and co-initiator and the concentration of applied photoinitiator. Novel derivatives of squaric acid could be the starting point for the design of new photoinitiating systems for radical and cationic polymerization based on squaraine dyes.

Received 27th September 2021,  
Accepted 22nd November 2021

DOI: 10.1039/d1py01294k

rsc.li/polymers

## 1. Introduction

Photochemically initiated polymerization reactions are among the most widely used and powerful strategies for the production of advanced polymer materials. In recent years, there has been enormous progress in the development of photopolymerization, which has resulted in an expansion in the scope of applications.<sup>1,2</sup> Currently, this technology is widely used in medicine,<sup>3,4</sup> 3D printing,<sup>5–7</sup> microelectronics,<sup>8</sup> the production of various types of coatings,<sup>9–11</sup> the packaging industry<sup>12</sup> and many others. For medicine, the photopolymerization process plays a key role in the production of dental fillings, hydrogels, bone scaffolds, wound dressings, etc.<sup>13–15</sup> The idea of 3D printing has opened up new directions in different areas, such as soft robotics, microfluidics, and the manufacture of smart clothing.<sup>16,17</sup> In the chemical industry, photopolymerization enables the production of paints, lacquers, varnishes, adhesives, laminates, etc.<sup>18</sup> The major advantages of the discussed method of cross-linking of polymerizable compositions are presented in Fig. 1.

As shown in Fig. 1, the production of novel polymeric materials by photopolymerization is economically advantageous. It is related to the low energy consumption, fast curing rates and high productivity of reactions. An ecological approach without the use of solvents and, hence, without the release of volatile organic compounds is a huge plus for environmental protection.<sup>19</sup> The advanced possibilities offered by photopolymerization and other listed benefits influence the variety of application areas.

Light-activated polymerization can occur *via* two basic mechanisms: radical and ionic (cationic or anionic). Generally, photopolymerization reactions require the introduction of an appropriate initiator into the photocuring composition.<sup>20</sup> The presence of a photoinitiator (PI) is a crucial element in the initiation step of the chain reaction. This molecule absorbs energy from a specified light source and forms free radicals. These active species attack mono- or multi-functional monomers and activate the unsaturated functional groups of the monomers, which leads to the production of linear or cross-linked polymers in a very short time.<sup>21</sup>

An active research area in the topic of photopolymerization is high-speed photoinitiators. The huge demand for new polymer materials obtained by photopolymerization is continually driving the global market for the increased production of these compounds. For this reason, numerous studies in the area of the synthesis of novel photoinitiators or improving known photoinitiators seem to be extremely important.<sup>22</sup>

Bydgoszcz University of Science and Technology, Faculty of Chemical Technology and Engineering, Department of Organic Chemistry, Seminaryjna 3, 85-326 Bydgoszcz, Poland. E-mail: nina@utp.edu.pl

† Electronic supplementary information (ESI) available. See DOI: 10.1039/d1py01294k

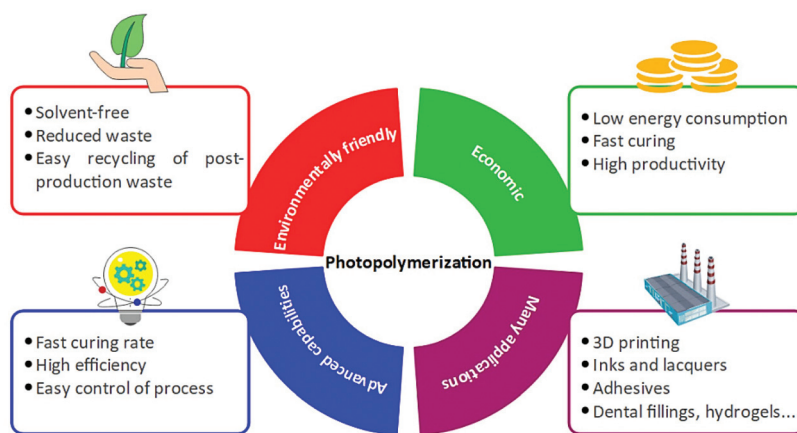


Fig. 1 Advantages of the photopolymerization process.

It should be noted that there are several important factors, which will be taken into account during the design of effective photoinitiating systems. The selection of an appropriate PI determines the kinetics of polymerization, as well as the final properties of the obtained polymer material. There are one-component, two-component and multi-component photoinitiating systems. Regardless of the number of components, the photoinitiators should comply with certain criteria. The highlights of the requirements for these compounds are presented in Fig. 2.<sup>23</sup>

One of the most important factors, which has a significant impact on the photoinitiating abilities, is matching the absorption spectrum of the PI to the characteristics of the chosen light source. It is known that the structure of a photoinitiator determines its spectral properties and directly determines the position of maximum absorption and the molar extinction coefficient. Therefore, by an appropriate modification of the structure of a PI, *e.g.* the introduction of a specific substituent, it is possible to achieve compatibility between the photoinitiator and the light. Indeed, photoinitiators which show a high molar absorption coefficient and high quantum efficiency are active light absorbers.<sup>24</sup> Moreover, the good thermal and temporal stability of PIs guarantee a long lifetime for photoinitiating compositions. An effective photoinitiator should be soluble in the polymerization mixture.

Non-toxicity and biocompatibility are also expected. These compounds should not have a negative impact on the final properties of the obtained products, such as yellowing or a reduction in the mechanical properties of the produced polymer materials.<sup>25</sup>

In order to obtain a high degree of monomer conversion and rate of polymerization, the parameters of the cross-linking process should be selected accordingly. First of all, attention should be paid to the type and intensity of the light source used. Nowadays, the use of low-power light sources is particularly desirable. Moreover, the curing of polymerizable mixtures not only by UV radiation, but most of all by using the visible region of radiation (Vis) is required.<sup>26</sup> Another significant parameter is selection of the appropriate concentrations of the photoinitiator and other additives. Furthermore, the structure and properties of the monomers used, the thickness of the polymerizing layer and the viscosity of the photocured formulation play key role in light-induced polymerization. What is predictable is that the photopolymerization will be more efficient both for thin layers and for monofunctional monomers.<sup>27</sup> In the case of radical polymerization, one cannot forget about oxygen inhibition. This phenomenon is especially unfavorable for the growing polymer chain because of the scavenging of radicals by oxygen molecules. Reduction in oxygen inhibition is possible: *e.g.* by using an inert atmo-



Fig. 2 Sample requirements for an effective photoinitiator.

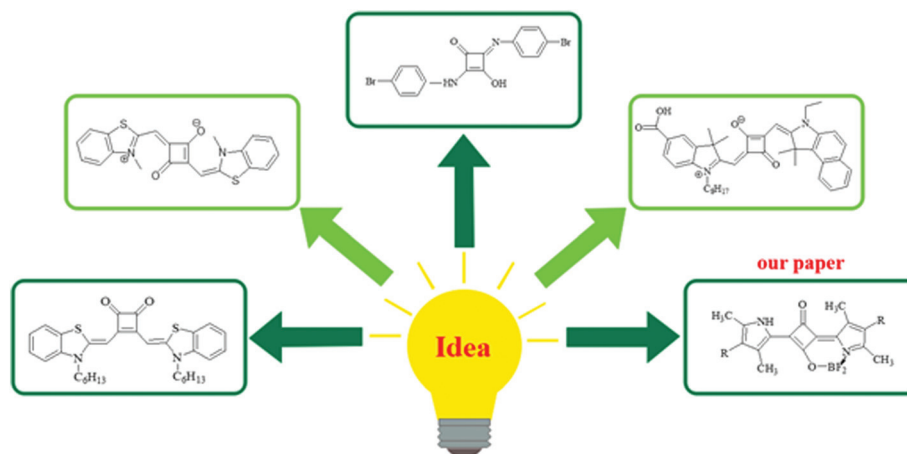


Fig. 3 Examples of squaraines used as photosensitizers in polymerization reactions.

sphere (nitrogen, argon, *etc.*).<sup>28</sup> As mentioned above, the planning of the photopolymerization reaction requires many parameters to be taken into account, which are first-class for obtaining high-kinetic parameters for these processes.

One example of a high-performance photoinitiator is a system based on squaraines (SQs). These PIs are arousing more and more interest among scientists. Until now, there have been only a small number of papers describing photoinitiators composed of squaraines in the role of photosensitizer.<sup>29</sup> A few examples of squaraine-based photoinitiating systems described in the literature are shown in Fig. 3.<sup>30–33</sup>

The possibility of using squaraine dyes in the role of photosensitizers is related to their unique properties of intensive and broad absorption and fluorescence bands, which extend from the visible to the near infrared region of the spectrum. Importantly, these dyes are distinguished by high molar extinction coefficients and good photostability.<sup>34</sup>

The squaraines are a promising group of organic dyes, which show huge potential for use as sensitizers in photopolymerization reactions, and were described by Giacometto and co-workers in 2021.<sup>29</sup> For this reason we decided to expand the group of squaraine sensitizers with new compounds *via* the modification of the structure of SQs based on a pyrrole scaffold. We synthesized two trifluoroborate complexes of squaraine dyes and used them as photosensitizers in photopolymerization studies. These compounds are an alternative to the well-known BODIPY dyes. To our knowledge, there is no information in the literature about an application of this type of compounds as photosensitizers in radical polymerization.

In this article we describe the synthesis, spectroscopic characteristics and fluorescence properties of squaraine dyes and their difluoroborate complexes, as well as kinetic studies of the radical polymerization of acrylates. The novelty of this paper is the application of novel squaraines and their difluoroborate complexes with a combination of iodonium (I1), borate (B2) and alloxonium (NO) salts as efficient photoinitiators for the radical polymerization of acrylates in the visible range of the spectrum.

## 2. Experimental section

### Materials

All substrates for the preparation of squaraine dyes PSQ1, PSQ2 and their difluoroborate complexes BPSQ1, BPSQ2 (Chart 1) were of reagent grade and purchased from commercial suppliers (Acros Organics, Aldrich Chemical Co., Poland). Tetramethylammonium *n*-butyltriphenylborate (B2) was synthesized in our laboratory, based on a previously described procedure.<sup>35</sup> Commercially available co-initiators, such as diphenyliodonium chloride (I1) and 1-methoxy-4-phenylpyridinium tetrafluoroborate (NO), were purchased from Alfa Aesar and Aldrich Chemical Co. (Poland), respectively, and used as received. 2-Ethyl-2-(hydroxymethyl)-1,3-propanediol triacrylate (TMPTA, from Aldrich Chemical Co., Poland) was applied as a model monomer to study the kinetics of radical photopolymerization experiments. The solvents used in the spectroscopic studies were supplied by Aldrich Chemical Co. (Poland) and used without further purification (purity  $\geq 99\%$ ).

### Structural characteristics

The chemical structures of the synthesized photosensitizers were characterized by nuclear magnetic resonance spectroscopy. The  $^1\text{H}$ ,  $^{13}\text{C}$ ,  $^{11}\text{B}$  and  $^{19}\text{F}$  isotope resonance spectra (NMR) were recorded with an Ascend III spectrometer operating at 400 MHz (Bruker, USA). Dimethylsulfoxide ( $\text{DMSO}-d_6$ ) was used as the solvent and tetramethylsilane (TMS) or trichlorofluoromethane ( $\text{CFCl}_3$  for  $^{19}\text{F}$  NMR) as the internal standard. The values of the chemical shifts ( $\delta$ ) are quoted in ppm relative to the internal standard and coupling constants ( $J$ ) are given in Hertz (Hz).

The melting point was measured on a Böethius apparatus (PGH Rundfunk, Fernsehen Niederdorf KR, Stollberg/E) and is uncorrected.

### Spectroscopic studies

The absorption and emission spectra of the synthesized dyes were registered in solvents of various polarity using an Agilent Technology UV-Vis Cary 60 spectrophotometer and a Hitachi

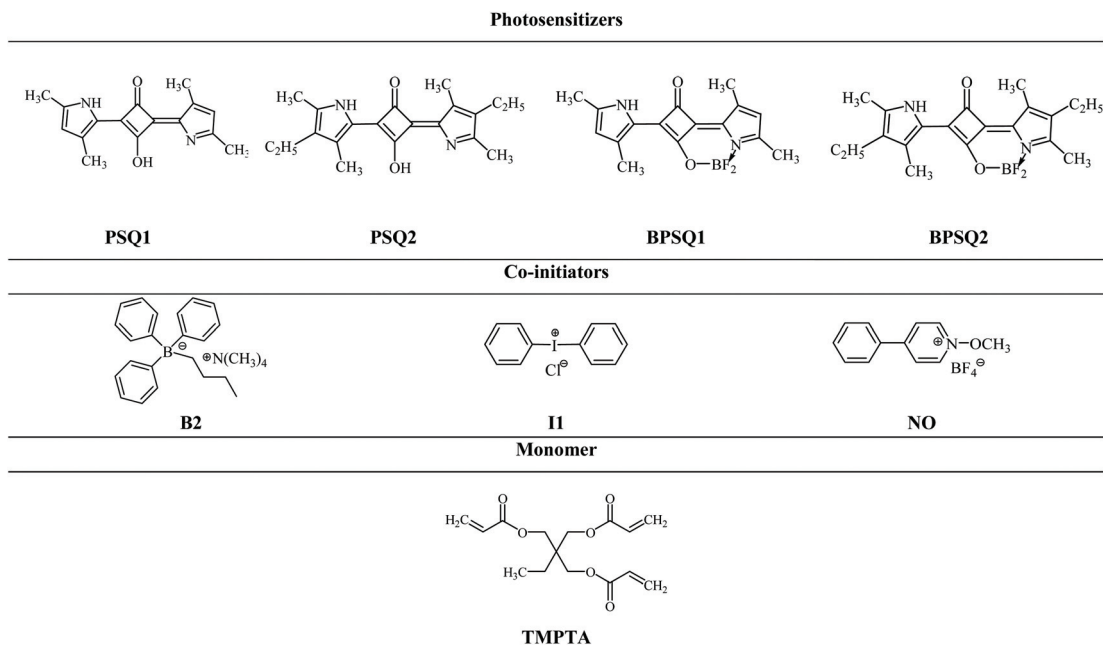


**Chart 1** Structures of the compounds of the photoinitiating systems studied.

F-7000 spectrofluorometer, respectively. The measurements were performed at ambient temperature (25 °C) in a standard quartz cuvette (1 cm). The UV-Vis and fluorescence spectra of the PSQs and BPSQs were recorded in solvents of different polarity, such as tetrahydrofuran (THF), ethyl acetate (AcOEt), acetone (ACE), ethanol (EtOH), methanol (MeOH), 1-methyl-2-pyrrolidinone (MP), dimethylformamide (DMF), acetonitrile (MeCN) and dimethylsulfoxide (DMSO). The concentration of the dye in the solvents of various polarity was about  $10^{-6}$  M.

The fluorescence quantum yields of the dyes ( $\Phi_{fl}$ ) were determined in the same solvents that were used for the spectroscopic studies. The fluorescence spectra of dilute solutions of these dyes ( $A \approx 0.1$ ) were registered by excitation at the maximum of the absorption band of the reference. The reference standard was Rhodamine 6G in ethanol solution ( $\lambda_{ex} = 546$  nm;  $\Phi_{ref} = 0.86$  (ref. 36)). The fluorescence quantum yield of all the tested dyes was estimated based on the following equation (eqn (1)):

$$\Phi_{fl} = \frac{\Phi_{ref} A_{ref} I_{dye} n_{dye}^2}{A_{dye} I_{ref} n_{ref}^2} \quad (1)$$

where  $\Phi_{ref}$  is the fluorescence quantum yield of the reference sample,  $A_{dye}$  and  $A_{ref}$  are the values of absorbance of the dye and reference at the excitation wavelength,  $I_{dye}$  and  $I_{ref}$  are the integrated emission intensities for the dye and reference, and  $n_{dye}$  and  $n_{ref}$  are the refractive indexes of the solvents used for the dye and reference, respectively.

Steady-state photolysis measurements were carried out under continuous irradiation at 514 nm with an air-cooled ion laser system, model 177-G01 (Spectra-Physics, USA). The average power of irradiation was  $50 \text{ mW cm}^{-2}$ . The light intensity was measured with a Coherent Model Fieldmaster power meter.

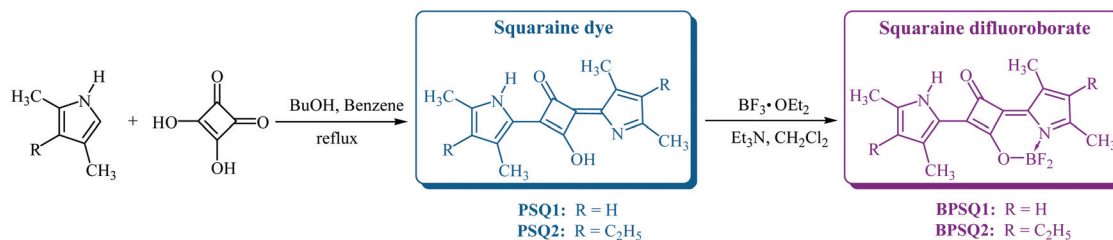
### Monitoring the kinetics of photopolymerization by photo-differential scanning calorimetry (photo-DSC)

In order to monitor the kinetics of the radical photopolymerization of 2-ethyl-2-(hydroxymethyl)-1,3-propanediol triacrylate (TMPTA), differential scanning calorimetry was used. The photopolymerization measurements were carried out using a differential scanning calorimeter DSC Q2000 (TA Instruments) equipped with a high-pressure mercury lamp (photo-DSC).

The measurements were conducted under isothermal conditions (25 °C) in a nitrogen atmosphere. The inert gas flow was  $50 \text{ ml min}^{-1}$ . A high-pressure mercury lamp was applied as the light source, which emitted radiation in the range from 300 to 500 nm. The intensity of the radiation was constant and equal to  $50 \text{ mW cm}^{-2}$ . The measurements were performed at a sampling interval of 0.05 s per point. A sample weight of  $30 \pm 0.1$  mg was placed into an open aluminum pan, and then maintained at the specified temperature (25 °C) for 2 min before each measurement run began. The heat emitted during the polymerization reaction was registered as a function of time.

The polymerization mixture was composed of 0.2 mL of 1-methyl-2-pyrrolidinone (MP), 1.8 mL of monomer (TMPTA) and an appropriate photoinitiator. The use of 1-methyl-2-pyrrolidinone was necessary because of the poor solubility of squaraines in the monomer. The polymerization experiments were carried out using various concentration of photoinitiators, as follows:  $5 \times 10^{-4}$  M,  $1 \times 10^{-3}$  M,  $2 \times 10^{-3}$  M and  $5 \times 10^{-3}$  M. Based on the obtained results, the degree of monomer conversion ( $C_{\%}$ ) and the rate of polymerization ( $R_p$ ) were determined using eqn (2) and (3), respectively.

The degree of conversion was estimated on the basis of the heat liberated in the polymerization reaction, which is directly proportional to the number of reactive groups (double bonds)



**Scheme 1** The synthesis of squaraine derivatives.

in the monomer molecule. By integrating the area under the exothermic peak, the percentages of conversion were obtained. These parameters were calculated using the formula presented below:

$$C\% = \frac{\Delta H_t}{\Delta H_0} \times 100 \quad (2)$$

where  $\Delta H_t$  is the heat evolved at time  $t$  in the polymerization reaction, and  $\Delta H_0$  represents the theoretical heat corresponding to the complete degree of conversion of the reactive group. For calculation of the  $C\%$  parameter, the value of the theoretical enthalpy for acrylate monomers of  $\Delta H_0 = 78.0$  kJ mol<sup>-1</sup> was used.<sup>37</sup>

The rate of polymerization ( $R_p$ ) is directly related to the total heat flow liberated during the polymerization reaction. This parameter was estimated on the basis of the formula presented below (eqn (3)):

$$R_p = \frac{dH/dt}{\Delta H_0} \quad (3)$$

where  $dH/dt$  denotes the heat flow evolved during the polymerization reaction.

Taking into account the maximum rate of polymerization ( $R_p^{\max}$ ) and the time required for the maximum rate of heat release ( $t^{\max}$ ) in the polymerization reaction, the overall ability for the initiation of the polymerization reaction ( $I_p$ ) may be calculated using eqn (4):

$$I_p = \frac{R_p^{\max}}{t^{\max}} \quad (4)$$

On the basis of the presented equations, the kinetic parameters of the polymerization process were calculated for the photoinitiating systems under study. The most efficient photoinitiator for the radical polymerization of acrylates was found.

### 3. Results and discussion

#### Synthesis of squaraines PSQs and BPSQs

Two symmetric squaraines based on a pyrrole unit, 2,4-bis(3,5-dimethylpyrrol-2-yl)squaraine (PSQ1) and 2,4-bis(4-ethyl-3,5-dimethylpyrrol-2-yl)squaraine (PSQ2), and their difluoroborate complexes, 2,4-bis(3,5-dimethylpyrrol-2-yl)squaraine difluoroborate (BPSQ1) and 2,4-bis(4-ethyl-3,5-dimethylpyrrol-2-yl)squaraine difluoroborate (BPSQ2), were synthesized and used

as photosensitizers in the light-induced polymerization process. The proposed dyes possess the characteristic structure for squaraines, which is a four-membered ring system derived from squaric acid connected by two moieties as electron donors.<sup>38</sup> The general procedure for the preparation of the tested squaraine derivatives is presented in Scheme 1.

The compounds PSQ1 and PSQ2 were synthesized according to the procedure described by Bonnett and co-authors.<sup>39</sup> In short, these dyes were obtained from the reaction of 2,4-dimethylpyrrole with 2-dihydroxycyclobuten-3,4-dione in an anhydrous mixture of butanol (BuOH) and benzene. The condensation reaction readily occurs at the highly reactive  $\alpha$ -position in the pyrrole ring to produce squaraines PSQ1 and PSQ2. Whereas BPSQ1 and BPSQ2 dyes were synthesized based on the procedure proposed by Kubota and co-workers.<sup>40</sup> These dyes are squaraine difluoroborates and are alternatives to typical BODIPYs. The compounds BPSQ1 and BPSQ2 were obtained as a result of the complexation reaction of squaraines PSQ1 or PSQ2, respectively, with boron trifluoride ethyl etherate ( $\text{BF}_3 \cdot \text{OEt}_2$ ) in the presence of triethylamine ( $\text{Et}_3\text{N}$ ) in anhydrous dichloromethane ( $\text{CH}_2\text{Cl}_2$ ). The squaraine difluoroborates were isolated by extraction with dichloromethane.

The details of the synthesis are given in ESI.†

The <sup>1</sup>H, <sup>13</sup>C, <sup>11</sup>B and <sup>19</sup>F NMR spectra confirmed the structure of the squaraine derivatives. The obtained data are in good agreement with the proposed chemical structures of these compounds. For example, one of the spectra of a synthesized dye is presented in Fig. 4. Other NMR spectra are shown in Fig. S4–S10 in ESI.†

As shown in Fig. 4, on the <sup>1</sup>H NMR spectrum of BPSQ1, the pronounced peaks derived from the protons of these dye molecules can be distinguished. The chemical shifts in the range from 2.36 ppm to 2.57 ppm correspond to the protons of methyl groups. The signal localized at 6.19 ppm for the methine groups can be perceived. At 11.42 ppm the peak derived from the proton of the imino group is observed; whereas, the presence of fluorine atoms is confirmed by signals at about -148.20 ppm (inset).

The chemical shift data, melting point values and yield of reaction of the tested dyes are summarized in Table 1. All of the synthesized compounds were obtained as violet-blue solids. The melting points are in the range from 230 °C for BPSQ2 to about 280 °C for PSQ2 and PSQ1. The melting point of the BPSQ1 crystals was observed at *ca.* 160 °C. The yields of the synthesis of PSQ1 and PSQ2 dyes achieved values of about

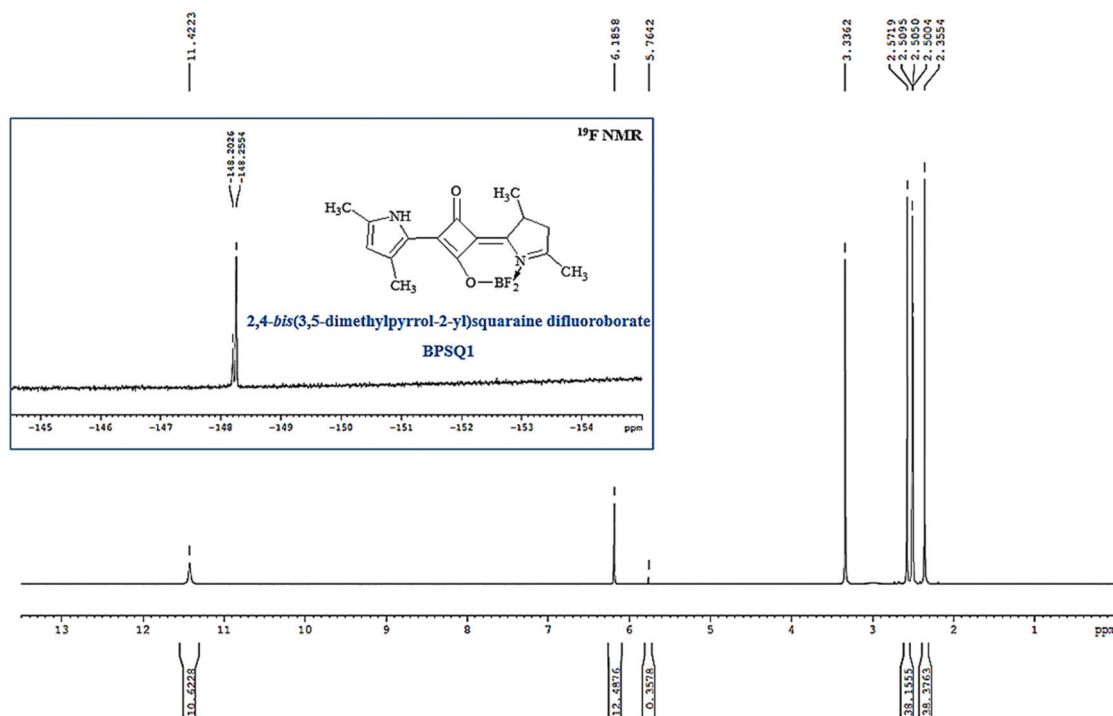


Fig. 4 The  $^1\text{H}$  NMR spectrum of BPSQ1 registered in deuterated DMSO. Inset: the  $^{19}\text{F}$  NMR spectrum of the same dye in  $\text{DMSO}-d_6$ .

Table 1 The characterization data of squaraine derivatives

Dye	Formula	Structure	Chemical shifts (ppm)	Yield (%)	M.p. ( $^{\circ}\text{C}$ )
PSQ1	$\text{C}_{16}\text{H}_{16}\text{N}_2\text{O}_2$		$^1\text{H}$ NMR: 2.36 (s, 6H), 2.50–2.57 (q, 6H), 6.19 (s, 2H), 11.42 (s, 2H) $^{13}\text{C}$ NMR: 13.5, 14.0, 116.9, 124.2, 136.9, 147.0, 171.6, 176.1	48	281–284
PSQ2	$\text{C}_{20}\text{H}_{24}\text{N}_2\text{O}_2$		$^1\text{H}$ NMR: 1.00–1.04 (t, 6H), 2.35 (s, 6H), 2.37–2.41 (t, 4H), 2.50–2.53 (q, 6H), 11.27 (s, 2H) $^{13}\text{C}$ NMR: 11.3, 12.3, 15.0, 17.2, 123.4, 129.5, 133.2, 144.6, 169.6	54	259–266
BPSQ1	$\text{C}_{16}\text{H}_{15}\text{BF}_2\text{N}_2\text{O}_2$		$^1\text{H}$ NMR: 2.36 (s, 6H), 2.50–2.57 (q, 6H), 6.19 (s, 2H), 11.42 (s, 2H) $^{13}\text{C}$ NMR: 13.5, 14.0, 116.9, 116.9, 124.0, 124.2, 136.8, 136.9, 146.8, 147.0, 171.7 $^{11}\text{B}$ NMR: –1.31 $^{19}\text{F}$ NMR: –148.26, –148.20	39	157–165
BPSQ2	$\text{C}_{20}\text{H}_{23}\text{BF}_2\text{N}_2\text{O}_2$		$^1\text{H}$ NMR: 1.00–1.04 (t, 6H), 2.35 (s, 6H), 2.37–2.41 (t, 4H), 2.50–2.53 (q, 6H), 11.27 (s, 2H) $^{13}\text{C}$ NMR: 11.3, 12.3, 15.0, 17.2, 123.4, 129.5, 133.2, 144.6, 160.7 $^{11}\text{B}$ NMR: –1.31 $^{19}\text{F}$ NMR: –148.26, –148.20	45	225–234

50%. On the other hand, the yields of the complexation reaction of these compounds were lower, in the range from 39% to 45% for BPSQ1 and BPSQ2, respectively.

### Characteristics of photoinitiators

One of the most important factors in photopolymerization experiments is adjusting the absorption spectrum of an appro-

priate photoinitiator to the emission spectrum of the light source. The important requirement is that the photosensitizer molecule should be highly sensitive to exposure to the light medium and show a high molar absorption coefficient. In order to determine the effectiveness of newly synthesized compounds for the role of the photosensitizers and, thus, the possibility of their interaction with co-initiators to generate

initiating radicals, the spectroscopic properties of these dyes were studied.

As mentioned above, the spectroscopic properties of squaraines were investigated in solvents of various polarities. Parameters, such as the position of maximum of absorption ( $\lambda_{ab}$ ), molar extinction coefficient ( $\epsilon$ ), position of maximum fluorescence ( $\lambda_{fl}$ ), Stokes shift ( $\Delta\bar{\nu}$ ), quantum yield of fluorescence ( $\Phi_{fl}$ ) and transition energy from the ground to excited state ( $E_{00}$ ) were calculated and are collected in Table 2.

From the data summarized in Table 2 and presented in Fig. 5, it can be seen that all the dyes absorb in a narrow range of the spectrum. The absorption band of the investigated compounds is located in the visible range of the spectrum and extends from *ca.* 500 nm to 600 nm. The absorption in this range is related to  $\pi \rightarrow \pi^*$  electron transitions in dye chromophores containing conjugated double bonds and pyrrole rings. The location of the absorption band of these compounds depends both on the properties of the solvent used and on the structure of the dye, *e.g.* the number of conjugated double bonds, the presence of aromatic rings and the nature of the substituent. Generally, it can be observed that the position of maximum absorption for squaraines overlaps with their difluoroborate analogues. The values of  $\lambda_{ab}$  oscillate from 551 nm to 566 nm for PSQ1 and BPSQ1 and from 559 to 574 nm for PSQ2 and BPSQ2, respectively.

Fig. 5(A) shows hypsochromic shifts of the absorption bands increasing with the polarity of the solvents. This phenomenon is referred to as negative solvatochromism. It is known that the polarity of the solvent has a significant effect

on the ground and excited states of a dissolved substance, due to difference in the energy gap between them. It should be highlighted that, with the increasing polarity of solvents, the interactions of the diluent with the dye molecules decreases (lower solvation free energy), causing the better stabilization of the molecule in the ground state relative to the first excited state. Such systems require higher energy for excitement of the dye. Therefore, the excited state of the molecule is less polar than the ground state, due to transfer of electron density from donor to acceptor after excitation. Based on the data summarized in Table 2, it can be concluded that for polar protic solvents, such as ethanol and methanol, the largest shifts of the absorption bands towards shorter wavelengths are observed.

It should be pointed that the introduction of a substituent in the form of an alkyl group (ethyl) to the pyrrole ring (PSQ2 and BPSQ2) results in a red shift of the absorption band in comparison with dyes without an additional substituent (PSQ1 and BPSQ1). Complexing the squaraines (PSQs) with an ethereal solution of boron trifluoride does not significantly affect the shape and position of the absorption bands. The bands of BPSQ1 and BPSQ2 dyes are almost identical to the bands corresponding to the appropriate squaraines PSQ1 and PSQ2.

The analysis of the fluorescence spectra of all the squaraine derivatives indicated that the investigated compounds emit in the visible region, in the range from 550 nm to 700 nm. The fluorescence bands are shifted towards the red region of the spectrum. The maximum fluorescence for squaraine derivatives is located between 562 nm and 614 nm. Indeed, the emission spectra are broader than the absorption spectra.

**Table 2** The spectral characteristics of squaraine derivatives

Dye	Parameter	Solvent								
		THF	AcOEt	ACE	EtOH	MeOH	MP	DMF	MeCN	DMSO
PSQ1	$\lambda_{ab}$ (nm)	560	556	556	551	549	566	562	553	565
	$\epsilon$ ( $10^5 \text{ dm}^3 \text{ mol}^{-1} \text{ cm}^{-1}$ )	1.98	2.03	0.77	0.70	0.65	0.59	2.13	1.00	0.59
	$\lambda_{fl}$ (nm)	581	578	575	571	569	<sup>a</sup>	565	573	<sup>a</sup>
	$\Delta\bar{\nu}$ ( $\text{cm}^{-1}$ )	645	685	594	636	640	<sup>a</sup>	94	631	<sup>a</sup>
	$\Phi_{fl}$ ( $10^{-3}$ )	7.23	10.17	4.26	6.49	2.63	14.95	6.26	3.99	9.83
	$E_{00}$ (eV)	2.18	2.20	2.20	2.21	2.22	<sup>a</sup>	2.20	2.21	<sup>a</sup>
PSQ2	$\lambda_{ab}$ (nm)	569	564	565	561	559	574	571	562	574
	$\epsilon$ ( $10^5 \text{ dm}^3 \text{ mol}^{-1} \text{ cm}^{-1}$ )	1.92	2.02	0.95	73 690	0.72	0.84	2.08	0.74	0.99
	$\lambda_{fl}$ (nm)	590	583	583	579	576	<sup>a</sup>	593	579	<sup>a</sup>
	$\Delta\bar{\nu}$ ( $\text{cm}^{-1}$ )	626	578	546	554	528	<sup>a</sup>	650	522	<sup>a</sup>
	$\Phi_{fl}$ ( $10^{-3}$ )	10.12	16.11	6.98	10.53	4.31	23.26	9.40	6.21	12.22
	$E_{00}$ (eV)	2.15	2.17	2.17	2.18	2.19	<sup>a</sup>	2.13	2.18	<sup>a</sup>
BPSQ1	$\lambda_{ab}$ (nm)	560	556	555	551	549	566	562	553	565
	$\epsilon$ ( $10^5 \text{ dm}^3 \text{ mol}^{-1} \text{ cm}^{-1}$ )	2.03	1.95	0.87	0.87	0.96	0.77	1.86	0.59	0.82
	$\lambda_{fl}$ (nm)	579	577	575	570	571	<sup>a</sup>	562	571	587
	$\Delta\bar{\nu}$ ( $\text{cm}^{-1}$ )	586	655	627	605	702	<sup>a</sup>	<sup>a</sup>	570	663
	$\Phi_{fl}$ ( $10^{-3}$ )	6.69	10.45	4.42	6.62	2.92	14.09	6.53	4.00	11.09
	$E_{00}$ (eV)	2.18	2.19	2.20	2.22	2.23	<sup>a</sup>	2.22	2.21	2.16
BPSQ2	$\lambda_{ab}$ (nm)	569	564	565	561	559	574	571	562	574
	$\epsilon$ ( $10^5 \text{ dm}^3 \text{ mol}^{-1} \text{ cm}^{-1}$ )	2.04	1.95	1.15	0.94	1.00	1.10	1.92	1.15	0.89
	$\lambda_{fl}$ (nm)	588	586	614	578	579	<sup>a</sup>	589	585	593
	$\Delta\bar{\nu}$ ( $\text{cm}^{-1}$ )	626	578	546	554	528	<sup>a</sup>	650	522	558
	$\Phi_{fl}$ ( $10^{-3}$ )	11.13	15.16	7.26	10.10	3.74	18.62	9.43	6.37	12.83
	$E_{00}$ (eV)	2.15	2.16	2.16	2.18	2.19	<sup>a</sup>	2.12	2.17	2.13

<sup>a</sup>The dye decomposed after excitation.

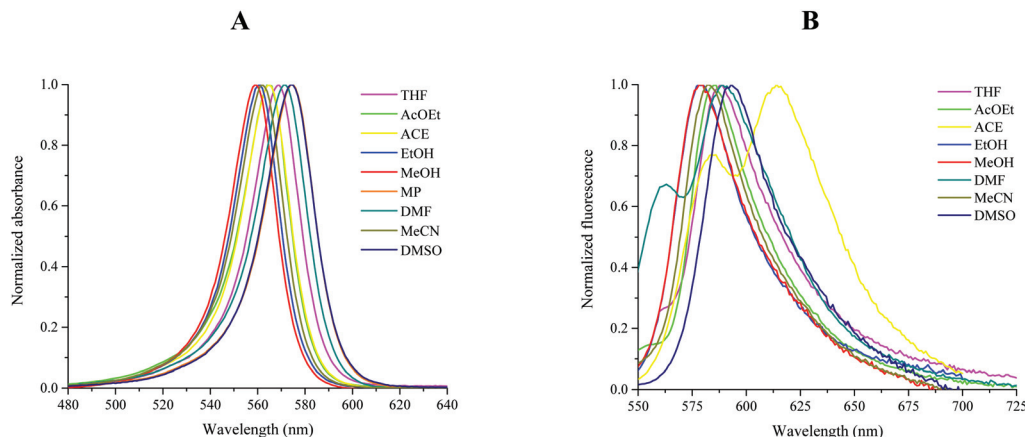


Fig. 5 The normalized absorption (A) and fluorescence (B) spectra of BPSQ2 complex in solvents of various polarity.

All of the synthesized compounds show high molar extinction coefficients. The value of this parameter exceeds  $10^5 \text{ dm}^3 \text{ mol}^{-1} \text{ cm}^{-1}$ . The Stokes shifts achieved relatively low values of *ca.*  $600 \text{ cm}^{-1}$ . Moreover, the studied dyes show low fluorescence quantum yields. This may be related to the main routes of deactivation, which are non-radiant processes with heat release: *e.g.* electron transfer or internal conversion. The  $\Phi_{\text{fl}}$  values range from  $2.63 \times 10^{-3}$  to  $23.26 \times 10^{-3}$ . Interestingly, higher quantum yields were obtained for dyes with an ethyl group attached to the pyrrole ring. The transition energy from the ground state to excited state reached similar values for all compounds. The average value of  $E_{00}$  energy is 2.20 eV.

On the basis of the obtained spectral data, it can be concluded that the proposed dyes fulfill the requirements which are necessary for using these compounds in the role of photosensitizers. In particular, the high molar absorption coefficients and spectroscopic characteristic adapted to the light source used suggest the possibility of good photosensitization.

As mentioned earlier, the presence of the initiator alone is usually insufficient to start the photopolymerization reaction. Commercial initiators, such Irgacure 2959 and diphenyl (2,4,6-trimethylbenzoyl)phosphine oxide (TPO), absorb over a narrow range of light. For this reason, it is important to determine the spectroscopic properties of the initiator and, if necessary, to combine it with a suitable light absorber. Therefore, the spectroscopic properties of the compounds used as co-initiators in the photopolymerization experiments were also examined. Fig. 6 illustrates the positions of the absorption bands of the chosen co-initiators and an example photosensitizer (BPSQ2).

As illustrated in Fig. 6, the co-initiators absorb in the ultraviolet, in contrast to squaraine dyes, whose absorption bands are shifted to the red region of the spectrum. Using only borate, iodonium or alkoxonium salts in photoinitiating systems would not be effective. However, in a combination of light absorbers, PSQ1, PQS2, BPSQ1 or BPSQ2 became promising photoinitiators. The data characterizing the spectroscopic properties of the co-initiators are presented in Table 3.

As shown in Table 3, the maximum absorption of B2 and I1 salts are at 252 nm, and for 1-methoxy-4-phenylpyridinium tetra-

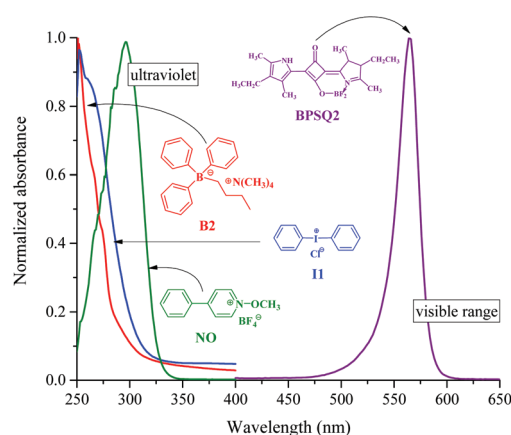


Fig. 6 The normalized absorption spectra of B2, I1, NO co-initiators and BPSQ2 photosensitizer recorded in ethyl acetate (AcOEt).

Table 3 The spectroscopic data of co-initiators

Co-initiator	Symbol	$\lambda_{\text{ab}}$ (nm)	$\epsilon$ ( $10^3 \text{ dm}^3 \text{ mol}^{-1} \text{ cm}^{-1}$ )
Tetramethylammonium <i>n</i> -butyltriphenylborate	B2	252	6.77
Diphenyliodonium chloride	I1	252	1.75
1-Methoxy-4-phenylpyridinium tetrafluoroborate	NO	295	2.91

fluoroborate (NO) it is at 295 nm. In comparison to photosensitizers, the values of the molar extinction coefficients for the co-initiators are much lower, of the order of  $10^3 \text{ dm}^3 \text{ mol}^{-1} \text{ cm}^{-1}$ .

### Photochemical stability of photosensitizers

In order to determine the photochemical stability of the photosensitizers a steady-state photolysis experiment was conducted. The steady-state photolysis of the squaraines themselves and with all co-initiators tested was studied to prove the photosensitizing capabilities of the dyes. All the components of photoinitiating systems were studied. Fig. 7 and S1–S3,<sup>†</sup> present the

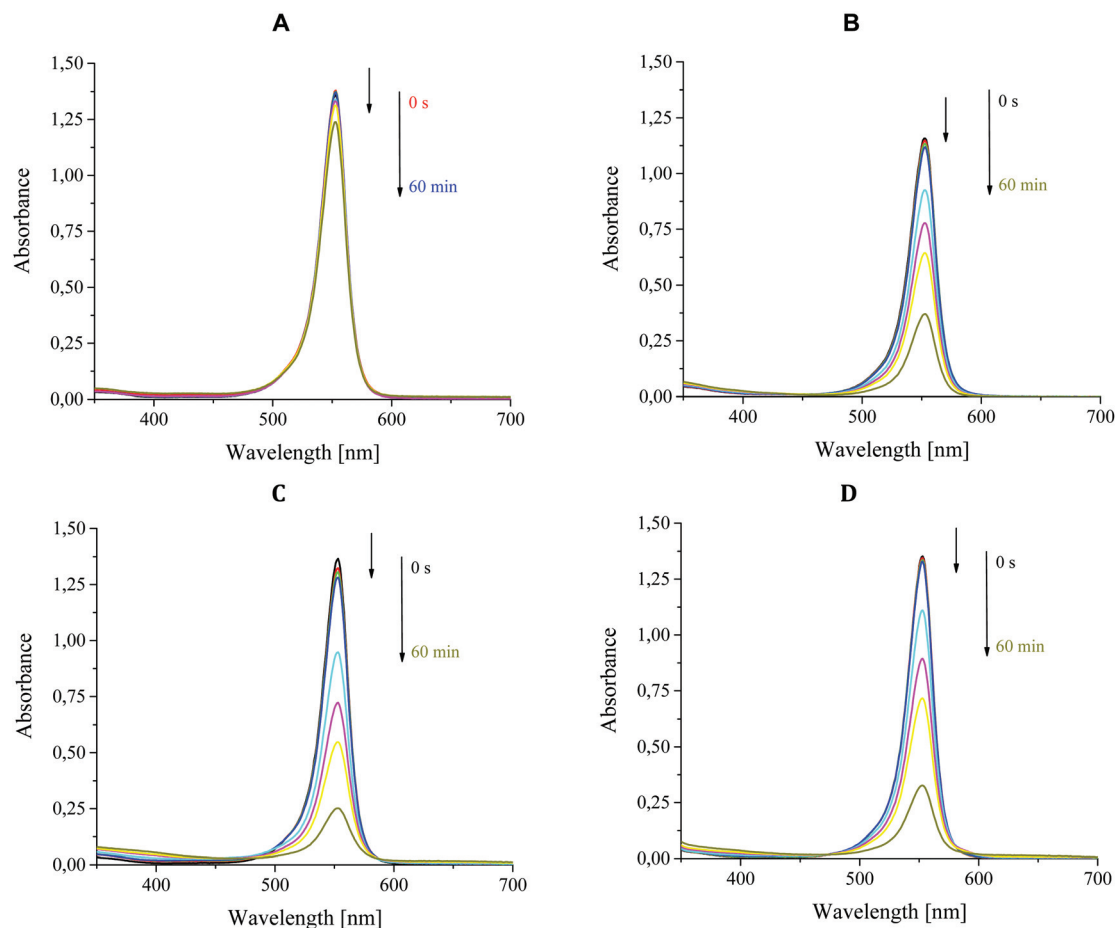


**Fig. 7** UV-Vis absorption spectra obtained upon photolysis of (A) PSQ1 alone, (B) PSQ1/B2, (C) PSQ1/I1 and (D) PSQ1/NO in acetonitrile upon irradiation at 518 nm (light intensity  $50 \text{ mW cm}^{-2}$ , co-initiator concentration  $1 \times 10^{-3} \text{ M}$ ).

photodegradation of the photosensitizers alone and in the presence of borate salt, iodonium salt and *N*-alkoxy pyridinium salt.

The most photochemically stable of the dyes tested is 2,4-bis(3,5-dimethylpyrrol-2-yl)squaraine (PSQ1). For dye PSQ1 alone in acetonitrile as a solvent, the intensity of the peak at  $\lambda_{\text{abs}}$  slightly decreased when irradiated with 514 nm wavelength (Fig. 7A). However, the photolysis rates accelerated when a co-initiator, *e.g.* borate salt (B2), iodonium salt (I1), or pyridinium salt (NO), was added (Fig. 7B–D). The addition of the co-initiator does not influence the position of the absorption band. Compounds PSQ1 and the difluoroborates of squaraines (BPSQ1 and BPSQ2) undergo photodegradation in acetonitrile solution under irradiation with visible light (514 nm) (Fig. S1A, S2A and S3A<sup>†</sup>). The photolysis rates also accelerated when the co-initiators were added (Fig. S1B–D, S2B–D and S3B–D<sup>†</sup>). The difluoroborate complex 2,4-bis(4-ethyl-3,5-dimethylpyrrol-2-yl)squaraine (BPSQ2) is the least photostable. The rate of photodegradation decreased from 20 min to 10 min when 1-methoxy-4-phenylpyridinium tetrafluoroborate (NO) was added.

For all the squaraines studied, similar degradation phenomena occurred during irradiation at 514 nm (Fig. S1–

S3<sup>†</sup>), with varying degrees of slope of absorbance, indicating interactions among the photosensitizers and co-initiators under irradiation.

### Kinetics of radical photopolymerization

The photoinitiating abilities of novel two-component systems for activating the radical polymerization process of trimethylolpropane triacrylate (TMPTA) were studied. New bimolecular photoinitiators consisting of squaraine derivatives and various co-initiators were proposed. The role of sensitizers was played by novel squaraine derivatives, such as 2,4-bis(3,5-dimethylpyrrol-2-yl)squaraine (PSQ1), 2,4-bis(4-ethyl-3,5-dimethylpyrrol-2-yl)squaraine (PSQ2), 2,4-bis(3,5-dimethylpyrrol-2-yl)squaraine difluoroborate (BPSQ1) and 2,4-bis(4-ethyl-3,5-dimethylpyrrol-2-yl)squaraine difluoroborate (BPSQ2). These squaraine dyes were combined with different co-initiators, such as tetramethylammonium *n*-butyltriphenylborate (B2), diphenyliodonium chloride (I1) and 1-methoxy-4-phenylpyridinium tetrafluoroborate (NO). The structures and abbreviations of the components of the tested photoinitiating systems are given in Chart 1.

The photopolymerization experiments were performed for different combinations of pairs of sensitizer and co-initiator. The influence of the structure of the photoinitiator on the kinetics of the radical polymerization of TMPTA was investigated. Moreover, the different concentrations of photoinitiators in the polymerization mixture were taken into account. Depending on the type of photoinitiating system used, various values of the kinetics parameters of polymerization were observed. The results obtained are summarized in Tables 4 and 5.

From the data summarized in Tables 4 and 5 and the kinetics curves presented in Fig. 8 it follows that all the proposed systems initiate the radical polymerization of acrylates. The highest degree of monomer conversion ( $C_{\%} = 12.4\%$ ) was

reached for the PSQ1/I1 combination. Unfortunately, polymerization in the presence of this combination shows one of the lower polymerization rates. More favorable results were obtained for systems with an NO co-initiator. Although the maximum degree of double bond conversion oscillates around 7–8%, the photocuring of monomers is already overlapping after first minutes of light exposure. These systems are very light sensitive. The slowest are systems with a basis of the B2 co-initiator. These PIs shows a 4-times lower rate of photopolymerization and conversion of about 2–5%.

In the case of the systems containing PSQ2 as photosensitizer, the highest degree of conversion of the reactive groups in the monomer equal to 12% were obtained in the presence of I1. The most efficient co-initiator also turned out to be NO due

**Table 4** The kinetic parameters of radical polymerization of TMPTA initiated by bimolecular photoinitiators composed of squaraines PSQ1 or PSQ2 and various radical sources

Sensitizer	Co-initiator	Concentration (M)	$Q^{\max}$ (mW)	$t^{\max}$ (min)	$R_p$ ( $10^{-4} \text{ s}^{-1}$ )	$I_p$ ( $10^{-7} \text{ s}^{-2}$ )	$C_{\%}$ (%)
PSQ1	B2	$5 \times 10^{-4}$	4.63	11.36	1.83	2.68	6.5
		$1 \times 10^{-3}$	11.65	10.49	4.60	7.31	4.9
		$2 \times 10^{-3}$	6.69	12.07	2.64	3.65	4.3
		$5 \times 10^{-3}$	5.06	13.01	2.00	2.56	4.4
	I1	$5 \times 10^{-4}$	6.88	3.69	2.71	12.24	0.8
		$1 \times 10^{-3}$	20.24	6.73	7.99	19.79	7.5
		$2 \times 10^{-3}$	10.37	7.95	4.09	8.57	6.9
		$5 \times 10^{-3}$	6.56	12.29	2.59	3.51	12.4
	NO	$5 \times 10^{-4}$	23.45	2.22	9.25	69.44	3.3
		$1 \times 10^{-3}$	46.31	2.31	18.30	132.03	7.1
		$2 \times 10^{-3}$	38.55	2.37	15.20	106.89	7.3
		$5 \times 10^{-3}$	19.56	2.29	7.72	56.19	8.1
PSQ2	B2	$5 \times 10^{-4}$	10.78	6.80	4.26	10.44	2.2
		$1 \times 10^{-3}$	3.81	15.43	1.50	1.62	2.6
		$2 \times 10^{-3}$	3.67	17.55	1.45	1.38	2.9
		$5 \times 10^{-3}$	5.35	15.65	2.11	2.25	6.5
	I1	$5 \times 10^{-4}$	8.99	6.99	3.55	8.46	12.0
		$1 \times 10^{-3}$	13.49	9.13	5.32	9.71	7.9
		$2 \times 10^{-3}$	6.64	11.25	2.62	3.88	4.4
		$5 \times 10^{-3}$	7.86	11.76	3.10	4.39	10.3
	NO	$5 \times 10^{-4}$	109.31	2.26	43.10	317.85	6.8
		$1 \times 10^{-3}$	25.55	2.29	10.10	73.51	4.6
		$2 \times 10^{-3}$	20.31	2.32	8.02	57.61	6.0
		$5 \times 10^{-3}$	15.89	2.26	6.00	44.25	5.4

**Table 5** The kinetic parameters of radical polymerization of TMPTA initiated by bimolecular photoinitiators composed of squaraine difluoroborates BPSQ1 or BPSQ2 and various radical sources

Sensitizer	Co-initiator	Concentration (M)	$Q^{\max}$ (mW)	$t^{\max}$ (min)	$R_p$ ( $10^{-4} \text{ s}^{-1}$ )	$I_p$ ( $\text{s}^{-2}$ )	$C_{\%}$ (%)
BPSQ1	B2	$5 \times 10^{-4}$	6.47	9.71	2.55	4.38	2.3
		$1 \times 10^{-3}$	7.14	14.75	2.82	3.19	6.0
	I1	$5 \times 10^{-4}$	5.13	9.08	2.02	3.71	1.8
		$1 \times 10^{-3}$	5.71	15.40	2.25	2.44	4.2
	NO	$5 \times 10^{-4}$	21.93	2.43	8.66	59.40	5.5
		$1 \times 10^{-3}$	31.73	2.26	12.50	92.18	6.3
BPSQ2	B2	$5 \times 10^{-4}$	11.12	9.75	4.39	7.50	4.1
		$1 \times 10^{-3}$	11.54	14.20	4.56	5.35	9.3
	I1	$5 \times 10^{-4}$	13.70	7.73	5.41	11.66	5.5
		$1 \times 10^{-3}$	14.12	9.27	5.57	10.01	10.7
	NO	$5 \times 10^{-4}$	44.19	2.19	17.40	132.42	6.4
		$1 \times 10^{-3}$	5.47	17.96	2.16	2.00	5.9

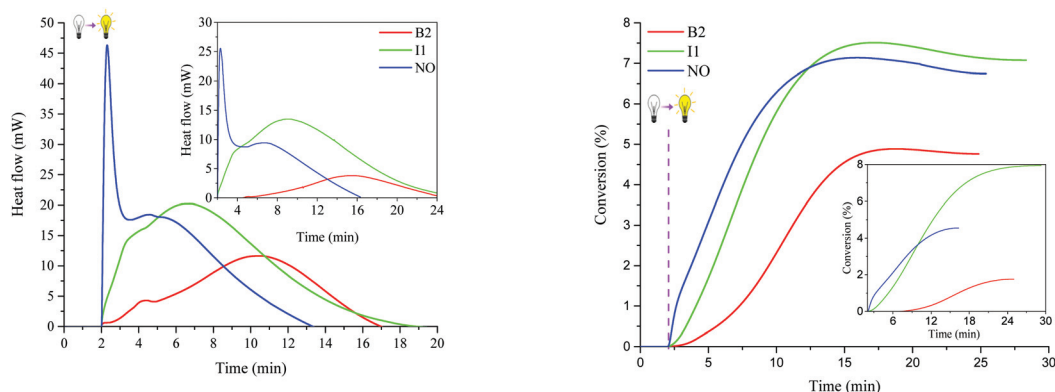


**Fig. 8** The kinetic curves registered during the radical polymerization of TMPTA initiated by two-component photoinitiating systems composed of 2,4-bis(3,5-dimethylpyrrol-2-yl)squaraine (PSQ1) in the presence of various co-initiators. Inset: the kinetic curves recorded during the radical polymerization of TMPTA initiated by photoinitiating systems containing 2,4-bis(4-ethyl-3,5-dimethylpyrrol-2-yl)squaraine (PSQ2) and various radical sources. The concentration of photoinitiator was  $1 \times 10^{-3}$  M.

to the highest heat flow of 109.31 mW and the conversion of 6.8%. This system is additionally characterized as having the fastest polymerization rate of all the dyes used as photosensitizers.

As was mentioned earlier, an important factor in the photopolymerization process is the concentration of photoinitiator in the polymerizable mixture. The obtained results confirm that in order to obtain high-speed PIs, the effect of photoinitiator concentration on the kinetics of the polymerization reaction should be investigated. The influence of this parameter for the photoinitiating abilities of the chain reaction for the following concentrations of co-initiator,  $5 \times 10^{-4}$  M,  $1 \times 10^{-3}$  M,  $2 \times 10^{-3}$  M and  $5 \times 10^{-3}$  M, is presented in Fig. 9.

As seen, in each case, the optimum concentration of photoinitiator mixture was  $1 \times 10^{-3}$  M. It turns out that the lowest

concentration of photoinitiator ( $5 \times 10^{-4}$  M) gives the worst kinetic result. Although, it must be noted, that the highest amounts of PI cause a slowing down of the speed of reaction. This may be explained by the inner filter effect. This phenomenon includes the dye sensitizers in high concentrations strongly absorbing radiation because of the high molar value absorption coefficients ( $\epsilon > 10^4$  dm<sup>3</sup> mol<sup>-1</sup> cm<sup>-1</sup>). This phenomenon effectively impedes the penetration of light to the lower layers of the polymerization mixture and leads to a slowing down or even complete inhibition of polymerization. For these reasons, the use of a high concentration of photoinitiator may be unfavorable, which translates into our data.

On the basis of data about the dependence of concentration on the rate of polymerization, photopolymerization experiments for PIs comprising difluoroborate complexes BPSQ1 or BPSQ2 were carried out for different concentrations of photoinitiators, as follows:  $5 \times 10^{-4}$  M and  $1 \times 10^{-3}$  M. The kinetic characteristics are presented in Fig. 10 and Table 5.

The highest degree of monomer conversion was achieved for the combinations of BPSQ1 with B2 ( $C_{\%} = 10.9\%$ ) and BPSQ2/I1 ( $C_{\%} = 9\%$ ). These photoinitiators, as in the case of PSQ1 and PSQ2, are characterized by a slow increase in polymerization rate and conversion during polymerization time. The maximum monomer conversion was obtained after 60 and 30 minutes of light exposure. These values disqualify these photoinitiators under these reaction conditions. The highest  $R_p$  value was achieved for PIs containing alkoxonium salt (NO). This is due to the highest heat flow of 51.99 mW and corresponds to a conversion of 6.2%. It is lower than in the case of the PSQ1/NO and PSQ2/NO photoinitiating systems, despite a higher concentration of photoinitiator ( $2 \times 10^{-3}$  M). From Table 5, it can be seen that this is the most effective concentration for both systems composed of onium salts I1 and NO. The polymerization rate  $R_p$  increases gradually

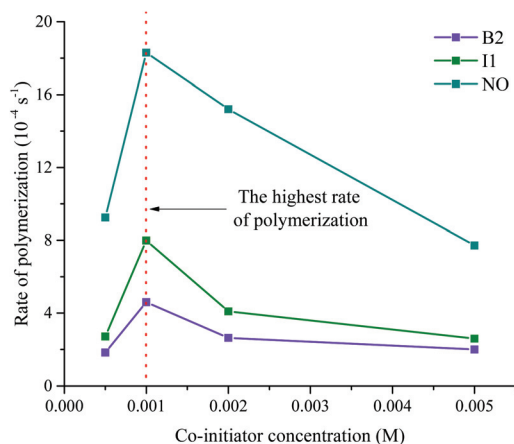


**Fig. 9** The effect of concentration of photoinitiator on the rate of radical polymerization of TMPTA. The concentration of 2,4-bis(3,5-dimethylpyrrol-2-yl)squaraine (PSQ1) is the same as for appropriate co-initiators and marked on the figure.

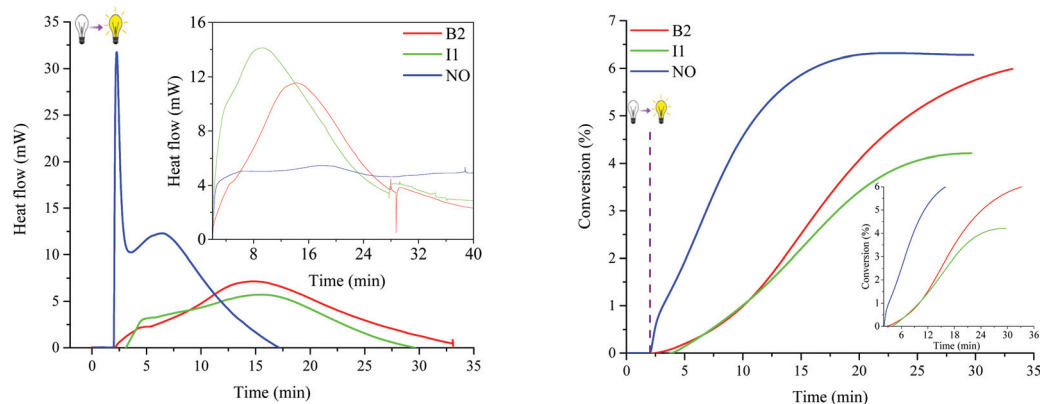


**Fig. 10** The kinetic curves registered during radical polymerization of TMPTA initiated by two-component photoinitiating systems composed of 2,4-bis(3,5-dimethylpyrrol-2-yl)squaraine difluoroborate (BPSQ1) in the presence of various co-initiators. Inset: the kinetic curves recorded during radical polymerization of TMPTA initiated by photoinitiating systems containing 2,4-bis(4-ethyl-3,5-dimethylpyrrol-2-yl)squaraine difluoroborate (BPSQ2) and various radical sources. The concentration of the photoinitiator was  $1 \times 10^{-3}$  M.

to this concentration and then successively decreases as a result of the internal filter effect. The changes in the rate of polymerization for BPSQ1/I1 photoinitiating systems with a variety of concentrations are not drastic. On the other hand, the system based on BPSQ1 dye and B2 is characterized by an almost linear dependence of the rate of polymerization on the photoinitiator concentration.

In order to evaluate the photoinitiation ability of the new systems, the values of their photoinitiation index ( $I_p$ ) were compared. Depending on the type of photoinitiator, different values of this parameter were obtained. Examples of the results are depicted in Fig. 11.

It can be seen that the photoinitiating systems composed of squaraine derivatives and 1-methoxy-4-phenylpyridinium tetrafluoroborate (NO) show the highest values of the  $I_p$  parameter. This may be related to the structure of this co-initiator. In the

described systems, the alkoxonium salt acts as an electron acceptor. The electron transfer process between the photosensitizer in the excited state and the co-initiator molecule is extremely effective. Therefore, the alkoxy radicals are formed in a relatively short time.

It should be pointed out that the lowest values of the photoinitiation indexes were obtained for PIs containing borate salt B2. In this case, the formation of the initiating radicals is less effective. The initiation of polymerization is also an effect of the electron transfer process between squaraine dye and borate salt, but this co-initiator acts as an electron acceptor in the two-component photoinitiating systems under study. It can be concluded that the phenyl and methoxy radicals formed from iodonium and alkoxonium salts show higher reactivity towards vinyl bonds in the monomer than boranyl radicals.

The efficiencies of the photoinitiating systems were also compared with other common initiators. Camphorquinone (CQ) in the presence of various co-initiators was studied under the same experimental conditions as the photoinitiators proposed by us. The following compounds, ethyl 4-*N*,*N*-dimethylaminobenzoate (EDMAB), diphenyliodonium chloride (I1) and *N*-phenylglycine (NPG), were applied as co-initiators. The structures of the components of common photoinitiating systems are shown in Chart 2.

The concentration of photosensitizer and co-initiators was  $1 \times 10^{-3}$  M, expected of photoinitiating systems composed of camphorquinone and diphenyliodonium chloride and *N*-phenylglycine. In this case, the concentration of co-initiator was one order of magnitude higher. Based on kinetic curves of the photopolymerization process (Fig. 12) it can be seen that the system of camphorquinone/*N*-phenylglycine under the same experimental conditions possesses the best photoinitiation ability. The lowest efficiency was observed for photoinitiators composed of diphenyliodonium chloride (I1) as a co-initiator. The degree of monomer conversion was low and

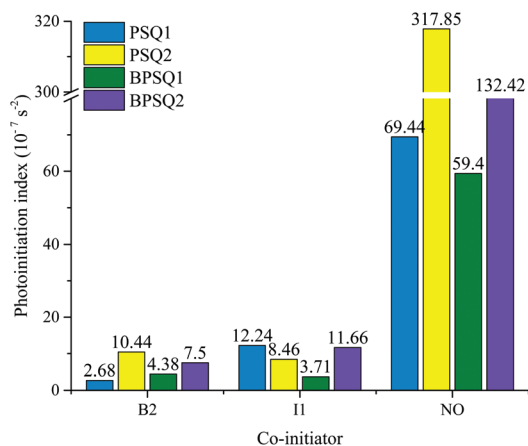


**Fig. 11** The values of photoinitiation indexes ( $I_p$ ) for various combinations of squaraine dye/radical source. The concentration of photoinitiator was  $5 \times 10^{-4}$  M.

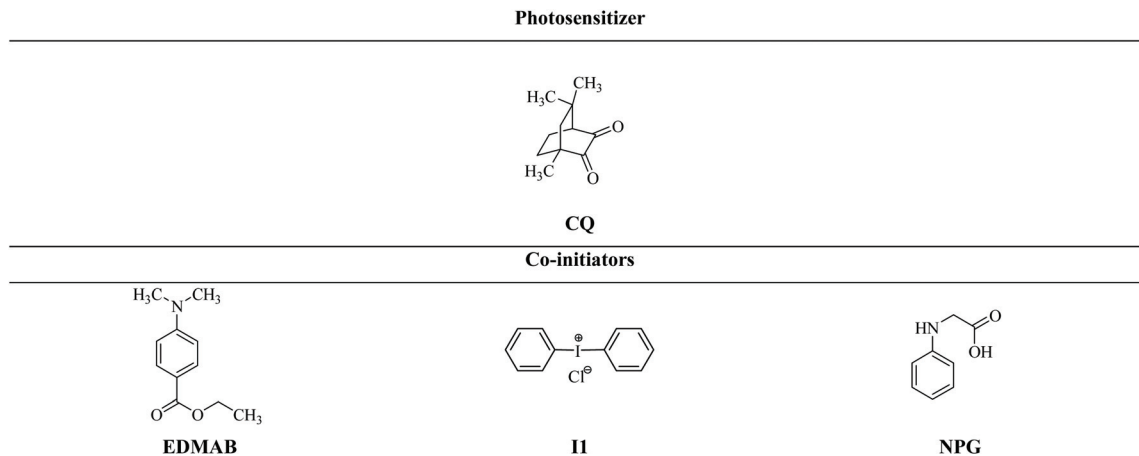


**Chart 2** Structures of components of common photoinitiating systems.

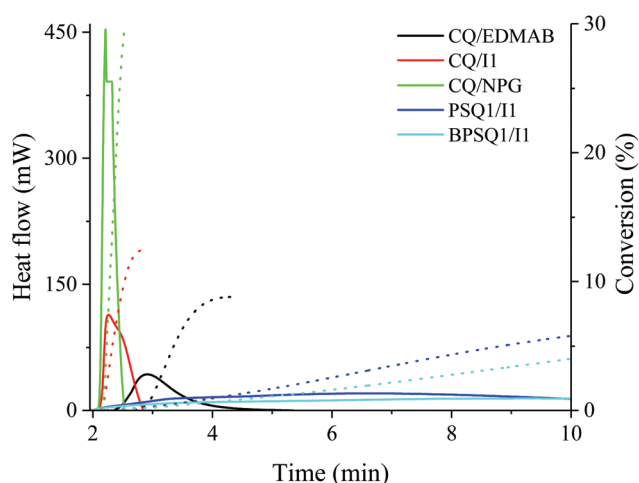


**Fig. 12** The comparison of the photoinitiating ability of systems composed of camphorquinone (CQ) and ethyl 4-*N,N*-dimethylaminobenzoate (EDMAB), diphenyliodonium chloride (I1) and *N*-phenylglycine (NPG) and photoinitiating systems composed of squaraine dye (PSQ1) and difluoroborate complex (BPSQ1) in the presence of diphenyliodonium chloride (I1).

ranged from 5% to 10%. The slightly higher value of conversion was achieved when camphorquinone was used as a photosensitizer, but in this case the concentration of the co-initiator was  $1 \times 10^{-2}$  M (one order of magnitude higher) than in the case of squarylium dyes and difluoroborate complexes.

The concentration of photosensitizers and co-initiator was  $1 \times 10^{-3}$  M or  $1 \times 10^{-2}$  M.

### Photosensitization

It is well known that one of the deactivation processes of an excited state of a photosensitizer may be an electron transfer between the dye and the co-initiator molecule. This is a non-radiative process. As was shown in Scheme S1,<sup>†</sup> the initiating radicals are formed as a result of a photoinduced electron

transfer process. The Gibbs free energy change ( $\Delta G_{et}$ ) of the charge transfer between the photosensitizer and the co-initiators was calculated using the Rehm–Weller equation (eqn (5)):

$$\Delta G_{et} = E_{ox}(D/D^{+}) - E_{red}(A^{-}/A) - E_{S1} - E_C \quad (5)$$

where  $E_{ox}(D/D^{+})$  and  $E_{red}(A^{-}/A)$ , are the oxidation potential and reduction potential, respectively.  $E_{S1}$  is the energy of the first excited state of the photosensitizer and was determined by identifying the crossing point between the normalized UV-Vis absorption and fluorescence spectra (Table 6), e.g.  $E_{S1} = 2.18$  eV and 2.17 eV for PSQ2 and its difluoroborate complex BPSQ2, respectively.  $E_C$  is the coulombic energy, which can be omitted from the calculation because neutral free radicals are formed during photoinduced electron transfer.

In this study, diphenyliodonium and *N*-alkoxypridinium salts were used as the electron acceptors, while the photosensitizer was an electron donor. In the case when *n*-butyltriphenylborate salt was used as a co-initiator, the dye played the role of an electron acceptor. The estimated values of free energy change for the electron transfer process are in the range from  $-132.8$  kJ mol<sup>-1</sup> to 76.52 kJ mol<sup>-1</sup>. In the PSQ2/B2 system the  $\Delta G_{et}$  was the highest, e.g. 76.52 kJ mol<sup>-1</sup>, whereas the  $\Delta G_{et}$  for BPSQ2/I1 (e.g.  $-132.8$  kJ mol<sup>-1</sup>) is lower than those for other systems. The lower  $\Delta G_{et}$ , the higher the efficiency of electron transfer. Only for iodonium and pyridinium salts were the free energy changes negative. Taking this into account, it may be

**Table 6** Electrochemical properties of selected photoinitiators

Photosensitizer	$E_{ox}^a/V$	$E_{red}^a/V$	$\Delta G_{et}^b/kJ\ mol^{-1}$		
			B2	I1	NO
PSQ2	0.31	-1.82	76.52	-132.8	-123.13
BPSQ2	0.51	-1.65	61.08	-112.52	-102.87

<sup>a</sup> Versus (Fc/Fc<sup>+</sup>).<sup>40</sup> <sup>b</sup>  $E_{ox}^b$  (B2) = 1.153 eV,<sup>41</sup>  $E_{red}$  (I1) =  $-0.494$  eV,<sup>45</sup>  $E_{red}$  (NO) =  $-0.594$  eV.<sup>41</sup>

concluded that the photoinitiated electron transfer *via* the photooxidizable mechanism is a spontaneous process. Thus, the results demonstrated that the intramolecular electron transfer between the photosensitizers PSQ2 and BPSQ2 and co-initiators: I1 and NO is thermodynamically allowed.

### Mechanism of free radical formation

It should be mentioned that we explained and described the mechanisms of primary and secondary processes occurring after irradiation of photoinitiating systems at 355 nm earlier.<sup>42–45</sup> The transient absorption spectra and decay kinetics were recorded using a nanosecond laser flash photolysis experiment.

As a reminder, the mechanism of active species formation is presented in ESI as Scheme S1.† The first step is absorption of light at an appropriate wavelength by squaraine dye. The photoexcited dye molecule encounters a co-initiator molecule, and accepts or donates an electron from or to the co-initiator, forming a photosensitizer-based radical anion or radical cation, respectively. Therefore, it was concluded that the first step of the photoreaction occurs between squarylum dye and co-initiator. The co-initiator reacts either as an electron donor or electron acceptor with an excited state of the dye. The squarylum dye may undergo both photoreduction and photooxidation processes; thus the photosensitizer may act as an electron acceptor or an electron donor. The role of the photosensitizer depends on the type of co-initiator. It was shown that in the presence of tetramethylammonium *n*-butyltriphenylborate salt, the radical anion of squaraine dye is formed, confirming the photoreducible mechanism of free radical formation.<sup>42–44</sup> On the other hand, in the presence of iodonium or alkoxyppyridinium salts the photooxidizable mechanism occurs and the radical cation of squaraine dye is formed and can be observed during nanosecond laser flash photolysis.<sup>42</sup> These processes lead to C–B bond cleavage in the boranyl radical, C–I bond cleavage in the diphenyliodonium radical<sup>44</sup> and N–O bond cleavage in the *N*-alkoxyppyridinium radical<sup>45</sup> and the formation of free radicals (*e.g.* butyl, phenyl, methoxy), that can start the polymerization chain reaction.<sup>43</sup>

The obtained results are our latest contribution to the design of novel photoinitiating systems for radical polymerization based on squaraine dyes. The proposed photoinitiators may be improved in the future in order to obtain high values of kinetic parameters of photopolymerization.

## 4. Conclusions

In conclusion, novel photoinitiators based on squaraine dyes for photocuring of acrylates were proposed in this article. The new photosensitizers in combination with borate (B2), iodonium salt (I1) and alkoxonium salt (NO) effectively initiated the radical polymerization of trimethylolpropane triacrylate (TMPTA) in visible light (Vis). It can be concluded that the efficiency of polymerization depends on the structure and concentration of the co-initiator. The use of an optimal concen-

tration of photoinitiator ( $1 \times 10^{-3}$  M) results in the best kinetic parameters of photopolymerization. The highest concentrations of photoinitiators cause the appearance of an inner filter effect, which is disadvantageous to the process. The synthesized sensitizers are not able to initiate the polymerization reaction independently, due to the negligible participation of dye radical ions in attacks on the double bonds of the monomer. Taking into account the structure of the sensitizer, it is worth underlining that the presence of additional electron-donating substituents, such as the ethyl group in PSQ2 and BPSQ2 dyes, has a positive effect on the rate of polymerization in the presence of the alkoxonium salt NO. The efficiency of photopolymerization depends on the reactivity of the initiating radicals in the following order: B2 < I1 < NO.

## Conflicts of interest

There are no conflicts to declare.

## Acknowledgements

The financial support of the Ministry of Science and Higher Education Republic of Poland (BN 8/2019) is gratefully acknowledged.

## References

- 1 D. C. Hoekstra, B. P. A. C. van der Lubbe, T. Bus, L. Yang, N. Grossiord, M. G. Debije and A. P. H. J. Schenning, *Angew. Chem., Int. Ed.*, 2021, **60**, 10935–10941, DOI: 10.1002/anie.202101322.
- 2 R. Brighenti and M. P. Cosma, *J. Mech. Phys. Solids*, 2021, **153**, 104456, DOI: 10.1016/j.jmps.2021.104456.
- 3 H. H. Kim, J. W. Kim, J. Choi, Y. H. Park and C. S. Ki, *Polymer*, 2018, **153**, 232–240, DOI: 10.1016/j.polymer.2018.08.019.
- 4 E. Sprick, J. M. Becht, B. Graff, J. P. Salomon, T. Tigges, C. Weber and J. Lalevée, *Dent. Mater.*, 2021, **37**, 382–390, DOI: 10.1016/j.dental.2020.12.0130109-5641.
- 5 E. S. Farrell, N. Ganonyan, I. Cooperstein, M. Y. Moshkovitz, Y. Amouyal, D. Avnir and S. Magdassi, *Appl. Mater. Today*, 2021, **24**, 101083, DOI: 10.1016/j.apmt.2021.1010832352-9407.
- 6 Z. Chen, J. Li, C. Liu, Y. Liu, J. Zhu and C. Lao, *Ceram. Int.*, 2019, **45**, 11549–11557, DOI: 10.1016/j.ceramint.2019.03.024.
- 7 E. Hola, J. Ortyl, M. Jankowska, M. Plich, M. Galek, F. Morlet-Savary, B. Graff, C. Dietlin and J. Lalevée, *Polym. Chem.*, 2020, **11**, 922–935, DOI: 10.1039/C9PY01551E.
- 8 Y. Xu, G. Noirbent, D. Brunel, F. Liu, D. Gimes, K. Sun, Y. Zhang, S. Liu, F. Morlet-Savary, P. Xiao, F. Dumur and J. Lalevée, *Eur. Polym. J.*, 2020, **132**, 109737, DOI: 10.1016/j.eurpolymj.2020.109737.

- 9 M. H. Narimatsu, C. F. Neto, R. M. Da Costa, L. Wang, J. F. S. Bombonatti and A. Y. Furuse, *Int. J. Adhes. Adhes.*, 2021, **111**, 102976, DOI: 10.1016/j.ijadhadh.2021.102976.
- 10 Y. Zhang, H. Miao and W. Shi, *Prog. Org. Coat.*, 2011, **71**, 48–55, DOI: 10.1016/j.porgcoat.2010.12.009.
- 11 S. Kasisomayajula, N. Jadhav and V. J. Gelling, *Prog. Org. Coat.*, 2021, **154**, 106190, DOI: 10.1016/j.porgcoat.2021.106190.
- 12 S. Liu, Y. Zhang, K. Sun, B. Graff, P. Xiao, F. Dumur and J. Lalevée, *Eur. Polym. J.*, 2021, **147**, 110300, DOI: 10.1016/j.eurpolymj.2021.110300.
- 13 P. K. Shah and J. W. Stansbury, *Dent. Mater.*, 2021, **37**, 578–587, DOI: 10.1016/j.dental.2021.01.0130109-5641.
- 14 M. Ha, A. Athirasala, A. Tahayeri, P. P. Menzes and L. E. Bertassoni, *Dent. Mater.*, 2020, **36**, 88–96, DOI: 10.1016/j.dental.2019.10.0130109-5641.
- 15 I. Chiulan, E. B. Heggset, Ş. I. Voicu and G. Chingacarrasco, *Biomacromolecules*, 2021, **22**, 1795–1814, DOI: 10.1021/acs.biomac.0c01745.
- 16 A. Bagheri and J. Jin, *ACS Appl. Polym. Mater.*, 2019, **1**, 593–611, DOI: 10.1021/acsapm.8b00165.
- 17 T. Spahiu, E. Canaj and E. Shehi, *J. Eng. Fibers Fabr.*, 2020, **15**, 1–8, DOI: 10.1177/1558925020948216.
- 18 K. Suyama and H. Tachi, *Prog. Org. Coat.*, 2016, **100**, 94–99, DOI: 10.1016/j.porgcoat.2016.02.0250300-9440.
- 19 C. Dietlin, S. Schweizer, P. Xiao, J. Zhang, F. Morlet-Savary, B. Graff, J. P. Fouassier and J. Lalevée, *Polym. Chem.*, 2015, **6**, 3895–3912, DOI: 10.1039/C5PY00258C.
- 20 J. Kabatc, K. Iwińska, A. Balcerak, D. Kwiatkowska, A. Skotnicka, Z. Czech and M. Bartkowiak, *RSC Adv.*, 2020, **10**, 24817–24829, DOI: 10.1039/D0RA03818K.
- 21 J. Li, Y. Peng, J. Peña and J. Xing, *J. Photochem. Photobiol., A*, 2021, **411**, 113216, DOI: 10.1016/j.jphotochem.2021.113216.
- 22 A. A. Perez-Mondragón, C. E. Cuevas-Suárez, J. A. González-López, N. Trejo-Carbajal and A. M. Herrera-González, *J. Photochem. Photobiol., A*, 2020, **403**, 112844, DOI: 10.1016/j.jphotochem.2020.112844.
- 23 W. Tomal and J. Ortyl, *Polymers*, 2020, **12**, 1073, DOI: 10.3390/polym12051073.
- 24 A. Eibel, D. E. Fast and G. Gescheidt, *Polym. Chem.*, 2018, **9**, 5107–5115, DOI: 10.1039/C8PY01195H.
- 25 R. Taschner, P. Gauss, P. Knaack and R. Liska, *J. Polym. Sci.*, 2020, **58**, 242–253, DOI: 10.1002/pol.20199929.
- 26 A. Balcerak, D. Kwiatkowska, K. Inieńska and J. Kabatc, *Polym. Chem.*, 2020, **11**, 5500, DOI: 10.1039/D0PY00763C.
- 27 P. Garra, C. Dietlin, F. Morlet-Savary, F. Dumur, D. Gignes, J. P. Fouassier and J. Lalevée, *Polym. Chem.*, 2017, **8**, 7088, DOI: 10.1039/C7PY01778B.
- 28 J. Pierrel, A. Ibrahim, C. Croutxé-Barghorn and X. Allonas, *Polym. Chem.*, 2017, **8**, 4596–4602, DOI: 10.1039/C7PY00974G.
- 29 N. Giacoletto, M. Ibrahim-Ouali and F. Dumur, *Eur. Polym. J.*, 2021, **150**, 110427, DOI: 10.1016/j.eurpolymj.2021.110427.
- 30 J. Kabatc, K. Kostrzewska, M. Kozak and A. Balcerak, *RSC Adv.*, 2016, **6**, 103851–103863, DOI: 10.1039/C6RA23060A.
- 31 P. Xiao, F. Dumur, T. T. Bui, F. Goubard, B. Graff, F. Morlet-Savary, J. P. Fouassier, D. Gignes and J. Lalevée, *ACS Macro Lett.*, 2013, **2**, 736–740, DOI: 10.1021/mz400316y.
- 32 A. Bonardi, F. Bonardi, G. Noirbent, F. Dumur, C. Dietlin, D. Gignes, J. P. Fouassier and J. Lalevée, *Polym. Chem.*, 2019, **10**, 6505–6514, DOI: 10.1039/C9PY01447K.
- 33 Y. He, W. Zhou, F. Wu, M. Li and E. Wang, *J. Photochem. Photobiol., A*, 2004, **162**, 463–471, DOI: 10.1016/S1010-6030(03)00390-3.
- 34 A. Balcerak, K. Iwińska and J. Kabatc, *Dyes Pigm.*, 2019, **170**, 107596, DOI: 10.1016/j.dyepig.2019.107596.
- 35 R. Damico, *J. Org. Chem.*, 1964, **29**, 1971–1976, DOI: 10.1021/jo01030a077.
- 36 J. Olmsted, *J. Phys. Chem.*, 1979, **83**, 2581–2584, DOI: 10.1021/j100483a006.
- 37 J. Brandrup and E. H. Immergut, *Polmer Handbook*, New York, Chichester, Brisbane, Toronto, Singapore, 3rd edn, 1989.
- 38 G. Xiao and H. Wang, *J. Photochem. Photobiol., C*, 2017, **31**, 84–113, DOI: 10.1016/j.jphotochemrev.2017.03.001.
- 39 R. Bonnett, M. Motevalli and J. Siu, *Tetrahedron*, 2004, **60**, 8913–8918, DOI: 10.1016/j.tet.2004.07.023.
- 40 Y. Kubota, M. Tsukamoto, K. Ohnishi, K. Funabiki and M. Matsui, *Org. Chem. Front.*, 2017, **4**, 1522–1527, DOI: 10.1039/C7QO00225D.
- 41 K. Kostrzewska, J. Ortyl, R. Dobosz and J. Kabatc, *Polym. Chem.*, 2017, **8**, 3464–3474, DOI: 10.1039/c7py00621g.
- 42 J. Kabatc, K. Kostrzewska, K. Jurek, M. Kozak, A. Balcerak and Ł. Orzeł, *J. Polym. Sci., Part A: Polym. Chem.*, 2017, **55**, 471–484, DOI: 10.1002/pola.28425.
- 43 J. Kabatc, *J. Polym. Sci., Part A: Polym. Chem.*, 2017, **55**, 1575–1589, DOI: 10.1002/pola.28525.
- 44 J. Kabatc, J. Ortyl and K. Kostrzewska, *RSC Adv.*, 2017, **7**, 41619–41629, DOI: 10.1039/c7ra05978g.
- 45 J. Kabatc, K. Kostrzewska, R. Dobosz, Ł. Orzeł and K. Jurek, *Part A: Polym. Chem.*, 2017, **55**, 2840–2850, DOI: 10.1002/pola.28693.

## Supporting Information

### **Novel photoinitiators based on difluoroborate complexes of squaraine dyes for radical polymerization of acrylates upon visible light**

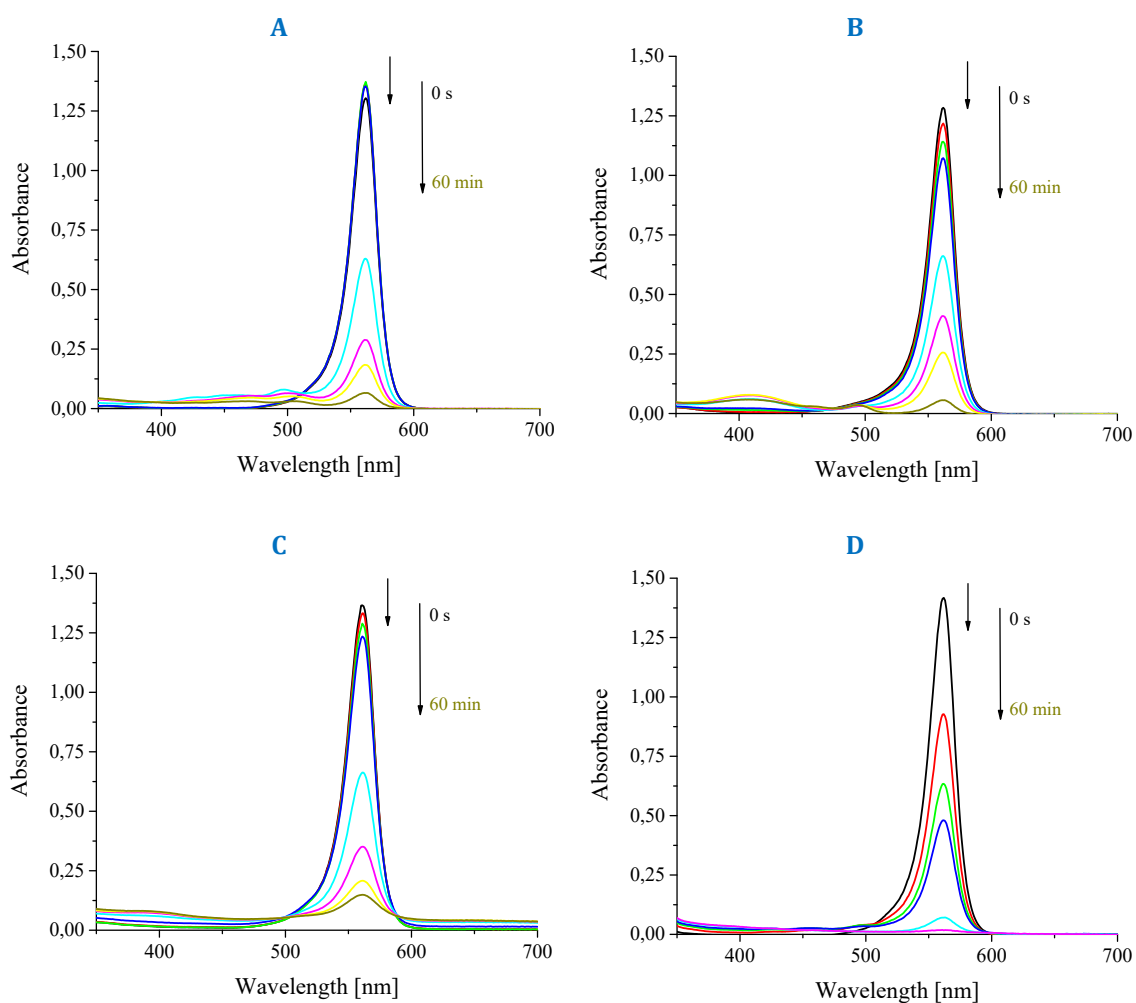
Alicja Balcerak, Dominika Kwiatkowska, and Janina Kabatc\*

*PBS University of Science and Technology, Faculty of Chemical Technology and Engineering,  
Seminaryjna 3, 85-326 Bydgoszcz, Poland*

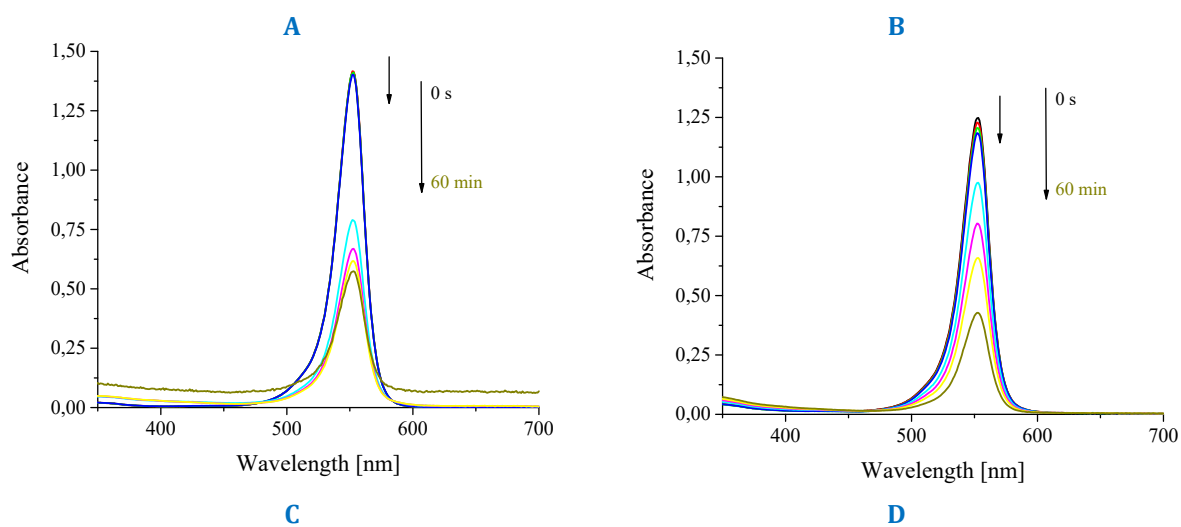
\* Corresponding author.

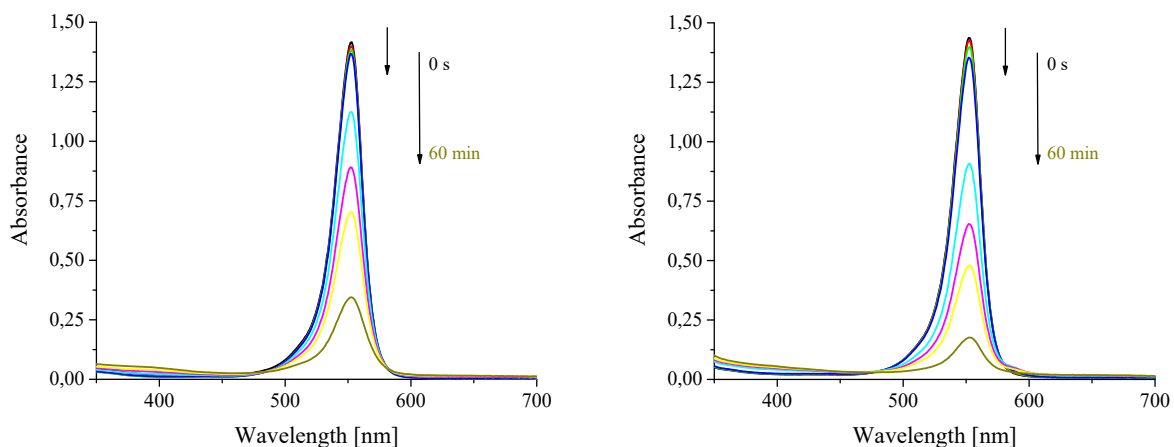
*E-mail address:* [nina@utp.edu.pl](mailto:nina@utp.edu.pl) (J. Kabatc)

## 1. Photodegradation - Steady state photolysis

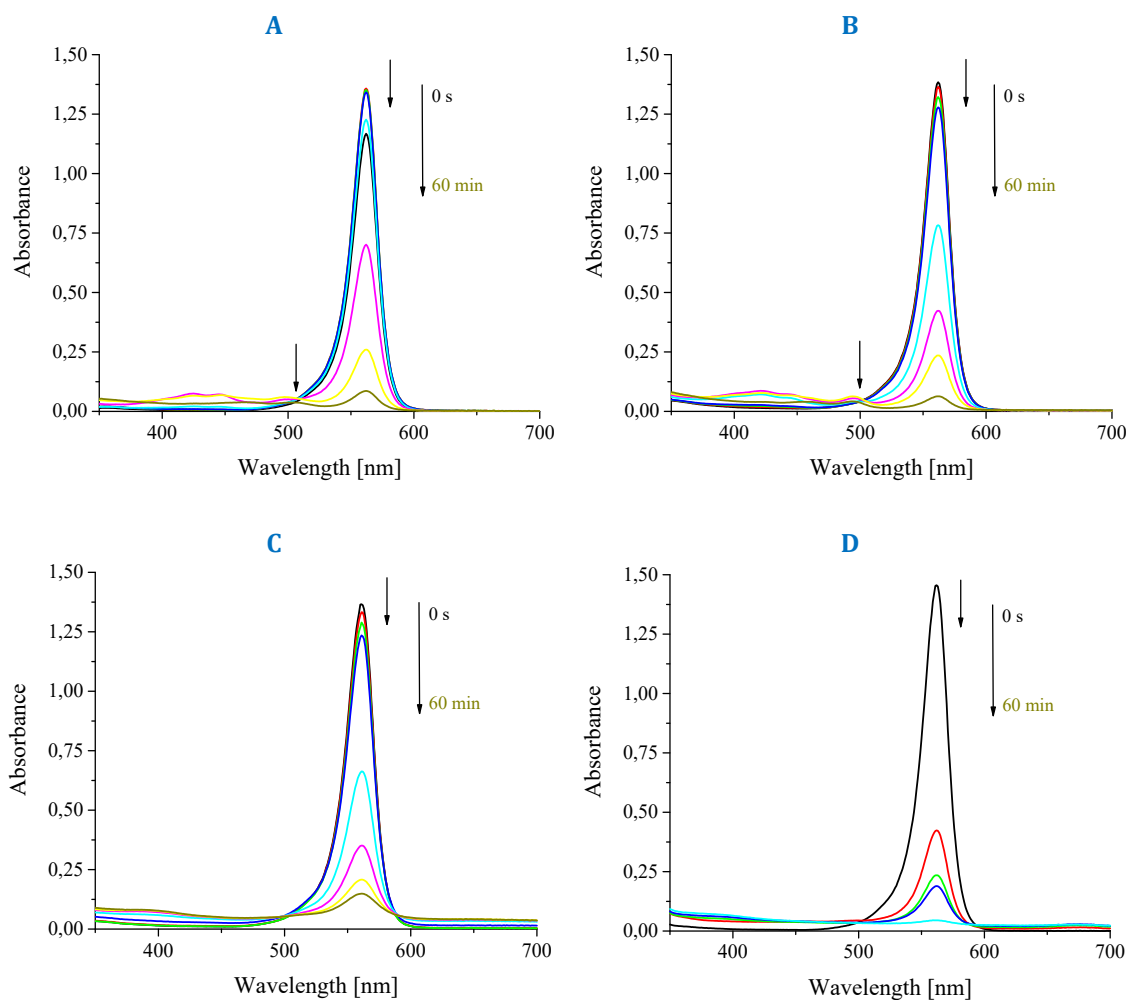


**Figure S1.** UV-Vis absorption spectra obtained upon photolysis of (A) PSQ2 alone, (B) PSQ2/B2, (C) PSQ2/I1 and (D) PSQ2/NO in acetonitrile upon irradiation at 518 nm (light intensity  $50 \text{ mW cm}^{-2}$ , co-initiator concentration  $1 \times 10^{-3} \text{ M}$ )



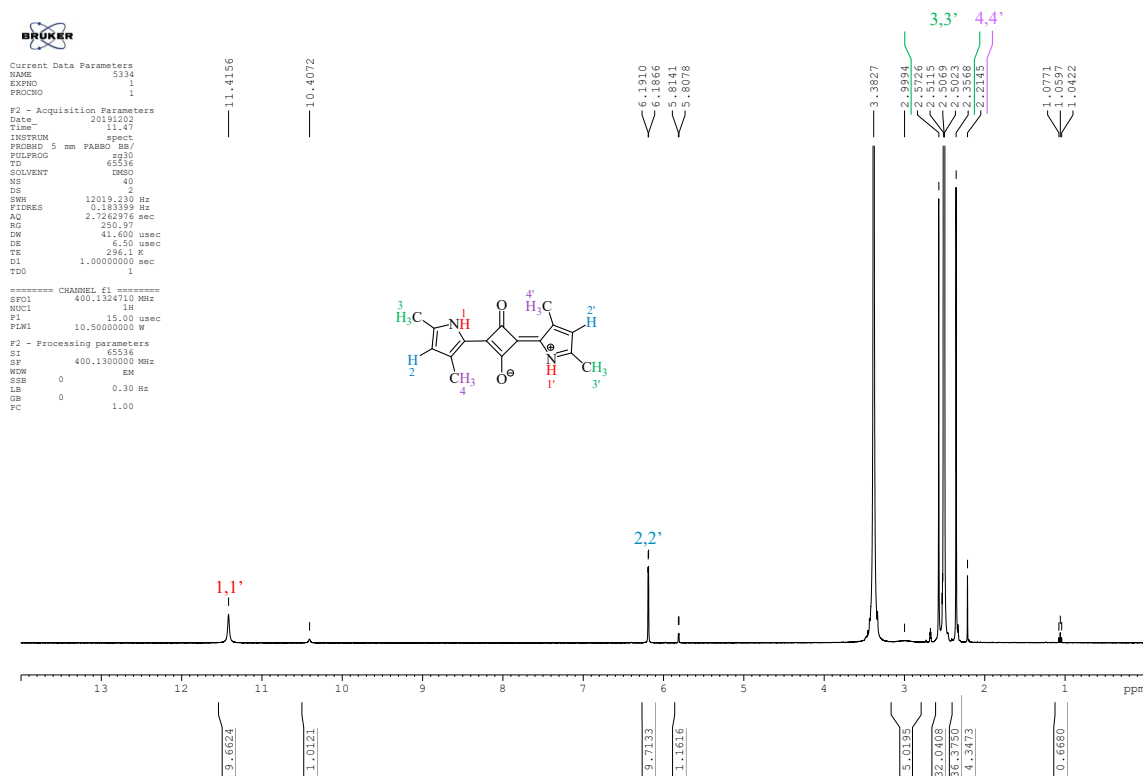


**Figure S2** UV-Vis absorption spectra obtained upon photolysis of (A) BPSQ1 alone, (B) BPSQ1/B2, (C) BPSQ1/I1 and (D) BPSQ1/NO in acetonitrile upon irradiation at 518 nm (light intensity  $50 \text{ mW cm}^{-2}$ , co-initiator concentration  $1 \times 10^{-3} \text{ M}$ )

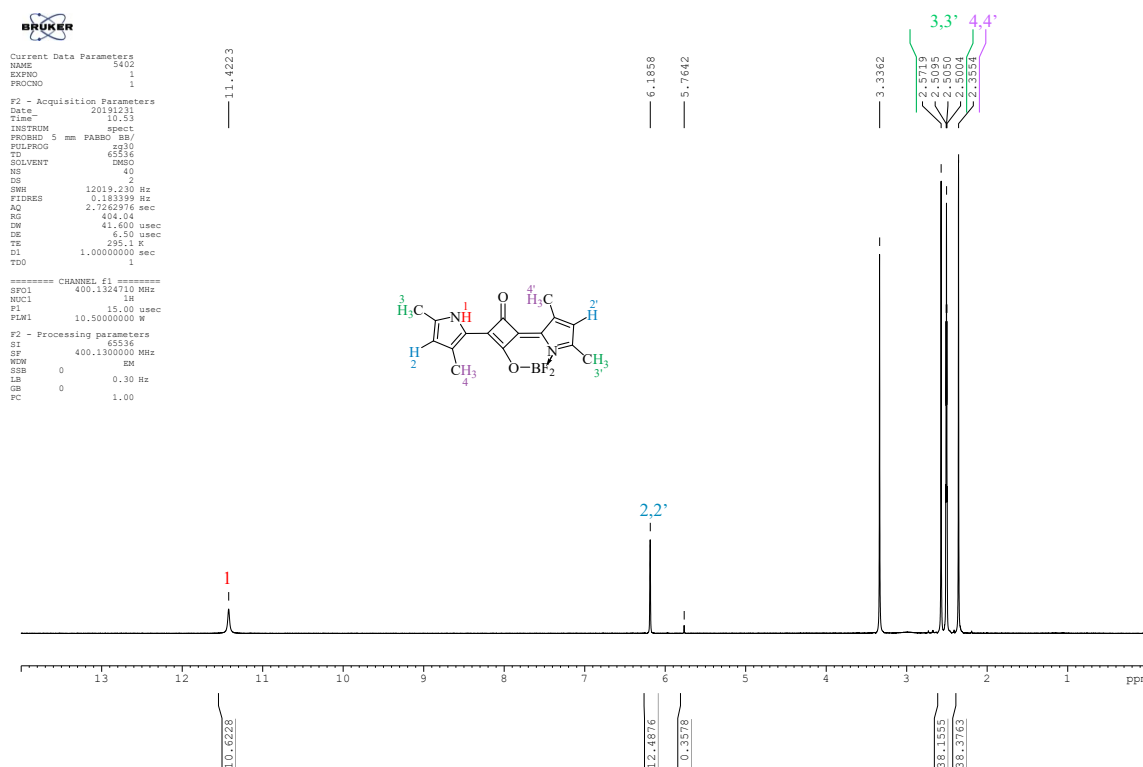


**Figure S3** UV-Vis absorption spectra obtained upon photolysis of (A) BPSQ2 alone, (B) BPSQ2/B2, (C) BPSQ2/I1 and (D) BPSQ2/NO in acetonitrile upon irradiation at 518 nm (light intensity  $50 \text{ mW cm}^{-2}$ , co-initiator concentration  $1 \times 10^{-3} \text{ M}$ )

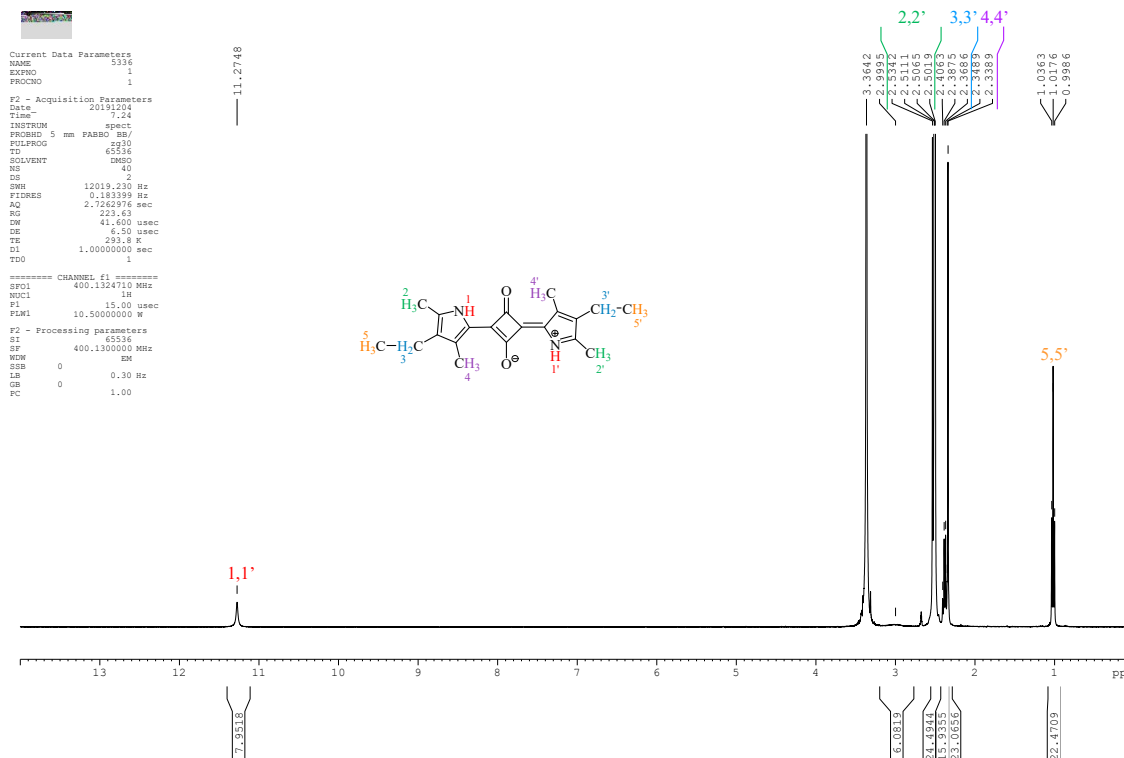
## 2. <sup>1</sup>H NMR spectra



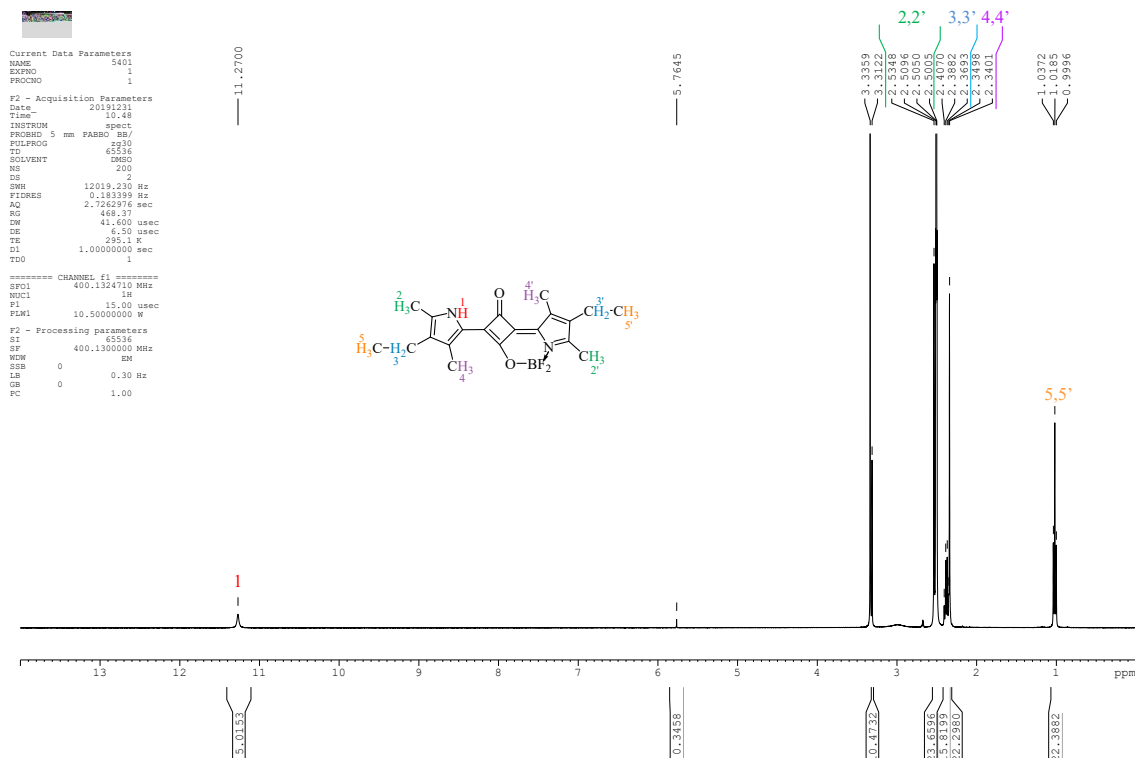
**Figure S4** <sup>1</sup>H NMR spectra of 2,4-bis(3,5-dimethylpyrrol-2-yl)squaraine (PSQ1) recorded in DMSO-d<sub>6</sub>



**Figure S5** <sup>1</sup>H NMR spectra of 2,4-bis(3,5-dimethylpyrrol-2-yl)squaraine dichloroborate complex (BPSQ1) recorded in DMSO-d<sub>6</sub>

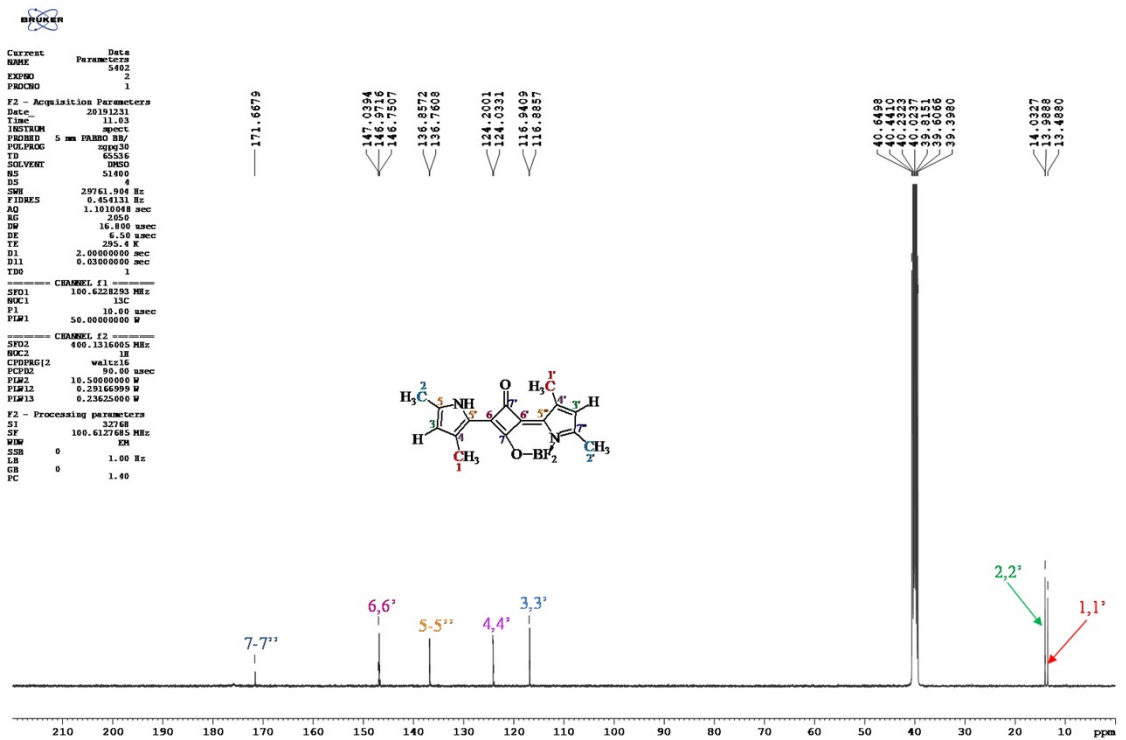
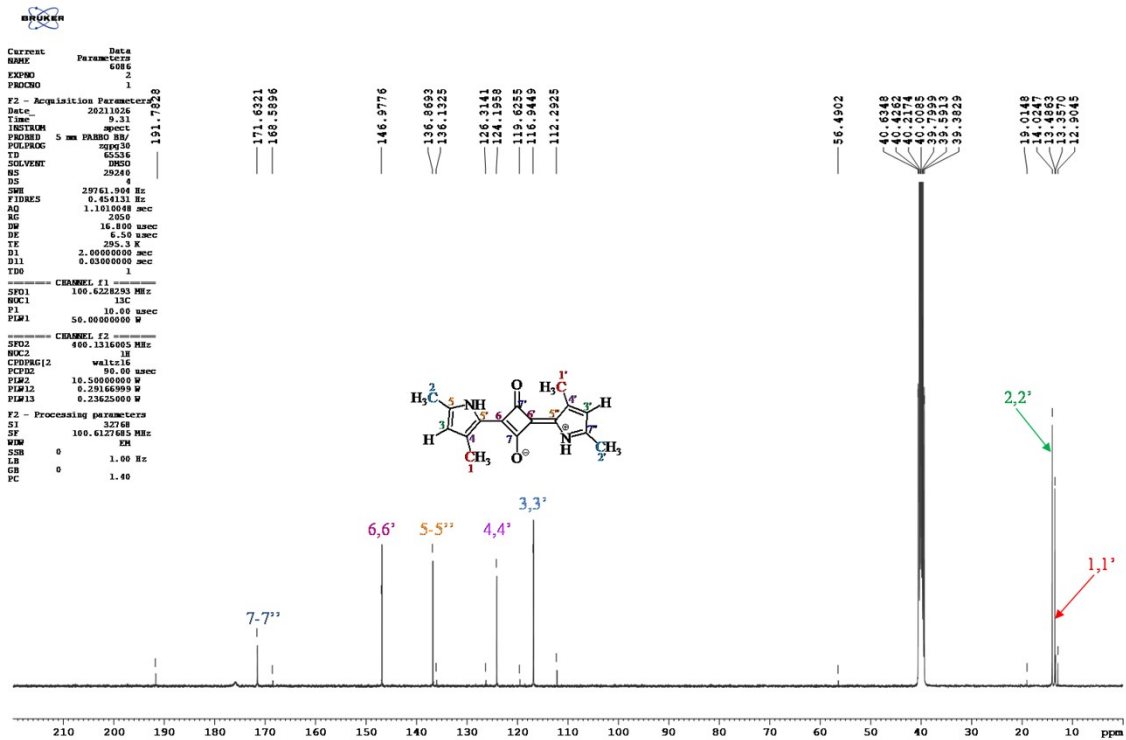


**Figure S6**  $^1\text{H}$  NMR spectra of 2,4-bis(4-ethyl-3,5-dimethylpyrrol-2-yl)squaraine (PSQ2) recorded in  $\text{DMSO-d}_6$



**Figure S7**  $^1\text{H}$  NMR spectra of 2,4-bis(4-ethyl-3,5-dimethylpyrrol-2-yl)squaraine (BPSQ2) difluoroborate complex recorded in  $\text{DMSO-d}_6$

### 3. $^{13}\text{C}$ NMR spectra



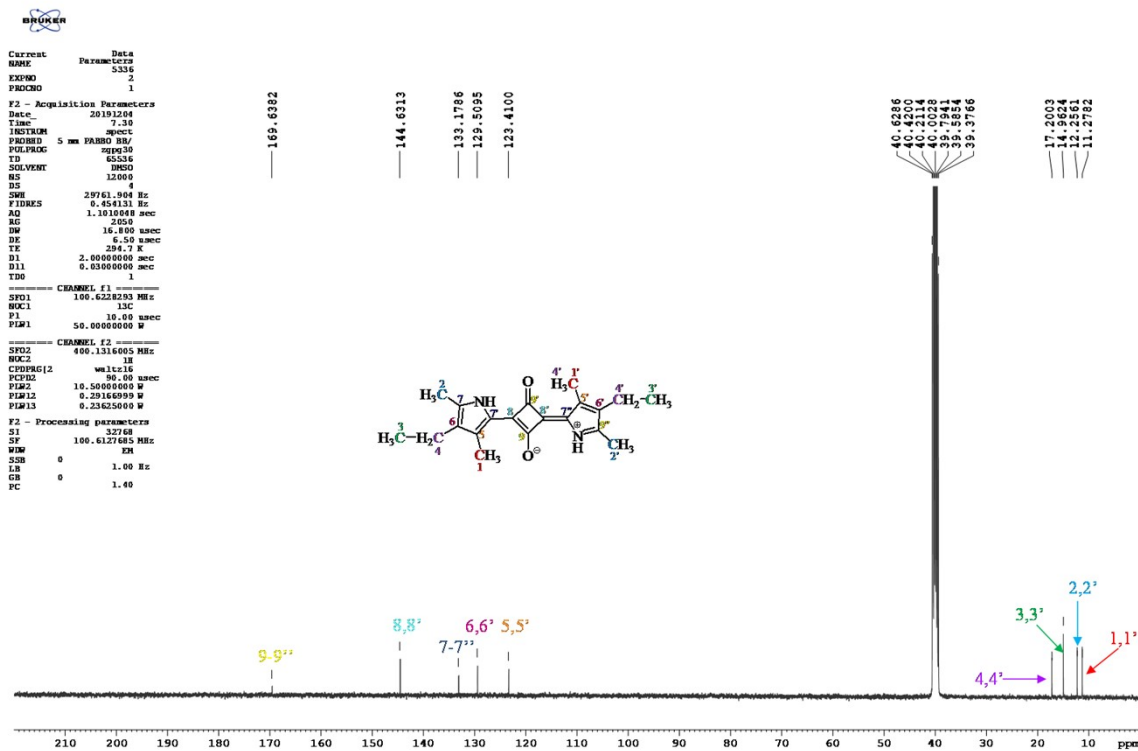


Figure S10  $^{13}\text{C}$  NMR spectra of 2,4-bis(4-ethyl-3,5-dimethylpyrrol-2-yl)squaraine (PSQ2) recorded in  $\text{DMSO-d}_6$

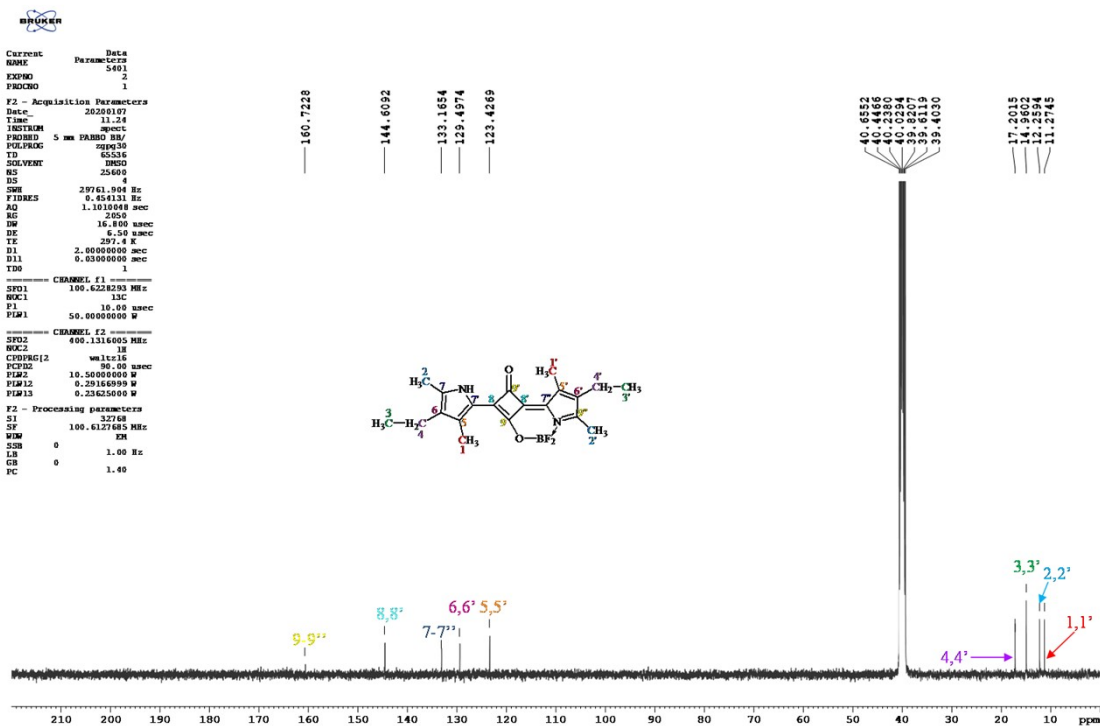


Figure S11  $^{13}\text{C}$  NMR spectra of 2,4-bis(4-ethyl-3,5-dimethylpyrrol-2-yl)squaraine dichloroborate complex (BPSQ2) recorded in  $\text{DMSO-d}_6$

#### 4. The procedure of synthesis of photosensitizers

#### 2,4-*bis*(3,5-dimethylpyrrol-2-yl)squaraine (PSQ1)

A mixture of 0.63 g (5.2 mmol) of square acid and 1 g (~ 1.1 cm<sup>3</sup>, 10.5 mmol) of 2,4-dimethylpyrrole in 50 cm<sup>3</sup> of anhydrous ethanol (99.8% anal) was heat under reflux for seven hours while stirring. The precipitated dye was filtered off and dried on air. Then it was crystallized from ethanol. Blue-violet dye crystals were obtained. The yield of the reaction was 75%.

#### 2,4-*bis*(4-ethyl-3,5-dimethylpyrrol-2-yl)squaraine (PSQ2)

A mixture of 0.63 g (5.2 mmol) of square acid and 1.29 g (~ 1.42 cm<sup>3</sup>, 10.5 mmol) of 3-ethyl-2,4-dimethylpyrrole in 50 cm<sup>3</sup> of anhydrous mixture of benzene/*n*-butanol (1:1) was heat under reflux for seven hours while stirring. The precipitated dye was filtered off and dried on air. Then it was crystallized from ethanol. Violet dye crystals were obtained. The yield of the reaction was 45%.

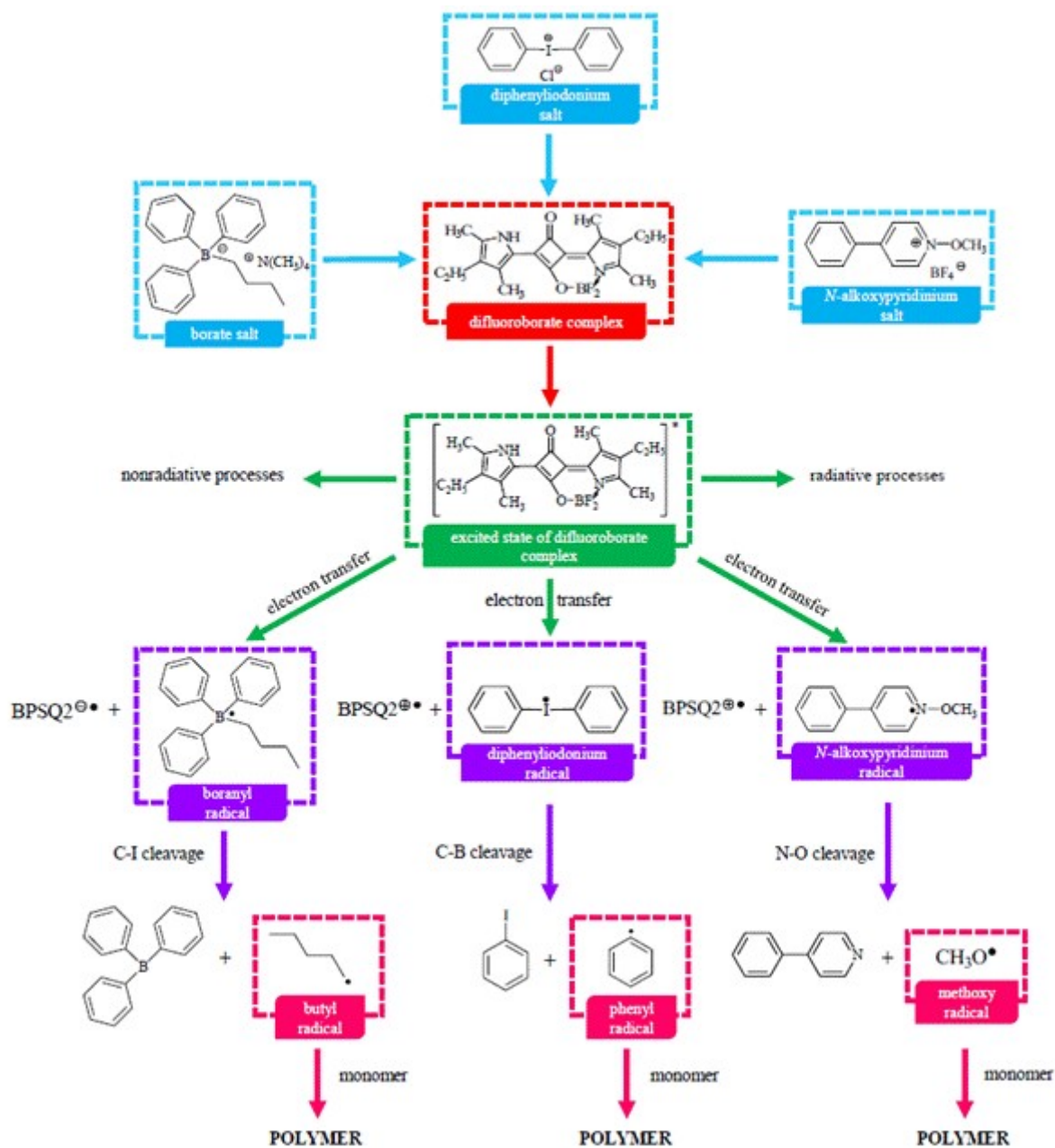
#### 2,4-*bis*(3,5-dimethylpyrrol-2-yl)squaraine difluoroborate (BPSQ1)

200 mg (0.75 mmol) of the PSQ1 dye was dissolved in 100 cm<sup>3</sup> of anhydrous dichloromethane (99.8%). Then 1.04 cm<sup>3</sup> of anhydrous triethylamine (7.5 mmol) and 0.94 cm<sup>3</sup> (7.5 mmol) of anhydrous boron trifluoride diethyl etherate were added in a 10-fold molar excess and stirred at room temperature for two days. Then 200 cm<sup>3</sup> of water was added to the solution and it was extracted twice with 100 cm<sup>3</sup> of dichloromethane. The resulting blue-violet dye was filtered off and dried. The reaction yield was 43%.

#### 2,4-*bis*(4-ethyl-3,5-dimethylpyrrol-2-yl)squaraine difluoroborate (BPSQ2)

100 mg (0,31 mmol) of the PSQ2 dye was dissolved in 40 cm<sup>3</sup> of anhydrous dichloromethane (99.8%). Then 0,43 cm<sup>3</sup> of anhydrous triethylamine (3.08 mmol) and 0.40 cm<sup>3</sup> (3.08 mmol) of anhydrous boron trifluoride diethyl etherate were added in a 10-fold molar excess and stirred at room temperature for two days. Then 150 cm<sup>3</sup> of saturated sodium chloride solution in water was added to the solution and it was extracted twice with 100 cm<sup>3</sup> of dichloromethane. The resulting blue-violet dye was filtered off and dried. The reaction yield was 53%.

### 5. The mechanism of free radical formation



**Scheme S1.** Mechanism of radical formation on the basis of photoinitiating systems composed of 2,4-bis(4-ethyl-3,5-dimethylpyrrol-2-yl)squaraine (PSQ2) and different co-initiators.